THE UNIVERSITY
of EDINBURGH

The Regulation of Notch Ligands Dll1 and Jag1 by Pax6 during Cortical Development

A thesis presented for the degree of Ph.D. at the University of Edinburgh

Elena Dorà, M.Sc, B.Sc (Hons)

2016

Abstract

The regulation of gene expression resulting in the formation of the mammalian cerebral cortex is tightly regulated by a group of transcription factors. The deletion of any one of these transcription factors results in numerous defects whose nature and severity depends on the role of the transcription factor in the regulation of complex gene regulatory networks involved in development. There is currently relatively little knowledge about the gene networks that these transcription factors control and how they exert their regulatory effects.

The paired-box transcription factor *Pax6* has been identified as a master regulator of gene networks involved in cortical development and its deletion results in numerous cortical defects such as an abnormally thin cortical plate and a vastly expanded proliferative zone. Previous work in our lab identified a list of candidate genes that are likely to be regulated by *Pax6* in the developing cortex. Members of the *Notch* signalling pathway were potential *Pax6* targets of particular interest since *Notch* signalling plays a crucial role in the maintenance of neural progenitor cells during development and consequently plays a critical role during corticogenesis.

Our work aims to identify the regulatory relationship between *Pax6* and *Notch* ligands *Dll1* and *Jag1* during cortical development. Analysis by flow cytometry and double labelling analysis of both gene and protein expression has provided insight into the relationship between *Pax6* and *Dll1* in progenitor cell subpopulations during cortical development. *In situ* hybridisation and qPCR results confirmed that loss of *Pax6* causes loss of *Dll1* expressing cells and downregulation of *Jag1*, indicating that both ligands are regulated by *Pax6.* Bioinformatic screening and analysis by luciferase assay suggests that *Jag1* is a likely candidate to be a direct target of *Pax6.*

Declaration

I hereby declare that this thesis has been composed by Elena Dorà, the undersigned, for the degree of Ph.D at the University of Edinburgh. This work has not been presented in any previous application for a degree and all work was performed by the undersigned unless otherwise stated in the text. All sources of information used have been specifically acknowledged in the text.

Elena Dorà, October 2016

Acknowledgements

Firstly, a big thank you to my supervisors Professor David Price and Dr John Mason for guiding me, providing suggestions, keeping me on track and generally putting up with me. I would also like to give a big thanks to all members of DBUG (past and present) for all of your help and for making my time in the lab fun. Particular thanks to Dr Martine Manuel for her help and for making sure I had enough samples for my endless counts! An extra special thanks to Mike Molinek for being the biggest help ever throughout my PhD, I'll miss our lab chats/rants a lot.

I would like to acknowledge the following: Dr Ian Simpson for his bioinformatics expertise and his patience when I bombarded him with questions about it. Dr Laura Lettice the Human Genetics Unit at the Western General, for providing me with genomic DNA. Dr Martin Waterfall from the FACS facility at Kings Buildings for his help and assistance with my flow cytometry experiments. Dr Lynn Powell for her luciferase assay help and advice. To all of the staff in the BRR, thanks for all of your help and for always being so nice whenever I was in the unit.

Thanks to Freya Hotson for producing a much more professional version of my hypothesis model from my less than professional looking sketches. Thanks to all of my project students for helping me with parts of this project. I'm sorry for being so pedantic! I'd also like to thank everyone who had to listen to me moan about cloning for the best part of two years and an extra special thank you to those who provided helpful troubleshooting suggestions.

Thank you to my sister Natalie for always being there to help me out in a lab related crisis and for reminding me that I could do this when the going got tough.

Thanks to my boyfriend Ross, you've had to put up with a lot! Thank you for all of your love and support. ily.

I’d also like to thank my brother-in-law Andy: thanks for plying me with wine whenever I had a bad science day. I’m not saying that alcohol solves problems or anything but it definitely helps!

Thanks to my furry friend Holly: You were there from the start and almost made it to the end of this journey with me. Thank you for all of the sofa cuddles you gave me when science was getting me down. I miss you.

A big thank you to my new furry friend Brook: you took over on those sofa cuddle duties, cheered me up and kept me sane during my write up. Thanks for the distractions you provided by needing walks and by chewing up some of my favourite clothes.

Finally, thank you to my Mum and Dad for the endless support and for always believing in me.

Table of contents

List of figures Page no.

Chapter One

Chapter 2

Chapter 3

Chapter 6

Chapter 7

List of tables

Chapter 1

Chapter 2

Chapter 3

Chapter 4

Chapter 5

Chapter 6

List of Abbreviations

$^{-/-}$ - Homozygous

$^{+/+}$ - Heterozygous

AMP – Ampcilin

AP – Apical Progenitors

bHLH – Basic Helix Loop Helix

BMPS – Bone Morphogenic Factor

BPs – Basal Progenitor Cells

cDNA – Complementary DNA

ChIP – Chromatin Immunoprecipitation

ChIP-seq – ChIP-sequencing

cKO – Conditional Knockout

CNS – Central Nervous System

CP – Cortical Plate

Ctx – Cortex

DI – Diencephalon

Dll1 – Delta-like 1

DNA – Deoxyribonucleic Acid

FACS – Fluorescence-activated Cells Sorting

Fgfs – Fibroblast Growth Factor

Fp6 – Floxed Pax6

GE – Ganglionic Eminences

GFP – Green Fluorescent Protein

HD – Paired-type Homeodomain

HEK293 – Human Embryonic Kidney

HP – Hippocampus

INPs – Intermediate Progenitor Cells

INP^{VZ} – INPs residing within the VZ

IZ – Intermediate Zone

Jag1 – Jagged 1

Jag1UE – Jag1 Upstream Enhancer

LB Broth – Lennox Broth

LGE – Lateral Ganglionic Eminence

Mash1 – Mammalian Achaete Scute Homolog 1

MGE – Medial Ganglionic Eminence

MZ – Marginal Zone

N - Number

N1-4 (Notch 1 – 4)

NEs – Neural Epithelial Cells

Ngn2 – Neurogenin2

NICD – Notch Intracellular Domain

PAX77 – Pax6 Overexpressing Mouse

PBS – Phosphate Buffered Saline

PD – Paired Domain

PNS – Peripheral Nervous System

PSPB – Pallial Subpallial Boundary

PWMs – Position Weight Matrixes

qPCR – Quantitative Real-Time Polymerase Chain Reaction

RBPj – DNA Binding Protein

RGCs – Radial Glial Cells

Sey – Small Eye

Sfrp2 – Secreted Frizzled-related Protein 2

SGZ – Subgranular Zone

Shh – Sonic Hedgehog

SNPs – Short Neural Precursor Cells

SP – Subplate

STWS – Scott's Tap Water Substitute

SVZ – Subventricular Zone

Tgfα – Transforming Growth Factor α

VZ – Ventricular Zone

Wnts – Wingless/Ints

WT – Wild Type

YAC – Yeast Artificial Chromosome

1.0 Introduction

1.1 The mammalian cerebral cortex

The mammalian cerebral cortex is a complex; multi-layered structure comprised of a variety of different neuronal cell subtypes, as well as non-neural glial cells (Tabata, 2015) and is predominantly accountable for both perceptual and cognitive functions, such as the process of conscious thought, emotions, memory and the ability to communicate (Martinez-Cerdeno, 2004). The study of cortical development during embryogenesis is of particular importance in our understanding of developmental (Manzini and Walsh, 2011) and neurodegenerative (Abdipranoto *et al*., 2008) diseases. Understanding how the cerebral cortex develops initially enables us to understand what happens when molecular mechanisms go wrong during development, such as occurs in autism (Hui *et al*., 2015), Fragile X syndrome (Fung *et al*., 2012) and cerebral palsy (MacLennan *et al*., 2015). Understanding how complex signalling pathways are disrupted in these diseases could potentially help to develop gene therapy approaches that could be implemented (Hui *et al*., 2015). Furthermore, the study of developmental processes such as neurogenesis can help develop gene therapy strategies for neurodegenerative diseases and brain injury, which could potentially regenerate cortical cells and effectively repair the cerebral cortex (Akhtar and Breunig, 2015; Lui and Deng, 2015). While there are some differences between species, mammalian cortical development is relatively well conserved and this thesis will focus on the development of the murine cerebral cortex unless otherwise stated.

The cerebral cortex forms from the dorsal region of the telencephalon during the process of embryogenesis, and the prerequisites required for its prospective development occur following embryonic gastrulation, with molecular cues manipulating a simple epithelial sheet of cells to ultimately result in the formation of a complex network of cells that constitute a fully formed and functional brain (Wilson and Rubenstein, 2000; Wilson and Houart, 2004). General organisation of

early forebrain patterning is well conserved in all vertebrates, and has been extensively studied in amphibian, avian and mammalian structures (Wilson and Houart, 2004). In terms of mammalian cortical development, the cellular and molecular processes are relatively similar with moderate differences between different species (Wilson and Rubenstein, 2000; Wilson and Houart, 2004).

1.2 Induction of the forebrain

The developmental onset of the mammalian telencephalon occurs early on during embryogenesis and is instigated by the process termed neurulation. Neurulation is initiated by the thickening of the ectoderm, the distal germinal layer formed during the primary stages of embryogenesis, and comprises three main stages (Morris-Kay, 1993). This commences with the aforementioned thickening of the ectodermal cells, forming the neural plate and eventually causing its pseudo stratification and the expression of molecular markers, which instigate the second stage of neurulation. Following the formation and thickening of the neural plate, the neural plate undergoes rostrocaudal lengthening, mediolateral narrowing and further apico-basal thickening. This results in the morphological modification of the once flat neural plate, allowing subsequent bending of the structure (Morris-Kay 1993; 1994). This stage of neurulation involves the folding of the neural plate and culminates in the formation of the neural tube (Figure 1.1), a hollow nerve cord that acts as the precursor of the adult central nervous system (CNS) and a majority of the peripheral nervous system (PNS). The mammalian brain consequently arises when the anterior portion of the neural tube closes to form three vesicles: the prosencephalon, mesencephalon, rhombencephalon (Smith and Schoenwolf, 1997). The prosencephalon consists of the telencephalon and diencephalon, and comprises the forebrain of the developing embryo. The telencephalic vesicles make up the telencephalon and develop as two laterally enlarging bulges that delineate them from the diencephalon (Smith and Schoenwolf, 1997; Götz, 2001).

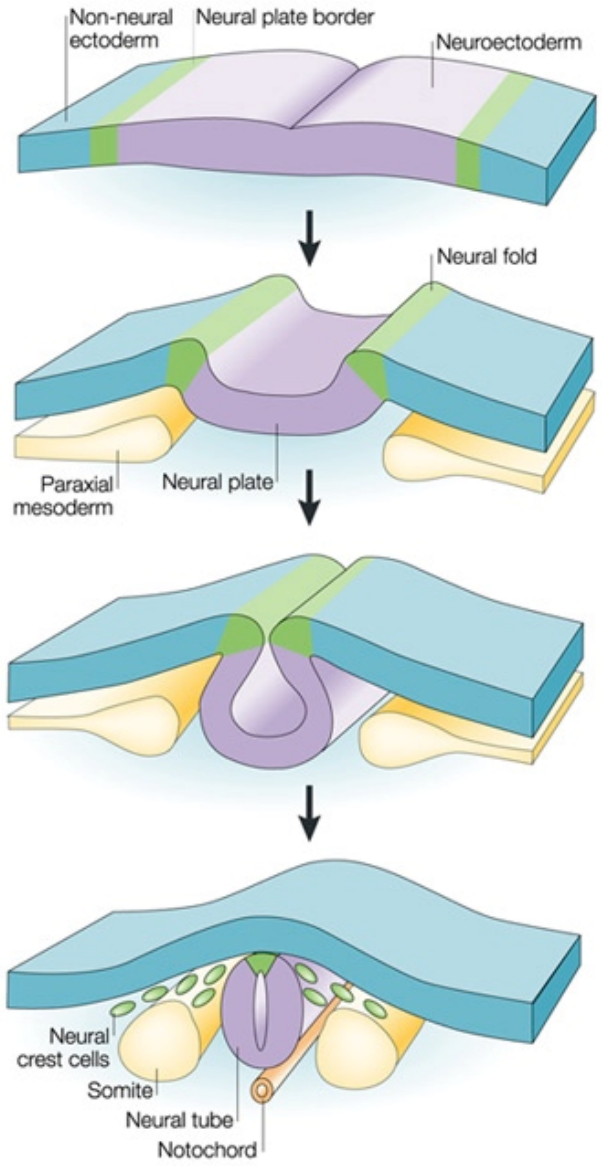

Figure 1.1 Early neurulation

Taken from Gammil and Bronner-Fraser, 2003. The neural plate forms from the thickening of ectodermal cells to produce the neural plate. During neurulation, the borders of the neural plate (neural folds) elevate to instigate the folding of the neural plate to form the neural tube. The neural tube acts as the precursor of both the CNS and PNS, with the anterior portion of the neural tube giving rise to the brain.

1.3 Early patterning of the telencephalon

During embryogenesis, development of the forebrain is guided by signals originating from four patterning centres: the rostral patterning centre, the caudodorsal centre, the ventral centre and the lateral centre (Figure 1.2 (Hoch *et al*., 2009). These molecular signals act to transform the aforementioned anterior neural plate into distinct forebrain structures, including the telencephalon (Rubenstein and Beachy, 1998; Wilson and Rubenstein, 2000; Wilson and Houart, 2004; Hoch *et al*., 2009). The induction of the telencephalon results from the accumulation of specific and highly controlled signalling, transcriptional and regulatory events, which coordinate the regional development of distinct telencephalic areas along the rostrocaudal and dorsoventral axes of the developing forebrain (Hoch *et al.,* 2009).

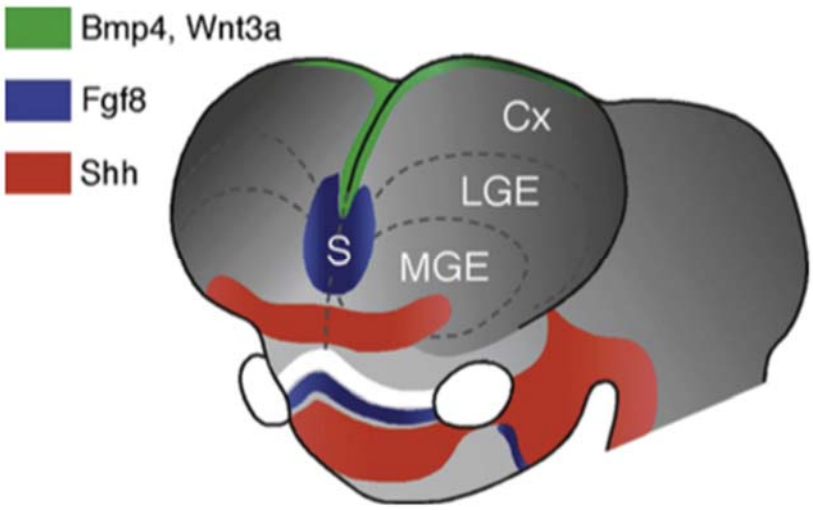

Figure 1.2 The signalling centres that instruct telencephalic development.

Taken from Hoch *et al*., 2009. The rostral signalling centre (S) (blue) is located in the anlage of the septum and secretes Fgfs. The caudodorsal signalling centre (green) is located at the cortical hem and secretes Wnts and BMPs. The ventral signalling centre (red) secretes Shh. There is also a lateral signalling centre located at the pallial-subpallial boundary PSPB (not shown) that secretes multiple factors including: Fgf7, Fgf15, neuregulins, Tgf, and Sfrp2.

The previously mentioned signalling centres responsible for the formation of the telencephalon act by contributing to the regionalisation of the forebrain and, consequently, the development of region-specific structures that comprise the forebrain (Figure 1.2) (Hoch *et al.,* 2009). The rostral patterning centre is embedded in the anlage of the septum and secretes fibroblast growth factors (Fgfs). The caudodorsal centre, located at the cortical hem, secretes Wnts and bone morphogenic factors (BMPs), while the ventral signalling centre is located at the commissural pre optic area and secretes sonic hedgehog (Shh). Lastly, the lateral centre, which is located at the cortex/LGE interface, secretes an abundance of factors including: Fgf7, Fgf15, neuregulins, transforming growth factor α (Tgfα) and the Wnt antagonist, secreted frizzled-related protein 2 (Sfrp2) (Figure 1.2) (Hoch *et al*., 2009).

Following neural induction, early regional specification of the telencephalon is mediated by the expression of *Fgf8*, *BMP* and *Shh* signalling, as well as the restriction of *Wnt* activity to dorsal domains by *Wnt* antagonists (Schneider *et al*., 2001; Haliagic *et al*., 2003; Ribes *et al*., 2006; Halilagic *et al*., 2007; Molotkova *et al*., 2007). The formation of the dorsal and ventral regions of the telencephalon swiftly follows the closure of the neural tube during the process of neurulation and is tightly controlled by growth and morphogenic signals responsible for regional pattering of the forebrain. The dorsal and ventral regions of the developing telencephalon give rise to the pallium (comprised of structures such as the cerebral cortex and hippocampus) and subpallium (comprised of the medial and lateral ganglionic eminences) respectively and their development relies upon the expression of opposing morphogen signals in order to specify their positional identity (Rubenstein and Beachy, 1998; Wilson and Rubenstein, 2000; Wilson and Houart, 2004; Hoch *et al*., 2009).

Positional identity of telencephalic structures relies upon the interplay and crossregulation of multiple signalling factors in order to specify structural identity along the DV axis of the developing forebrain. The pallium and subpallium

principally arise from the activity of opposing morphogens; Shh from the ventral signalling centre and the secretion of Bmps and Wnts from the dorsal signalling centre respectively, allowing specification of positional identity along the DV axis (Hoch *et al*., 2009). The ventral secretion of Shh is present from early on during the process of shaping the forebrain, originating originally from the anterior mesoderm and then later from the ventral hypothalamus and rostroventral telencephalon as the telencephalon develops in its complexity (Wilson and Houart, 2004). On the other hand, morphogens responsible for specifying a dorsal structure are secreted from the paramedial neuroectoderm and the dorsal midline (Hoch *et al*., 2009). However, *Shh* and *Bmps*/*Wnts* are not solely responsible for the development of the pallium and subpallium, with multiple additional factors such as the *Fgf* family and transcription factors *Gli3* and *Pax6* to name but a few also playing a vital role during telencephalic patterning (Rubenstein and Beachy, 1998; Wilson and Rubenstein, 2000; Wilson and Houart, 2004; Hoch *et al*., 2009).

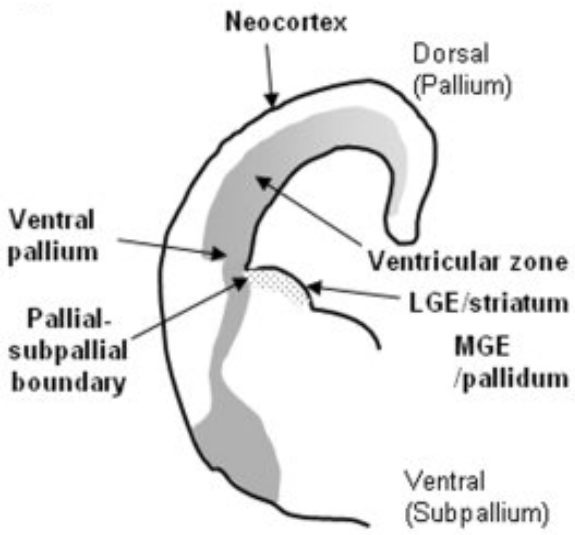

Figure 1.3 The structures of the developing telencephalon

Taken from Cocas *et al.,* 2001. A schematic representation of the structures that make up the developing telencephalon during embryogenesis. The telencephalon is divided into the pallium and subpallium and are separated by the pallial subpallial boundary (PSPB). The pallium includes the developing cortex (neocortex) and the subpallium includes the ganglionic eminences (LGE and MGE) The location of all structures are depicted by black arrows.

As mentioned, Fgfs are required during telencephalic development. Fgfs originate from the RPC and are a major contributor to the specification of the telencephalon into dorsal and ventral domains by their regulation of signalling factors residing at the pallial-subpallial boundary (PSPB) (Hoch *et al*., 2009). The PSPB resides between the pallium and subpallium and secretes a variety of signals, such as Fgf7, Fgf15, Sfrp2 and members of the Egf family, which act to define a molecular boundary between the pallium and subpallium as well as instructing development of forebrain structures (Assimacopoulos *et al*., 2003; Borello *et al*., 2008). Additionally, *Fgfs* are responsible for the activation of *Shh* and *Nkx2.1* expression, which are both required for specification of the ventral region of the telencephalon. The activation of *Shh* by Fgf signalling induces the lateral ganglionic eminences (LGE) and medial

ganglionic eminences (MGE) that constitute the subpallium of the telencephalon. It is likely that Shh instigates this in part at least by its repression of the transcription factor Gli3, a factor that instigates a dorsal telencephalic fate over a ventral fate (Ishibashi and McMahon, 2002; Rallu *et al*., 2002; Rash and Grove, 2007; Ulloa and Briscoe, 2007).

An abundance of experimental evidence suggests that the aforementioned morphogens secreted at the PSPB are of key importance during specification of telencephalic structures. It has been suggested that these signals potentially restrict Wnt activity to the dorsal telencephalon, consequently encouraging ventral specification (Assimacopoulos *et al*., 2003). Past studies using *Pax6*$^{-/-}$ mice observed that mutant embryos display a severe disruption of the PSPB and lack the anti-hem signals that are expressed there, resulting in telencephalic structures forming incorrectly (Yun *et al*., 2001). Furthermore, it has been suggested that the signals secreted at the PSPB either control the transcription factors Pax6 and Gsh2, or are controlled by them to compartmentalise the telencephalon into its specific regions (Yun *et al*., 2001; Hoch *et al*., 2009; Cocas *et al*., 2011). This notion is due to research by Yun *et al*., (2001) which showed that *Pax6*$^{-/-}$ mutant embryos see a dorsal expansion of ventral telencephalon gene expression and *Gsh2*$^{-/-}$ mutant embryos see a ventral expansion of dorsal telencephalon gene expression. In wild-type (WT) embryos, Pax6 and Gsh2 are expressed in the pallium and subpallium respectively, and their expression patterns abut the PSPB, so the previously mentioned observations are particularly interesting in terms of how patterning of the telencephalon is achieved (Yun *et al*., 2001). Cocas et al., (2011) provided further evidence of the mutual relationship between Pax6 and Gsh2 to co-repress one another, where specific loss of Pax6 in Gsh2 expressing cells saw an expansion of the LGE of the subpallium, consequently distorting the formation of the telencephalon (Cocas *et al*., 2011). However, regardless of whether anti-hem signals regulate *Pax6* and *Gsh2* or vice versa, transcription factors *Pax6* and *Gsh2* and anti-hem signals at the PSPB are critical during the specification of structures that comprise the telencephalon (Hoch *et al*., 2009).

1.4 Cortical development

During embryogenesis, the cerebral cortex develops as a result of the process of neurogenesis and the migration of the resulting generated neurons from the ventricular zone (VZ), and at later stages in the subventricular zone (SVZ), of the telencephalon during embryonic development (Manuel *et al*., 2015). Neurogenesis is essentially the process that generates the neurons that come together to craft the structures that comprise the fully formed brain. During neurogenesis, neurons are produced from neural progenitor cells residing within the proliferative zone of the developing brain. The vast majority of neurogenesis occurs during embryonic development when a vast number of neurons are required to produce the developing brain, but neurogenesis continues postnatally while the brain continues to develop (Anderson and Vanderhaeghen, 2014). Furthermore, adult neurogenesis continues thereafter in a small number of structures such as the olfactory bulb and hippocampus (Eriksson *et al*., 1998; Temple and Alvarez-Buylla, 1999; Ma *et al*., 2010).

The generation of new neurons during embryonic neurogenesis implicates different types of cell division that are specific to different progenitor cell types and produce different cell types as a result (Laguesse *et al*., 2015). These cell divisions are: symmetrical progenitor cell divisions, asymmetrical progenitor cell divisions and terminal symmetrical progenitor divisions. Symmetrical cell divisions produce two new progenitor cells and replenish the proliferative cell pool as a result (Figure 1.4), while asymmetrical divisions generate a single neuron and one new progenitor cell, therefore still replenishing the progenitor cell population and allowing subsequent rounds of neurogenesis to take place (Figure 1.4). However, terminal symmetrical divisions produce two neurons, consequently diminishing the progenitor cell pool within the proliferative zone. Throughout development of the cerebral cortex, neural progenitor cells residing in both the VZ and SVZ, that constitute the proliferative zone of the cortex, carry out all three types of cell division depending on which

progenitor cell subtype they are (Chenn and McConnell, 1995; Farkas and Huttner, 2008; Noctor *et al*., 2004; Laguesse *et al*., 2015).

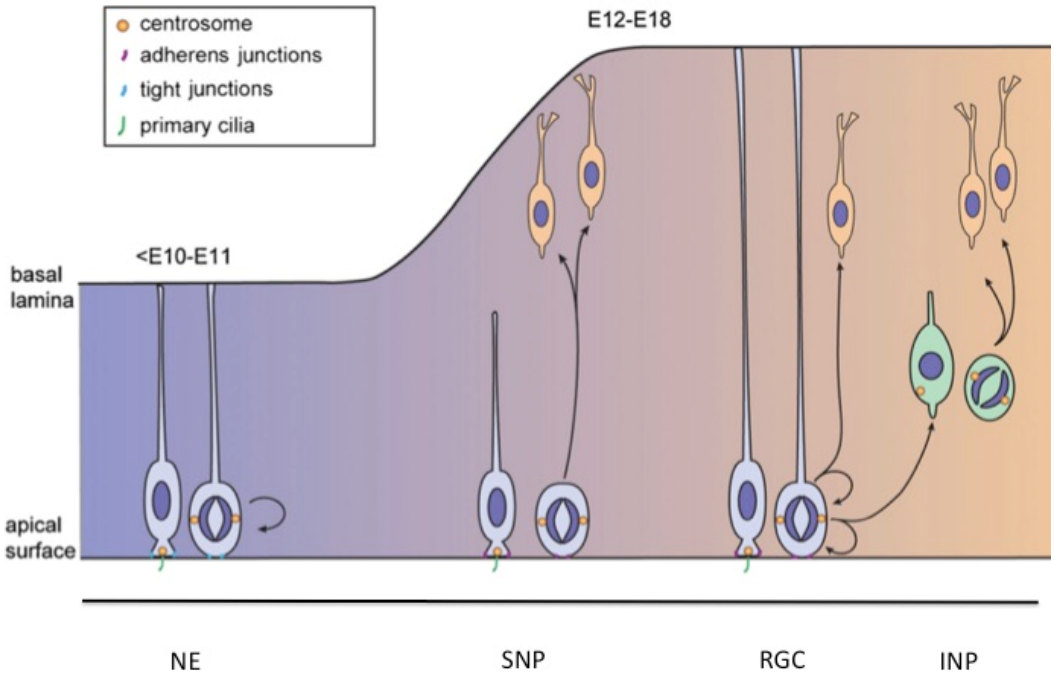

Figure 1.4 Cell divisions and progenitor cell subtypes during cortical neurogenesis

Taken from Laguesse *et al*., 2015. Apical progenitors (APs) encompass neuroepithelial cells (NEs), short neural precursor cells (SNPs), radial glial cells (RGCs). NEs divide symmetrically to self- renew and expand the surface area of neural tube or to produce two RGCs. During neurogenesis, RGCs divide asymmetrically to produce one RGC and one neuron (direct neurogenesis), or one RGC and one intermediate progenitor cells (INP) (indirect neurogenesis). SNPs have no attachment to the basal lamina and tend to generate two neurons. INPs are basal progenitors (BPs) and reside in the SVZ. INPs are not attached to the apical membrane or the basal lamina. INPs retract their processes during M-phase and produce either two new INPs or two neurons by symmetric division.

1.5 Progenitor cell sub populations

Classically, three distinctive types of neural progenitor cells were proposed to be involved in cortical development and are distinguished by differing cellular

morphology, mitotic divisions, molecular expression, regional position, and daughter cell fate (Huttner *et al*., 2005; Pontious *et al*., 2007). These subpopulations are: neuroepithelial cells (NEs), radial glial cells (RGCs), and intermediate progenitor cells (INPs). In addition to the three classically defined progenitor cell populations, a further population has been identified; short neural precursor cells (SNPs).

NEs are categorically the primary progenitor cell type and all subsequent progenitor cell subtypes are derived solely from them (Laguesse *et al*., 2015). In principle, NEs are neural stem cells, or stem cells of the CNS, in that they have acquired a neural fate although their eventual neuronal cell fate is yet to be determined. NEs have the ability to produce any type of neuronal cell and each subsequent differentiation into a different progenitor cell subtype further restricts neural cell fate (Götz and Huttner, 2005). NEs derive from the ectoderm during neural induction and display similar features to epithelial cells, most notably an apical-basal polarity during the process of cellular mitosis (Huttner *et al., 2005).*

The formation of cortical layers relies upon the production of RGCs by NEs. RGCs are formed when NEs undergo asymmetric cell division, producing one new NE and one RGC. Generally speaking, RGCs have similar properties to NEs but do differ from the latter by their expression of astroglial markers and their further restricted eventual cell fate (Laguesse *et al*., 2015). Due to the fact that RGCs are more fate restricted than their neural precursors and also essentially replace them in the progenitor zone, the vast majority of neurons that comprise the cerebral cortex are generated directly from them (Götz *et al.,* 2005, Heins *et al.,* 2008). As previously mentioned, progenitor cell subtypes are distinguished by unique characteristics, such as distinct molecular expression and how they undergo cellular mitosis and division. RGCs are widely recognised as expressing molecular markers such as Pax6, Sox2 and Olig2 - providing a relatively quick and reliable way to identify the progenitor cell type by immunohistochemical analysis. RGCs have also been identified by previous studies as characteristically projecting from the apical surface of the VZ, and extending through the neural cell layers towards the basal lamina by basal processes. RGCs undergo mitosis towards the apical surface of the VZ, and divide

asymmetrically to produce one daughter cell that continues to reside within the VZ and either one neural precursor cell or one INP which migrate from the VZ to form the layers of the cortex or to reside within the SVZ respectively (Figure 1.4) (Noctor *et* al., 2001; Götz and Huttner, 2005; Huttner *and* Kosodo, *2005*; Hevner, 2006; Tan and Shi, 2013). Alongside RGCs, the VZ also contain an additional subpopulation of progenitor cell, SNPs. SNPs undergo symmetric cell divisions only to produce pairs of neurons and are consequently unable to self-renew unlike other progenitor cell subtypes (Gal *et al*., 2006; Tan and Shi, 2013; Manuel *et al*., 2015).

INPs are transient amplifying neural progenitor cells, in that they undergo a more restricted round of cell divisions before terminating and differentiating as neural precursor cells (Farkas and Huttner, 2008). INP cells differ from RGCs in that they undergo symmetric cell division, producing either two INP cells that continue to reside within the SVZ, or two neural precursor cells that migrate from the progenitor zone to create the neuronal layers of the cerebral cortex (Figure 1.5) (Haubensak *et al*., 2004; Miyata *et al*., 2004; Noctor *et al*., 2004). Furthermore, INPs undergo basal cell divisions within the proliferative zone of the developing cortex and differ from RGCs in terms of their expression of genes unique to their cell subtype, such as the transcription factor Tbr2 (Englund *et al., 2005)*. These distinct differences between INPs and fellow progenitor cell subtypes were identified by previous studies conducted by groups investigating progenitor cells during embryogenesis, and incorporated time-lapse imaging analysis of slice cultures and by in-depth gene expression analysis (Hevner, 2006; Pontious, 2007; Pierfelice *et al*., 2011).

Interestingly, although the majority of INPs are located within the SVZ and they are classically defined as residing within this region of the proliferative zone of the developing cerebral cortex, a fraction of INPs have been identified as being located within the VZ. INPs residing within the VZ (INP^{VZ}s) were initially identified by their expression of the transcription factor Tbr2, as RGCs do not express it. Additionally, INPs lack the apical end feet that are characteristic of RGCs and INPs residing within the VZ are no exception (Götz and Huttner, 2005). Why a small number of INPs are found within the VZ is still not entirely clear, however it has been

suggested that they are newly generated INPs in the process of migrating into the SVZ (Englund *et* al., 2005; Corbin *et al*., 2009), suggesting that INP^{VZ} cells could be the link between RGCs and INPs, in that they have newly differentiated and could potentially still retain characteristics of RGCs, as well as beginning to acquire INP characteristics.

1.6 Laminar organisation of the cerebral cortex

As previously discussed, the cerebral cortex is comprised of layers of neurons that are produced during embryogenesis by the process of corticogenesis; neurogenesis which is specific to cortical development. The formation of the layers of the cortex during cortical development is the product of the radial migration of newly generated neurons produced by cellular differentiation (Chenn and McConnell, 1995; Götz, 2001). Neural cell division occurs as the nucleus of the cell moves from an apical to a basal position, towards the pial surface. S phase, when DNA replication commences, occurs at the pial surface and M phase, when mitosis occurs, takes place at the ventricular surface. As previously discussed, the cerebral cortex initially consists of the VZ only and its development occurs as progenitor cells divide to yield neurons. The newly generated neurons cease to have contact with the ventricular surface and settle underneath the pial surface to aid the formation of a layer of the cortex. As the process of neurogenesis continues, newly generated neurons proceed with forming additional cortical layers directly beneath the pial surface, guided by the processes of RGCs that retain a constant connection via a process with the pial surface (Figure 1.4) (Götz 2001; 2002; Rakic, 1972; 1988).

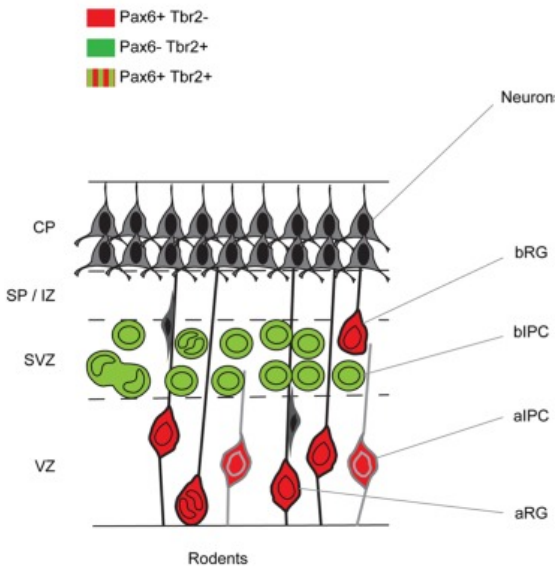

Figure 1.5 The formation of cortical layers during development of the cerebral cortex

Taken from Manuel *et al*., (2015). A coronal section through the developing cortex depicting progenitor cell subtypes residing in the VZ and SVZ and the migration of neurons to form the cortical plate (CP), subplate (SP) and intermediate zone (IZ). that will form the layers of the adult cortex. Progenitor cells are colour coded to show if they express Pax6 (RGCs) or Tbr2 (INPs).

The developing cortex undergoes rounds of neurogenesis during embryonic development until it consists of three neuronal layers: the marginal zone (MZ), subplate (SP) and cortical plate (CP); and two proliferative layers, the VZ and SVZ, that together comprise the proliferative zone. Neurons produced initially after neurogenesis commences to form the preplate of the developing cortex (Götz and Sommer, 2005). During this early stage, the processes of RGCs that aid neuronal migration do not guide neurons to their destination. Later on, neurons migrating with the aid of RGC guidance settle in the preplate, dividing it into two layers, the marginal zone and the subplate, forming the cortical plate between them (Levitt *et al*., 1997). Following cortical plate formation, the SVZ develops directly above the VZ, producing an additional proliferative layer (Figure 1.4) (Götz, 2001).

In terms of the adult cerebral cortex, its layers are numbered according to their proximity to the pial surface, with the MZ of the developing cortex forming the first layer. Neurons which formed the cortical plate develop into layers 2-6 and the subplate forms layer 6b of the adult cortex (Götz, 2001).

1.7 A comparison between mice and humans

While mammalian embryonic cortical development is relatively conserved from species to species, there are some distinct differences amongst some. This is most notable when comparing murine cortical development to human cortical development during embryogenesis, where the obvious differences in cortical morphology reflect the different progenitor cell subpopulations and their characteristic cell divisions (Florio and Huttner *et al*., 2014). First and foremost, the human cerebral cortex is roughly around 1000 times larger than that of the mouse, with this stark difference in size largely being attributed to the increased level of neurogenesis that occurs during human – and more generally, primate - embryonic development (Azevedo *et al*., 2009).

In comparison to mice, the SVZ of primates is much larger and contains both and inner (ISVZ) and outer (OSVZ) region. While the ISVZ predominately contains INPs akin to the INPs found in the murine SVZ, the OSVZ is comprised mainly of radial glial-like outer radial glial cells (ORGCs) (Florio and Huttner *et al*., 2014). ORGCs are similar to their RGC counterparts located in the VZ but differ morphologically as they do not have an apical process and instead only have a basal process extending towards the pial surface. Furthermore, ORGCs are incapable of directly generating neurons unlike their RGC counterparts, instead undergoing self-renewing and proliferative asymmetric cell divisions in order to generate one ORGC and one INP, as well as neurogenic divisions (Fietz *et al*., 2010; Hansen *et al*., 2010; Reillo *et al*., 2011). While ORGCs are generally associated with primates, they have also been observed in the SVZ of mice but only contribute a small percentile of the total progenitor cell population of the SVZ in comparison (Manuel *et al*., 2015). To

put it simply, ORGCs in the OSVZ of the human/primate cortex undergo multiple rounds of self amplification in order to maintain the proliferative cell pool, and the majority of primate cortical neurons are generated by ORGC neurogenic divisions as a result (Florio and Huttner *et al*., 2014).

An additional difference between the developing cortex of mice and humans is the difference between INPs of the SVZ and ISVZ in terms of their proliferative and differentiative abilities. While INPs located in the SVZ of the murine cortex undergo symmetrical divisions in order to produce a pair of INPs or a pair of neurons, INPs in the ISVZ of the primate cortex can yield any other INP subtype and undergo additional rounds of amplification unlike their murine counterparts (Haubensak *et al*., 2004; Miyata *et al*., 2004; Noctor *et al*., 2004).

Lastly, in humans, PAX6 is expressed by progenitors in the VZ, ISVZ and OSVZ. This contrasts with the expression of Pax6 in mice where it is restricted to RGCs. Furthermore, while Pax6 and Tbr2 are expressed sequentially in mice and are associated as markers of RGCs and INPs respectively, many cells co-express Pax6 and Tbr2 in the developing cortex of primates (Englund *et al*., 2005; Cappello *et al*., 2006; Manuel *et al*., 2015).

1.8 The role of notch signalling during cortical development

Notch signalling occurs throughout the process of embryogenesis and also plays a key role in a variety of biological processes postnatally (Guruharsha *et al*., 2012; Mathieu *et al*., 2013). During embryogenesis, *Notch* signalling is involved in a variety of developmental processes including somatogenesis (Wahi *et al*., 2014), organogenesis (Fortini *et al*., 2012) and neurogenesis (Egger *et* al., 2011; Pierfelice *et al*., 2011). During the process of cortical neurogenesis in the mouse, *Notch* signalling plays a critical role in the regulation of the progenitor pool (Corbin *et al*., 2009). The key importance of *Notch* signalling during neurogenesis was initially identified in *Drosophila*, where it was discovered that a disruption in the *Notch*

cascade resulted in the generation of too many neurons and a consequent radical depletion of the neural progenitor pool (Artavanis-Tsakonas *et al*., 1999). The classical view of Notch signalling is that a cell fated to differentiate into a neuron signals to a neighbouring cell, supressing cell fate and thus maintaining the proliferative cell pool. This mechanism, termed 'lateral inhibition' was discovered initially in *Drosophila* neuroblasts (Campos-Ortega, 1993) and has subsequently also become the universally accepted model for Notch signalling in the vertebrate CNS (Pierfelice *et al*., 2011). As a result, the role of *Notch* signalling during embryonic neurogenesis has been extensively researched in multiple animal models such as mammalian cell lines, Xenopus and chick embryos, as well as mouse embryos. Notable research included gain-of-function studies that observed that the activation of *Notch* signalling inhibits neuronal differentiation and promotes the maintenance of progenitor cells (Gaiano *et al*., 2000; Hitoshi *et al*., 2002; Yoon *et al*., 2005), and over-expression studies in Xenopus that revealed increased expression of the *Notch* ligand Delta inhibits neurogenesis and increases preservation of the progenitor cell pool (Chitnis *et al*., 1995). These studies determined that activation of *Notch* signalling influenced cell fate during neurogenesis, similar to the original *Notch* research conducted using *Drosophila* (Chitnis *et al*., 1995; Coffman *et al*., 1993; Henrique *et al*, 1995, 1997; Kopan *et al*., 1994; Nye *et al*., 1994; Pierfelice *et al*., 2011; Wettstein *et al*., 1997).

While *Notch* signalling is of key importance during embryonic neurogenesis, it is also crucial during development of the cerebral cortex specifically (corticogenesis), with the pathway playing a vital role in the regulation of cell proliferation and differentiation that allow the neuronal layers that make up the cortex to form correctly (Egger *et al*., 2012). In mammals, a simplified overview of the *Notch* signalling pathway is as follows: Proneural genes (e.g. *Mash1* and *Ngn2*) induce the expression of *Notch* ligand genes, the *Delta-like* (*Dll*) and *Jagged* (*Jag*) families. *Notch* ligands move to the surface of a neighbouring progenitor cell, binding to one of the four *Notch* receptors (*N1-N4*). This results in the intramembranous cleavage of *Notch* receptors by the γ-secretase complex, which in effect releases the active form of *Notch*, referred to as the *Notch* intracellular domain (NICD). The NICD

translocates to the nucleus of the cell, where it forms a complex with the DNA binding protein (RBPj). The newly formed NICD/RBPj complex acts to induce the expression of target proneural inhibitor genes, such as the basic helix-loop-helix *Hes* and *Hey* families, which act to supress neurogenesis by antagonizing the function of the aforementioned proneural genes initially responsible for activating the *Notch* signalling cascade (Figure 1.6). Failure to fully activate *Notch* signalling results in all neural progenitor cells differentiating into early-born neurons and an extreme reduction in the progenitor cell pool (Pierfelice *et al*., 2011; Imayoshi *et al*., 2013). This would result in the proliferative zone of the cortex failing to produce the necessary spectrum or number of cells, resulting in the failure of the cerebral cortex to form correctly (Oshtsuka *et al*., 1999; Gaiano *et al*., 2000; Yoon and Gaiano 2005; Louvi *et al*., 2006; Basak and Taylor 2007; Kageyama *et al*., 2008a; Corbin *et* al., 2009; Pierfelice *et al* 2011).

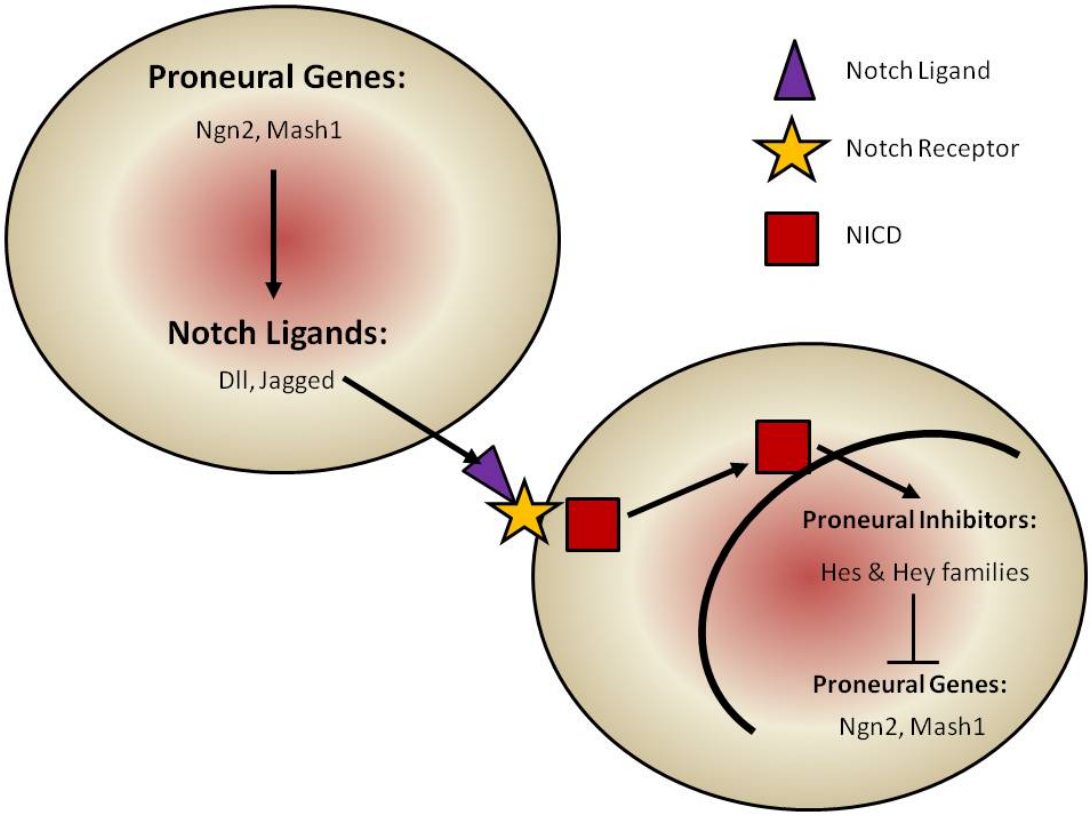

Figure 1.6 A simplified overview of *Notch* signalling

A cell fated to differentiate into a neuronal cell expresses proneural genes (*Ngn2*, *Mash1*), which activate *Notch* ligands (*Dll* and *Jag*). *Notch* ligands then activate the *Notch* receptors on the surface of a neighbouring cell, cleaving the active form of *Notch* (NICD). The NICD translocates to the cell nucleus and activates the proneural inhibitor genes (*Hes* and *Hey* families), which in turn inhibit proneural gene expression, consequently supressing neural differentiation.

1.9 Mechanisms of *Notch* signalling

In terms of mammalian cortical development, the aforementioned lateral inhibition hypothesis suggests that intracellular regulation between a neuronal fated cell and its neighbouring cell inhibits the latter from differentiating into a neuron also (Pierfelice *et al*., 2011). Lateral inhibition accounts for the maintenance of the neural progenitor

pool during the process of neurogenesis in order to give rise to the required number and full spectrum of cells necessary for the formation of complex brain structures during embryonic development (Kageyama *et al*., 2008b). In situ hybridisation analysis has shown that proneural genes and *Notch* ligand genes involved in the signalling pathway are expressed at varying levels in the proliferative zone, forming distinctive 'salt and pepper' expression patterns. The classic view of *Notch* signalling suggests that lateral inhibition is responsible for the formation of these salt and pepper patterns of gene expression and is based on neurogenesis studies in *Drosophila melanogaster* and *Caenorhabditis elegans* vulva development studies (Artavanis-Tsakonas *et al*., 1999). It is suggested that initially all neural progenitor cells express proneural genes and *notch* ligands at similar levels, but as neurogenesis continues during development some cells express higher levels of these genes due to stochastic variations and consequently possess the ability to activate *Notch* signalling in adjacent cells far more efficiently. This results in the latter cells expressing high levels of proneural inhibitor genes (such as *Hes1*), therefore inhibiting the expression of proneural genes and consequently, *Notch* ligand genes. As a consequence, the former cells are affected less by *Notch* signalling and subsequently up-regulate proneural and *Notch* ligand genes to a higher degree. Therefore, the classic view of *Notch* signalling suggests that lateral inhibition works to amplify stochastic variations between neighbouring cells, consequently resulting in the aforementioned characteristic salt and pepper expression patterns of proneural genes and *Notch* ligands (Kageyama *et al*., 2008b). This suggests that cells expressing proneural and *Notch* ligand genes are fated to differentiate into postmitotic neurons. However, it has been argued that the salt and pepper expression patterns of some *Notch* signalling genes are merely a snapshot of gene expression and therefore do not account for subsequent gene expression levels or the fate of the progenitor cells in question (Kageyama *et al*., 2008b).

While this was the universally accepted view of *Notch* signalling for a lengthy period of time, more recent research has challenged the current view of lateral inhibition, showing that the expression of some *Notch* genes changes dynamically within single neural progenitor cells during embryogenesis (Shimojo *et al*., 2008; Kageyama *et al*.,

2009). Real-time imaging carried out in the 2008 study by Shimojo *et al*., (2008) demonstrated that that the bHLH proneural inhibitor gene *Hes1* oscillates in a cyclical fashion within neural progenitor cells in a period of 2-3 hours. Additionally, live imaging further showed that the proneural gene *Ngn2* and the *Notch* ligand *Dll1* are also expressed in an oscillatory manner but with an inverse correlation to *Hes1* (Figure 1.7 B). In other words, when *Hes1* expression is high, *Ngn2* and *Dll1* expression is low, and vice versa, during oscillations (Shimojo *et al*., 2008). As a result of these observations coupled with the knowledge that *Hes1* inhibits proneural gene expression, it has been suggested that *Hes1* regulates the observed *Ngn2* oscillations and that *Dll1* oscillations are regulated in turn by *Ngn2* (Kageyama *et al*., 2008b). As a result, it is likely that these oscillations are essential for the maintenance of the neural progenitor pool during embryonic development by keeping progenitor cells in a proliferative, undifferentiated state due to their mutual activation of *Notch* signalling. However, the exact mechanism that initiates and controls these oscillations of *Notch* genes remains unknown.

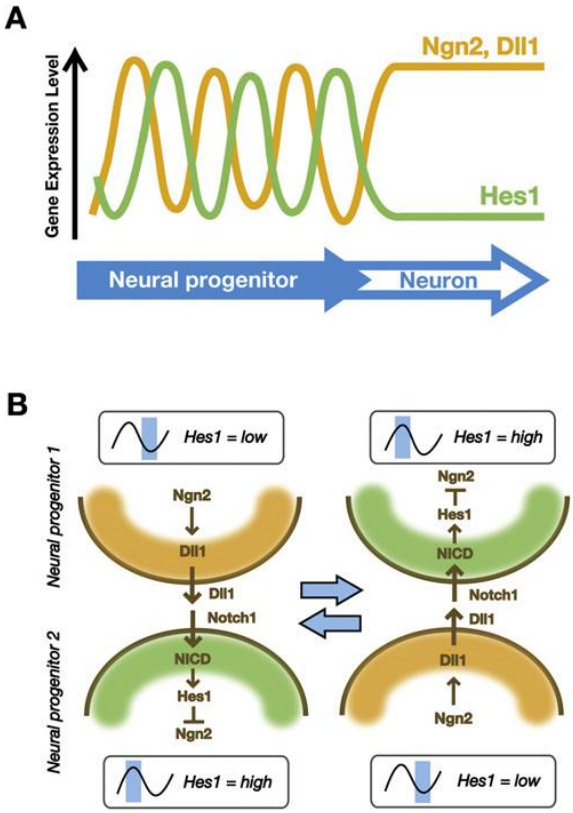

Figure 1.7 An overview of *Notch* oscillations during lateral inhibition

Taken from Shimojo *et al*., 2008b. (A) Levels of *Hes1* and *Ngn2*/*Dll1* expression oscillate in proliferating neural progenitor cells with opposing levels of expression from one another. When *Hes1* expression is high, *Ngn2*/*Dll1* expression is low and vice versa. When a cell commits to differentiating, *Hes1* expression remains low and *Ngn2*/*Dll1* remains high. (B) The revised view of lateral inhibition suggests that when *Hes1* expression is low in a cell, the neighbouring cell it signals to displays high *Hes1* expression and vice versa.

It was originally believed that only postmitotic neurons express *Notch* ligand genes such as *Dll1* and that in turn only they could activate *Notch* signalling in neural progenitors to keep them in their undifferentiated state. However, it was later determined that *Notch* ligands are also expressed by neural progenitor cells early on in development (prior to embryonic stage E11.5) before they have started to give rise

to neurons (Guillemot and Joyner, 1993; Bettenhausen *et al*., 1995; Lindsell *et al*., 1996; Sommer and Anderson, 1996; Nieto *et al*., 2001; Hatakeyama *et al*., 2004; Hatakeyama and Kageyama, 2006; Hämmerle and Tejedor, 2007; Nelson and Reh, 2008). However, *Hes1* is not expressed by postmitotic neurons and consequently, their oscillatory control of *Notch* signalling cannot apply to the maintenance of all neural progenitors. It has therefore been suggested that the cyclic expression of *Ngn2* and *Dll1* is a mechanism required to initiate neuronal differentiation and following that, acts as a secondary source by which *Notch* signalling is activated in neural progenitor cells (Shimojo *et* al., 2009; Kageyama *et al*., 2008b). Consequently, a revised version of the classic model of lateral inhibition (Figure 1.6 B) has been suggested in order to account for the oscillatory expression of *Notch* genes in neural progenitor cells (Kageyama *et al*., 2008b).

The revised lateral inhibition hypothesis accounts for the salt and pepper expression patterns of the *Ngn2* and *Dll1* by suggesting that their dynamic expression varies from cell to cell, resulting in the oscillations of cells occurring out of sync with one another. Consequently, the unsynchronised oscillations occurring in neural progenitor cells would cause differing gene expression levels from cell to cell, resulting in the distinct salt and pepper expression patterns for the above-mentioned *Notch* genes (Kageyama *et al*., 2008b; Imayoshi *et al.,* 2013; Imayoshi *et al*., 2014; Shimojo *et al.,* 2016; Shimojo and Kageyama, 2016). Numerous *Notch* genes have been observed to oscillate in neural progenitor cells during embryonic development, including the proneural genes *Ngn2* and *Mash1*, the *Notch* ligand *Dll1*, and the proneural inhibitor genes *Hes1, Hes5 and Hes7* (Kageyama *et al*., 2008b; Shimojo *et al.,* 2008; Imayoshi *et al.,* 2013; Imayoshi *et al*., 2014; Shimojo *et al.,* 2016; Shimojo and Kageyama, 2016). Evidence that components of the Notch signalling pathway oscillate in neural progenitor cells during forebrain development was initially discovered by Shimojo *et al*., (2009), who observed dynamic oscillations of *Hes1*, *Ngn2* and *Dll1* by live image analysis of their expression in single cells. In order to achieve this, ubiquitinated firefly luciferase reporters under the control of the *Hes1*, *Ngn2* or *Dll1* promoter were used and biolumiensance levels were monitored in both dissociated and slice cultures taken from the telencephalon of embryos that had been

electroporated with the luciferase construct of choice (Shimojo *et al*., 2009). *Hes1* levels were found to be high when *Ngn2/Dll1* levels were low and vice versa, while the sustained up-regulation of *Ngn2/Dll1* in a cell resulted in the sustained down-regulation of Hes1 and the expression of the neuronal marker Tuj1. This suggests that components of the *Notch* signalling pathway oscillate dynamically in order to keep neuronal progenitors in an undifferentiated state until they are selected by a yet to be identified mechanism that causes them to differentiate into a neuron (Shimojo *et al*., 2009). Further work by Imayoshi *et al.,* (2013; 2014) identified that Hes1 is not only responsible for periodically repressing the proneural gene Ngn2, but also Mash1. Furthermore, it was observed that oscillatory expression of Mash1 promotes neural progenitor cell proliferation, while its sustained expression induces neuronal differentiation, suggesting that Mash1 is capable of promoting opposing functions that are dependant on its expression dynamics (Imayoshi *et al*., 2013; Imayoshi *et al*., 2014; Shimojo and Kageyama, 2016). In light of these findings, it can be assumed that oscillatory vs. sustained expression of proneural factors is crucial in cell proliferation and differentiation during brain development (Shimojo and Kageyama, 2016).

Further investigations of the dynamic expression of Notch pathway components was recently undertaken by Shimojo and colleagues, who found that Dll1 protein expression also oscillates dynamically in neural progenitor cells (Shimojo *et al*., 2016). Quantification of time-lapse imaging found that the average period of Dll1 oscillation was ~2.3 hours, a similar length to that of Hes1 oscillations (Shimojo *et al*., 2008; Shimojo *et al*., 2016). Furthermore, it was found that in a number of dividing neural progenitor cells, Dll1 was distributed between both daughter cells but that Dll1 expression had begun to oscillate in an anti-phase manner between them, suggesting that these cells remained as progenitor cells following cell division (Shimojo *et al*., 2016). In order to further analyse the effects of Dll1 oscillations on cell proliferation and differentiation, two type of transgenic mice were generated: Type1, where introns were removed causing Dll1 expression to be accelerated by ~6 minutes in comparison to WT controls, and Type2, where Dll1 expression was delayed by ~6 minutes compared to the WT control. In both types of *Dll1* mutant,

Dll1 expression patterns appeared similar to that of WT mice, however, Dll1 oscillations were quenched, as were Hes1 oscillations. Furthermore, both *Dll1* mutant types were found to have an increase in the expression of the INP marker Tbr2 and the neuronal marker Tuj1 when compared to WT control embryos, as well as a reduction in the size of the VZ and a reduction in mitotic cells within the VZ, suggesting that a premature cell cycle exit for neural progenitors when Dll1 expression is steady as opposed to dynamic. Additionally, it was found that there was an overall reduction in brain size in *Dll1* Type1 and Type2 mutant embryos, but an increase in thickness of post-mitotic neuronal layers when compared to WT controls, suggesting that the dampening of Dll1 oscillations subsequently disrupts Hes1 oscillatory expression, resulting in accelerated neuronal differentiation at the expense of the progenitor cell population. Overall, this suggests that dynamic expression of Dll1 favours the maintenance of progenitor cells in their proliferative state, while sustained Dll1 expression favours neuronal differentiation during embryogenesis (Shimojo *et al*., 2016). Furthermore, due to the fact that continuous, sustained Dll1 expression results in the quenching of Hes1 and Hes7 oscillations and consequently neural defects, it can be suggested that the correct dynamic expression of Dll1 is of great importance for normal Notch pathway signallingand as a result, correct embryonic brain development (Shimojo *et al*., 2016).

Following the initial study of Notch oscillations in neural stem cells by Shimojo *et* al., (2008), it was suggested that Notch signalling is only required for maintenance of the neural progenitor cell pool and unlikely to be required for neuronal selection. This assumption was based on the fact that dynamic expression of *Ngn2* and *Dll1* was only observed in progenitor cells (Shimojo *et* al., 2008). The classic model of lateral inhibition stated that the expression of *Ngn2* and *Dll1* by a cell meant that it was selected for a neuronal fate, but the oscillatory expression of these genes indicate that their fate remains unrestricted and that the expression of these genes does not automatically determine their fate (Kageyama *et al*., 2008b). As a result, it has been concluded that the salt and pepper patterns of expression that were previously thought to indicate neuronal selection, are in fact merely the evidence of oscillatory expression (Kageyema et al., 2008b). However, while evidence suggests that *Notch*

signalling does not directly control neuronal fate, it cannot be completed excluded as a likely candidate for exerting control upon the process. While it has been suggested that neuronal selection is likely to actually be regulated by Numb, a gene that has been implicated in regulating elements of *Notch* signalling, it is perhaps a rash assumption that the aforementioned *Notch* gene oscillations do not have an effect on neuronal selection. It has been suggested that cyclic expression can lead to the gradual accumulation of downstream factors that induce neuronal differentiation, such as the cell cycle exit gene *BM88* that is known to induce neuronal differentiation (Politis *et al*., 2007). If this was to be the case, the number of oscillatory cycles of *Notch* genes could potentially be acting as a molecular clock, therefore determining when postmitotic neurons are generated (Kageyama *et al*., 2008b).

Recent analysis of Notch oscillations have identified that the Notch ligand *Dll1* of the effects of Dll1 oscillatory expression vs sustained expression suggested that the precise timing of Dll1 expression is of the utmost importance to correct neural development. The fact that the acceleration of delay of Dll1 expression by just ~6 minutes results in severe dampening of the oscillatory expression of Dll1 and proneural inhibitors Hes1 and Hes7 and a subsequent decrease in embryonic brain size attests to this, along with the fact that the quenching of Hes1 by Dll1 was highly unexpected due to the fact that Hes1 oscillates autonomously in the presence of steady NICD levels in neural progenitor cells (Shimojo and Kageyama, 2016). Furthermore, while oscillations in neural progenitor cells have been found to be out-of-phase between neighbouring cells, Notch oscillations in the PSM have been found to occur in-phase of one another. This negates the original hypothesis that the salt and pepper expression pattern of *Dll1* is characteristic of oscillatory expression, but rather a trademark of out-of-phase oscillations that occur specifically in neural progenitor cells. It has been suggested that the out-of-phase oscillations of Dll1 observed in neural progenitor cells may be of importance to producing a diverse range of neural cell types and that it would be of interest to observe what happens to neural development if out-of-phase oscillations were switched to in-phase

oscillations and in order to better understand the significance of phase control of oscillations (Shimojo *et al.,* 2016; Shimojo and Kageyama, 2016).

While the traditional view of *Notch* signalling has been adapted to account for the oscillatory expression of *Notch* genes in neural progenitor cells, how these oscillations are controlled and induced is unknown. It is possible that that a further cellular mechanism of *Notch* signalling could initiate these oscillations. During the process of *Notch* signalling, *Notch* ligands act upon *Notch* receptors in two distinctly different ways. While the generalised view of *Notch* signalling sates that *Notch* ligands bind to the *Notch* receptors of neighbouring cells, *Notch* ligands are capable of binding to the receptors on the surface of the cell that secreted them (del Álamo *et al*., 2011). This phenomenon is referred to as 'Cis-inhibition', while the more traditional act of *Notch* ligands binding to *Notch* receptors on the surface of neighbouring cells is termed 'Trans-activation'. While trans-activation results in the activation of proneural repressor genes, cis-inhibition blocks the cleavage of the NICD, in turn preventing the expression of proneural inhibitor genes and resulting in the up-regulation of proneural genes and *Notch* ligand genes (del Álamo *et al*., 2011). Cis-inhibition was first discovered in *Drosophila melanogaster* where evidence of the repression of *Notch* by its ligands in a cell-autonomous manner was revealed by overexpression studies (Couso *et al.,* 1995; Doherty *et* al., 1996; Klein *et* al., 1996; de Celis *et al*., 1997; Glittenberg *et al*., 2006). Evidence of cis-inhibition has also been shown in vertebrates with overexpression studies conducted in chick, *Xenopus laevis* and mouse (Franklin *et* al., 1999; Sakamoto *et* al., 2002; Itoh *et al*., 2003), suggesting that cis-inhibition is a conserved mechanism of *Notch* signalling. It has been proposed that *Notch* signalling utilises both cis-inhibition and trans-activation in order to promote both cell maintenance and differentiation (Lowell *et al*., 2000; Estrach *et al*., 2008). However, exact mechanisms underlying cis-inhibition and the consequences of cis-interactions still remain poorly understood (del Álamo *et al*., 2011).

It is plausible that cis-inhibition and trans-activation could be involved in controlling *Notch* oscillations that have been observed in neural progenitor cells. This would

account for the cyclical expression of *Ngn2* and *Dll1*, as there are multiple *Notch* receptors on the surface of a cell. This would suggest that an onslaught of cis-inhibition and trans-activation could occur upon a progenitor cell, potentially activating and repressing the expression of downstream genes involved in neuronal differentiation until their levels peak to the point that they win out the majority and a cell differentiates, as suggested by Kageyama *et al*., (2008b). However, while this hypothesis may provide an explanation for why oscillations of *Notch* genes occur, it does not fully account for what actually drives *Notch* expression and controls its regulation of the progenitor pool. What drives *Notch* signalling and its oscillations remains elusive. It could be postulated that *Notch* could be driven by Numb (Kageyama *et al*., 2008b), a collection of factors working together, or by an as yet unidentified master regulator.

1.10 *Pax6* and cortical development

The paired-box transcription factor *Pax6* is expressed from E8.5 during murine embryogenesis in an abundance of developing structures, including the forebrain (Walther and Gruss, 1991; Stoykova and Gruss 1994; Geotgala et al., 2011). *Pax6* belongs to the class IV Pax transcription factors, which characteristically have two DNA binding domains, a paired domain (PD) and a paired-type homeodomain (HD), as well as a C-terminal transactivation domain (Mansouri *et al*., 1996; Chi and Epstein, 2002). The PD and HD recognise different *Pax6* consensus binding sites and it is likely that they regulate distinct developmental processes during embryogenesis by regulating specific gene targets both cooperatively and independently of one another (Jun and Desplan, 1996; Singh *et al*., 2000; Mikkola *et al*., 2001; Chi and Epstein, 2002; Xie and Cvekl, 2011). *Pax6* expression is important for successful development of multiple regions of the mammalian CNS, acting at a molecular level upon its formation. *Pax6* expression is vital for cell proliferation and differentiation during embryonic neurogenesis in the mammalian telencephalon, including the developing cerebral cortex (Sansom *et al.,* 2009). In the developing cerebral cortex of WT embryos, *Pax6* displays a very distinct high rostrolateral to low caudomedial

gradient expression pattern (Figure 1.8 B-D) (Manuel *et al*., 2014). *Pax6* expression is mainly restricted to the mitotically active VZ of the pallium and in a small region of the ventral pallium at the level of the pallial-subpallial boundary (PSPB) (Walther and Gruss, 1991; Stoykova *et al*., 2000).

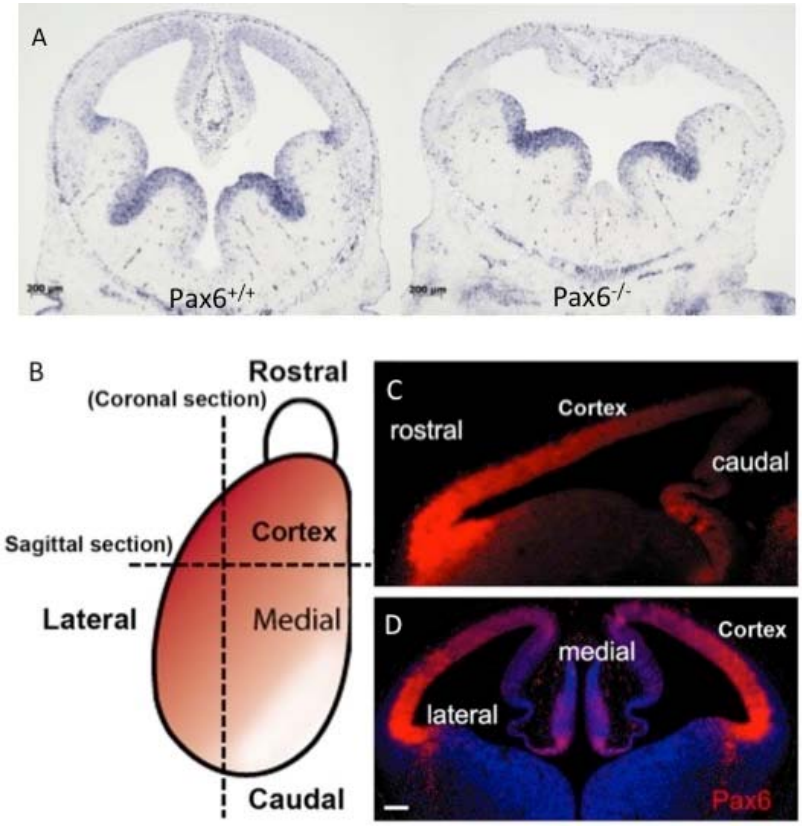

Figure 1.8 The effects of loss of *Pax6* expression during development and *Pax6* expression in the developing cerebral cortex

Taken from Manuel *et al*., 2015 (B-D). (A) A coronal section of the brain of a $Pax6^{+/+}$ and a $Pax6^{-/-}$ embryo stained for *Jag1*. The structures of the forebrain appear malformed in the $Pax6^{-/-}$ embryo. (B) A diagram of *Pax6* expression illustrating that *Pax6* is normally in a high rostrolateral to low caudomedial gradient in the developing cortex of WT embryos. (C) *Pax6* expression in a sagittal section (D) *Pax6* expression in a coronal section.

The importance of *Pax6* for development of the CNS is demonstrated by the multiplicity of CNS defects observed in *Pax6* mutants. A spontaneous mutation in

Pax6 known as the small eye (Sey) mutation is caused by a point mutation in the *Pax6* gene, resulting in the production of a non-functional form of the protein. Sey is predominantly characterised by a radical reduction in eye size and can affect either one copy (heterozygous) or both copies (homozygous) of the *Pax6* gene (Hill *et al*., 1991). Heterozygous mutations in human *PAX6* result in the congenital eye malformation termed aniridia (Hanson *et al*., 1993), while homozygous *PAX6* mutations result in multiple CNS defects, specifically in the eye, forebrain, cerebellum and spinal cord; as well as individuals who are homozygous for *PAX6* characteristically dying at birth. Furthermore, heterozygous ($Pax6^{+/-}$) mutant mouse embryos are phenotypically characterised as having a reduced eye size in comparison to their wild type (WT) counterparts while the eyes in homozygous ($Pax6^{-/-}$) mutant embryos fail to form at all (Hill *et* al., 1991; Stoykova *et al*., 2000). Previously mentioned forebrain defects in $Pax6^{-/-}$ mutants include an abnormally thin CP and an enlarged proliferative zone in the developing cerebral cortex (Schmahl *et al*., 1993; Caric *et al.,* 1997).

As *Pax6* is expressed in RGCs located in the VZ of the cortex, it is generally accepted that *Pax6* is of key importance during cortical development and that *Pax6* is a key regulator of cell proliferation and differentiation during corticogenesis (Stoykova *et* al., 2000; Englund *et al*., 2005; Georgala *et al*, 2011a; 2011b); Mi *et al*., 2013a; 2013b). Previous research focused on the role of *Pax6* during cortical development has indicated that specific levels of *Pax6* are required for normal development to occur during embryogenesis. The 2007 study by Quinn *et al.,* utilising $Pax6^{-/-} \leftrightarrow Pax6^{+/+}$ chimeras, detected an under-representation of $Pax6^{-/-}$ progenitor cells in the developing cerebral cortex and that loss of Pax6 increases neural differentiation suggesting that Pax6 helps to maintain the progenitor cell pool during corticogenesis (Quinn *et al*., 2007). Furthermore, research into the effects of overexpression of *Pax6* undertaken using Pax6 overexpressing (*PAX77*) transgenic mice, utilised BrdU labelling to show a reduction in the number of proliferating progenitors in the rostral and medial regions of the cortex, where Pax6 levels are highest (Manuel et al., 2007).

Furthermore, studies involving *Pax6*$^{-/-}$ mutants detected severe developmental brain defects, including an inability to form proper thalamocortical connections (Pratt *et al*., 2000; Pratt *et al*., 2002; Piñon *et al*., 2008; Simpson *et al*., 2009).

1.11 *Pax6* as a master regulator of corticogenesis

As previously described, during formation of the mammalian brain, it is crucial that cell proliferation and differentiation are tightly controlled and coordinated as regulation of the number of generated neurons and progenitor cell subtypes has a profound influence upon the functional properties of the CNS (Walcher *et al*., 2013). The molecular mechanisms governing embryonic neurogenesis are relatively unknown. However, it is widely accepted that early patterning of the brain and progenitor cell fate are greatly influenced by transcriptional regulators (Zaret and Carrol, 2011). It has been suggested that certain transcription factors act as master regulators to coordinate developmental processes, such as neurogenesis, at a molecular level, by exerting their regulatory effects upon complex downstream gene networks (Davidson, 2010; Peter and Davidson, 2011; Xie *et* al., 2013; Sun *et al*., 2015). However, the molecular mechanisms by which these regulatory proteins exert their effects remain poorly understood (Walcher *et al*., 2013).

Pax6 acts as one of the aforementioned master regulators in various structures comprising the CNS (Hanson and Van Heyingen, 1995; Dohrmann *et al.*, 2000; Kozmik *et al*., 2008; Osumi *et al*., 2008) and, as previously discussed, has been identified as having a crucial role in correct CNS development due to its key regulatory role over patterning, cell fate and proliferation (Hanson and Van Heyningen, 1995; Stoykova *et al*., 1996; Stoykova *et al*., 1997; Götz *et al*., 1998; Chapouton *et al*., 1999; Stoykova *et al*., 2000; Toresson *et al*., 2000; Yun *et al*., 2001; Estivill-Torrus *et al*., 2002; Heins *et al*., 2002; Haubst *et al*., 2004; Quinn *et al*., 2007; Sansom *et al*., 2009; Tuoc *et al*., 2009).

At the onset of neurogenesis, Pax6 is expressed predominantly to influence arealisation of the cortex and regulation of neural progenitor cell proliferation

(Bishop *et al*., 2000, 2002; Muzio *et al*., 2003; Muzio and Mallamac, 2003; Hevner *et al*., 2006; Manuel *et al*., 2015). Previous research into the role of Pax6 during embryonic development of the forebrain has highlighted the regulatory role of the transcription factor in both temporal and spatial control of cell cycle duration cell cycle exit, cell cycle length and proliferation; as well as its implication in the temporal and spatial control of cell cycle duration in cortical progenitor cells (Manuel *et al*., 2015). For example, it has been documented that a loss of Pax6 leads to a reduction in the cell cycle duration of cortical progenitor cells and an increase in the proportion of asymmetrical cell divisions, resulting in a surge in the production of post-mitotic neurons and as a result, a reduction of progenitor cells within the proliferative zone of the cortex (Warren *et al*., 1999; Estivill-Torrus *et al*., 2002; Walcher *et al*., 2013). Additionally, cultured *Pax6-/-* cortical cells displayed inhibited progenitor cell proliferation (Estivill-Torrus *et al*., 2002).

For example, gain-of-function studies have demonstrated that forced expression of Pax6 diminishes progenitor cell proliferation *in vitro* (Heins *et al*., 2002; Hack *et al*., 2004; Cartier *et al*., 2006); while the 2007 study by Manuel *et al*., (2007) that utilised *PAX77* (Pax6 overexpressing) embryos, found a reduction in proliferating neural progenitor cells in the areas of the developing cortex where Pax6 expression levels are highest (Manuel *et al*., 2007). Furthermore, INPs located the rostral and caudal areas of the developing cortex in *PAX77* mice proliferate at a much slower rate in comparison to WTs.

As previously mentioned, it has been determined that Pax6 regulates both cell cycle length and cell cycle exit, with past studies indicating that Pax6 primarily exerts a repressive effect upon cell cycle progression of progenitor cells within the cerebral cortex; and Pax6 expression levels confirming its region and age specific role in the regulation of neural progenitor proliferation (Manuel *et al*., 2015). Early on during the process of corticogenesis, expression levels of Pax6 vary between different cortical regions but its expression levels become increasingly uniform as the embryo develops (Mansouri *et al*., 1994; Stoykova and Gruss, 1994; Manuel *et al*., 2007). When the Pax6 expression gradient is at its steepest during early cortical

development (E12.5), areas found to have the highest levels of Pax6 expression correlate with regions where cell cycle duration is longest (Manuel *et al*., 2015). Furthermore, a loss of Pax6 results exclusively in a shortening of the cell cycle in areas where there would have been high Pax6 expression normally (Manuel *et al*., 2015). These findings indicate that the effects that Pax6 exerts upon the cell cycle of cortical progenitor cells are associated with its expression levels. This was further supported by the 2013 study by Mi *et al*., where cell cycle parameters were examined in different cortical regions during different stages of embryonic development using mouse models with a conditional inactivation of Pax6 or a constitutive inactivation of Pax6 (Mi *et al*., 2013a); Manuel *et al*., 2015). Consequently, the fact that Pax6 is expressed in a gradient during early cortical development, the dosage-dependent effects of Pax6 on cell proliferation are of great importance in terms of understanding how the cerebral cortex is organized into regions of specific cryoarchitectures and functions (Manuel *et al*., 2015).

While it is widely accepted that *Pax6* regulates developmental processes, such as corticogenesis, and advances have been made in identifying *Pax6*-regulated genes implicated in the process of neurogenesis (Xie and Cvekl, 2007; Wolf *et al.,* 2009; Sansom *et al*., 2009; Carr, 2009; Xie *et* al., 2013; Sun *et* al., 2015), many of the gene networks regulated by *Pax6* and how *Pax6* is specifically exerting its regulatory effects upon these genes remain unidentified and unexplained. Some advances into understanding how Pax6 regulates progenitor cell proliferation during corticogenesis have been made by identifying targets of Pax6. These include the cyclin-dependent kinases and their activating cyclins (Cdk4, Cdk6, Cdca2, Cdca7) which are responsible for cell cycle progression (Sansom *et al*., 2009; mi *et al.,* 2013 a, b).

As previously stated, *Pax6* possesses two DNA binding domains, the PD and the HD, with both recognizing different *Pax6* consensus binding sites. This suggests that the PD and HD are likely to regulate distinct functions by controlling specific gene targets (Chi and Epstein, 2002), both separately or cooperatively of one another (Jun and Desplan, 1996; Singh *et al*., 2000; Mikkola *et al*., 2001; Mishra *et al*., 2002; Xie and Cvekl, 2001). Previous studies have identified that the HD is involved in lens

formation during embryogenesis and has little involvement in development of the forebrain (Haubst *et al.,* 2004; Ninkovic *et al*., 2010). This suggests that the PD facilitates the effects *Pax6* exerts upon development of the mammalian forebrain (Walcher *et al*., 2013). The *Pax6* PD possesses two subdomains, an N-terminal PAI subdomain and a C-terminal RED subdomain, which can bind cooperatively or independently of one another to their cognate sites (Epstein *et al*., 1994a; Yamaguchi *et al*., 1997). Moreover, recent investigations into how *Pax6* utilizes particular subdomains of the PD, to coordinate patterning and neurogenesis in the developing forebrain, using mutations of the RED and PAI subdomains, showed that only the PAI subdomain affects neurogenesis as embryos with PAI mutations had similar neurogenic defects to $Pax6^{-/-}$ mutants (Walcher *et al*., 2013). In short, Pax6 exerts its regulatory effects upon its target genes by binding to target DNA sequences through one or both of the aforementioned DNA-binding domains (Bertuccioli *et al*., 1996; Jun and Desplan, 1996; Sheng *et al*., 1997; Singh *et al*., 2000; Walcher *et al*., 2013), and transcriptional regulation of Pax6 target genes is mediated by a carboxy terminal proline/serine/threonine (PST) rich transactivation domain (Singh *et al*., 1998, 2001; Tang *et al*., 1998; Manuel *et al*., 2015).

1.12 *Pax6* controls progenitor cell proliferation via regulation of *Notch* signalling

Amongst the numerous gene candidates for regulation by *Pax6* during cortical development, members of the *Notch* signalling pathway are consistent and of particular interest due to their role during the process of embryonic neurogenesis. Research centred around identifying transcriptional targets has predominately utilised sequencing strategies such as DNA microarray analysis, chromatin immunoprecipitation (ChIP) and the newer approach of ChIP-sequencing (ChIP-seq), allowing the study of protein-DNA interactions and gene expression levels. Furthermore, research following on from sequencing analysis has yielded evidence of direct binding between Pax6 and its target genes (Scardigli *et al*., 2001; 2003; Carr *et al*., 2009 Sansom *et al*., 2009; Mi *et al*., 2013a; Xie *et al*., 2013; Sun *et al*., 2015)

(Table 1.1). Although steps are being taken to determine which genes *Pax6* regulates and how its regulatory control over complex gene networks controls forebrain development, relatively little is currently known about the scope of *Pax6*'s regulatory effects and, as a result, it is an area of embryonic development which continues to be of importance to investigate.

Table 1.1 Examples of identified Pax6 targets

Paper	Key Identified Targets	Method Used
Scardigli *et al.,* 2002; 2003	Ngn2	EMSA, Transgenic Mice
Carr, 2009	Ngn2, Mash1, Jag1, N1	Microarray
Sansom *et al*., 2009	Cdk4, Mcm3, Cdca2, Cdca7	ChIP-chip, Microarray
Mi *et al*., 2009	Cdk6	ChiP, EMSA, Luciferase Assay
Xie *et al*., 2013	Isl1	ChIP-chip, Microarray
Sun *et al*., 2015		

Previous work in our lab has also concentrated on identifying targets of *Pax6* and undertaking the challenge of identifying which genes are directly regulated by the transcription factor, as well as highlighting how these regulatory relationships allow *Pax6* to orchestrate its considerable control over forebrain development (Carr 2009; Mi *et al*., 2013a). Previous microarray analysis carried out on the PSPB of *Pax6*$^{-/-}$ mice identified a list of candidate genes that were likely to be regulated by *Pax6*. The list included a number of genes implicated in the *Notch* signalling pathway such as the proneural genes *Ngn2* and *Mash1*, the *Notch* ligand *Jag1*, and the *Notch* receptor N1. Research into previously published literature identified the *Notch* ligand *Dll1* and the bHLH proneural inhibitor Hes5 as targets of *Pax6* (Sansom *et al*., 2009). As previously discussed, the *Notch* signalling pathway is crucial during the process of corticogenesis due to its role in maintaining the pool of proliferative cells required to

ensure that the cortex develops correctly. Additionally, *Pax6* is involved in the process of cell proliferation during cortical development (Stoykova *et* al., 2000; Estivill-Torrus et al., 2002; Englund *et al*., 2005; Manuel et al., 2007; Quinn et al., 2007; Georgala et al., 2011b; Mi et al., 2013a; 2013b). One of the interests of our lab has been to explore the role of *Pax6* during cortical development and, consequently, investigating the relationship between *Pax6* and the *Notch* signalling pathway was of particular interest. Initial investigations determined that a number of *Notch* pathway genes were down-regulated in the cortex of *Pax6*$^{-/-}$ mutant embryos (Carr, 2009), although not all of the *Notch* genes displayed altered expression when tested by in situ hybridisation analysis previously carried out during an Msc project (Dorà, 2011). Out of the *Notch* pathway genes initially investigated by in situ hybridisation, the *Notch* ligands *Dll1* and *Jag1* were determined to be the targets of *Pax6* that were of greatest interest to pursue further. Microarray analysis provided *Jag1* as a likely target of Pax6 (Carr, 2009). *Dll1* on the other hand, appears more likely to be indirectly regulated by *Pax6* rather than directly regulated, as ChiP-Seq analysis carried out by Sansom *et al.* (2009) did not identify *Dll1* as a *Pax6* target but hypothesised that *Dll1* was a likely indirect target of *Pax6* (Sansom *et al*., 2009). However, past determining direct or indirect regulation of target genes by master regulators, an important relationship between *Pax6* and *Notch* could exist in terms of the process of neurogenesis. Due to the role of *Notch* ligand genes and the known functions of *Pax6*, a potential relationship between the two on a cellular level would be particularly interesting and could provide insight into mechanisms involved in the regulation of cell proliferation, such as how Pax6 exerts its regulatory effects upon proliferation via its interactions with key genes implicated in Notch signalling.

In order to explain how the *Notch* ligands and *Pax6* could be interacting with one another, a model was designed by interpreting findings documented in the literature (Figure 1.9). The model suggests that *Pax6* drives the proliferation of progenitor cells by regulating the *Notch* ligands *Jag1* and *Dll1*. However, the relationship between *Pax6* and these two ligands is likely to differ. In the model depicted in Figure 1.8, *Jag1* is expressed in RGCs within the VZ of the developing cortex (Nelson *et al*., 2013; Chapter 4). It has been shown that *Pax6* is expressed within

RGCs also (Götz *et al*., 1998). As a result, we have predicted that the suggested direct regulatory relationship between *Pax6* and *Jag1* occurs exclusively within RGCs residing in the VZ (Figure 1.8 depicted by a solid green arrow). As for *Dll1*, our hypothesis suggests that the regulatory relationship between *Pax6* and the ligand is likely to be indirect and far more complex. Study of previously published literature on *Dll1* expression in the developing cerebral cortex revealed startling contradictions over which progenitor cell population *Dll1* is expressed in, with studies stating that the gene is expressed in the VZ (Campos *et al*., 2001), in INPs in the SVZ (Mizutani *et al*., 2007; Kawaguchi *et al*., 2008; Yoon *et al*., 2008) and within both ventricular and subventricular zones (Nelson *et al*., 2013). The latter study, which concentrated on the expression of *Dll1* protein in the developing telencephalon, showed that *Dll1* was expressed in INP cells within the SVZ and also expressed by a subpopulation of INP that reside basally within the VZ (INP^{vz}). As previously discussed, it has been suggested that INP^{VZ}s are the link between RGCs and INPs, in that INP^{VZ}s are actually INPs newly generated from RGCs in the VZ and are simply migrating to their correct position in the SVZ where they will undergo proliferation and/or differentiation (Englund *et* al., 2005; Corbin *et al*., 2009). If this is indeed the case, INP^{VZ} could be considered as a cell type making the transition from a RGC to an INP and could very well express markers for both cell types at varying levels. This would account for *Dll1* expression in the VZ as INP^{VZ}s would start to express INP markers as they migrate to the SVZ. Furthermore, the proneural gene *Ngn2* is expressed in both the VZ and the SVZ. This is likely due to the fact that both RGCs and INPs are capable of making the shift to differentiate into neuronal cells, coupled with what we know about the oscillatory expression of *Ngn2* in proliferating cells. However, due to the cyclical expression of *Ngn2*, it is highly likely that *Ngn2* is also expressed in INP^{VZ}s and could therefore act as the regulatory link between *Pax6* and *Ngn2* if they were both expressed in INP^{VZ}s simultaneously. Therefore, we hypothesise that there is likely to be a stage that transitioning INP^{VZ}s may still express *Pax6* when *Dll1* is expressed.

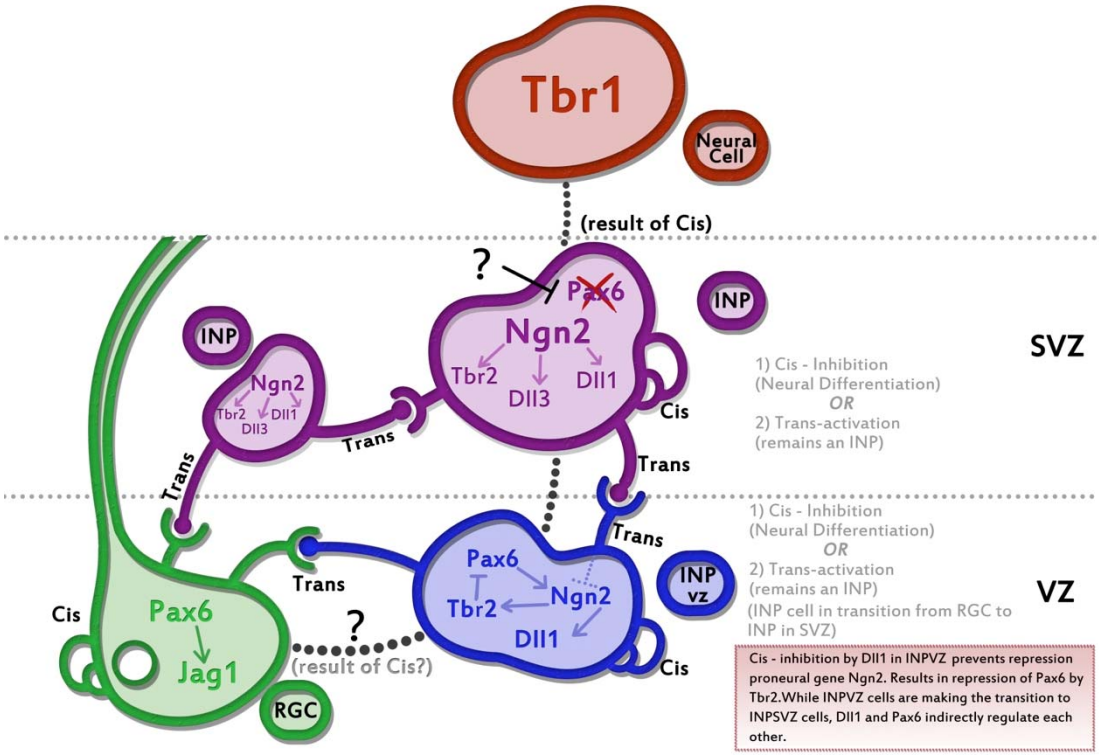

Figure 1.9 Model of project hypothesis

Pax6 directly regulates the expression of *Jag1* in RGCs residing in the VZ (green cell). Newly generated INPs by RGCs (INP^{vz}) migrate from the VZ to the SVZ where they settle as mature INPs. INP^{vz} s (blue cell) begin to express *Ngn2*, *Dll1* and Tbr2 and in turn begin to lose *Pax6* expression. Cis-inhibition by *Dll1* in INP^{VZ}s prevents repression of *Ngn2*, resulting in the repression of *Pax6* by Tbr2. Consequently, *Dll1* and *Pax6* indirectly regulate each other in INP^{VZ} cells. Mature INP cells in the SVZ (purple cell) express *Dll1*, *Ngn2* and Tbr2 but no longer express *Pax6*. Cis-inhibition of a cell promotes neural differentiation, while trans-activation between cells promotes remaining in a proliferative state. Arrows = activation. Repression symbol = repression. Dotted lines depict differentiation and migration of a cell.

Our interpretation of the literature further expanded our model to explore the notion that while INP^{VZ} cells are migrating to the SVZ, where they would become mature INP cells, *Pax6* and *Dll1* could mutually co-regulate one another. It is plausible that transitioning INP^{VZ}s could express RGC markers and INP markers simultaneously at varying levels, providing a tangible link between RGCs and INPs. As a result, we

hypothesise that newly generated INP^{VZ} cells still retain *Pax6* expression, resulting in the activation of both *Ngn2* and *Dll1* expression (Figure 1.9 depicted by solid blue arrows). Activation of *Ngn2* by *Pax6* would also results in the activation of the INP marker Tbr2. Tbr2 has been shown to repress *Pax6* (Englund *et al*., 2005; Sessa *et al*., 2008; Ochai *et al*., 2009; Kovach *et al*., 2012) and thus, as the INP^{VZ} migrates towards the SVZ, Tbr2 levels would increase and consequently diminish Pax6 expression until the transcription factor is no longer expressed. This phenomenon would most likely occur at a reduced rate due to the cyclical expression of *Ngn2* and *Dll1* in proliferative cells, meaning that expression of Tbr2 would slowly increase and *Pax6* expression would gradually decrease. We further hypothesise that the aforementioned *Notch* signalling mechanisms of cis-inhibition and trans-activation would aid this event. As previously discussed, cis-inhibition promotes neural differentiation and trans-activation encourages the cell to remain in a proliferative state (del Álamo *et al*., 2011). However, due to *Notch* oscillations in proliferating cells, a cell targeted by cis-inhibition does not guarantee that the cell will automatically differentiate as the cyclical nature of *Notch* indicates that the effect may be more gradual. Subsequently, we believe that the act of cis-inhibition in INP^{VZ}s prevents the repression of the proneural gene *Ngn2*, resulting in the repression of *Pax6* by Tbr2. If this is the case, while INP^{VZ}s are making the transition to INPs in the SVZ, *Dll1* and *Pax6* mutually regulate one another indirectly.

1.13 Aims

Chapter 3: The aim was to investigate the effects of *Pax6* levels on *Dll1* expression in the cerebral cortex, thereby testing the possibility of regulation of *Dll1* by *Pax6* (Figure 1.9).

Chapter 4: The aim was to investigate the effects of *Pax6* levels on *Jag1* expression in the cerebral cortex, thereby testing the possibility of regulation of *Jag1* by *Pax6* (Figure 1.9).

Chapter 5: The aim was to determine which progenitor cell subpopulation *Dll1* is expressed in in the cerebral cortex and to further characterise how *Pax6* and *Dll1* interact with one another during neurogenesis (Figure 1.9).

Chapter 6: The aim was to determine whether *Jag1* is directly regulated by *Pax6* by identifying potential binding sites for Pax6 surrounding the *Jag1* gene and testing them.

2.0 Methods and materials

2.1 Solutions and suppliers

All chemicals were supplied by Sigma Aldrich or Thermo Fisher Scientific, unless stated otherwise and were of laboratory standard purity.

2.2 Mice

All procedures were performed under licence in accordance with the Animals (Scientific Procedures) Act 1986.

2.2.1 *Pax6*$^{-/-}$ mice

Pax6$^{-/-}$ mouse embryos were derived from Pax6^{SeyEd} heterozygote (Pax6$^{+/-}$) crosses maintained on an inbred Swiss background, and wild-type siblings were used as controls. The Pax6^{SeyEd} allele has a premature stop codon caused by a point mutation. This point mutation prevents the production of functional Pax6 (Hill *et al*., 1991). Pregnant females were sacrificed by anaesthesia followed by cervical dislocation. Embryos were dissected from the uterus at gestational age E11.5, E12.5, E13.5 and E14.5.

2.2.2 *PAX77* transgenics

PAX77 hemizygous mice (Schedl et al., 1996) (*PAX77*) carry 5 to 7 copies of a 420Kb human PAX6 YAC (Y593) with all copies incorporated at the same locus. The integrated copies are referred to as the *PAX77* transgene. The *PAX77* line was maintained on a CD1 background (Manuel *et al*., 2007).

2.2.3 *Emx1CreEr*^{T2}*;Pax6*$^{loxP/loxP}$ transgenics

For conditional inactivation of Pax6 in the developing cortex, a transgenic line carrying $Pax6^{loxp}$ (Simpson *et al*., 2009), *Emx1-CreER*^{T2} (Kessaris *et al*., 2006) ND Rosa26-YFP (Srinivas *et al.,* 2001) alleles were generated. Cre expression was induced with 10mg single dose of tamoxifen by gavage (Sigma UK) at E9.5 (50mg/ml^{-1} in corn oil, Sigma UK). Pregnant females were sacrificed by anaesthesia followed by cervical dislocation. Embryos were dissected from the uterus at gestational age E12.5 and E13.5.

2.2.4 Ngn2-Cre transgenics

Homologous recombination in embryonic stem cells was used to replace the *Ngn2* coding sequence with *Cre* (Danielian *et al*., 1998) using the same strategy that generated *Ngn2* knockouts (Fode *et al*., 1998). *Ngn2-Cre* mice bred onto a C57Bl6/J background were crossed to Rosa26-loxp reporter mice (Soriano, 1999) to generate an Ngn2-Cre mouse line that produces *Ngn2-/-* embryos (Zirlinger et al., 2002).

2.2.5 Tissue collection

Embryos were dissected out in ice-cold RNAse free phosphate buffered saline (PBS) and heads were removed and kept.

2.3 Tissue preparation

2.3.1 Tissue fixation

Following dissection, tissue fixed in 4% PFA/ 1X PBS overnight. Fixed tissue was then washed three times in PBS. Tissue was cryoprotected in 30% sucrose/1X PBS at 4°C overnight or until the tissue sunk. Tissue was then equilibrated in a 50:50 mixture of 30% sucrose:OCT (Thermo Scientific) for one hour on a rocking platform. Tissue was embedded in the same 50:50 30% sucrose:OCT mixture and

frozen on dry ice. Tissue was embedded at an orientation suitable for coronal sectioning. Frozen tissue was stored at -80°C until required.

2.3.2 Cryostat sectioning

Frozen tissue for cryosectioning was transported on ice from -80°C storage freezers to the cryostat. Blocks were allowed to come up to temperature for 30 minutes prior to sectioning. OCT embedding medium was used to attach the tissue to the chuck at -20°C. Cryostat sections were cut at 10µm or 12µm (for fluorescent staining) and mounted on superfrost positively charged slides. Sections were then stored at -20°C until required. All sections cut were coronal and 8 sections were mounted per slide as standard. Slides displaying Rostral, medial and caudal sections (from the front, middle and towards the back of the cortex, respectively) were selected for all expression analysis (Figure 2.1).

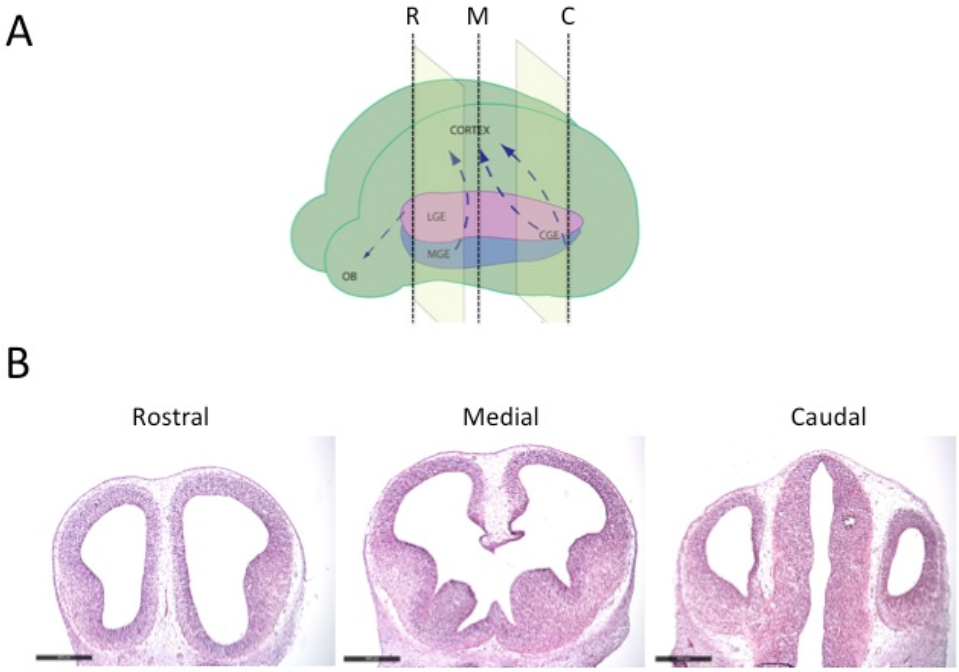

Figure 2.1 Selection of cortical sections for staining

A brief summary of how coronal forebrain sections were selected for expression analysis. (A) A schematic depicting roughly where the rostral, medial and caudal areas of the cortex reside within a mouse embryo head. (B) An example of a rostral, medial and caudal section of the forebrain at E12.5 in a WT embryo. R= Rostral. M = Medial. C= Caudal. Scale bars = 500µl.

2.4 PCR genotyping

2.4.1 Preparation of genomic DNA

Genomic DNA was extracted from embryonic limb tissue. Tissue was lysed in 75µl of hotshot lysis buffer (25mM NaOH; 0.2mM EDTA) at 96°C for 30 minutes and

then cooled to 4°C. 75µl of neutralising buffer (40mM Tris-HCl) was then added to stop the reaction. 1µl of this solution was added to 24µl of PCR reaction mix.

2.4.2 Genotyping of *PAX77* mice and *Emx1CreEr^{T2};Pax6$^{loxP/loxP}$* mice

PCR reaction mix:
2.5mM dNTPs - 2.5µl
TPSX loading dye - 5µl
25µM Fp6 primer mix (F and R primers) – 0.5µl
Taq polymerase – 0.2µl
ddH_2O – 15.8µl

Table 2.1 Primers for genotyping by PCR

Genotype	Primer Sequence
PAX77	Human Pax6 Forward 5'CCGTGTGCCTCAACCGTA Reverse 5'CACGGTTTACTGGGTCTGG Mouse Pax6 Forward 5' GAGGGTTTCCTGGATCTGG Reverse 5' CGCAAATACACCTTTGCTCA
Fp6	Forward 5' AAATGGGGGTGAAGTGTGAG Reverse 5' TGCATGTTGCCTGAAAGAAG
Ngn2	Ngn2 Wt Forward 5'GGACATTCCCGGACACACAC Reverse 5'AGATGTAATTGTGGGCGAAG Ngn2Cre Forward 5'GGACATTCCCGGACACACAC Reverse 5'AATCGCGAACATCTTCAGGT

For *PAX77*, Fp6 and Ngn2 primers, cycle conditions were as follows:
94°C for 1 minute
(96°C for 30 seconds, 59°C for 30 seconds, 72°C for 30 seconds) for 35 cycles

2.4.3 Agarose gel electrophoresis

PCR samples were run on a 2% agarose gel (1.5g agarose, 75ml TBE (Tris/Borate/EDTA)) at 115V for 1 hour.

2.5 Histological analysis

2.5.1 Haematoxylin and eosin staining

H&E staining was carried out on adjacent sections to in situ hybridisation sections and repeats were stained simultaneously for each developmental stage. Frozen sections stored at -20°C were brought to RT for 30 minutes prior to staining. Slides were then rinsed under running water for 2 minutes before being dipped in Haematoxylin for 2 minutes. Slides were then rinsed under running water for 2 minutes and then placed in Scott's Tap Water Substitute (STWS) (Leica) for 2 minutes. Slides were then rinsed under running water for 2 minutes before being dipped in alcoholic Eosin. Slides were then dipped in running water, before being placed in Potassium Aluminium for 2 minutes. Slides were then rinsed under running water for 2 minutes before being dehydrated through a series of alcohol dips at increasing concentrations: 70%, 90%, 95% and two absolute alcohol dips. Slides were then dipped in Xylene and slides were mounted with coverslips using DPX mounting medium (Fisher).

2.6 Plasmids

The following DNA plasmids were used: Dll1, Jag1 and Ngn2. Dll1 was kindly gifted by the lab of Dr Thomas Theil from the Centre for Integrative Physiology at the University of Edinburgh. Jag1 was kindly gifted by the lab of Dr Kim Dale from the School of Life Sciences at the University of Dundee. Ngn2 was readily available from our own lab.

2.6.1 Plasmid transformation

Transformations were set up in 14ml PP tubes and plasmids were heat shocked into JM109 competent cells (Promega) according to Promega protocol instructions, in order to amplify the gene of interest. Plasmid heat shock reactions are shown in the tables below (Jin and Lloyd, 1997).

Table 2.2 Heat Shock reaction

Reaction Component	Standard Reaction	Positive Control	Negative Control
Plasmid	2µl	2µl	0µl
Competent Cells	100µl	100µl	100µl
ddH_20	0µl	0µl	2µl

250µl of ampicillin was added to 250ml of agar before pouring into petri dishes to ensure that only cells which had taken up the plasmid grew. Dishes were then left to set and stored upside down until required to prevent contamination from condensation droplets. JM109 competent cells (Promega) and DNA plasmids were thawed on ice. In order to insert the DNA into the cells, tubes were placed on ice for 30 minutes. Tubes were then placed in the water bath at 42°C for 90 seconds before being placed back on ice. 450µl of SOC medium was added to each test tube. Tubes

were then incubated at 37°C in a shaking oven for 60 minutes. Three separate dilutions, a 1:10 positive control (using N1 plasmid which has been previously validated) and an undiluted no plasmid control (competent cells only and no in situ plasmid), were set up in tubes as shown in the table below.

Table 2.3 Transformation Dilutions

Component	Undiluted	1:10	1:100	Control
Plasmid	100µl	10µl	1µl	0µl
SOC Medium	0µl	90µl	100µl	100µl

100µl of each dilution was streaked onto individual agar plates using sterilised glass rods. Plates were then incubated overnight at 37°C. 500µl of ampicillin (AMP) was then added to 500ml of Lennox broth (LB broth) and 2ml of LB + Amp was added to four separate test tubes. Colonies were then selected from 1:100 dishes and one colony was put into each individual tube. Tubes were placed in a shaking oven and incubated at 37°C for 2 hours. 200ml of LB + Amp was then poured into a conical flask with 1ml of one of the four 3ml starter cultures and was incubated overnight at 37°C in a shaking oven.

2.6.2 Plasmid Midi Prep

Plasmid midi prep was performed using a Qiagen HiSpeed plasmid maxi kit. Cells were harvested from 200ml of culture at 6000xg for 15 minutes at 4°C. Centrifuge tubes were then inverted to remove all traces of supernatant. The bacteria pellet formed during centrifugation was then resuspended in 10ml of chilled Buffer P1by gently vortexing the mix until dissolved. 10ml of buffer P2 was then added and the tube inverted 6 times before being incubated at RT for 5 minutes. The lysate was then poured into the barrel of a QIA filter cartridge and incubated at RT for 10 minutes. A HiSpeed Maxi Tip was then equilibrated by applying 10ml of buffer QBT

and allowing the column to empty by gravity flow. A plunger was then fitted to the QIAfilter Maxi Cartridge and the cell lysate filtered into the equilibrated HiSpeed Tip. The HiSpeed Maxi Tip was then washed with 20ml of Buffer QC by gravity flow. Collected DNA was then eluted with 15ml of Buffer QF. 10.5ml of isopropanol was added to precipitate the eluted DNA and the mix was incubated at RT for 5 minutes. The eluate/isoproanol mix was then passed through a QIA precipitator before being washed with 2ml of 70% ethanol. The membrane of the QIA precipitator was then dried by passing air through by force twice. The QIA precipitator was then attached to a 5ml syringe and held over a 1.5ml collection tube. 1ml of Tris buffer (10mM Tris pH 8.0 + 1mM EDTA) was added to the 5ml syringe and DNA was eluted into the 1.5ml collection tube. Eluate was then transferred to a new 5ml tube with the QIA precipitator attached and DNA was eluted for a second time into a 1.5ml collection tube. DNA was then measured using a Nanodrop and stored at -20°C until required.

2.6.3 DNA Digest

DNA digest reactions for each plasmid is shown in the tables below. Restriction enzymes and buffers were supplied by New England Biolabs. Digests were incubated at 37°C for 2 hours.

An example of the digest mix follows:
(DNA concentration was required to be 10ug and the following was adjusted accordingly).
ddH_2O – 164.5µl
DNA – 10.5µl
10X Buffer - 20µl
Enzyme (100,000 units/ml) - 5µl

Table 2.4 Plasmid digest information

Plasmid	Restriction enzyme
Dll1	EcoR1
Jag1	EcoR1
Ngn2	BamHI

2.6.4 DNA Clean-up

600µl of Isopropanol and 200µl of buffer QG (Qiagen) were added to the digest mix. The mix was then applied to a QIA quick spin column (Qiagen) in a 2ml collection tube and centrifuged for 1 minute in order to bind the DNA to the column membrane. Flow-through was discarded and 0.5ml of buffer QG was added to the QIA quick spin column. The QIA spin column was then centrifuged for 1 minute and flow through was discarded. 0.75ml of buffer PE (Qiagen) was then added to the QIA spin column which was then centrifuged for 1 minute. Flow through was discarded. Centrifugation for 1 minute was repeated to dry the QIA quick spin column. The QIA quick spin column was then placed in a clean 1.5ml tube and DNA was eluted by adding 30µl of buffer EB (Qiagen). Following application of buffer EB, the column and collecting tube was left to sit for 1 minute and then centrifuged for 1 minute. Flow through was retained in the 1.5ml collecting tube and stored at -20°C.

2.6.5 Plasmid Analysis

Uncut, cut and cleaned plasmids, and Dig-labelled probes were visualised using agarose gel electrophoresis. A 1% agarose gel was used to visualise products used for in situ hybridisation. All agarose gels contained Sybrsafe in order for DNA bands to be seen under ultraviolet light. All agarose gels were run at 100 V for 45 minutes.

2.7 DIG-labelled Antisense RNA Probes

Labelling mixes (Roche) were made up for each probe in 1.5ml test tubes and were incubated at 37°C for 2 hours. Labelling mix was as follows:

ddH_2O - 12µl
Plasmid digest - 10µl
10X transcription buffer - 2µl
Dig label mix (10x solution with: 10 mM ATP, CTP, GTP (each), 6.5 mM UTP, 3.5 mM DIG-11-UTP) - 2µl
RNA polymerase (≥20 U/µl) - 2µl

Table 2.5 Plasmid polymerase information

Plasmid	RNA ploymerase
Dll1	T3
Jag1	T3
Ngn2	T7

2µl of DNase (2,000 U/mg) (Roche) was then added to the tubes and the mix was incubated for an additional 15 minutes at 37°C. The following was then added to the reaction mix:

0.2M EDTA (pH8) - 2µl
4M LiCl - 2.5µl
100% ETOH - 75µl

Tubes were then stored at -20°C overnight. Tubes were then removed from -20°C storage and centrifuged for 15 minutes to remove supernatant. The remaining pellet was then washed twice in 70% EOH. The pellet was left to dry (until clear) and was then suspended in 100µl of H_2O and stored at -20°C.

2.8 In situ hybridisation staining

2.8.1 Hybridisation

Sections were selected in a rostral-caudal series; an additional slide was included to act as a no probe control. All slides were mounted with 8 sections as standard. Preliminary in-situ runs using a new probe included a positive control in order to validate the tissue and reagents (N1 probe which has been previously validated by our lab). A no probe control was used as a negative control. Sense probes were not utilised as a negative control. Slides were defrosted at room temperature (RT) for 30 minutes prior to hybridisation. Slides were defrosted in their storage box to prevent RNA degradation by condensation. A sealable plastic box was then lined with two sheets of Tork roll soaked in 100ml of 50% formamide/ 1X salt (1ml of 10X salt). The box was incubated at 65°C until required.

<u>10X Salt:</u>
NaCl – 22.8g
Tris HCl (pH 7.5) – 2.8g
Tris Base – 0.27g
$NaH_2PO_4.2H_2O$ – 1.56g
Na_2HPO_4 – 1.42g
0.5M EDTA – 20ml
ddH_2O – up to 200ml

Probes were thawed quickly and diluted in hybridisation solution in 1.5ml screw cap tubes. Probe dilution was optimised for each individual probe. A range of concentrations were used (1:250, 1:500, 1:1000, 1:10000, 1:15000, 1:25000) and the dilution that produced the clearest stain was selected. This process was repeated for each batch of labelled probe. Hybridisation/probe mixes were then vortexed vigorously in order to allow the probe to mix thoroughly. Diluted probes were then denatured on a hot block at 85-90°C for 10 minutes. Denatured probes were then

centrifuged briefly. Sections were outlined with a hydrophobic pen and 20µl of diluted probe was pipetted directly onto each section. Slides were then placed in the pre-prepared sealable plastic box and incubated at 65°C overnight.

2.8.2 Post-hybridisation

Slides were transferred from the sealed box to a glass Coplin jar. Sections were then washed in wash buffer (pre-warmed to 70°C) for 15 minutes at 70°C. This was repeated for 2X 30 minutes using fresh wash buffer each time. Slides were transferred to a new Coplin jar and incubated in 1X MABT at RT on a rocker for 30 minutes. This step was then repeated.

Wash Buffer:
1X SSC – 15ml
50% formamide – 150ml
0.1% Tween-20 - 300µl
ddH_2O – 135ml
5X MABT

0.5M Maleic Acid – 29.1g
NaOH – 16g
0.75M NaCl – 21.9g
0.5% Tween 20 – 2.5ml
ddH_2O – up to 500ml

2.8.3 Blocking and antibody staining

A box was lined with 2 sheets of Tork roll soaked with PBS in order to prepare a humidified environment. Slides were removed from 1X MABT (5X MABT diluted in PBS) and then edges were dried. Sections were then outlined using a hydrophobic pen. Reactions were blocked by adding 200µl of blocking solution (20% heat-

inactivated sheep serum/ 2% blocking reagent in 1X MABT) onto each slide. Slides were then incubated in the pre-prepared humidified box at RT for 1 hour. Blocking solution was removed and 100µl of anti-DIG antibody diluted in 1:1500 blocking solution was then added to the slides in order to detect RNA expression. Slides were placed back in the humidified box and incubated at 4°C overnight.

2.8.4 Post-antibody washes

Slides were transferred to a glass Coplin jar and sections were washed 5 times for 20 minutes each in fresh 1X MABT at RT on a rocker. Sections were equilibrated in pre-staining buffer twice for 10 minutes at RT with rocking.

Pre-staining buffer:

5M NaCl – 6ml
1M $MgCl_2$ – 15ml
1M Tris-pH 9.5 – 30ml
Tween 20 - 300µl
ddH_2O – 250ml

2.8.5 Colour reaction

In order to visualise RNA expression, 1.4ml of nitro-blue tetrazolium and 5-bromo-4-chloro-3'-indolyphosphate (NBT/BCIP) complex was added to staining buffer before being directly added to a foil wrapped Coplin jar. The staining reaction was then incubated in the dark at RT for ~24-48 hours until developed. The staining reaction was then stopped by transferring slides to a new Coplin jar and washing in 1X PBS several times. Slides were then left in 1X PBS for 2 days at 4°C.

Stain Buffer:
5M NaCl – 2ml
1M Tris pH 9.5 – 10ml

$\underline{ddH_2O}$ – 83ml

Slides were then removed from 1X PBS and mounted with coverslips using Aquatex mounting medium. Slides were left to dry and then stored at 4°C until required for imaging.

2.9 Double fluorescent in situ hybridisation staining

2.9.1 Hybridisation

Refer to 2.6.1 for Hybridisation protocol. Both Digoxygenin (DIG) labelled and Dinitrophenyl (DNP) labelled probes were diluted in the same tube of hybridisation mix.

2.9.2 Post-hybridisation

Slides were transferred from the sealed box to a glass Coplin jar. Sections were then washed in wash buffer (pre-warmed to 70°C) for 15 minutes at 70°C. This was repeated for 2X 30 minutes using fresh wash buffer each time. Slides were transferred to a new Coplin jar and incubated in TNT buffer (0.1 M TrisHCl, 0.15 M NaCl, 0.05% Tween-20) at RT on a rocker for 30 minutes. This step was then repeated.

2.9.3 Blocking and DIG antibody staining

An immunohistochemistry box was lined with 2 sheets of Tork roll soaked with PBS in order to prepare a humidified environment. Slides were removed from TNT buffer and slide edges were dried using a square of tissue paper. Sections were then outlined using a hydrophobic pen. Reactions were blocked by adding 150µl of TNB blocking solution (0.1M TrisHcl pH7.5, 0.15M NaCl, 0.5% Perkin Elmer blocking

reagent in ddH_20) onto each slide. Slides were then incubated in the pre-prepared humidified box at RT for 1 hour.
Blocking solution was removed and 100µl of anti-DIG POD antibody diluted in 1:500 TNB blocking solution was then added to the slides in order to detect RNA expression. Slides were placed back in the humidified box and incubated at 4°C overnight.

2.9.4 Post-antibody washes and detection of DIG probe

Slides were transferred to a glass Coplin jar covered in foil and sections were washed 3 times for 5 minutes each in fresh TNT at RT on a rocker. 100µl of Cyanine3 tyramide diluted 1:500 in amplification diluted and 100µl was added to each slide. Slides were then incubated at RT for 10 minutes. Slides were then transferred to a glass Coplin jar and covered in foil and sections were washed 5 times for 5 minutes each with fresh TNT buffer.

2.9.5 Peroxidase inactivation and detection of DNP probe

100µl of 10mM HCl was then added to each slide and slides were then incubated for 30 minutes at RT, in order to inactivate deposited peroxidase. Slides were then placed in a glass Coplin jar covered in foil and sections were washed 3 times for 5 minutes each in TNT. 100µl of anti-DNP POD antibody diluted in 1:500 TNB blocking solution was then added to the slides in order to detect RNA expression. Slides were placed back in the humidified box and incubated at 4°C overnight.

2.9.6 Post-antibody washes and detection of DNP probe

Slides were transferred to a glass Coplin jar covered in foil and sections were washed 3 times for 5 minutes each in fresh TNT at RT on a rocker. 100µl of fluorescein tyramide diluted 1:50 in amplification diluent was added to each slide. Slides were then incubated at RT for 10 minutes. Slides were then transferred to a glass Coplin

jar and covered in foil and sections were washed 5 times for 5 minutes each with fresh TNT buffer.

2.9.7 Counterstain with DAPI

Slides were transferred back into the humidified box and 100µl of DAPI diluted 1:1000 in 1X PBS was added to each slide. Slides were incubated at RT for 5 minutes. Slides were then transferred to a glass Coplin jar and covered in foil and sections were washed 3 times for 5 minutes each with fresh 1X PBS. Slides were then removed from 1X PBS and mounted with 22mm X 50mm coverslips using Vectashield (Vectorlabs) hard set mounting medium. Slides were left to dry in the dark and were then stored at 4°C until required for imaging.

2.10 Double immunofluorescence/fluorescent in situ hybridisation staining

2.10.1 Antigen retrieval

Sections were selected in a rostral-caudal series; an additional slide was included to act as a no probe control. Slides were defrosted at RT for 30 minutes prior to hybridisation. Slides were defrosted in their storage box to prevent RNA degradation by condensation. Slides were washed for 10mins in 10mM sodium citrate. Slides were placed in a plastic Coplin jar and placed in a 95°C water bath for 90°C. Slides were then removed and left to cool down for 20mins. Slides were then washed in PBS.

2.10.2 Hybridisation

Refer to 2.10.1 for Hybridisation protocol.

2.10.3 Post-hybridisation

Refer to 2.7.2 for post-hybridisation protocol.

2.10.4 Blocking and DIG antibody staining

An immunohistochemistry box was lined with 2 sheets of Tork roll soaked with 1X PBS in order to prepare a humidified environment. Slides were removed from TNT buffer and slide edges were dried using a square of tissue paper. Sections were then outlined using a hydrophobic pen. Reactions were blocked by adding 150µl of TNB blocking solution (0.1M TrisHCl pH7.5, 0.15M NaCl, 0.5% Perkin Elmer blocking reagent in ddH_20) onto each slide. Slides were then incubated in the pre-prepared humidified box at RT for 1 hour.

Blocking solution was removed and 100µl of anti-DIG POD antibody diluted in 1:500 TNB blocking solution was then added to the slides in order to detect RNA expression. Slides were placed back in the humidified box and incubated at 4°C overnight.

2.10.5 Post-antibody washes and detection of DIG probe

Slides were transferred to a glass Coplin jar covered in foil and sections were washed 3 times for 5 minutes each in fresh TNT at RT on a rocker. 100µl of Cyanine3 tyramide diluted 1:500 in amplification diluted and 100µl was added to each slide. Slides were then incubated at RT for 10 minutes. Slides were then transferred to a glass Coplin jar and covered in foil and sections were washed 5 times for 5 minutes each with fresh TNT buffer.

2.10.6 Blocking and antibody staining

Slides were blocked for 30 minutes in 10% goat serum in PBT in the dark. Slides were then incubated O/N at 4°C in rabbit anti-Tbr2 (ab23345) (Abcam) 1:100 in block in the dark.

2.10.7 Post antibody washes and secondary antibody staining

Slides were washed 4 x 15mins in PBT in the dark and then incubated O/N at 4°C in goat anti-rabbit IgG alexa fluor® 488 (ab150077) (Abcam) 1:400 in block in the dark.

2.10.8 Post antibody washes and counterstain with DAPI

Slides were washed 4x15mins in PBT in the dark. Slides were then counterstained with DAPI (Thermo Fisher Scientific) 1:1000 in 1X PBS for 5mins in the dark. Slides were then washed 2x 5mins in PBT in the dark. Slides were then mounted with Vectashield (Vectorlabs) hard set mounting medium. Slides were left to dry in the dark and were then stored at 4°C until required for imaging.

2.11 Quantitative polymerase chain reaction

2.11.1 Dissection of cortical tissue

The uterus of Sey females at gestational stage E12.5, E13.5 and E14.5 were dissected out and placed into ice-cold RNAse free 1X PBS in a petri dish. Embryos were then dissected out genotyped by eye with WT and *Pax6*$^{-/-}$ kept and *Pax6*$^{+/-}$ discarded. Embryos were then decapitated and the brain was removed using forceps and a beaver blade. Telencephalic vesicles were removed from the brain and cortices dissected and placed in 1.5ml eppendorf and placed immediately on dry ice. Whole WT brains were taken to act as a control.

2.11.2 Preparation of RNA

RNA was extracted from dissected cortical tissue using Qiagen RNeasy kit. A QIAshredder spin column was used to disrupt membranes and homogenise the lysate. 70% RNase free ethanol was added to assist the binding of RNA to the membrane of the RNeasy spin column. Traces of genomic DNA were eradicated by

on-column DNase digestion (Qiagen RNeasy kit). Contaminants were removed by washing with buffer RPE (Qiagen) and the RNA was then eluted in RNAse free ddH_2O. RNA was then stored at -80°C.

2.11.3 Reverse transcription

Cortical RNA was reverse transcribed to cDNA using Invitrogen Superscript III First-Strand Synthesis Supermix kit as follows:
RNA - 8 µl
Random hexamers (50ng/ µl) - 1µl
Annealing buffer - 1µl
The mix was incubated at 65°C for 5mins and then chilled on ice for 5mins.
The following was added to the mix:
2X First-Strand reaction mix - 10µl
Superscript III/RNase out enzyme mix - 2µl
The mix was then vortexed briefly and incubated for 10mins at 25°C followed by 50mins at 50°C and then 5mins at 85°C. Samples were then chilled on ice and stored at -20°C.

2.11.4 qPCR protocol

Standards for qPCR were prepared as follows:

Table 2.6 qPCR Standards

1000	250	62.5	15.62	1000	250	62.5	15.625
WT 1	Sey 1	WT 2	Sey 2	WT 3	Sey 3	-rt	H_2O

Tube 1000 ➔ 4.5µl + H_2O ➔ 4µl + 12ul H_2O ➔ 3µl + 9ul H_2O

The qPCR reaction mix was prepared as follows:

H_2O – 7µl

Primer Mix – 0.5µl

SYBR green – 12.5µl

cDNA – 5µl

Table 2.7 PCR primers for qPCR

Gene	Primer Sequence
GAPDH	Forward 5'GGGTGTGAACCACGAGAAAT Reverse 5'CCTTCCACAATGCCAAAGTT
Jag1	Forward 5'GGAAGACAAGCCAAGGACCA Reverse 5'GTGCTTGCACTGGGTTTCTG
Dll1	Forward 5'GGATACTCTAGGAGAGCAAGG Reverse 5'CTTCTTGTTGACGAACTCCT

2.11.5 qPCR programme

Cycle conditions for qPCR for all primers were as follows:

95°C for 15 minutes

(94°C for 15 seconds, 55°C for 30 seconds and 72°C for 30 seconds, plate read) 35 cycles

Perform melting curve from 60°C to 90°C; read every 1°C; hold for 001 seconds between reads

2.11.6 qPCR analysis

qPCR results were produced using OpticonMonitor™ analysis software version 1.08. Results were then exported and statistical analysis was carried out using Excel. Results were normalised to GAPDH and one tailed paired student t-tests carried out.

2.12 Cloning

2.12.1 Selection of Jag1UE predicted enhancer element

Identification of the Jag1 enhancer element was made by bioinformatic screening using a customised track on the UCSC Genome Browser. The customised Jag1 track was developed by Dr Ian Simpson (Institute for Adaptive and Neural Computation, School of Informatics, University of Edinburgh). The customised track implemented the Mouse Dec. 2011 (GRCm38/mm10) assembly and compared the Jag1 gene to various Pax6 binding motifs

2.12.2 Amplification of Jag1UE from genomic DNA

Primers (Figure 6.4) were designed to clone our region of interest (Jag1UE) from genomic DNA. The following programme was used:
94°C for 1min
(94°C for 30secs, 55°C for 30secs and 68°C for 3mins and 30secs) 20 cycles

Jag1UE was then run on a 2% agarose gel at 80V for 60mins and the approximately 3.5Kb band was cut from the gel on a UV box and a gel extraction was carried out using a Qiagen QIAquick Gel Extraction Kit according to kit instructions.

Jag1UE was sequenced by Eurofins Genomics DNA sequencing service in order to validate the fragment.

2.12.3 In fusion PCR

Cloning was carried out using a Clontech® In-Fusion® HD Cloning Kit according to kit instructions. Jag1UE and a pGL4.23 construct (Promega) with a mimimal promoter were used. Bacterial transformations were carried out according to kit instructions. Colonies were selected and minipreps were carried out using a Qiagen QIAprep Spin Miniprep Kit according to kit instructions. Mini preps were sequenced

by Eurofins Genomics DNA sequencing service in order to validate them as pGL4.23+Jag1UE.

2.13 Routine cell culture techniques

2.13.1 Cell culture conditions

Cell lines were maintained at 37°C in 5% CO_2. Media suitable for the selected cell line was used at 37°C and stored at 4°C. Media was routinely changed every 24-48 hours and the cells passaged at regular intervals to ensure the maintenance of a constant, healthy stock of cultured cells.

2.13.2 HEK 293 cell line

The human embryonic kidney (HEK 293) cell line was used (Graham and Smiley 1977). The cell line was maintained in standard culture conditions in Dulbecco's Modified Eagle Serum (D-MEM) (Invitrogen) containing 10% Foetal Bovine Serum (FBS) and routinely passaged.

2.13.3 Cell culture conditions

1ml of HEK 293 cells, stored in liquid nitrogen, were thawed rapidly and suspended in 9ml of Dulbecco's Modified Eagle Serum (D-MEM) (Invitrogen) containing 10% Foetal Bovine Serum (FBS) (check FBS source) in a universal tube. Cells were then pelleted by centrifugation at 5000rpm for 5 minutes and supernatant was discarded. Cells were then re-suspended in 4mls of D-MEM + 10% FBS and transferred to a T25 flask. Cells were incubated overnight at 37°C. Cells were fed with D-MEM + FBS the subsequent day and then transferred to a T75 flask, with 5mls of media.

2.13.4 Cell passage

Cell passage was carried out at regular intervals to ensure the maintenance of a constant stock of cultured cells maintained in the optimum conditions for growth. Cells were grown to confluence in 75cm^2 flask before being passaged.
Cells were dissociated in 3ml of 1X Trypsin/EDTA (0.25% Trypsin/0.02% EDTA) at 37°C, 7ml of culture media was added to the flask to inactivate the trypsin. The cell mixture was centrifuged at 1000 revolutions per minute (rpm) for 5 minutes. Supernatant was discarded and the cell pellet was re-suspended in 10ml of fresh media. Cells were maintained in standard conditions as stock cells.

2.13.5 Freezing and defrosting cell lines

Cells were grown to confluence in 75cm^2 culture flasks and dissociated in trypsin, 7ml of culture media was added to inactivate the trypsin. The cells were pelleted by centrifugation at 1000rpm for 5 minutes. Cell pellets were re-suspended in 1ml of freezing buffer and transferred to pre-chilled cryovials. Freezing was carried out slowly to minimise cell damage, first on dry ice, before being transferred to a -80°C freezer for 24-48 hours, and then long term storage in liquid nitrogen.
Cells frozen in cryovials were defrosted rapidly at 37°C and placed in a volume of fresh media. Cells were then pelleted by centrifugation at 1000rpm for 5 minutes and supernatant was discarded. The cell pellet was re-suspended in fresh media to prevent DMSO toxicity and transferred to a 25cm^2 culture flask. Cells were left to adhere overnight at 37°C and the media was then removed and replaced with fresh media to feed cells and to remove any dead ones.

Freezing Buffer
12ml DMEM
4ml FBS
4ml DMSO

2.13.6 Transient transfections

Transient transfections were carried out in the HEK 293 cell line, in cells which had reached 70-90% confluence.

2.13.7 Lipofectamine 2000

Cells were plated in a 24 well plate at 1 x 10^5 cells per well in 1ml of fresh media and incubated at 37°C overnight. Transfections were carried out using 5µl of Lipofectamine 2000 (Invitrogen) mixed in 50µl of OptiMEM (Thermo Fisher) per well. The lipofectamine/OptiMEM mix was incubated at RT for 5 minutes. A DNA cocktail of the required constructs was prepared to give a final working concentration of 815ng per well, with each well containing an increasing concentration of the CMV Pax6 construct (pCMV-Pax6 construct was generated by inserting full-length Pax6 cDNA into a pCMV-Script plasmid (Stratagene)) (Da Mi *et al*., 2013 a)). The empty CMV construct was used to make up the total concentration of DNA. A replicate of three was carried out for each Pax6 concentration. Each experiment included experimental transfections using the developed Jag1UE luciferase construct (Chapter 6, Figure 6.5) and a control experiment using an empty pGL4.23 luciferase vector (Chapter 6, Figure 6.4) (Promega). Luciferase constructs were used at a concentration of 30ng per well and the control SV40 Renilla vector (Promega) (Figure 2.1) was used at a concentration of 15ng (Table 2.8 and Table 2.9).

Table 2.8 Jag1UE experimental transfection DNA mix

1	**2**	**3**	**4**	**5**	**6**
0ng Pax6	50ng Pax6	100ng Pax6	200ng Pax6	0ng Pax6	0ng Pax6
500ng Empty	500ng Empty	500ng Empty	500ng Empty	500ng Empty	500ng Empty
300ng Jag1UE	300ng Jag1UE	300ng Jag1UE	300ng Jag1UE	300ng Jag1UE	300ng Jag1UE
15ng Renilla	15ng Renilla	15ng Renilla	15ng Renilla	15ng Renilla	15ng Renilla

Table 2.9 Pgl4.23 control transfection DNA mix

1	**2**	**3**	**4**	**5**	**6**
0ng Pax6	50ng Pax6	100ng Pax6	200ng Pax6	0ng Pax6	0ng Pax6
500ng Empty	500ng Empty	500ng Empty	500ng Empty	500ng Empty	500ng Empty
300ng pGL4.23	300ng pGL4.23	300ng pGL4.23	300ng pGL4.23	300ng pGL4.23	300ng pGL4.23
15ng Renilla	15ng Renilla	15ng Renilla	15ng Renilla	15ng Renilla	15ng Renilla

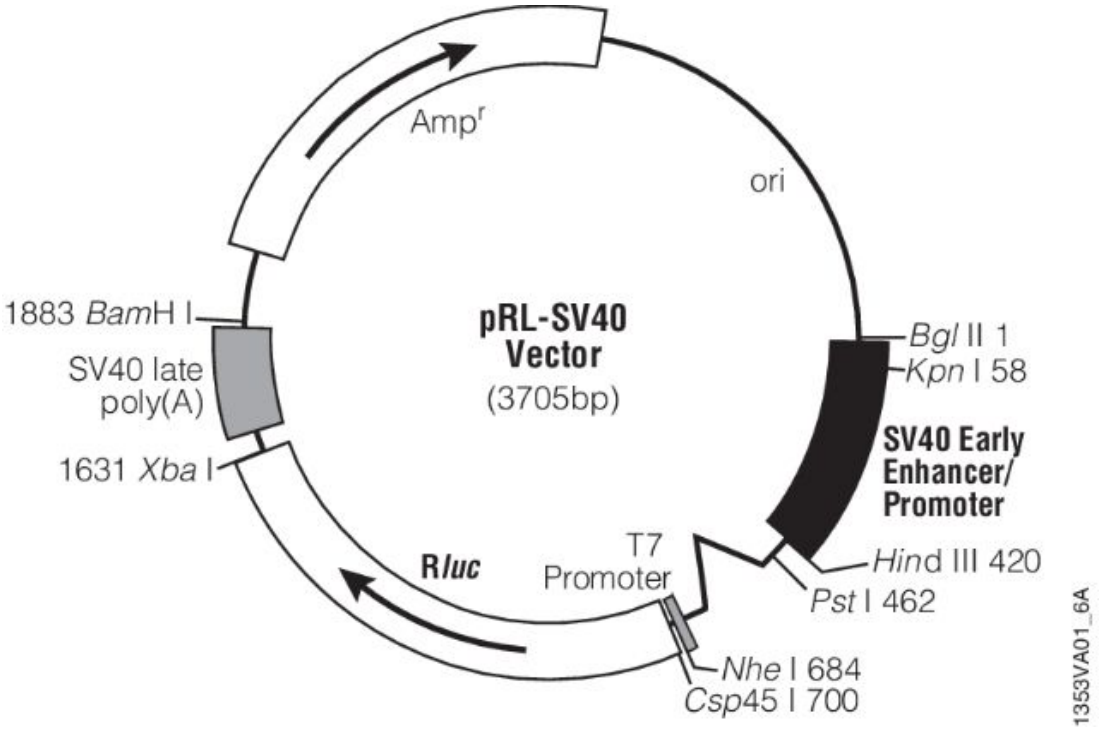

Figure 2.2 SV40 renilla vector

A plasmid map detailing the Promega SV40 Renilla Vector used as a control during luciferase assay analysis.

The DNA cocktail was mixed with OPTIMEM and incubated at RT for 5 minutes. The lipofectamine solution and DNA solutions were then mixed and incubated for 20 minutes at RT. 50µl of the final mix was then added to each well and incubated for 48 hours at 37°C until cells displayed a transfection efficiency of 70-80%. Media was changed 6 hours after transfection and 24 hours following transfection. Transfection efficiency was checked using a GFP microscope.

2.14 Luciferase assay

48 hours post transfection, media was removed and cells were washed in 1X PBS. 100µl of passive lysis buffer (Promega) was then added to each well and cells were

incubated for 15 minutes on a shaker at RT. A cell scraper was then used to help lift any remaining cells from the surface of the well. The cell lystate solution was then aliquoted into 2ml Eppendorf tubes and spun down at 4°C by centrifugation at 13000rpm for 5 minutes. Following centrifugation, 20µl of the supernatant was added per well to a 96 well assay plate (bio-rad). The remaining sample volume was stored at -20°C and used for western blot analysis.
Lysates were then analysed using a Promega Dual Luciferase Reporter Assay System (DLR) kit (Promega) according to kit instructions (see appendix1). Assays were carried out using a GloMax 96 Microplate Luminometer with dual injectors (Promega) using a DLR specific protocol (see appendix 2).

2.14.1 Quantification

Results were then compiled in Microsoft Excel and quantified using Microsoft Excel and Prism software.

2.15 Western blot analysis

2.15.1 Preparation of cell lysate for western blot

Transfected HEK 293 cells previously lysed for luciferase assay analysis were defrosted and placed on ice. The samples were transferred into 1.5µl eppendorf tubes and 1µl of β-Mercaptethanol (Sigma Aldrich) was added to each tube in a fumehood. A volume of 4X protein running buffer (Li-COR) containing 1:10 β-Mercaptethanol was added and the samples were then boiled for 10 minutes on a hot block in order to denature the proteins.

2.15.2 One-dimensional electrophoresis

One-dimensional electrophoresis was used to separate proteins according to their molecular weight for further analysis. An adaptation of the discontinuous polyacrylamide system described by Laemmli (1970) using precast gels was

implemented. 4-12% Bis Tris pre-cast 1mm 12 well polyacrylamide gels (NuPAGE) were rinsed in ddH2O and set up in a western blot gel tank. Gels were fully immersed in fresh MOPS 1X running buffer (50ml NuPAGE MOPS SDS running buffer + 950ml ddH_2O).
Samples were loaded into the gels along with a pre-stained protein ladder (PageRuler). Samples were then run at a constant voltage of 200V for 50 minutes.

2.15.3 Protein transfer

Following sample separation, samples were transferred to a nitrocellulose membrane. Standard methods were used (Appendix 3). The transfer was carried out at 100V with a current limit of 0.4A at 4°C for 1 hour. Care was taken to ensure that the cassette was completely immersed in transfer buffer and that all air bubbles were removed from the cassette.

2.15.4 Western blotting

Following the transfer, nitrocellulose membranes were stained for 5 minutes in 0.1% Ponceau S solution (Sigma) in 5% acetic acid (Fisher Scientific) in order to visualise the separated protein bands and assess sample quality. The nitrocellulose membrane was then rinsed in ddH2O and blocked in blocking buffer (5% dry milk powder + 0.25% PBT). Western blots were carried out using optimum concentrations of both primary and secondary antibodies (Table 2.10).

Table 2:10 Primary and secondary antibody concentrations

Antibody	Source	Concentration
GAPDH	Abcam. Catalogue No. ab8245	1:5000
Pax6	Millipore Catalogue No. AB2237	1:1000

AF680 goat anti-mouse IgG (H+L)	ThermoFisher Catalogue No. A-21057	1:3000
AF790 goat anti-rabbit IgG (H+L)	ThermoFisher Catalogue No. A-11367	1:3000

2.15.5 Incubation with primary antibodies

Blots were incubated with primary antibodies diluted in blocking buffer overnight at 4°C. Primary antibodies used were: mouse anti-GAPDH (Abcam) and rabbit anti-Pax6 (Millipore). The nitrocellulose membrane was equally covered by the solutions and rocked gently. Following incubation the blot was washed 3 x 10 min in 0.25% PBT.

2.15.6 Incubation with the secondary antibodies

Blots were incubated with secondary antibody diluted in blocking buffer for 45 minutes at room temperate. Secondary antibodies used were: AF680 goat anti-mouse IgG (H+L) (ThermoFisher) and AF790 goat anti-rabbit IgG (H+L) (ThermoFisher). The nitrocellulose membrane was equally covered by the solutions and rocked gently. Following incubation the blot was washed 3 x 10 min in 0.25% PBT and then washed 2 x 5min in 1X PBS**.**

2.15.7 Imaging

The Nitrocellulose membrane was removed from PBS and covered in a thin layer of cling film. Bubbles were carefully removed to ensure that the samples were imaged correctly. The Nitrocellulose membrane was then imaged using a Li-COR Odyssey (Li-COR Biosciences) and Odyssey software. Samples were scanned at varying levels of exposure to ensure that optimum exposure levels were identified.

2.15.8 Quantification

Samples scanned at optimum exposure levels were then quantified using imageJ. Pax6 intensity levels were normalised to GAPDH intensity levels for each sample.

2.16 Cell dissociation

Dissociation of cortical cells was carried out using a Papain Dissociation Kit (Worthington Biochemical Corporation).

2.16.1 Preparation of papain dissociation kit reagents

100ml of Earle's Balanced Salt Solution (EBSS) was oxygenated for 3-5 minutes and aliquoted into 20ml universal tubes. Ovomucoid inhibitor was prepared by adding 32mls of oxygenated EBSS to vial 4, containing ovomucoid powder and shaken well to suspend. The ovomucoid inhibitor was then placed in a 37°C incubator for to dissolve the powder fully. DNAse was dissolved in 500µl of oxygenated EBSS and stored in a Bijou for later use. Papain solution was prepared by dissolving Papain powder in 5mls of oxygenated EBBS and 250µl of DNAse solution was added prior to placing the Papain solution into a 37°C incubator.

2.16.2 Dissection of embryonic cortices

The uterus of *Pax6*$^{-/-}$ females at gestational stage E12.5 and E14.5 were dissected out and placed into EBSS in a petri dish. Embryos were then dissected and placed into a fresh dish of EBSS and genotyped by eye and sorted into control and mutants. Embryos were then decapitated and the brain was removed using forceps and a beaver blade. Telencephalic vesicles were removed from the brain and cortices dissected and placed in a bijou containing EBSS on ice. Control cortices were grouped together and Sey cortices were also grouped together.

2.16.3 Dissociation of embryonic cortical cells

EBSS and cortical tissue sections were then transferred to a conical centrifuge tube and EBSS was removed with a sterile pipette. 2mls of prepared Papain solution was then added in its placed and the tube was placed in a 37°C incubator for 45 minutes to allow the cortical tissue to be digested. Cells were then suspended in solution by gentle pipetting with a round-ended sterile pipette. Cells were then centrifuged at 300g (1500rpm) for 5 minutes and supernatant was removed and discarded. A low-ovo solution was then prepared by mixing 1.35mls of EBSS, 300µl of ovomucoid inhibitor and 75µl DNAse, and cells were suspended in the mix. 5mls of ovomucoid inhibitor was then added to a new centrifuge tube and cell suspension was added very slowly to the top of the ovomucoid solution. The tube containing the ovomucoid inhibitor/cell mix was then centrifuged at 70g (~500rpm) for 5 minutes. Supernatant was then removed and the dissociated cells re-suspended in 5mls of culture medium.

2.16.4 Estimation of cell concentration

20µl of the final cell suspension was pipetted onto a haemocytometer and counts were carried out using a light microscope (Leica). Counts were carried out for four different areas and the average was calculated for the number of cells in $x10^4$ in 1ml in order to calculate how many were in the prepared 5ml solution.

2.16.5 Fixation of dissociated cells

Following the estimation of cell concentration, cells were pelleted by centrifugation and supernatant was discarded. For 20,000 cells, 250µl of 1X PBS was added to the pelleted cells in order to re-suspend them, and 750µl of ice-cold 100% ethanol was then slowly added while mixing the cell suspension. Cells were then stored at -20°C until required.

2.17 Flow cytometry

2.17.1 Staining cells

$1x10^6$ cells (5ml of 200, 000 cell/ml suspension) were pelleted by centrifugation at 5000rpm and supernatant was discarded. Cell pellets were then re-suspended in 50µl of FACS buffer (1X PBS and 0.5% bovine serum albumins (BSA)).
Primary antibody mix was prepared in a total volume of 50µl per cell sample. Primary antibodies were titrated by flow cytometry analysis and used at an optimised ratio of 1:100 for Sox-2 af488 and Tbr2 pe-ef610 (eBioscience), and a ratio of 1:50 for Dll1 APC (BioLegend). Optimisation was carried out for the reported experiments in this thesis. Primary antibodies were diluted in FACS buffer to a total volume of 50µl and added to the cell sample. Cell samples were then incubated for 1 hour in the dark at RT.
Cells were then washed with 1ml of FACS buffer and pelleted by centrifugation at 5000rpm. Supernatant was then discarded and cell pellets were re-suspended in 110µl of DNA dye solution (0.11µl of 10mg/ml Hoechst 33342 stock solution and 109.89µl FACS buffer). Samples were then incubated for 1 hour in the dark at RT.

Cell samples were then washed with 1ml of FACS buffer and pelleted by centrifugation at 5000rpm, supernatant was discarded and cells were re-suspended in 300µl of FACS buffer and stored at 4°C until required.

2.17.2 Flow cytometry analysis

Cell samples were run on an LSRII and analysed using FlowJo V10.

2.18 Cell counts

Cell density for Dll1 expressing cells and total cell density were quantified using images produced from in situ hybridisation and H&E staining experiments. Sample

areas were defined at caudal, medial and rostral regions of the cortex. Within these regions, a sub region was defined by dividing analysis of the cortex into the dorsal cortex and the ventral cortex. A replicate of 3 sections per region, per embryo were analysed for each mutant and their control littermate. An N of three was used for each genotype and developmental stage, other than analysis of Dll1 density in *PAX77* embryos at E12.5 where an N of 5 was used and the left telencephalic lobe was defined as the sample area for each individual embryo. For each section, a high powered image (X40) of both the dorsal and ventral areas of the developing cortex were taken.

The width of the cortex of each replicate was measured and a square was drawn on the cortex with each side equating to the width recorded. The boxed area was treated as the sample area. Total number of cells within the cortex was recorded and the sample area was calculated (cortex width mm^2). Cell density was then calculated (no. cells x 0.01 ÷ area, chosen in order to reduce size of graph axis). The average cell density for each region was calculated and statistical analysis by Two-way ANOVA and Tukey's multiple comparison test was conducted.

Cell count analysis was carried out using ImageJ software and statistical analysis was carried out using Prism 6 software.

2.19 Identification of the VZ and the SVZ in the embryonic cortex

Identification of the SVZ was achieved by immunohistochemistry. The SVZ marker Tbr2 was used in order to visualise the SVZ and separate it from the VZ in the proliferative zone (Figure 2.3).

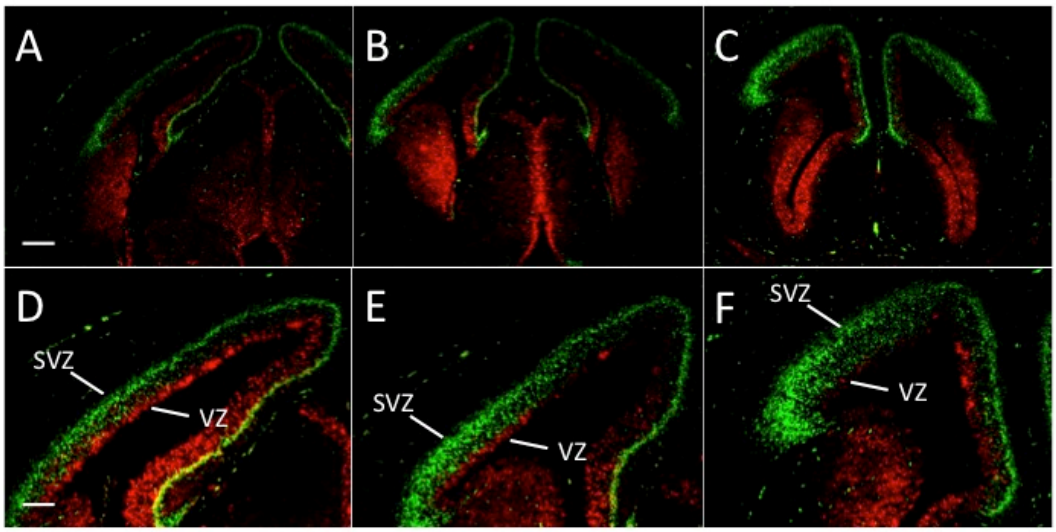

Figure 2.3 Identification of the VZ and the SVZ in the telencephalon

Panels showing an E14.5 WT telencephalon double stained by in situ hybridisation/immunohistochemistry with *Dll1* (red) and Tbr2 (green). (A and D) Caudal section (B and E) Medial section (C and F) Rostral section. Tbr2 is a well established marker of INPs residing in the SVZ, allowing separation of the SVZ (Green) from the VZ (red) in the cortex telencephalic vesicles. (A-C) Scale bars = 80µm (D-F) Scale bars = 60µm

3.0 Analysis of *Dll1* gene expression in the developing cortex of *Pax6* mutants

3.1 Introduction

Dll1, the mouse homolog of the Drosophila gene *Delta1* (*Dll1)*, is one of four genes in the *Dll* family (*Dll1-4*). The *Dll1* family, along with the *Jagged* family (comprised of *Jagged 1-2*) form the group of Notch ligands responsible for the cleavage and activation of the NICD in a neighbouring cell, inhibiting its differentiation into a neural cell and consequently, preserving the progenitor cell pool required for the cortex to form correctly (Chapter 1.7). As a result, *Dll1* is a crucial element of the Notch signalling pathway and therefore of great importance in maintaining the balance between cell proliferation and differentiation during the process of cortical neurogenesis (Campos *et* al., 2001; Kageyama *et* al., 2008a; 2008b; Pierfelice *et al*., 2011; Nelson *et al*., 2013).

A disruption in the levels of *Dll1* expression has been documented to have adverse effects during embryonic development and postnatally. An increase in *Dll1* has been linked to brain tumor development (Ignatova *et al.*, 2002; Purow *et al*., 2005; de Antonellis *et al., 2011*; Zhang *et al.*, 2011), while a decrease in *Dll1* expression prevents correct arteriogenesis (Limbourg *et al*., 2007; Van den Akker *et al*., 2007). However, despite the clear role of *Dll1* in forebrain development (Pierfelice *et al*., 2011; Shimojo *et al*., 2008; Nelson *et al*., 2013), few studies have addressed how an alteration in *Dll1* expression levels would affect corticogenesis.

Past studies, which have observed the expression of *Dll1* during neurogenesis, have observed a punctate expression pattern throughout the developing telencephalon. This expression pattern has a striking resemblance to the proneural gene *Ngn2*, which directly regulates *Dll1* expression (Shimojo *et al*., 2008). In terms of the cortex specifically, there has been some controversy over the precise location of *Dll1* expression within the proliferative zones of the developing cortex. Campos *et al*.

(2001) originally reported *Dll1* to be expressed in the VZ between E12.5-E14.5 of embryonic development (Campos *et al*., 2001), while subsequent research has suggested that *Dll1* is expressed solely within the SVZ and is a cell marker for INPs (Mizutani *et al*., 2007; Kawaguchi *et al*., 2008; Yoon *et al*., 2008). Furthermore, recent studies by Nelson *et al*. (2013) have suggested that *Dll1* is predominately expressed within the SVZ but is also expressed at lower levels in the VZ, in a sub population of INPs that reside there (Nelson *et al*., 2013).

As previously discussed (Chapter 1), microarray analysis of potential *Pax6* targets has suggested *Dll1* as a likely candidate. A study by Sansom *et al*. (2013) proposed *Dll1* to be regulated by *Pax6* from their chromatin immunopreciptiation (ChIP) analysis of the *Pax6*$^{-/-}$ mutant and *PAX77* mutant. However, *Dll1* has yet to be confirmed as a *Pax6* target and no *Dll1* expression pattern analysis has been conducted in *Pax6* mutants.

Due to published research directly suggesting *Dll1* to be regulated by *Pax6*, and other genes implicated in the Notch signalling pathway also being classified as potential targets (Carr, 2009; Sansom *et al*., 2009), it stands to reason that *Dll1* could be a Pax6 target. In order to ascertain whether *Dll1* could be regulated by Pax6 expression, analysing *Dll1* gene expression in the *Pax6*$^{-/-}$ mutant, which is null for Pax6 expression, provides a clear insight.

If *Dll1* expression is affected by a loss of *Pax6*, it is plausible that its expression will also be affected by varying levels of *Pax6*. As a result, analysis of *Dll1* expression in the *PAX77* overexpressing mutant and the floxed *Pax6* conditional knockout (Fp6 cKO) mutant would provide insight into how differing *Pax6* levels affect *Dll1* expression in the developing cortex. Previous work on the *PAX77* mutant has shown that an increase in *Pax6* expression results in a depletion of the progenitor pool due to a decrease in progenitor cell proliferation vs. differentiation (Manuel *et al*., 2007; Georgala *et al*., 2011). Additionally, analysis using a floxed *Pax6* transgenic line expressing a tamoxifen inducible Cre recombinase targeted to the *Emx1* locus (*Emx1CreEr*^{T2}*;Pax6*$^{loxP/loxP}$) (Kessaris *et al*., 2006; Simpson *et al*., 2009), allowing

the knockdown of *Pax6* at specific stages of development and exclusively in the cortex from E9.5, will give further insight into the role of *Pax6* during telencephalic development and how it affects the complex gene networks that it controls (Simpson *et al*., 2009).

3.2 Analysis of *Dll1* gene expression in *Pax6*$^{-/-}$ mutants

In order to better understand the effects of Pax6 on *Dll1*, in situ hybridisation analysis of *Dll1* gene expression in *Pax6*$^{-/-}$ mutants was carried out in a developmental series of embryonic stages E11.5-E13.5, spanning the peak of neurogenesis. WT littermates acted as controls. Due to the fact that *Dll1* was suggested as a potential indirect target of Pax6 by Sansom *et al*., 2009, it was anticipated that Dll1 gene expression would be altered in *Pax6*$^{-/-}$ embryos.

At E11.5, *Dll1* was observed to have a punctate expression pattern throughout the telencephalic vesicles (Figure 3.1 A-C) and the diencephalon (Figure 3.1 B-C) of WT embryos. A punctate expression pattern was also observed in telencephalic vesicles (Figure 3.1 D-F) and diencephalon of *Pax6*$^{-/-}$ mutant embryos (Figure 3.1 E-F). *Dll1* expression remained uniform throughout the cortex and no obvious gradient was observed from a rostral to caudal position. No striking difference in *Dll1* expression was observed between WT controls and *Pax6*$^{-/-}$ mutants at a low powered magnification (Figure 3.1 A-F). A comparison of *Dll1* expression between WT controls and *Pax6*$^{-/-}$ mutants at a higher power of magnification suggested that the number of cells expressing *Dll1* may be reduced throughout the developing cortex. The cerebral cortex of *Pax6*$^{-/-}$ mutant embryos also appeared notably thinner, particularly in rostral cortical regions, in comparison to the cortex of WT controls (Figure 3.1 G-L).

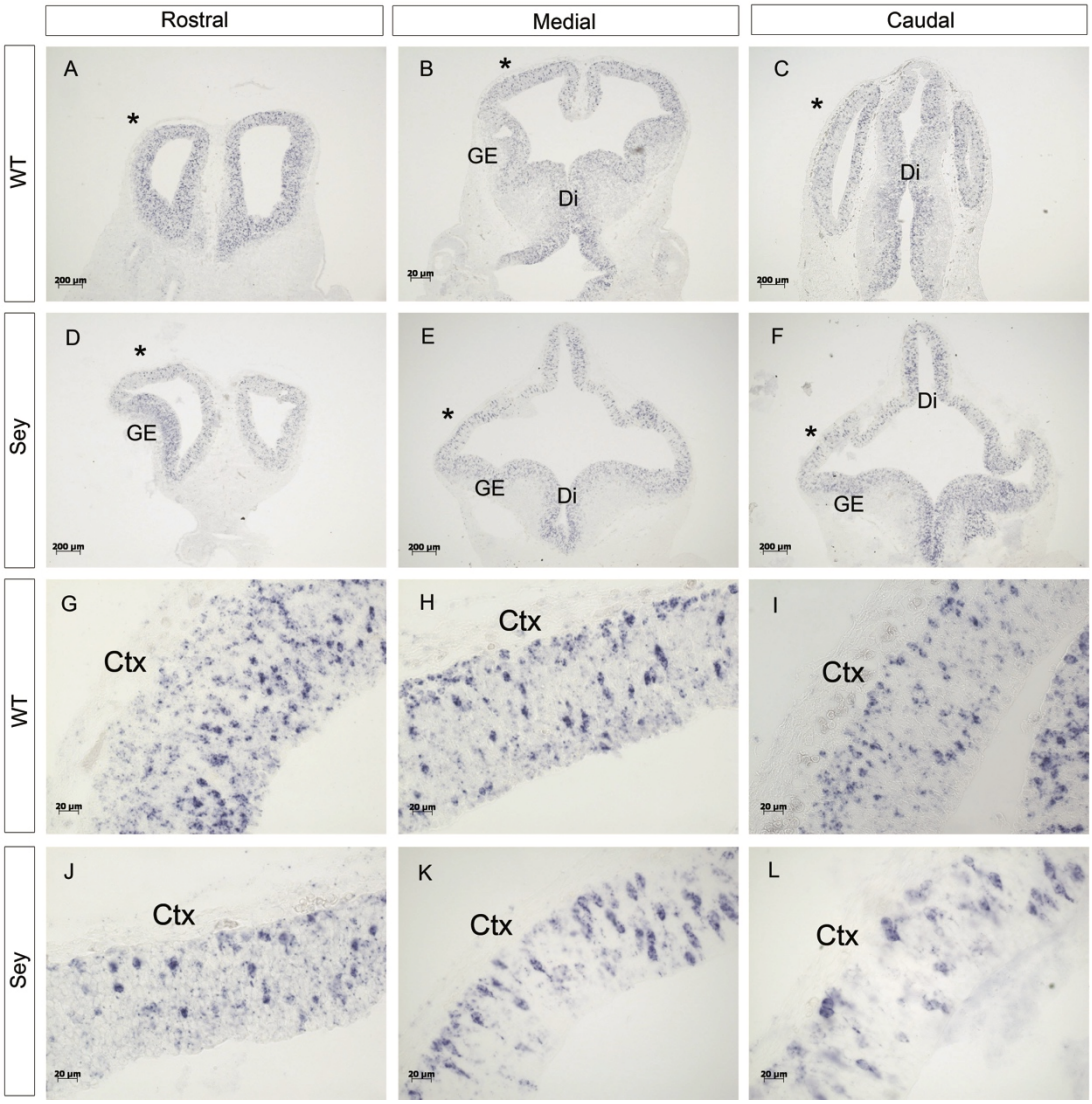

Figure 3.1 *Dll1* gene expression in the developing forebrain of *Pax6*$^{-/-}$ embryos at E11.5.

(A-C) *Dll1* gene expression in a WT control embryo. (A) *Dll1* expression in the rostral region of the WT forebrain. (B) *Dll1* expression in the medial region of the WT forebrain. (C) *Dll1* expression in the caudal region of the WT forebrain. (D-F) *Dll1* expression in a Sey mutant embryo. (D) *Dll1* expression in the rostral region of the Sey forebrain. (E) *Dll1* expression in the medial region of the Sey forebrain. (F) *Dll1* expression in the caudal region of the Sey forebrain. (G-I) *Dll1*s punctate expression pattern in the developing cerebral cortex of WT control embryos at E11.5. (J-L) The number of *Dll1* expressing cells appears reduced in the cortex of Sey mutant embryos at E11.5. (A-F) Scale bars = 200µm. (G-L) Scale bars = 20µm. Sey = *Pax6*$^{-/-}$. WT = *Pax6*$^{+/+}$. * indicates the cortex and is the area of cortex that is

shown at higher magnification in G-L. GE = ganglionic eminence. Di = diencephalon. Ctx = cortex. (N=3 embryos).

At E12.5, *Dll1* was observed to have a similarly punctate expression pattern throughout the telencephalic vesicles (Figure 3.2 A-C) and the diencephalon (Figure 3.2 B-C) of WT embryos and *Pax6*$^{-/-}$ embryos (Figure 3.2 D-F and E-F). The number of cells expressing *Dll1* appears to be higher at E12.5 (Figure 3.2) when compared to E11.5 (Figure 3.2). *Dll1* expression remains uniform throughout the cortex at E12.5 and no obvious difference was observed at a low magnification between WT control embryos and *Pax6*$^{-/-}$ mutants (Figure 3.2 A-F). Examination of the cortex at a higher power magnification also observed a potential decrease in the number of *Dll1* expressing cells in *Pax6*$^{-/-}$ mutants (Figure 3.2 J-L) when compared to WT controls (Figure 3.2 G-I).

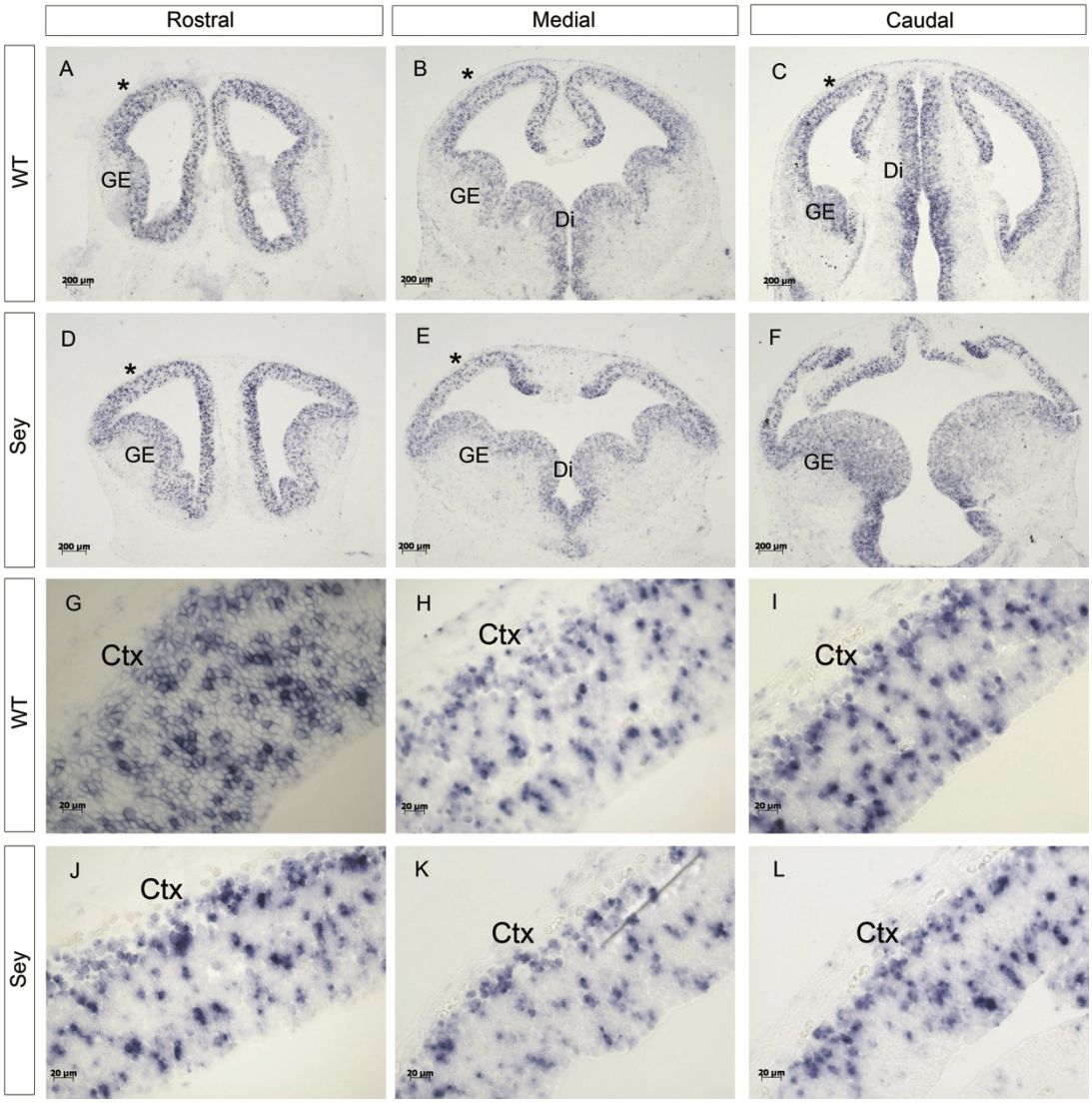

Figure 3.2 *Dll1* gene expression in the developing forebrain of *Pax6*$^{-/-}$ embryos at E12.5

(A-C) *Dll1* gene expression in a WT control embryo. (A) *Dll1* expression in the rostral region of the WT forebrain. (B) *Dll1* expression in the medial region of the WT forebrain. (C) *Dll1* expression in the caudal region of the WT forebrain. (D-F) *Dll1* expression in a Sey mutant embryo. (D) *Dll1* expression in the rostral region of the Sey forebrain. (E) *Dll1* expression in the medial region of the Sey forebrain. (F) *Dll1* expression in the caudal region of the Sey forebrain. (G-I) *Dll1*s punctate expression pattern in the developing cerebral cortex of WT control embryos at E12.5. (J-L) The number of *Dll1* expressing cells appears reduced in the cortex of Sey mutant embryos at E12.5. (A-F) Scale bars = 200µm. (G-L) Scale bars = 20µm. Sey = *Pax6*$^{-/-}$. WT = *Pax6*$^{+/+}$. * indicates the cortex and is the area of cortex that is shown at higher magnification in G-L. GE = ganglionic eminence. Di = diencephalon. Ctx = cortex. (N=3 embryos).

At E13.5, the punctate expression pattern of *Dll1* remains consistent with the expression observed at E11.5 and E12.5. *Dll1* expression remains consistent throughout the telencephalic vesicles (Figure 3.3 A-C) and diencephalon (Figure 3.3 B-C) in WT controls and in *Pax6*$^{-/-}$ mutants (Figure 3.3 D-F and E-F). In WT embryos, *Dll1* expression appears to be denser in the VZ of the developing cortex when compared to the SVZ. This difference is evident in the rostral and medial regions of the cortex (Figure 3.3 A-B) but does not appear to be the case in the caudal region of the cortex (Figure 3.3 C). In contrast, *Pax6*$^{-/-}$ embryos do not display denser expression of *Dll1* in the VZ (Figure 3.3 D-F). Analysis of the cortex at a higher magnification also presented a likely reduction in the number of cells expressing *Dll1* in *Pax6*$^{-/-}$ mutants (Figure 3.3 G-I) when compared to WT controls (Figure 3.3 J-L)

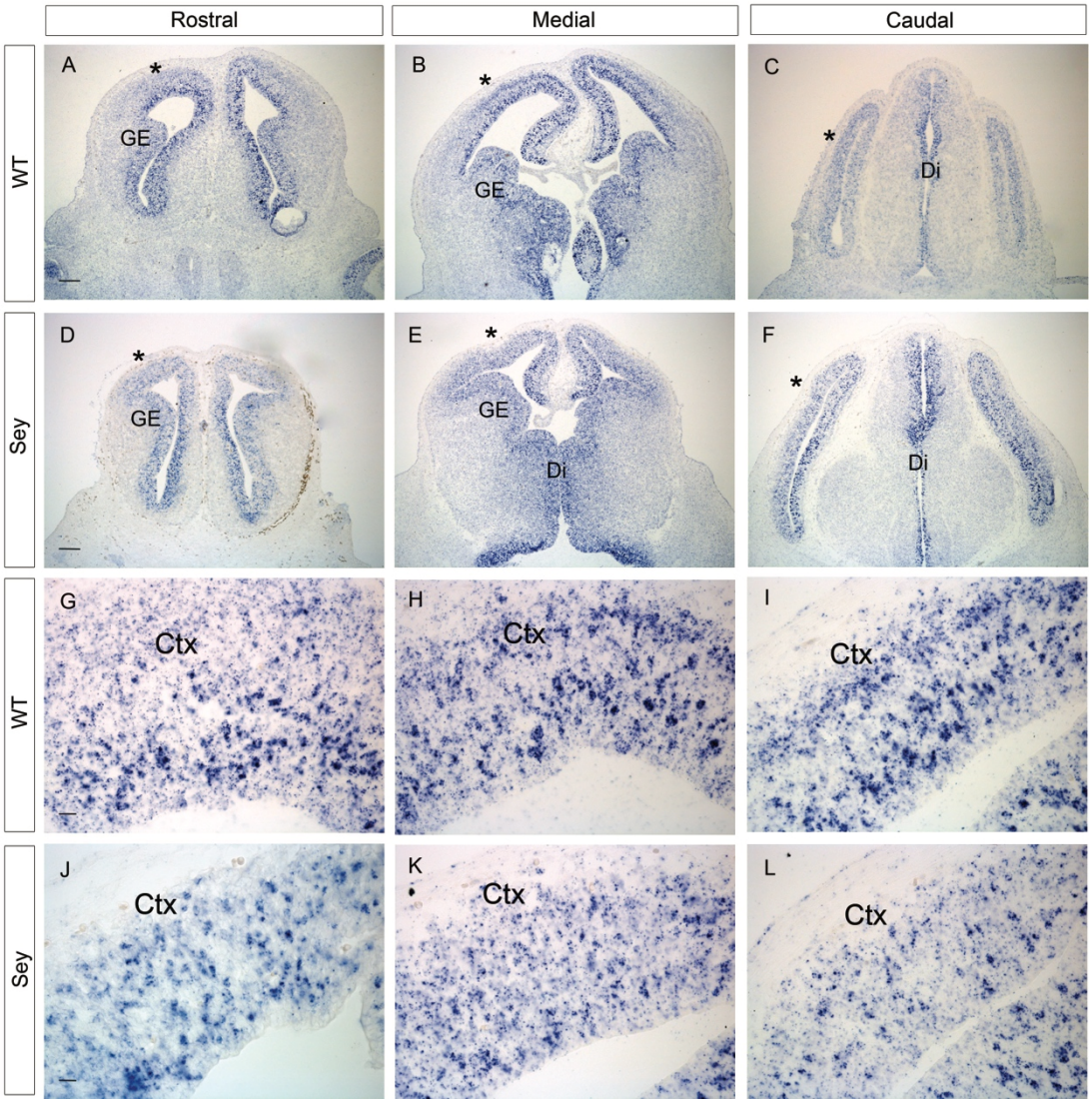

Figure 3.3 *Dll1* gene expression in the developing forebrain of *Pax6*$^{-/-}$ embryos at E13.5

(A-C) *Dll1* gene expression in a WT control embryo. (A) *Dll1* expression in the rostral region of the WT forebrain. (B) *Dll1* expression in the medial region of the WT forebrain. (C) *Dll1* expression in the caudal region of the WT forebrain. (D-F) *Dll1* expression in a Sey mutant embryo. (D) *Dll1* expression in the rostral region of the Sey forebrain. (E) *Dll1* expression in the medial region of the Sey forebrain. (F) *Dll1* expression in the caudal region of the Sey forebrain. (G-I) *Dll1*s punctate expression pattern in the developing cerebral cortex of WT control embryos at E13.5 Expression appears to be denser in the VZ. (J-L) The number of *Dll1* expressing cells appears reduced in the cortex of Sey mutant embryos at E13.5. (A-F) Scale bars = 200µm. (G-L) Scale bars = 20µm. Sey = *Pax6*$^{-/-}$. WT = *Pax6*$^{+/+}$. * indicates the cortex and is the area of cortex that is shown at higher magnification in G-L. GE = ganglionic

eminence. Di = diencephalon. Ctx = cortex. (N=3 embryos). Analysis carried out by project student Gabrielle Clark.

Analysis of *Dll1* gene expression in *Pax6*$^{-/-}$ embryos identified that there appeared to be less *Dll1* expressing cells when compared to WT control littermates. However, the difference in expression is very subtle and could only be seen at a high power of magnification. It was concluded that the images would need to be quantified by cell count in order to confirm that there was a reduction in the mutant embryos. It was also concluded that it would of interest to observe the effects of different levels of Pax6 on *Dll1* expression in order to learn more about the relationship between the two genes.

3.3 Analysis of *Dll1* gene expression in *PAX77* mutants

Due to the fact that *Dll1* expression appeared reduced in some areas of cortex at E11.5-E13.5 in *Pax6*$^{-/-}$ embryos, in situ hybridisation analysis of *Dll1* gene expression in *PAX77* mutants was carried out in a developmental series of embryonic stages E11.5-E13.5, spanning the peak of neurogenesis. WT littermates acted as controls. As *Dll1* expression appeared reduced in *Pax6*$^{-/-}$ embryos, it was anticipated that Dll1 expression would increase in the PAX77 embryos as they overexpress Pax6.

At E11.5, both WT control embryos and *PAX77* mutant embryos have a punctate expression pattern, identical to the pattern observed in the *Pax6*$^{-/-}$ mutant embryos and their WT littermates. *Dll1* expression remains uniform throughout the telencephalic vesicles and the diencephalon of both WT (Figure 3.4 A-C and B-C) and *PAX77* embryos (Figure 3.4 D-F and E-F). No difference in expression pattern was detected in *PAX77* embryos when compared to their WT littermates at a low magnification (Figure 3.4 A-C and D-F). No difference in expression pattern was detected in the cortex of *PAX77* mutants (Figure 3.4 G-I) compared to WT controls (Figure 3.4 J-L) when analysed at a higher magnification.

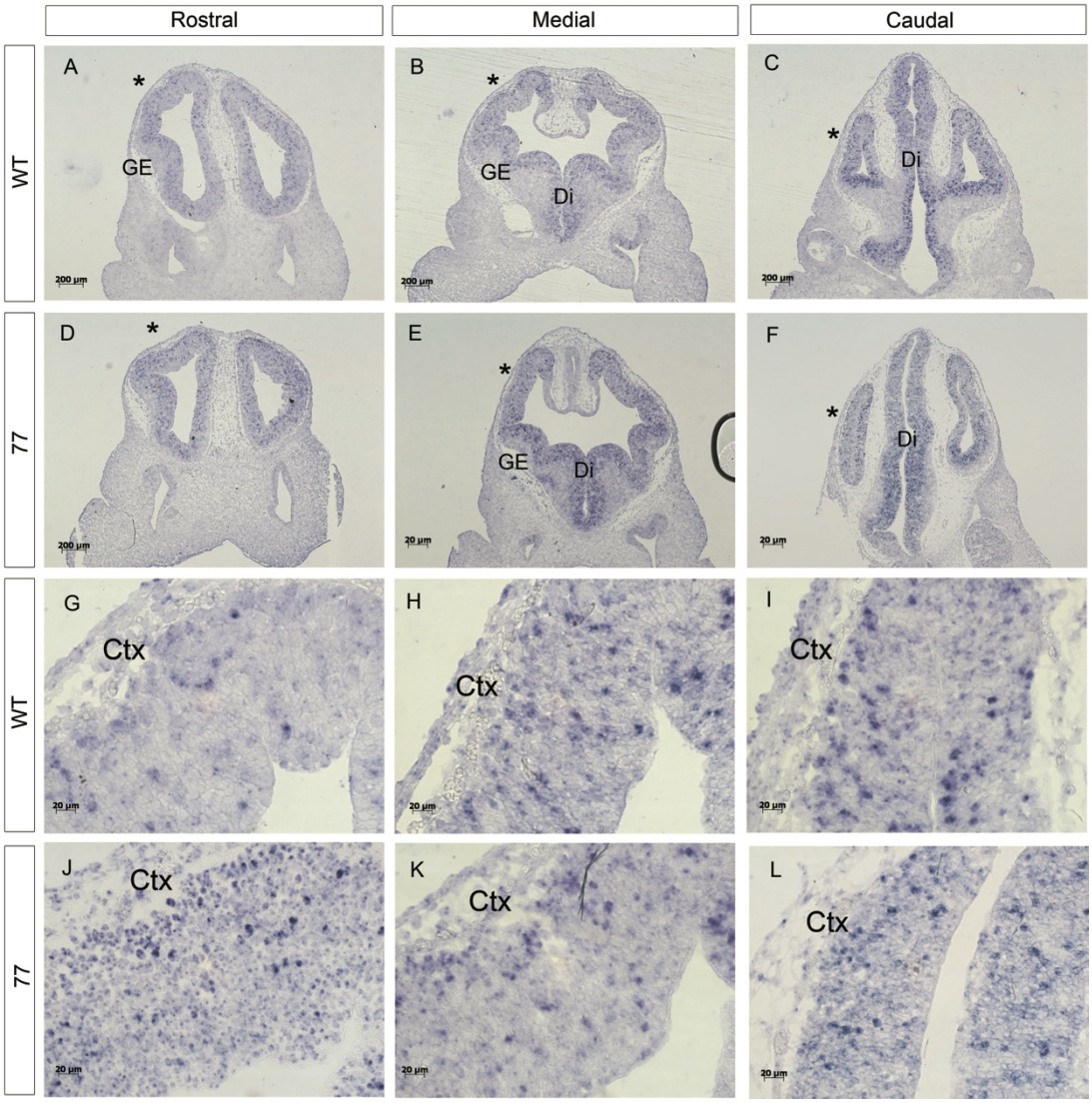

Figure 3.4 *Dll1* gene expression in the developing forebrain of *PAX77* embryos at E11.5

(A-C) *Dll1* gene expression in a WT control embryo. (A) *Dll1* expression in the rostral region of the WT forebrain. (B) *Dll1* expression in the medial region of the WT forebrain. (C) *Dll1* expression in the caudal region of the WT forebrain. (D-F) *Dll1* expression in a *PAX77* mutant embryo. (D) *Dll1* expression in the rostral region of the *PAX77* forebrain. (E) *Dll1* expression in the medial region of the *PAX77* forebrain. (F) *Dll1* expression in the caudal region of the *PAX77* forebrain. (G-I) *Dll1*s punctate expression pattern in the developing cerebral cortex of WT control embryos at E11.5. (J-L) No obvious difference is evident in the cortex *PAX77* mutant embryos when compared to WT controls at E11.5. (A-F) Scale bars = 200µm. (G-L) Scale bars = 20µm. * indicates the cortex and is the area of cortex that is

shown at higher magnification in G-L. GE = ganglionic eminence. Di = diencephalon. Ctx = cortex. (N=3 embryos).

At E12.5, *PAX77* mutant embryos exhibit the punctate expression pattern as their WT control littermates (Figure 3.5 A-C and D-F). Uniform *Dll1* expression is observed throughout the telencephalic vesicles (Figure 3.5 A-C) and the diencephalon (Figure 3.5 B-C) in WT controls and in *PAX77* mutants (Figure 3.5 D-F and E-F). No difference in expression between WT and *PAX77* embryos was detected at a low magnification (Figure 3.5 A-C and D-F) or at a higher magnification (Figure 3.5 G-I and J-L).

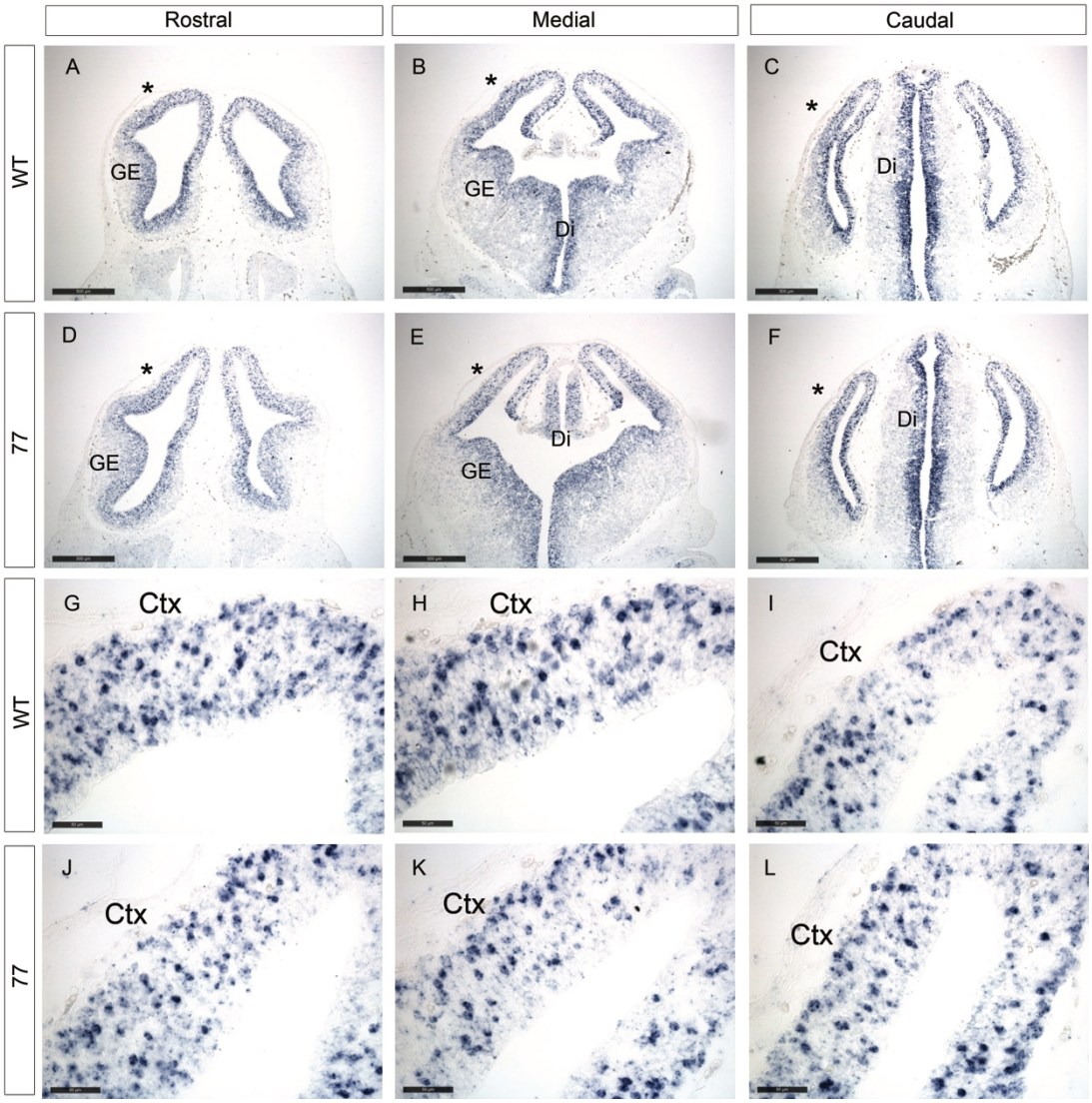

Figure 3.5 *Dll1* gene expression in the developing forebrain of *PAX77* embryos at E12.5

(A-C) *Dll1* gene expression in a WT control embryo. (A) *Dll1* expression in the rostral region of the WT forebrain. (B) *Dll1* expression in the medial region of the WT forebrain. (C) *Dll1* expression in the caudal region of the WT forebrain. (D-F) *Dll1* expression in a *PAX77* mutant embryo. (D) *Dll1* expression in the rostral region of the *PAX77* forebrain. (E) *Dll1* expression in the medial region of the *PAX77* forebrain. (F) *Dll1* expression in the caudal region of the *PAX77* forebrain. (G-I) *Dll1*s punctate expression pattern in the developing cerebral cortex of WT control embryos at E12.5. (J-L) No obvious difference is evident in the cortex *PAX77* mutant embryos when compared to WT controls at E12.5. (A-F) Scale bars = 200µm. (G-L) Scale bars = 20µm. * indicates the cortex and is the area of cortex that is

shown at higher magnification in G-L. GE = ganglionic eminence. Di = diencephalon. Ctx = cortex. (N=3 embryos). Analysis carried out by project student Milena Blaga.

At E13.5, both WT and *PAX77* embryos continue to display a uniformly punctate expression pattern for *Dll1* throughout the telencephalic vesicles (Figure 3.6 A-C) and diencephalon (B-C). At a higher magnification, WT embryos display an increase in *Dll1* expressing cells in the VZ (Figure 3.6 G-I) when compared to the SVZ. This increase in *Dll1* expression does not appear to be present in the VZ of *PAX77* littermates (Figure 3.6 J-L).

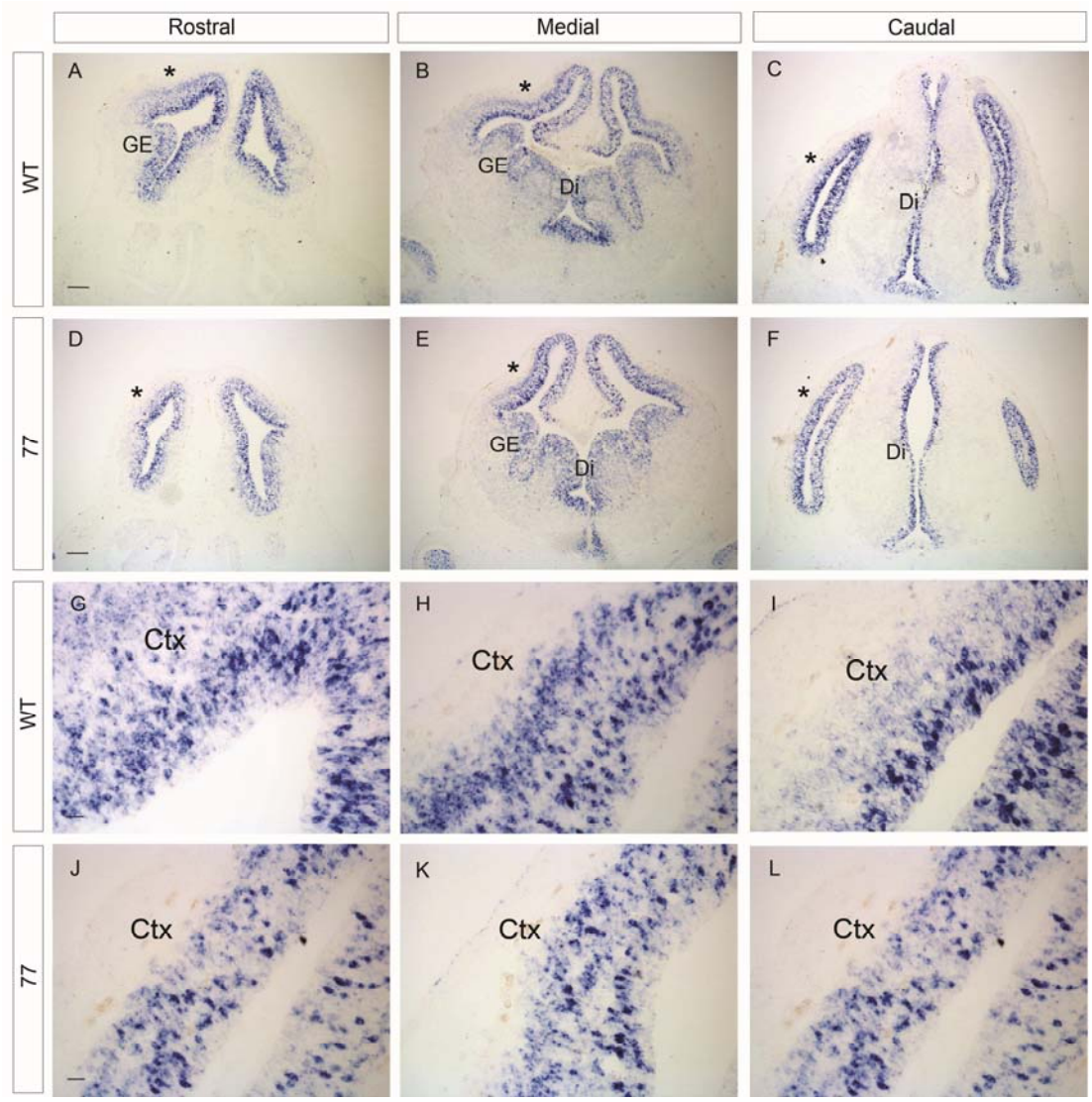

Figure 3.6 *Dll1* gene expression in the developing forebrain of *PAX77* embryos at E13.5

(A) *Dll1* expression in the rostral region of the WT forebrain. (B) *Dll1* expression in the medial region of the WT forebrain. (C) *Dll1* expression in the caudal region of the WT forebrain. (D-F) *Dll1* expression in a *PAX77* mutant embryo. (D) *Dll1* expression in the rostral region of the *PAX77* forebrain. (E) *Dll1* expression in the medial region of the *PAX77* forebrain. (F) *Dll1* expression in the caudal region of the *PAX77* forebrain. (G-I) *Dll1* appears to be most densely expressed in the VZ of the developing cortex. (J-L) The denser expression of *Dll1* in the VZ appears to be lost in *PAX77* mutants when compared to WT controls. (A-F) Scale bars = 200µm. (G-L) Scale bars = 20µm. * indicates the cortex and is the area of cortex that is shown at higher magnification in G-L. GE = ganglionic eminence. Di

= diencephalon. Ctx = cortex. (N=3 embryos). Analysis carried out by project student Gabrielle Clark.

Analysis of *Dll1* gene expression in *PAX77* embryos identified no discernable difference when compared to WT control embryos. However, quantification of Dll1 expression would be required to confirm that there is no difference in the *PAX77* mutants.

3.4 Analysis of *Dll1* gene expression in cKO Fp6 mutants

While *Pax6*$^{-/-}$ embryos provide an excellent model to study the effects of a loss of Pax6 on cortical development, the fact that Pax6 is never present allows for compensation from other genes that could reduce the detrimental effect of a loss of Pax6 expression. In order to combat this potential compensatory effect, a conditional knockout for Pax6 exclusively in the cortex was also used. *In* situ hybridisation analysis of *Dll1* gene expression in *Emx1CreEr*^{T2}*;Pax6*$^{loxP/loxP}$ (herein referred to as 'cKO') was carried out in a developmental series of embryonic stages E12.5-E13.5. Heterozygous littermates for *Emx1CreEr*^{T2}*;Pax6*$^{loxP/loxP}$ embryos (herein referred to as 'controls') were used at controls. Embryonic stage E11.5 was excluded from the series due to the fact that previous analysis of the cKO mutants carried out in our lab has indicated that tamoxifen injections at E9.5 do not sufficiently knock down *Pax6* by E11.5. As a result, E11.5 was excluded from analysis.

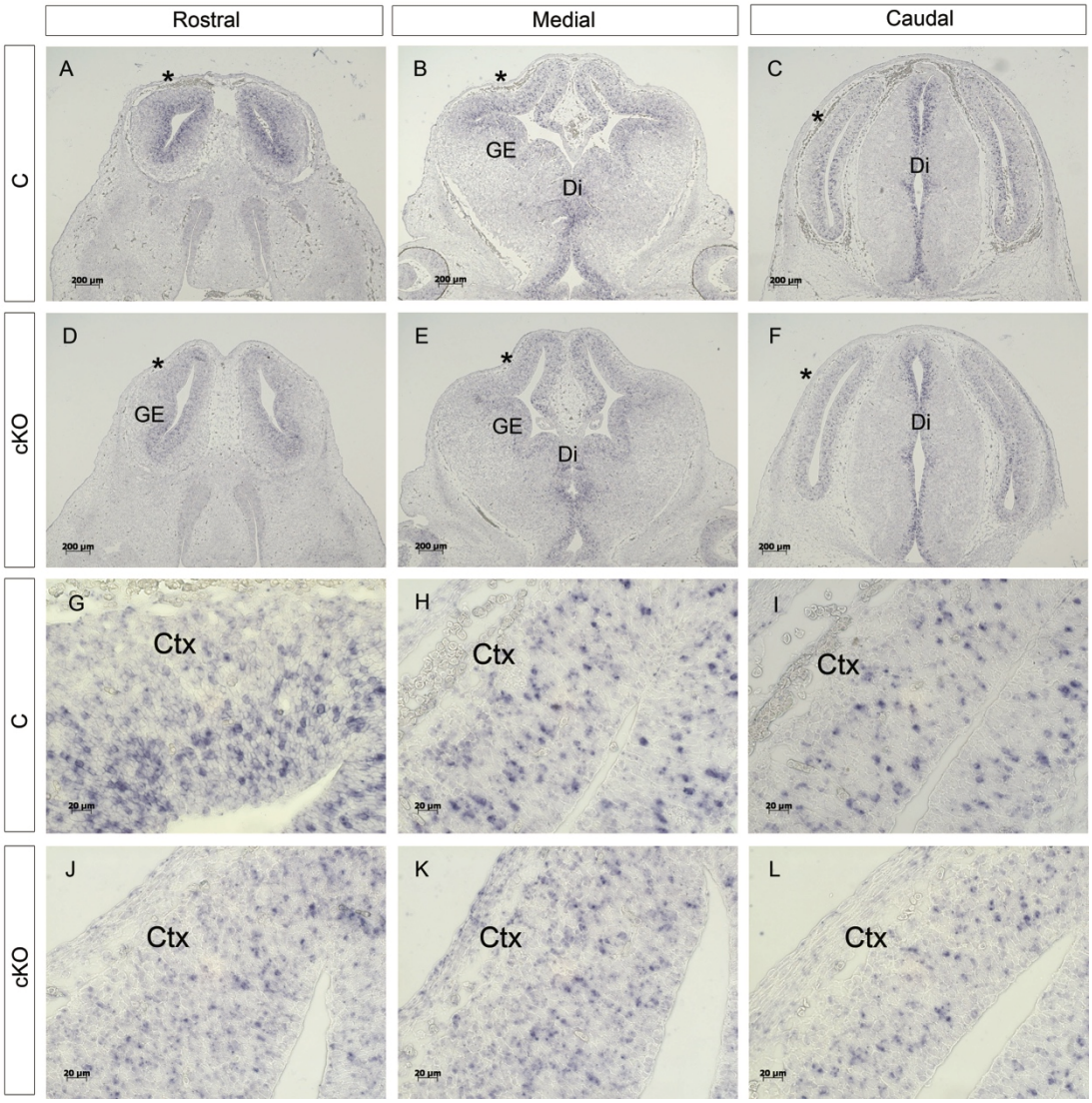

Figure 3.7 *Dll1* gene expression in the developing forebrain of cKO embryos at E12.5

(A-C) *Dll1* gene expression in a WT control embryo. (A) *Dll1* expression in the rostral region of the WT forebrain. (B) *Dll1* expression in the medial region of the WT forebrain. (C) *Dll1* expression in the caudal region of the WT forebrain. (D-F) *Dll1* expression in a cKO mutant embryo. (D) *Dll1* expression in the rostral region of the cKO forebrain. (E) *Dll1* expression in the medial region of the cKO forebrain. (F) *Dll1* expression in the caudal region of the cKO forebrain. (G-I) *Dll1*s punctate expression pattern in the developing cerebral cortex of WT control embryos at E12.5. (J-L) The number of *Dll1* expressing cells appears reduced in the cortex of cKO mutant embryos at E12.5. (A-F) Scale bars = 200µm. (G-L) Scale bars = 20µm. * indicates the cortex and is the area of cortex that is shown at higher magnification in G-L. GE = ganglionic eminence. Di = diencephalon. Ctx = cortex. (N=3 embryos).

At E12.5, *Dll1* expression remained punctate and uniform throughout the telencephalic vesicles and the diencephalon of control (Figure 3.7 A-C and B-C) and cKO mutant (Figure 3.7 D-F and E-F) embryos. No difference in expression was observed at a lower magnification when comparing cKO mutants (Figure 3.7 B-C) to their control littermates (Figure 3.7 A-C). A potential reduction in the staining intensity of *Dll1* was observed in the cKO cortex at a higher power magnification (Figure 3.7 J-L) when compared to the cortex of control embryos (Figure 3.7 G-I). At E13.5, *Dll1* expression was also observed to be punctate throughout the telencephalic vesicles and the diencephalon of control embryos (Figure 3.8 A-C and B-C) and cKO littermates (Figure 3.8 D-F and E-F). No difference in the expression of *Dll1* was observed between control embryos and cKO embryos when observed at a low power of magnification. Images taken at a high power magnification suggested that staining could potentially be reduced in cKO embryos (Figure 3.8 G-L). As was the case with *Pax6*$^{-/-}$ analysis at E13.5, *Dll1* expression appears to be denser in the VZ of the cortex of both control embryos (Figure 3.8 G-I) and cKO mutants (Figure 3.8 J-L).

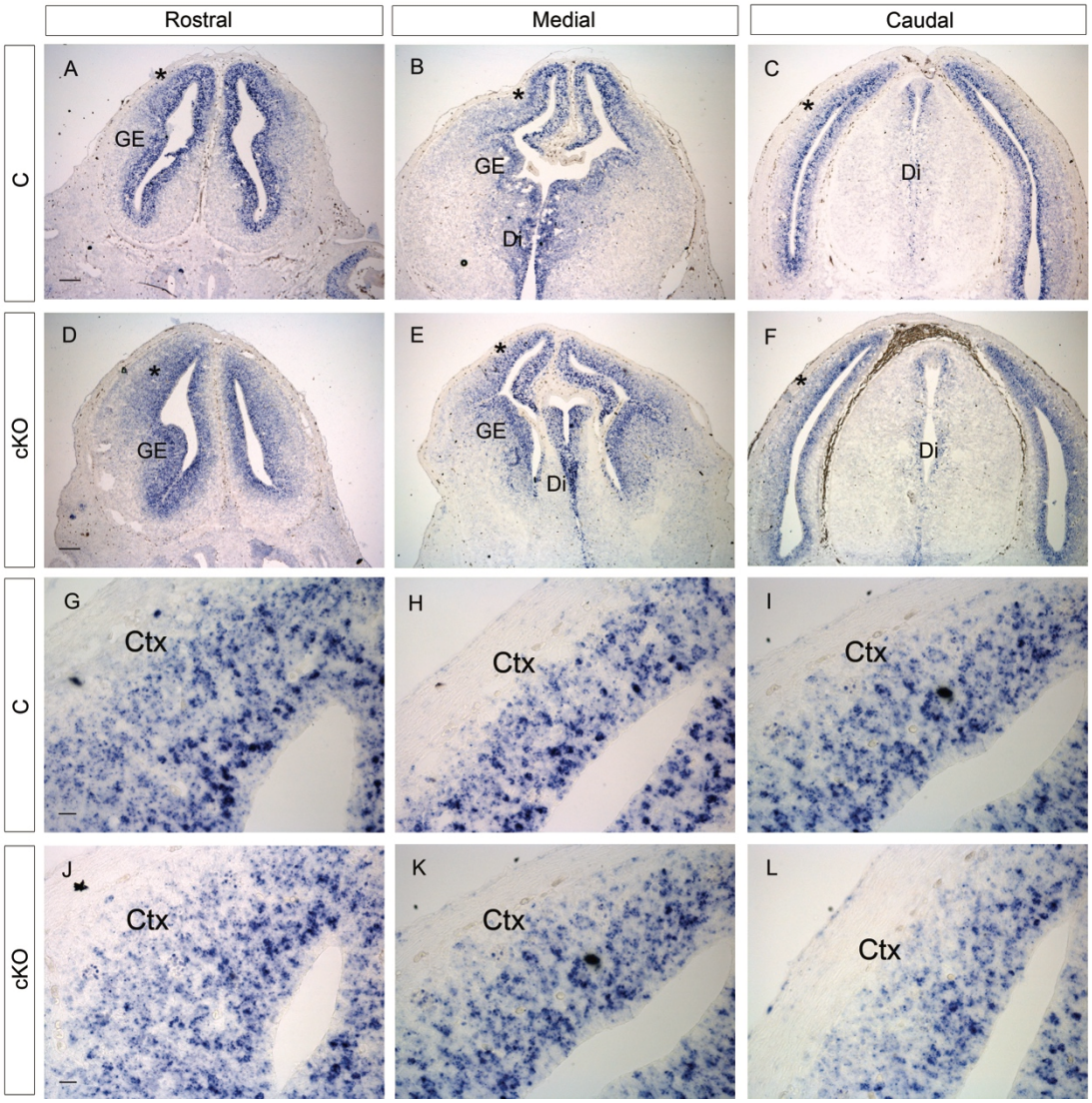

Figure 3.8 *Dll1* gene expression in the developing forebrain of cKO embryos at E13.5

(A-C) *Dll1* gene expression in a WT control embryo. (A) *Dll1* expression in the rostral region of the WT forebrain. (B) *Dll1* expression in the medial region of the WT forebrain. (C) *Dll1* expression in the caudal region of the WT forebrain. (D-F) *Dll1* expression in a cKO mutant embryo. (D) *Dll1* expression in the rostral region of the cKO forebrain. (E) *Dll1* expression in the medial region of the cKO forebrain. (F) *Dll1* expression in the caudal region of the cKO forebrain. (G-I) *Dll1*s punctate expression pattern in the developing cerebral cortex of WT control embryos at E13.5. *Dll1* expression appears denser in the VZ. (J-L) The number of *Dll1* expressing cells appears reduced in the cortex of cKO mutant embryos at E13.5. (A-F) Scale bars = 200µm. (G-L) Scale bars = 20µm. * indicates the cortex and is the area of cortex that is shown at higher magnification in G-L. GE = ganglionic eminence. Di =

diencephalon. Ctx = cortex. (N=3 embryos). Analysis carried out by project student Gabrielle Clark.

As was the case with the *Pax6*$^{-/-}$ embryos, analysis of *Dll1* expression in cKO mutants suggested a decrease in the number of *Dll1* expressing cells in the developing cortex when compared to WT control littermates. However, due to the subtlety of the difference observed, it was concluded that quantification of the images by cell count analysis would be required for confirmation.

3.5 Cell count analysis of *Dll1* gene expression in *Pax6*$^{-/-}$ mutants

In order to confirm the observations made by in situ hybridisation analysis, cell counts of the images were performed as described in chapter 2 (Chapter 2.18) (Figure 3.9). Cell counts were performed on *Dll1* in situ slides and H&E slides. H&E cell counts allowed us to assess whether total cell density was affected in the cortex of mutant embryos when compared to their control littermates. This allowed us to validate any significant difference in *Dll1* density.

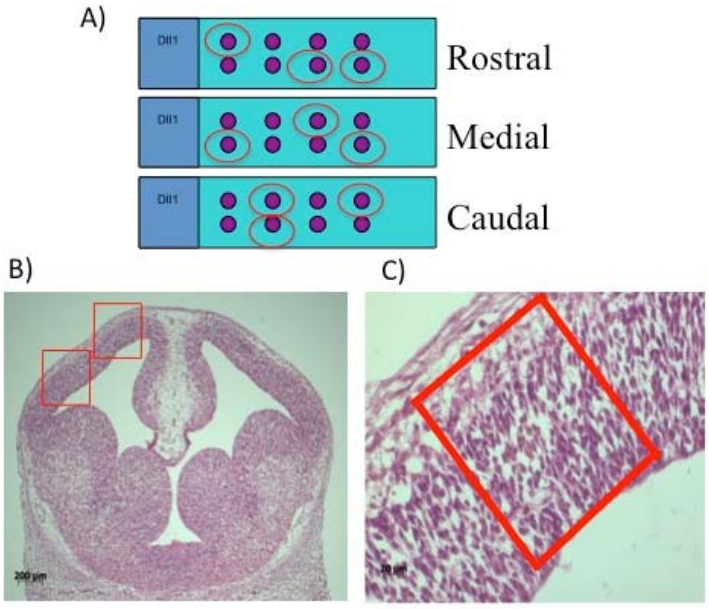

Figure 3.9 Example of cell count sample selection

(A) Three replicate sections were selected for each cortical region. (B) An example of the dorsal and ventral regions of the cortex selected for cell counts. (C) An example of a cell count area produced by measuring the width of the cortex for each sample.

3.5.1 E11.5

Two-way ANOVA results for the dorsal region of the developing cortex (Figure 3.10 A) determined that there were no interaction, region or genotype effects found when comparing the WT control and *Pax6*$^{-/-}$ mutant data sets, with all P values found to be non-significant (NS). All Tukey multiple comparison tests were also not significant. The ventral region of the cortex (Figure 3.9 B) was found to have no interaction or region effect, but did have a genotype effect (P=0.0331) when analysis by two-way ANOVA was carried out at E11.5. However, Tukey's multiple comparison tests were all non-significant.

Two-way ANOVA analysis of the total density of cells in the dorsal region of WT and *Pax6*$^{-/-}$ cortices (Figure 3.9 C) reported that there were no interaction, region or genotype effects, and that all Tukey's multiple comparison tests were non-significant. However, in the ventral region of the cortex (Figure 3.9 D), analysis by two-way ANOVA reported a region effect (P=0.0195) and Tukey's multiple comparison tests yielded no significant differences.

Figure 3.10 Cell density in the cortex of *Pax6*$^{-/-}$ embryos at E11.5

(A) *Dll1* density in the dorsal region of the cortex. (B) *Dll1* density in the ventral region of the cortex. (C) Total cell density in the dorsal region of the cortex. (D) Total cell density in the ventral region of the cortex. (A-B) No significant decrease in *Dll1* density was detected when comparing Sey mutants to WT controls. (C-D) No significant decrease in cell density was detected when comparing Sey mutants to WT controls. Sey = *Pax6*$^{-/-}$. WT = *Pax6*$^{+/+}$. N=3.

3.5.2 E12.5

Statistical analysis of *Dll1* expression in the dorsal region of the developing cortex at E12.5 (Figure 3.11 A) demonstrated a genotype effect (P=0.0004) between Wt and

Pax6$^{-/-}$ embryos. The implementation of Tukey's multiple comparison tests reported a significant difference between caudal Wt: caudal *Pax6*$^{-/-}$ (P=0.0056). The ventral region of the developing cortex (Figure 3.10 B) showed a genotype effect (P= <0.0001) by two-way ANOVA, while Tukey's multiple comparison tests yielded a significant difference between rostral Wt: rostral *Pax6*$^{-/-}$ (P=0.0008), medial Wt: medial *Pax6*$^{-/-}$ (P=0.0003), caudal Wt: caudal *Pax6*$^{-/-}$ (P=0.0168).

Analysis of the total density of cells in the dorsal region of the developing cortex (Figure 3.10 C) by two-way ANOVA reported no interaction, region or genotype effect, and all Tukey's multiple comparison tests were not significant. However, analysis of the ventral region of the cortex (Figure 3.11 D) reported a region effect (P=0.0205) by two-way ANOVA and a significant difference between rostral *Pax6*$^{-/-}$: caudal *Pax6*$^{-/-}$ (P=0.0201) when analysed by Tukey's multiple comparison tests.

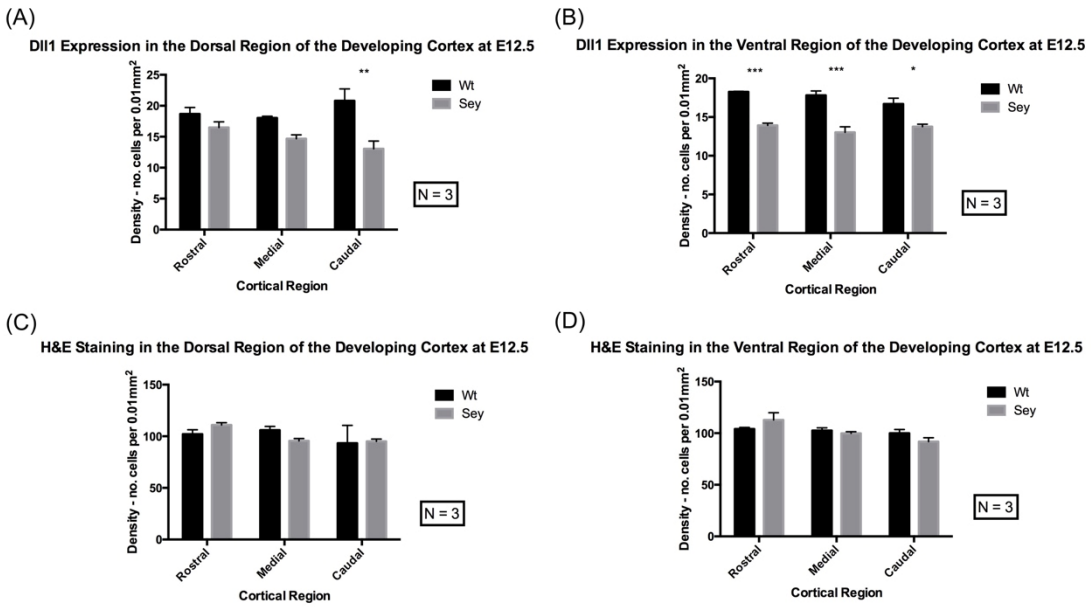

Figure 3.11 Cell density in the cortex of *Pax6*$^{-/-}$ embryos at E12.5

(A) *Dll1* density in the dorsal region of the cortex. A significant decrease in *Dll1* density is observed in the dorsal-caudal region of the cortex when comparing Sey to WT. (**P=0.0329). (B) *Dll1* density in the ventral region of the cortex. *Dll1* expression in the ventral region of the cortex in WT controls and Sey mutants. A significant decrease in Dl11 density was observed in all regions of the ventral cortex when comparing Sey mutants to WT controls. (Rostral ***P=0.0008, Medial ***P=0.0003, *P=0.0168). (C) Total cell density in the dorsal region of the cortex. (D) Total cell density in the ventral region of the cortex. (C-D) No significant decrease in cell density was detected when comparing Sey mutants to WT controls. Sey = *Pax6*$^{-/-}$. WT = *Pax6*$^{+/+}$. N=3.

3.5.3 E13.5

Two-way ANOVA testing carried out on Dll1 expression of samples from the dorsal region of the cortex at E13.5 (Figure 3.11 A) observed interaction (P=0.0292), region (P=0.0133) and genotype (P=<0.0001) effects. Further analysis by Tukey's multiple comparison testing found significant differences between rostral Wt: caudal Wt (P=0.0167); medial Wt: medial *Pax6*$^{-/-}$ (P=0.0141); caudal Wt: caudal *Pax6*$^{-/-}$ (P=0.0028). Evaluation of the ventral region of the cortex at E13.5 (Figure 3.12 B)

displayed a genotype effect (P=0.0118) but no significant differences were detected by Tukey's multiple comparison test.

Two-way ANOVA analysis of the total density of cells in the dorsal region of Wt and *Pax6*$^{-/-}$ cortices (Figure 3.11 C) reported that there was no interaction effect. However, a region effect (P=0.0325) and genotype effect (P=0.0475) were reported. All Tukey's multiple comparison tests were non-significant. However, in the ventral region of the cortex (Figure 3.11 D), analysis by two-way ANOVA reported a region effect (P=0.0006) but no interaction or genotype effect. Tukey's multiple comparison tests yielded a significant difference between rostral:Sey vs. caudal:Sey (P=0.0228) and medial:Wt vs. caudal:WT (p=0.0431).

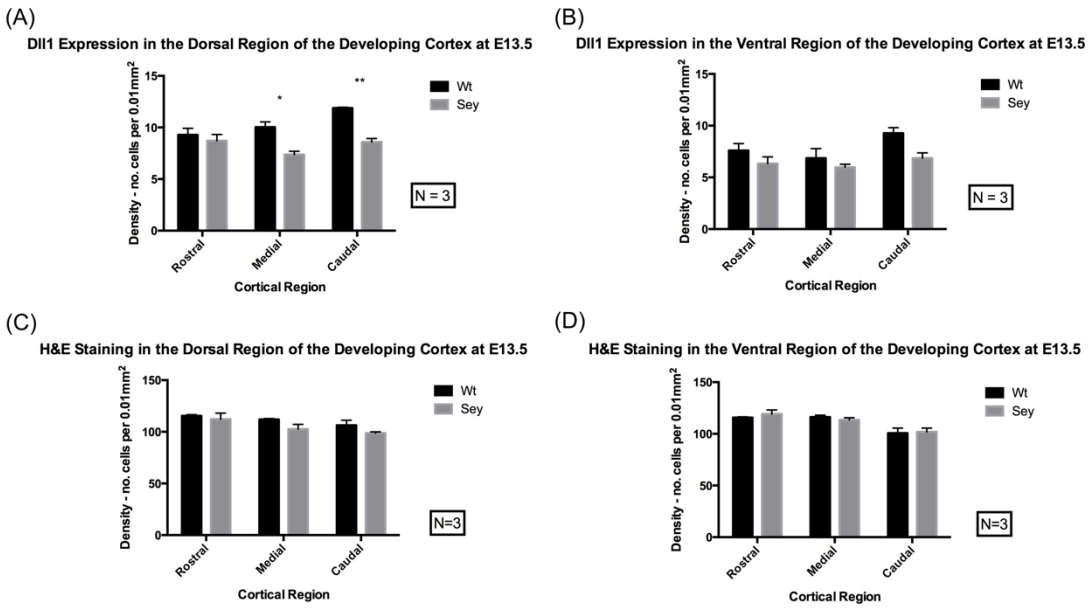

Figure 3.12 Cell density in the cortex of *Pax6*$^{-/-}$ embryos at E13.5

(A) *Dll1* density in the dorsal region of the cortex. A significant decrease in *Dll1* density is observed in the dorsal-medial and dorsal-caudal regions of the cortex when comparing Sey to WT. (* P=0.0118, ** P=0.0275). (B) *Dll1* density in the ventral region of the cortex. No significant decrease in *Dll1* density was observed in any ventral region of the cortex. *Dll1* expression in the ventral region of the cortex in WT controls and Sey mutants. (C) Total cell density in the dorsal region of the cortex. (D) Total cell density in the ventral region of the cortex. (C-D) No significant decrease in cell density was detected when comparing Sey mutants to WT controls. Sey = *Pax6*$^{-/-}$. WT = *Pax6*$^{+/+}$. N=3. Analysis carried out by project student Gabrielle Clark.

3.6 Cell count analysis of *Dll1* gene expression in *PAX77* mutants

3.6.1 E11.5

Analysis by two-way ANOVA of both the dorsal (Figure 3.12 A) and ventral (Figure 3.12 B) region of the cortex at E11.5 found no interaction, region or genotype effects, and all Tukey's multiple comparison tests were found to have no significant difference.

Two-way ANOVA analysis of the total density of cells in the dorsal (Figure 3.12 C) and ventral (Figure 3.12 D) regions of Wt and *PAX77* cortices reported that there were no interaction, region or genotype effects, and that all Tukey's multiple comparison tests were non-significant.

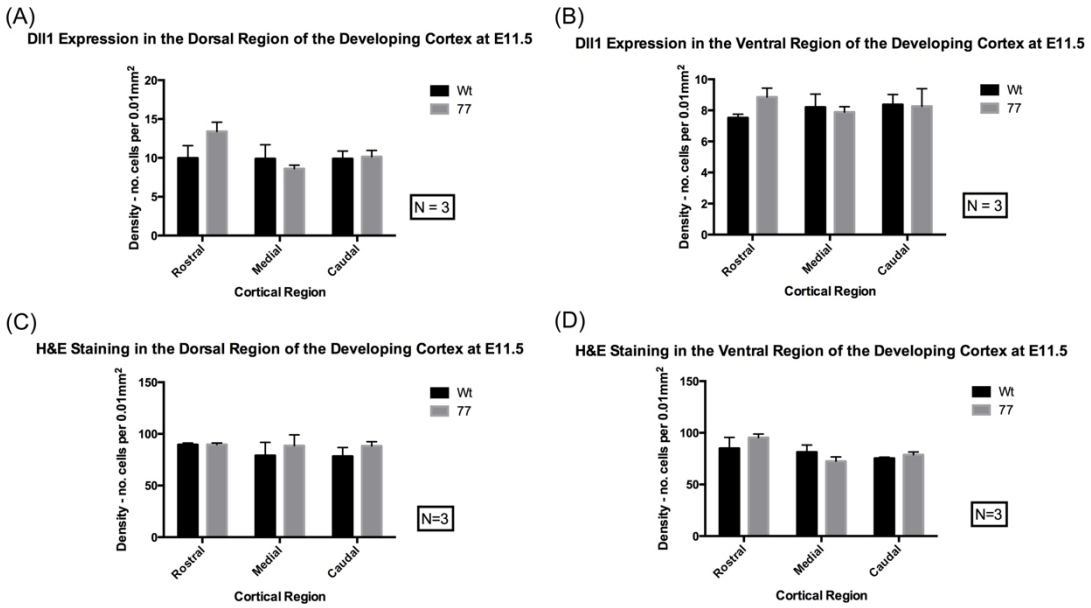

Figure 3.13 Cell density in the cortex of *PAX77* embryos at E11.5

(A) *Dll1* density in the dorsal region of the cortex. (B) *Dll1* density in the ventral region of the cortex. (C) Total cell density in the dorsal region of the cortex. (D) Total cell density in the ventral region of the cortex. (A-B) No significant difference in *Dll1* density was detected in the dorsal or ventral regions of the cortex when directly comparing cortical regions of WT controls and *PAX77* mutants. (C-D) No significant difference in total cell density was detected in the dorsal and ventral regions of the cortex when directly comparing cortical regions of WT controls and *PAX77* mutants. N=3.

3.6.2 E12.5

The dorsal region of the cortex (Figure 3.13 A) was found to have a region effect (P=0.0256) and a genotype effect (0.0022), while multiple comparison testing found

a significant difference between rostral Wt: Caudal *PAX77* (P=0.0147) and Medial Wt: Caudal *PAX77* (P=0.0248). However, the ventral region of the cortex (Figure 3.13 B) yielded no interaction, region or genotype effects, and all comparison tests were not significant.

Analysis of the total number of cells in both the dorsal (Figure 3.13 C) and ventral (Figure 3.13 D) regions of the cortex yielded no interaction, region or genotype effects by two-way ANOVA. All Tukey's multiple comparison tests for both regions were also not significant.

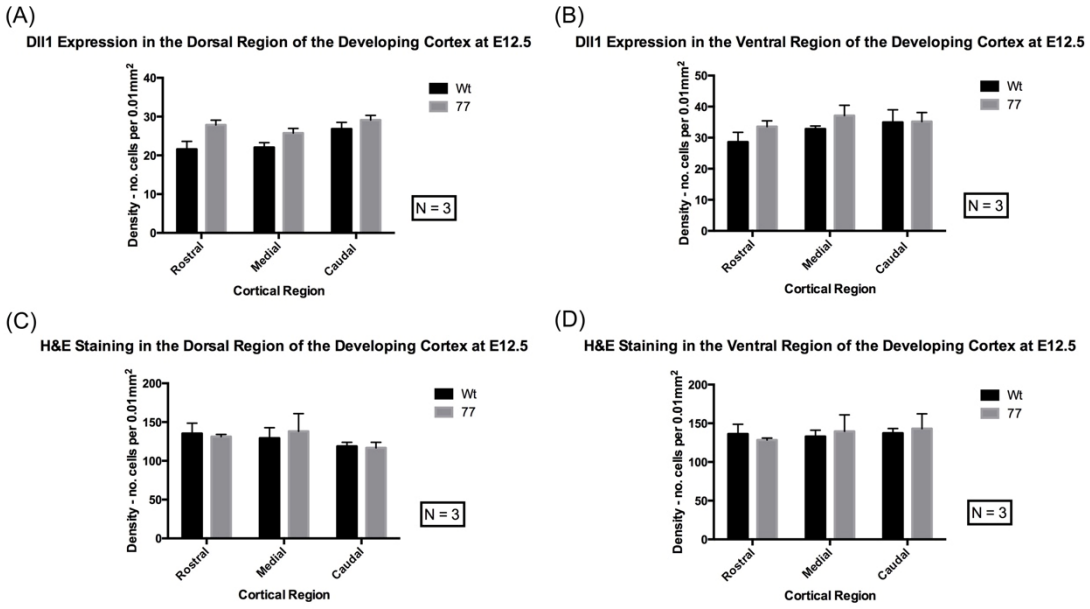

Figure 3.14 Cell density in the cortex of *PAX77* embryos at E12.5

(A) *Dll1* density in the dorsal region of the cortex. (B) *Dll1* density in the ventral region of the cortex. (C) Total cell density in the dorsal region of the cortex. (D) Total cell density in the ventral region of the cortex. (A-B) No significant difference in *Dll1* density was detected in the dorsal or ventral regions of the cortex when directly comparing cortical regions of WT controls and *PAX77* mutants. (C-D) No significant difference in total cell density was detected in the dorsal and ventral regions of the cortex when directly comparing cortical regions of WT controls and *PAX77* mutants. N=3. Analysis carried out by project student Milena Blaga.

3.6.3 E13.5

Analysis of the dorsal region of the cortex (Figure 3.14 A) and ventral region of the cortex (Figure 3.14 B) found no interaction, region or genotype effects at E13.5. All multiple comparison tests were reported as non-significant.

Two-way ANOVA analysis of the total density of cells in the dorsal (Figure 3.14 C) and ventral (Figure 3.14 D) regions of Wt and *PAX77* cortices reported that there were no interaction, region or genotype effects, and that all Tukey's multiple comparison tests were non-significant.

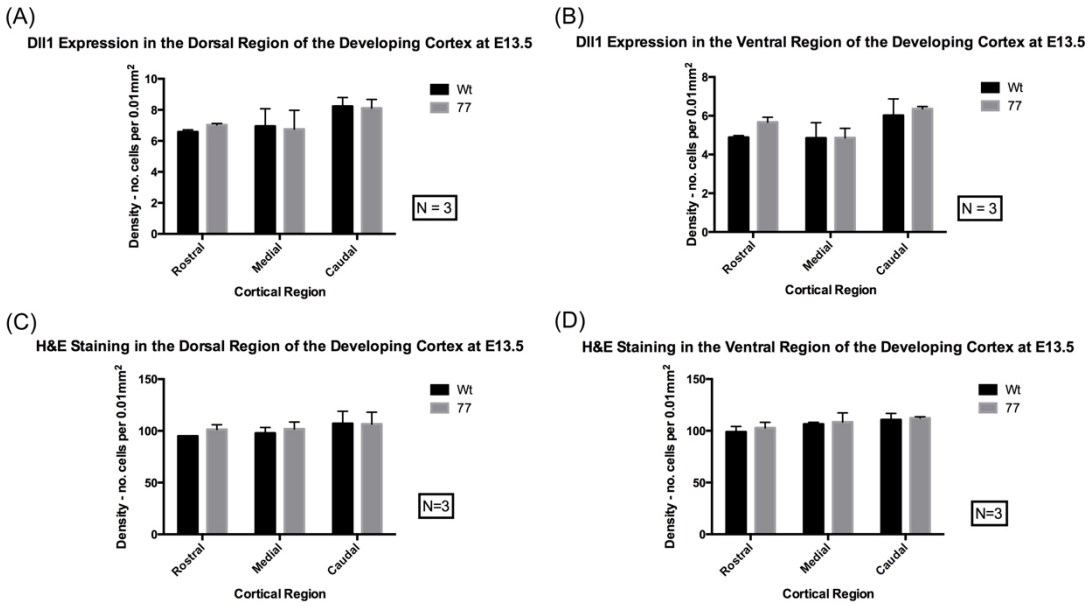

Figure 3.15 Cell density in the cortex of *PAX77* embryos at E13.5

(A) *Dll1* density in the dorsal region of the cortex. (B) *Dll1* density in the ventral region of the cortex. (C) Total cell density in the dorsal region of the cortex. (D) Total cell density in the ventral region of the cortex. (A-B) No significant difference in *Dll1* density was detected in the dorsal or ventral regions of the cortex when directly comparing cortical regions of WT controls and *PAX77* mutants. (C-D) No significant difference in total cell density was detected in the dorsal and ventral regions of the cortex when directly comparing cortical regions of WT controls and *PAX77* mutants. N=3. Analysis carried out by project student Gabrielle Clark.

3.7 Cell count analysis of *Dll1* gene expression in cKO mutants

3.7.1 E12.5

Analysis of *Dll1* expression in the dorsal region of the cortex at E12.5 (Figure 3.15 A) identified a genotype effect (P=<0.0001) when analysis by two-way ANOVA was carried out, but there were no reported interaction or region effects. A variety of significant differences between both region and genotype were reported by Tukey's multiple comparison tests: rostral C: rostral cKO (P=0.0046), medial C: medial cKO (P=0 Analysis of the ventral region of the cortex (Figure 3.15 B) detected an effect for both region (P=0.0043) and genotype (P=0.0003), while multiple comparison testing detected numerous significant differences between combinations of regions and genotype (Table 3.1)

Table 3.1 cKO E12.5 significant Tukey's testing

Tukey's Multiple Comparisons Test	**P Value**	**P Value Summary**
Rostral:C vs. Rostral:cKO	0.0046	**
Rostral:C vs. Medial:cKO	0.0022	**
Rostral:C vs. Caudal:cKO	0.0040	**
Rostral:cKO vs. Medial:C	0.0076	**
Rostral:cKO vs. Caudal:C	0.0075	**
Medial:C vs. Medial:cKO	0.0036	**
Medial:C vs. Caudal:cKO	0.0066	**
Medial:cKO vs. Caudal:C	0.0036	**
Caudal:C vs. Caudal:cKO	0.0065	**

Two-way ANOVA analysis of the total density of cells in the dorsal (Figure 3.15 C) region of control and cKO cortices reported that there were no interaction, region or genotype effects, and that all Tukey's multiple comparison tests were non-significant. However, two-way ANOVA analysis of the ventral region reported a

region (P=0.0014) and genotype (0.0395) effect, while analysis by Tukey's multiple comparison testing showed a significant difference between rostral:cKO vs. caudal:cKO (P=0.0019).

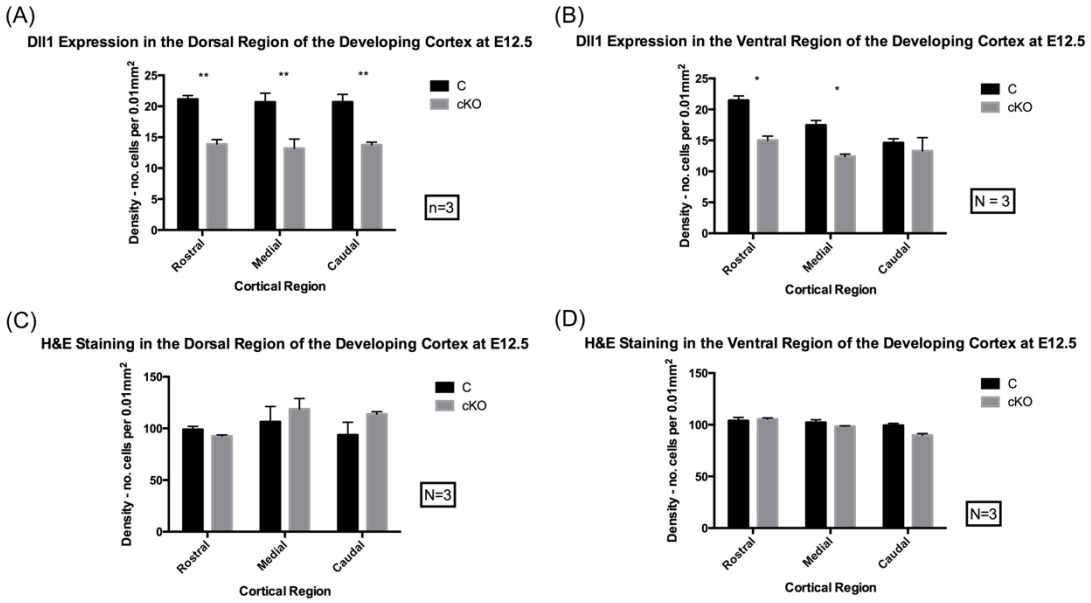

Figure 3.16 Cell density in the cortex of cKO embryos at E12.5

(A) *Dll1* density in the dorsal region of the cortex. A significant decrease was detected between all dorsal regions of the cortex when comparing cKO mutants to WT controls. (** Rostral P=0.0046, **Medial P=0.0036, ** Caudal P=0.0065). (B) *Dll1* density in the ventral region of the cortex. A significant decrease was detected between the rostral regions and the medial regions of the ventral cortex when cKO mutants were compared to WT controls. (* Rostral P=0.0102, * Medial P=0.0487). (C) Total cell density in the dorsal region of the cortex. (D) Total cell density in the ventral region of the cortex. (C-D) No significant difference in total cell density was detected in the dorsal and ventral regions of the cortex when directly comparing cortical regions of WT controls and *PAX77* mutants. N=3.

3.7.2 E13.5

Two-way ANOVA results for the dorsal region of the cortex at E13.5 (Figure 3.16 A) detected both region (P=0.0043) and genotype (P=0.0003) effects, while Tukey's

multiple comparison tests reported multiple significant differences between both genotype and regions. In contrast, while a genotype effect (P=0.0005) was detected in the ventral region of the cortex (Figure 3.16 B), all multiple comparison tests were found to be non-significant.

Total cell density. Dorsal (Figure 3.16 C). Ventral (Figure 3.17 D).
Two-way ANOVA analysis of the total density of cells in the dorsal (Figure 3.16 C) region of Wt and cKO cortices reported that there were no interaction, region or genotype effects, and that all Tukey's multiple comparison tests were non-significant. However, two-way ANOVA analysis of the ventral (Figure 3.16 D) region observed a region effect (P=0.0012) and analysis by Tukey's multiple comparison tests found a significant difference between rostral:C vs. caudal:C (P=0.0205).

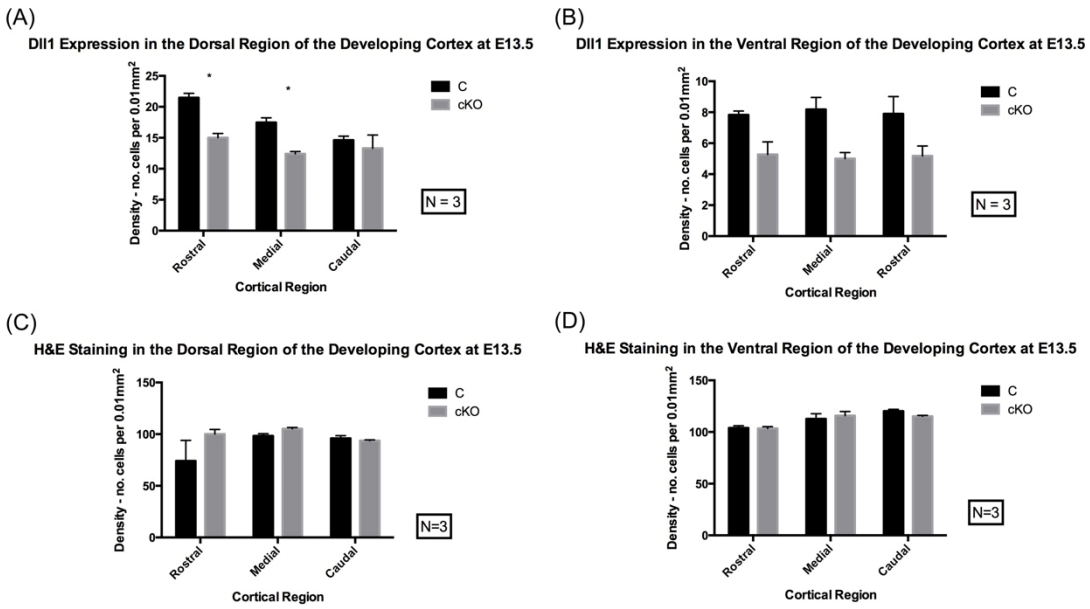

Figure 3.17 Cell density in the cortex of cKO embryos at E13.5

(A) *Dll1* density in the dorsal region of the cortex. A significant decrease was detected between the rostral regions and the medial regions of the ventral cortex when cKO mutants were compared to WT controls. (* Rostral P=0.0102, * Medial P=0.0487). (B) *Dll1* density in the ventral region of the cortex. No significant difference in *Dll1* density was detected in the ventral cortex when comparing WT controls and *Pax6*$^{-/-}$ mutants. (C) Total cell density in the dorsal region of the cortex. (D) Total cell density in the ventral region of the cortex. (C-D) No significant difference in total cell density was detected in the dorsal and ventral regions of the cortex when directly comparing cortical regions of WT controls and *PAX77* mutants. N=3. Analysis carried out by project student Gabrielle Clark.

Cell count analysis of *Dll1* density in *Pax6*$^{-/-}$ and cKO embryonic cortices observed a reduction in *Dll1* density in some cortical regions at specific embryonic stages when compared to WT controls; while analysis of *PAX77* embryos identified no significant change in *Dll1* density when compared to their WT littermates. Further quantification of *Dll1* in the cortex by qPCR would also be beneficial in order to support these findings.

3.8 qPCR analysis of *Dll1* gene expression in *Pax6*$^{-/-}$ mutants

Further analysis of *Dll1* in the developing cortex from E12.5-E14.5 was carried out by qPCR (Figure 3.18). No significant difference in *Dll1* expression was detected at E12.5 or E13.5 when *Pax6*$^{-/-}$ mutants were compared to WT controls. A significant decrease (P=0.0575) in *Dll1* expression in the cortices of *Pax6*$^{-/-}$ mutants when compared to Wt control cortices was observed at E14.5.

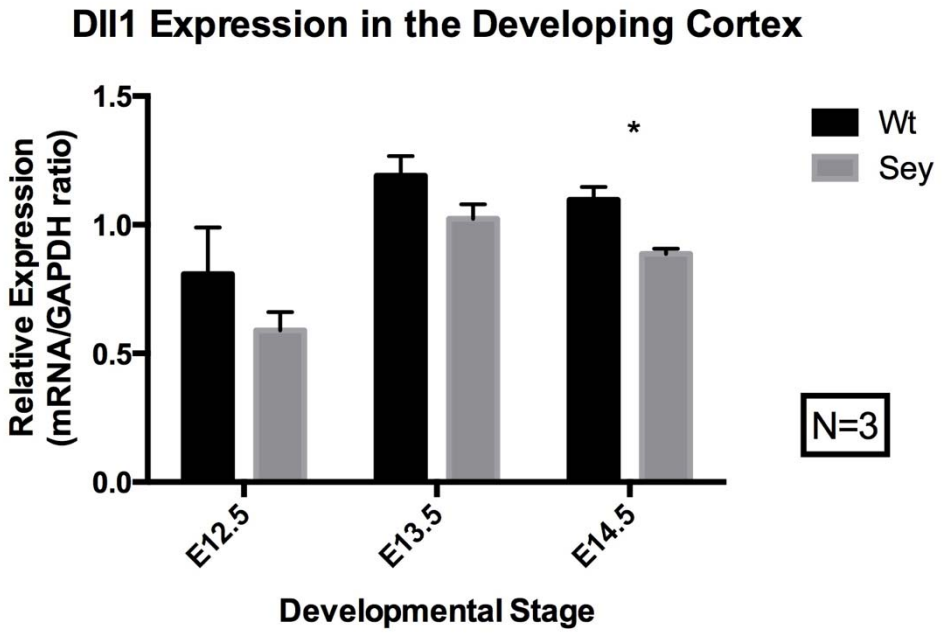

Figure 3.18 *Dll1* gene expression in the developing cortex of *Pax6*$^{-/-}$ embryos

Detection of *Dll1* gene expression in the developing cortex by qPCR. qPCR was carried out on three developmental stages (E12.5-E14.5) on *Pax6*$^{-/-}$ mutants and WT control littermates. Results were normalised to GAPDH. A significant decrease in *Dll1* expression was detected in *Pax6*$^{-/-}$ mutants at E14.5. * P=0.05. N=3.

Analysis by qPCR did not reflect the findings of the previously described cell count analysis, with no significant decrease in *Dll1* expression observed at E12.5 and E13.5, despite there being a decrease in *Dll1* density in specific cortical regions at these stages of embryonic development.

3.9 Discussion

Although the expression pattern of *Dll1* in the developing forebrain has previously been documented, *Dll1* gene expression in the forebrain of embryos with differing levels of *Pax6* has not been investigated. Initial investigation into the effects of *Pax6* levels on *Dll1* by in situ hybridisation observed a similar, punctate expression pattern throughout the telencephalon of *Pax6*$^{-/-}$, *PAX77* and cKO cortices. *Dll1*s punctate expression pattern bears a striking resemblance to the expression pattern of the proneural gene *Ngn2*. As previously discussed, *Ngn2* has been reported as a direct regulator of several Notch ligands, including *Dll1*. Furthermore, previous studies by Shimoji et al., (2008) have highlighted the complementary oscillatory expression levels that *Ngn2* and *Dll1* exhibit, most likely to be a result of the direct activation of *Dll1* by *Ngn2* (Shimojo *et al*., 2009). As a result, it is unsurprising that *Ngn2* and *Dll1* share a near identical type of expression pattern to one another. The fact that *Ngn2* directly regulates *Dll1* provides a tangible connection to *Pax6* and the Notch ligand. Work by Scardigli *et al.,* (2003) provided evidence that *Ngn2* is a direct target of *Pax6*, with multiple enhancer sites for *Pax6* being located upstream of *Ngn2* (Scardigli *et al*., 2003). The evidence that *Pax6* directly regulates the gene that is responsible for the activation of *Dll1* automatically typecasts *Dll1* as a candidate for indirect regulation by *Pax6*. Initial examination of the mutant cortices in comparison to their control littermates found there to be no obvious difference in expression patterns. However, in situ images produced at a higher power of magnification suggested that there may potentially be fewer *Dll1* expressing cells in the developing cortex of *Pax6*$^{-/-}$ mutants and cKO mutants when compared directly with control littermates. Examination of *PAX77* samples did not display a discernible difference from Wt controls. While analysis of gene expression by in situ hybridisation provides insight into expression patterns and provides insight into differences in gene expression in mutants compared to WT controls, they are not directly quantitative.

In order to quantify the suspected change in *Dll1* expression that was observed by in situ hybridisation in the cortex of embryos mutant for *Pax6*, cell count analysis was carried out on the in situs for each mutant of interest and their Wt controls. In order to verify that any significant difference detected was the result of a loss of *Pax6* and not just an increase or decrease in cell density within the cortex of mutant embryos,

cell counts on the total number of cells within the cortex of mutant samples and their control counterparts were also undertaken. Previous work by Sansom et al., suggested *Dll1* to be a potential *Pax6* target, and *Dll1* was listed as a gene target of *Pax6* in their microarray data. However, there has previously been no expression analysis undertaken to confirm this (Sansom *et al*., 2009).

Cell count analysis of the *Pax6*$^{-/-}$ mutant from E11.5-E13.5 showed no significant decrease in density of cells expressing *Dll1* density at E11.5, but a significant decrease in *Dll1* density begins to be detected from E12.5, with a decrease in *Dll1* expression being observed in the dorsal-caudal region of the cortex when Wt and *Pax6*$^{-/-}$ are compared, contributing to the genotype effect that was identified by two-way ANOVA. The fact that the ventral region was found to have a genotype effect of greater significance, and a high number of significantly different multiple comparison tests which included a significant decrease in *Dll1* cell density in each specified region of the *Pax6*$^{-/-}$ cortex when compared to its control, was of particular interest. The ventral region of the developing cortex is where *Pax6* expression is at its highest, suggesting that at E12.5, *Dll1* cell density is potentially tightly controlled by the level of *Pax6* expression. However, this trend is lost by E13.5, with the dorsal region of the cortex being affected by *Pax6* to a greater extent than the ventral region of the cortex.

A reduced cell density of *Dll1* expressing cells in the cortex of *Pax6*$^{-/-}$ mutants when compared to WT controls was observed in a variety of cortical regions from E12.5. However, no obvious pattern emerged for the significant differences between cortical regions, genotype or developmental stage. Although the lack of pattern could be entirely random, it could be that *Dll1* is required at higher levels in specific cortical areas at specific stages of development. Furthermore, oscillations in *Dll1* expression could be contributing to the random pattern in regional and genotypic significant differences. This would be due to the fact that the cell counts have been performed on a snapshot of what oscillating *Dll1* expression levels were like at the specific time that each embryo was sacrificed. As a result, *Dll1* expression levels may be vastly diverse in embryos taken from different litters and may even differ to a degree from

their littermates. Furthermore, embryos from a different litter are even more likely to be prone to differing levels of *Dll1* expression, due to the fact that the specific stages that the embryo was taken at are not going to be identical as a result of estimated times of fertilisation and varying times for sample collection. Consequently, some samples may be older than others and as a result, there would be an even larger variation in oscillatory cycles. While this minute variance in developmental stage by a matter of hours would normally make little difference to the analysis of gene expression, caution should be applied when analysing genes proven to oscillate within a period of 2-3 hours (Shimojo *et* al., 2008). In order to rule out any discrepancy in results due to *Dll1* oscillations, any future cell counts for *Dll1* need to be carried out with each N taken from the same litter, allowing *Dll1* levels to be as close as possible to one another for each sample.

Dll1 cell density increases in Wt cortices from E11.5-E12.5, but reduces at E13.5. This is likely to be due to a reduction in the size of the VZ as the SVZ forms. As previously discussed, *Dll1* expression appears to become denser in the VZ at E13.5. This decrease could be the result of the sample area being produced from the width of the cortex, as the proportion of *Dll1* positive cells within the sample area will have reduced dramatically. In order to remedy this, analysis of *Dll1* expression in the future may need to implement a sample area restricted to the width of the VZ only, where *Dll1* expression is at its highest, or apply two sample areas in later developmental stages to account for the VZ and the SVZ.

Cell count analysis observed little significant difference in *Dll1* expression in *PAX77* mutants, with the only significant differences being found at E12.5 in the dorsal region of the cortex between different dorsal cortical regions of the cortex when genotypes were compared. The fact that the *PAX77* over expressing mutant routinely used by our lab is heterozygous, carrying 5-7 copies of a 420 kb human *Pax6* YAC, may account for no significant change in *Dll1* expression from E11.5-E13.5. It could be the case that co-effectors could be responsible for maintaining *Dll1* levels by compensating for an increase in *Pax6*. Therefore it may be probable that a higher level of *Pax6* might be required to alter *Dll1* levels, suggesting that the use of the

homozygous *PAX77* mutant that contains 10-14 copies of *Pax6* would be beneficial for this study and an effect may be observed (Manuel *et al*., 2007).

Cell count analysis for the cKO mutant observed a greater effect when compared to the *Pax6*$^{-/-}$ mutant. This is likely to be due to the fact that in the naturally occurring *Pax6*$^{-/-}$ mutation, co-effectors compensate for a loss of *Pax6*. However, a sudden knockout of *Pax6* at E9.5 followed by a collection of the embryos within 72-96 hours, would most likely prevent these compensatory mechanisms. It can therefore be suggested that losing *Pax6* at a specific time point is more detrimental to *Dll1* expression than if *Pax6* was never expressed to begin with (Lewandoski *et al*., 2001; Simpson *et al*., 2009).

Analysis of *Dll1* gene expression was also carried out by qRT-PCR. A significant decrease in *Dll1* expression was detected at E14.5 (P=0.0575) but no significant decrease was observed at E12.5 or E13.5. This data conflicts with the previously discussed cell count analysis data, where specific regions of the cortex were found to be significantly different at both E12.5 and E13.5. This could be the a result of using the entire cortex for qPCR, as any subtle regional decreases could potentially be lost when detecting *Dll1* levels as a whole in the cortex. Future qPCR analysis using specific cortical regions could remedy this issue and give a more accurate account of *Dll1* expression. Furthermore, technical error when dissecting the cortex could also affect the result, as accidentally including tissue from the ventral area of the telencephalon where *Pax6* is not expressed and *Dll1* levels would not be affected, would undoubtedly mask the reduction of *Dll1* levels in the cortex where *Pax6* is expressed.

Despite the discrepancies between experimental techniques used to analyse *Dll1* expression in the developing cortex of mutant embryos exhibiting different levels of *Pax6*, it can be implied that *Pax6* regulates *Dll1* expression on some level. The subtle decreases in *Dll1* expression in specific cortical regions at specific stages of embryonic development suggest that *Dll1* is more likely to be indirectly regulated by

Pax6 rather than a direct target. However, the notion that *Dll1* could be a direct target cannot be completely disregarded without further experimental evidence.

STAGE/COMPARISON	*DLL1* DORSAL	*DLL1* VENTRAL	CELL DENSITY DORSAL	CELL DENSITY VENTRAL
E11.5 WT/SEY	No difference	No difference	No difference	No difference
E12.5 WT/SEY	Caudal – reduced *Dll1* in Sey	Rostral, Medial, Caudal – reduced *Dll1* in Sey	No difference	No difference – WT/Sey but difference Rostral/Caudal – Sey
E13.5 WT/SEY	Sey: Medial and Caudal – reduced *Dll1* WT: Rostral/Caudal, high *Dll1* in Caudal	Genotype effect	No difference WT/Sey	No difference WT/Sey Sey: Rostral/Caudal Wt: Medial/Caudal
E11.5 WT/*PAX77*	No difference	No difference	No difference	No difference
E12.5 WT/*PAX77*	Rostral WT/Caudal *PAX77* Medial WT/Caudal *PAX77*, high in Caudal *PAX77*	No difference	No difference	No difference
E13.5 WT/*PAX77*	No difference	No difference	No difference	No difference
E12.5 C/CKO	cKO: reduced *Dll1* in all dorsal regions	Sey: reduced *Dll1* in Rostral and Medial regions	No difference	No difference cKO: Rostral/Caudal, Caudal low
E13.5 C/CKO	cKO: Reduced *Dll1* in Rostral and Medial regions	Genotype effect	No difference	Region effect WT: Rostral/Caudal, Caudal high

Table 3.1 Chapter 3 results summary

A summary of the cell count analysis detailed in chapter 3. Summary of the statistical analysis by ANOVA and Tukey's multiple comparison testing of the density of *Dll1* expressing cells and total cell density in WT/Sey embryos at E11.5-E13.5; WT/*PAX77* embryos at E11.5-E13.5; and C/cKO embryos at E12.5-E13.5. Region specific significant differences and any genotype effects are reported.

4.0 Analysis of *Jag1* expression in the developing cortex of *Pax6*$^{-/-}$ mutant mice

4.1 Introduction

The mammalian *Jag1* gene, a ligand and member of the Notch signalling family, is one of two genes which comprises the *Jagged* family, the mammalian homolog of the *Drosophila Serrate* family. *Jag1* was initially discovered in the rat, when isolation of a cDNA clone observed that the newly identified gene was able to activate *Notch* receptors in a similar manner to its *Drosophila* counterpart (Lindsell *et al*., 1995).

As previously discussed, *Jag1* is a key component of the *Notch* signalling pathway and is consequently involved in the proliferation and differentiation of neural progenitor cells during murine embryonic neurogenesis (Basak and Taylor 2007; Corbin *et* al., 2009; Gaiano *et al*., 2000; Götz and Sommer 2005; Kageyama *et al*., 2008b; Pierfelice *et al*., 2011). As well as the well-documented involvement of *Jag1* in murine neurogenesis, *Jag1* has been implicated in maintaining neural progenitors during human embryonic development, with its down-regulation resulting in abnormal differentiation of progenitor cells, and an increase in the expression of *Jag1* observed in neuroectodermal spheres (Woo *et al.*, 2009; Li *et al., 2015*).

A link between *Jag1* and brain tumors has recently been established, with an over-expression of the ligand observed in childhood medulloblastoma (Fiaschetti *et al*., 2014). Additionally, an increase in *Jag1* expression has also been identified in human glioblastomas (Jubb *et al*., 2012; Liu *et al*., 2014). This is of particular interest due to the fact that *Pax6* has been identified as a suppressor of tumor formation in *in vivo* murine models for gliomagenesis, and provides a link between the genes of interest in our hypothesis for their interaction with one another during corticogenesis (Appolloni *et al*., 2012).

In the murine developing telencephalon, it has been reported Jag1 protein is expressed in the developing cortex, with highest expression at the pallial subpallial boundary (PSPB) and particularly strong staining also observed in the ganglionic eminences of the telencephalon at E14.5 (Nelson *et al*., 2013). Previous research has found Jag1 to be enriched in the RGC population, suggesting that Jag1 is involved in *Notch* signalling in a specific progenitor cell subpopulation during the process of neurogenesis (Nelson *et al*., 2013). Despite recent advances in our knowledge of the expression pattern of Jag1 protein and research implementing FACS to identify the cell population that Jag1 is expressed in during cortical development, there is little documentation of the expression pattern of the *Jag1* gene during murine forebrain development.

While information concerning the role of *Jag1* during embryonic forebrain development is scarce, the role of *Jag1* during postnatal and adult forebrain development has been documented. Research into postnatal and adult neurogenesis in the dentate gyrus has identified that Jag1 is expressed specifically in transient amplifying cells residing in the subgranular zone (SGZ) of the dentate gyrus (Breunig *et al*., 2007; Lavado *et al*., 2010; Imayoshi and Kageyama, 2011) and that conditional inactivation of the gene Prox1 results in the loss of Jag1 expressing transient amplifying cells, resulting in a reduction in Notch signalling in neural stem cells (NSCs) in the SGZ (Lavado *et al*., 2010). Furthermore, a recent study by Lavado and Oliver demonstrated that Jag1 is necessary for neurogenesis in the adult dentate gyrus by demonstrating that the inactivation of *Jag1* reduces neural stem cell maintenance and proliferation in the SGZ (Lavado and Oliver, 2014).

Previous microarray research by our group has identified *Jag1* as a potential target of *Pax6*. *Jag1* was found to be down-regulated at the PSPB of E12.5 $Pax6^{-/-}$ mutants, with a fold change of -1.625 (Carr, 2009). As previously discussed in the case of *Dll1*, no analysis of the expression pattern of *Jag1* in the developing cortex has been conducted in *Pax6* mutant embryos. Due to the fact that *Jag1* has been identified as a gene down-regulated in the cortex of $Pax6^{-/-}$ mutant embryos, it has been hypothesised that a reduction in the expression of *Jag1* in the developing cortex will

be observed when analyzed by in situ hybridisation. Furthermore, as previously discussed in the case of the *Notch* ligand *Dll1*, it would stand to reason that an effect observed in the cortex of embryos homozygous for *Pax6* might suggest that a variance in *Jag1* expression could also be observed in embryos which express increased levels of *Pax6*, and that embryos with a timed knock down of *Pax6* exclusively within the developing cerebral cortex could provide insight into how *Pax6* exerts its regulatory effects without compensation from other genes involved in neurogenesis (Chapter 3.1).

4.2 Analysis of *Jag1* expression in *Pax6*$^{-/-}$ mutants

In order to confirm the microarray data carried out by our lab (Carr, 2009) and confirm that *Jag1* expression is reduced in *Pax6*$^{-/-}$ embryos when compared to WT embryos, in situ hybridisation analysis of *Jag1* expression was carried out in *Pax6*$^{-/-}$ mutant embryos and their WT littermate counterparts at E11.5 and E12.5 of embryonic development. Analysis was also carried out at the later developmental stage of E14.5, when the SVZ has formed and progenitor cell subpopulations have been established.

Analysis of *Jag1* expression in WT embryos at E11.5 showed strong staining in the ganglionic eminences of the developing telencephalon (red arrows, Figure 4.1 A-C). Staining was also observed at the PSPB (black arrows, Figure 4.1 A-C), and lighter staining observed in the developing cortex (asterisk, Figure 4.1, A-C). In *Pax6*$^{-/-}$ mutant embryos, *Jag1* expression in the ganglionic eminences (red arrows, Figure 4.1 D-F) remains consistent with staining observed in WT littermates. Staining at the PSPB of *Pax6*$^{-/-}$ mutant embryos appears reduced (black arrows, Figure 4.1 D-F), while staining in the cortex appears unaffected (asterisk, Figure 4.1 D-F).

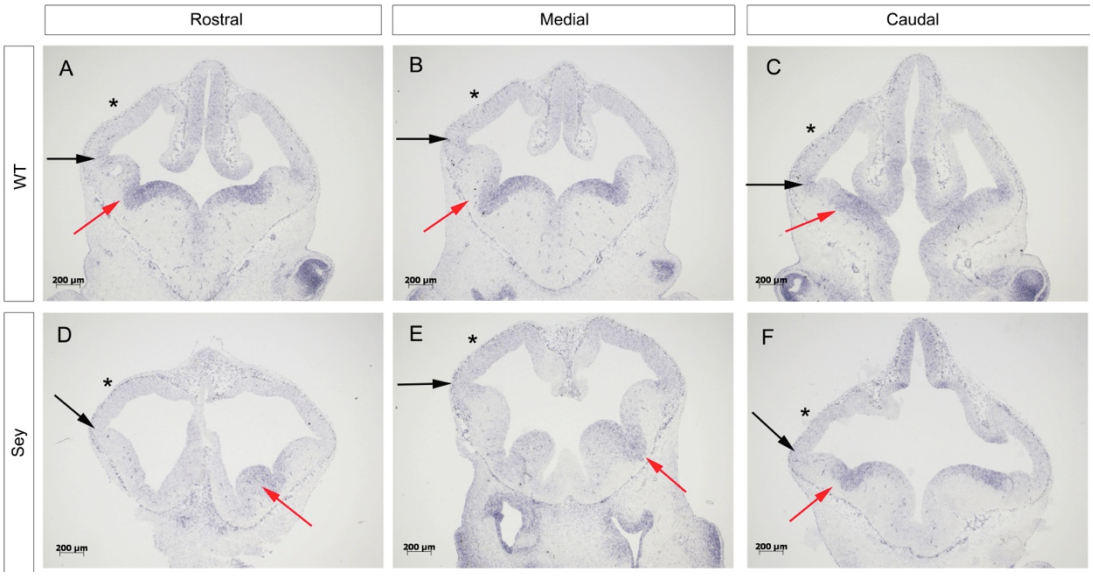

Figure 4.1 *Jag1* gene expression in the developing forebrain of *Pax6*$^{-/-}$ embryos at E11.5

(A-C) *Jag1* expression in the forebrain of a WT control embryo. (A) Expression in the rostral region of a WT forebrain. (B) *Jag1* expression in the medial region of a WT forebrain. (C) *Jag1* expression in the caudal region of a WT forebrain. (A-C) Black arrows indicate the PSPB where there is strong *Jag1* expression and red arrows indicate the ganglionic eminences where there is also strong *Jag1* expression. (D-E) *Jag1* expression in the forebrain of a Sey mutant embryo. (D) *Jag1* expression in the rostral region of a Sey forebrain. (E) *Jag1* expression in the medial region of a Sey mutant forebrain. (F) *Jag1* expression in the caudal region of a Sey mutant forebrain. (D-F) Black arrows indicate the PSPB. A loss of *Jag1* expression at the PSPB in Sey mutant embryos is shown. Red arrows indicate the presence of strong *Jag1* expression in the ganglionic eminences at E11.5. (A-D) * indicates the cortex. Wt = *Pax6*$^{+/+}$ and Sey = *Pax6*$^{-/-}$. Scale bars = 200µm. (N=3 embryos).

At E12.5, *Jag1* exhibited weak staining within the dorsal region developing cortex, with staining appearing strongest in the medial section in WT embryos (Figure 4.2 B). Strong staining was exhibited at the PSPB (black arrows, Figure 4.2 A-C) and within the ganglionic eminences in WT controls (red arrows, Figure 4.2 A-C). This expression pattern corresponds well with previously reported protein expression pattern studies for *Jag1* (Nelson *et al*., 2013). However, in the cortices of *Pax6*$^{-/-}$ mutant embryos, *Jag1* expression appeared reduced in the cortex (asterisk, Figure 4.2

D-F) when compared to the cortices of WT littermates (asterisk, Figure 4.2 A-C), and was entirely gone at the PSPB (black arrows, Figure 4.2 D-F). Staining remained unchanged in the ganglionic eminences (red arrows, Figure 4.2 D-F).

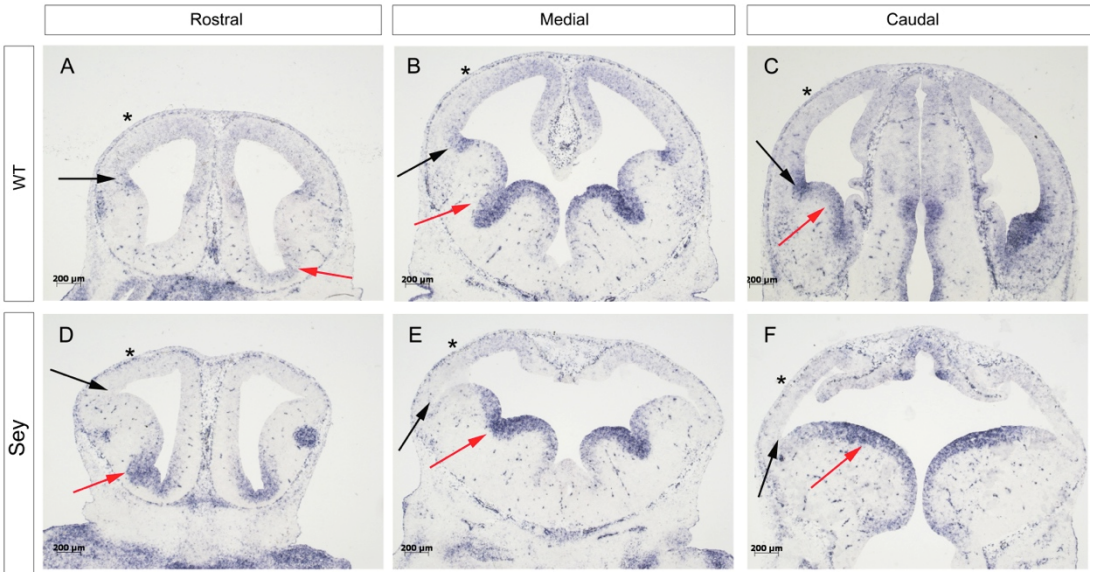

Figure 4.2 *Jag1* gene expression in the developing forebrain of *Pax6*$^{-/-}$ embryos at E12.5

(A-C) *Jag1* expression in the forebrain of a WT control embryo. (A) *Jag1* expression in the rostral region of a WT forebrain. (B) *Jag1* expression in the medial region of a WT forebrain. (C) *Jag1* expression in the caudal region of a WT forebrain. (A-C) Black arrows indicate the PSPB where there is strong *Jag1* expression, and red arrows indicate the ganglionic eminences where there is strong *Jag1* expression. *Jag1* expression is also observed in the developing cortex. (D-E) *Jag1* expression in the forebrain of a Sey mutant embryo. (D) *Jag1* expression in the rostral region of a Sey forebrain. (E) *Jag1* expression in the medial region of a Sey mutant forebrain. (F) *Jag1* expression in the caudal region of a Sey mutant forebrain. (D-F) Black arrows indicate the loss of *Jag1* expression at the PSPB in Sey mutant embryos and red arrows indicate strong *Jag1* expression in the ganglionic eminences at E12.5. *Jag1* expression in the developing cortex appears reduced in Sey mutants. (A-F) * indicates the cortex. Wt = *Pax6*$^{+/+}$ and Sey = *Pax6*$^{-/-}$. Scale bars = 200µm. (N=3 embryos).

In situ analysis at E14.5 showed staining in the ganglionic eminences (red arrows, Figure 4.3 A-C) and at the PSPB (black arrows, Figure 4.3 A-C) of WT embryos, while staining that was observed in the cortex (asterisk, Figure 4.3 A-C) at earlier gestational stages was found to no longer be present. In contrast, mutant littermates retained the staining observed in the ganglionic eminences of WT controls but *Jag1* expression was lost at the PSPB (black arrows, Figure 4.3 D-F). As was the case with their WT counterparts, no *Jag1* expression was observed in the cortex of *Pax6*$^{-/-}$ mutant embryos at E14.5 (asterisk, Figure 4.3 D-F).

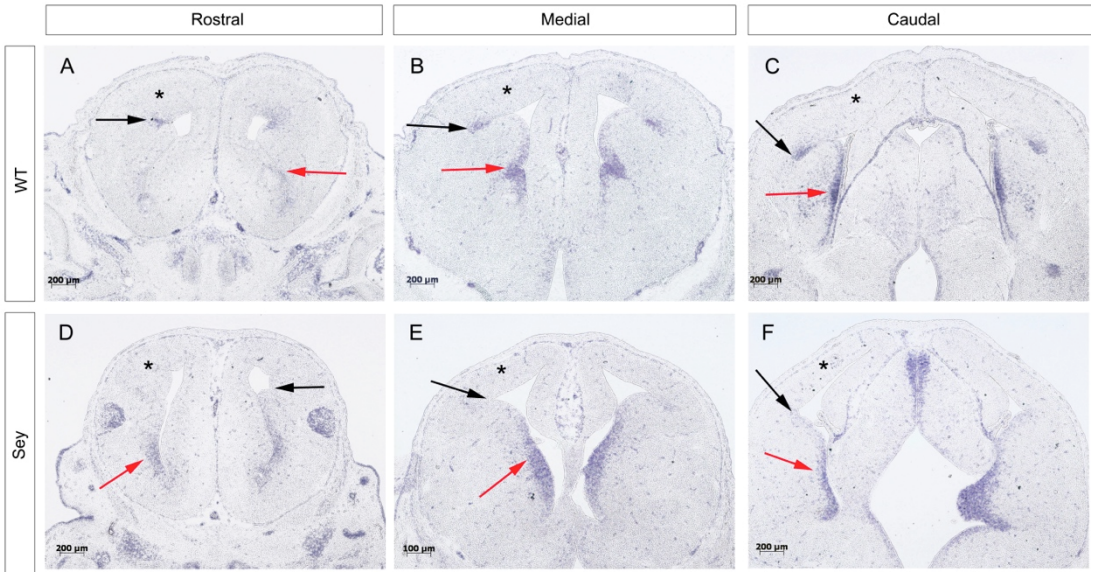

Figure 4.3 *Jag1* gene expression in the developing forebrain of *Pax6*$^{-/-}$ embryos at E14.5

(A-C) *Jag1* expression in the forebrain of a WT control embryo. (A) *Jag1* expression in the rostral region of a WT forebrain. (B) *Jag1* expression in the medial region of a WT forebrain. (C) *Jag1* expression in the caudal region of a WT forebrain. (A-C) Black arrows indicate the PSPB where *Jag1* expression is present and red arrows indicate the ganglionic eminences where *Jag1* expression is present. (D-E) *Jag1* expression in the forebrain of a Sey mutant embryo. (D) *Jag1* expression in the rostral region of a Sey forebrain. (E) *Jag1* expression in the medial region of a Sey mutant forebrain. (F) *Jag1* expression in the caudal region of a Sey mutant forebrain. (D-F) Black arrows indicate the loss of *Jag1* expression at the PSPB in Sey mutant embryos and red arrows indicate strong *Jag1* expression in the ganglionic eminences at E14.5. (A-D) * indicates the cerebral cortex. Wt = *Pax6*$^{+/+}$ and Sey = *Pax6*$^{-/-}$. Scale bars = 200µm. (N=3 embryos).

In situ hybridisation analysis of *Jag1* in *Pax6*$^{-/-}$ embryos confirmed a decrease in expression at the PSPB of mutant embryos when compared to WT embryos. A less dramatic decrease was also visible in the main body of the developing cortex. Furthermore, in situ hybridisation analysis allowed us to characterise *Jag1* expression in the developing telencephalon, with strong expression observed at the PSPB and in the ganglionic eminences, and lighter expression throughout the cortex observed in WT embryos. Analysis of mutant embryos saw a complete loss at the

PSPB and a small decrease in the cortex, while staining in the ganglionic eminences remained. As was the case with in situ analysis of *Dll1* expression (Chapter 3), the results for *Jag1* in *Pax6*$^{-/-}$ embryos piqued our interest as to how increased levels of Pax6 or timed deletions of Pax6 would affect *Jag1* expression. Consequently, in situ analysis was carried out using *PAX77* and cKO mutant embryos at E12.5 in order to compare the effects on Jag1 expression at the embryonic stage where it was most affected in *Pax6*$^{-/-}$ embryos. Due to the results from *Pax6*$^{-/-}$ in situ analysis of *Jag1*, it is likely that a greater decrease in expression will be observed in the cortex of cKO mice, as the likelihood of compensation will be greatly reduced; while *Jag1* expression in *PAX77* embryos will increase due to increased levels of Pax6.

4.3 Analysis of *Jag1* gene expression in *PAX77* mutants

At E12.5, *Jag1* expression in *PAX77* mutant embryos closely mimics the expression pattern observed in *Pax6*$^{-/-}$ mutants at the same developmental stage (Figure 4.4). A slight decrease in expression was observed in the developing cortex (asterisk, Figure 4.4 D-F), along with the abolition of expression at the PSPB (black arrows, Figure 4.4 D-F), while *Jag1* expression in the ganglionic eminences remained unchanged (red arrows, Figure 4.4 D-F) when compared to WT control littermates (red arrows, Figure 4.4 A-C). As expected, *Jag1* expression in WT control littermates for *PAX77* expression analysis was consistent with the expression pattern observed in WT controls from *Pax6*$^{-/-}$ in situ hybridisation analysis at E12.5 (Figure 4.2, Figure 4.4).

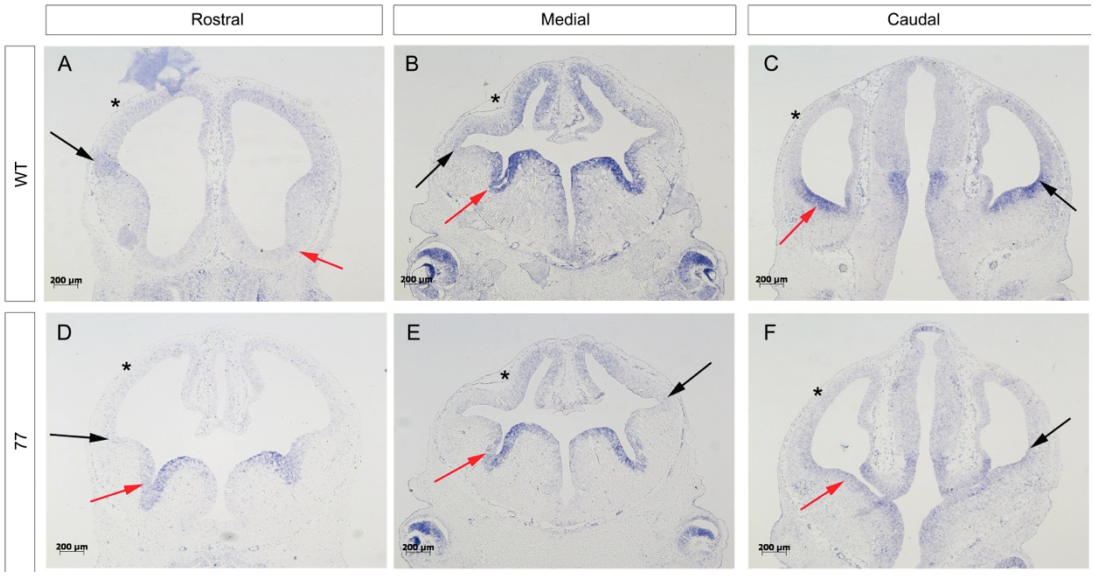

Figure 4.4 *Jag1* gene expression in the developing forebrain of *PAX77* embryos at E12.5

(A-C) *Jag1* expression in the forebrain of a WT control embryo. (A) *Jag1* expression in the rostral region of a WT forebrain. (B) *Jag1* expression in the medial region of a WT forebrain. (C) *Jag1* expression in the caudal region of a WT forebrain. (A-C) Black arrows indicate the PSPB where there is *Jag1* expression and red arrows indicate the ganglionic eminences where there is strong *Jag1* expression. *Jag1* expression is also observed in the developing cortex. (D-E) *Jag1* expression in the forebrain of a *PAX77* mutant embryo. (D) *Jag1* expression in the rostral region of a *PAX77* mutant forebrain. (E) *Jag1* expression in the medial region of a *PAX77* mutant forebrain. (F) *Jag1* expression in the caudal region of a *PAX77* mutant forebrain. (D-F) Black arrows indicate the PSPB where there is a loss of *Jag1* expression in *PAX77* mutant embryos and red arrows indicate the ganglionic eminences where there is strong *Jag1* expression at E12.5. *Jag1* expression in the developing cortex appears reduced in *PAX77* mutants. (A-D) * indicates the cortex. Wt = $Pax6^{+/+}$ and Sey = $Pax6^{-/-}$. Scale bars = 200µm. (N=3 embryos). In Situ hybridisation carried out by project student Milena Blaga.

Interestingly, analysis of *Jag1* expression at E12.5 observed a complete loss of expression at the PSPB in *PAX77* embryos, and a reduction in expression in the main body of the developing cortex. This result is identical to the $Pax6^{-/-}$ data at E12.5, an

unexpected result as both a loss and increase of Pax6 expression had the same effect on *Jag1* expression.

4.4 Analysis of *Jag1* expression in cKO mutants

At E12.5, *Jag1* expression in control embryos remained similar to the expression patterns observed in the aforementioned analysis of control littermates from *Pax6*$^{-/-}$ and *PAX77* embryos at E12.5, with strong staining observed at the PSPB and in the ganglionic eminences, and a lighter level of expression evident in the cortex (asterisk, Figure 4.5 D-F). However, unlike in the case of *Pax6*$^{-/-}$ and *PAX77* mutant embryos, the *Emx1CreEr*^{T2}*;Pax6*$^{loxP/loxP}$ (hereinafter referred to as cKO) embryos did not display a reduction in staining at the PSPB (black arrows, Figure 4.5 D-F).

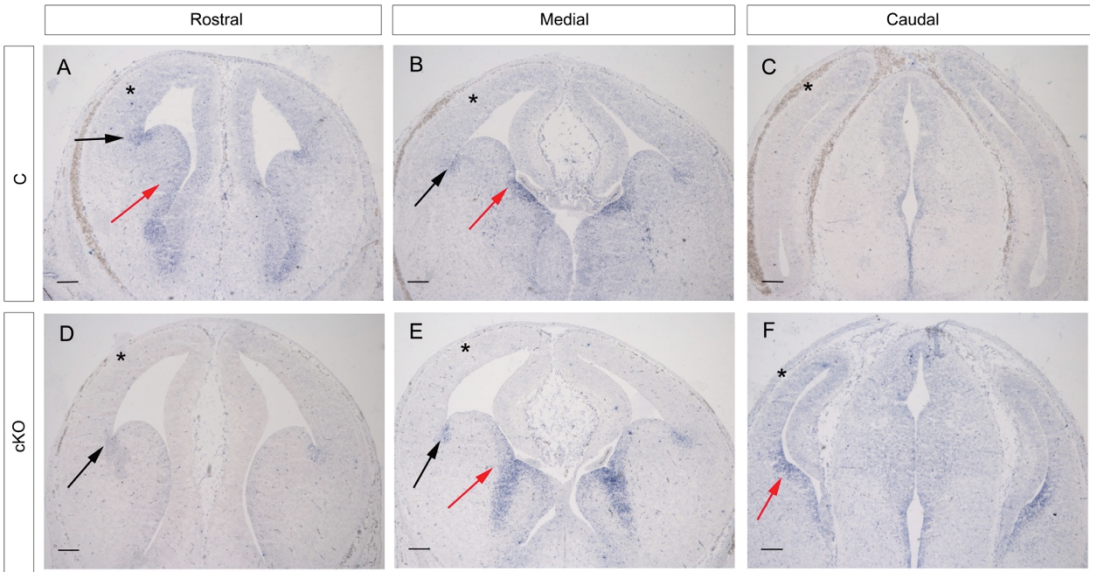

Figure 4.5 *Jag1* gene expression in the developing forebrain of cKO embryos at E12.5

(A-C) *Jag1* expression in the forebrain of a control embryo. (A) *Jag1* expression in the rostral region of a control forebrain. (B) *Jag1* expression in the medial region of a control forebrain. (C) *Jag1* expression in the caudal region of a control forebrain. (A-C) Black arrows indicate the PSPB where there is *Jag1* expression and red arrows indicate the ganglionic eminences where there is strong *Jag1* expression. *Jag1* expression is also observed in the developing cortex. (D-E) *Jag1* expression in the forebrain of a cKO mutant embryo. (D) *Jag1* expression in the rostral region of a cKO mutant forebrain. (E) *Jag1* expression in the medial region of a cKO mutant forebrain. (F) *Jag1* expression in the caudal region of a cKO mutant forebrain. (D-F) Black arrows indicate the PSPB where there is *Jag1* expression in cKO mutant embryos and red arrows indicate the ganglionic eminences where there is strong *Jag1* expression at E12.5. *Jag1* expression in the developing cortex appears reduced in cKO mutants. (A-D) * indicates the cortex. Wt = $Pax6^{+/+}$ and Sey = $Pax6^{-/-}$. Scale bars = 200µm. (N=3 embryos).

4.5 qPCR analysis of *Jag1* expression in $Pax6^{-/-}$ mutants

In order to quantify the decrease in *Jag1* expression observed in $Pax6^{-/-}$ embryonic cortices and to determine whether overall *Jag1* mRNA levels were altered, qRT-PCR was carried out at E12.5 and E14.5 (Figure 4.6). It was hypothesised that a significant decrease in *Jag1* would be detected due to the complete loss of the gene

at the PSPB. However, no significant decrease in *Jag1* expression in the cortex of *Pax6*$^{-/-}$ mutants was observed when compared to *Jag1* expression in the cortex of WT control embryos at E12.5 (p=0.136) or at E14.5 (p=0.164) when analyzed by two-tailed paired students t-test.

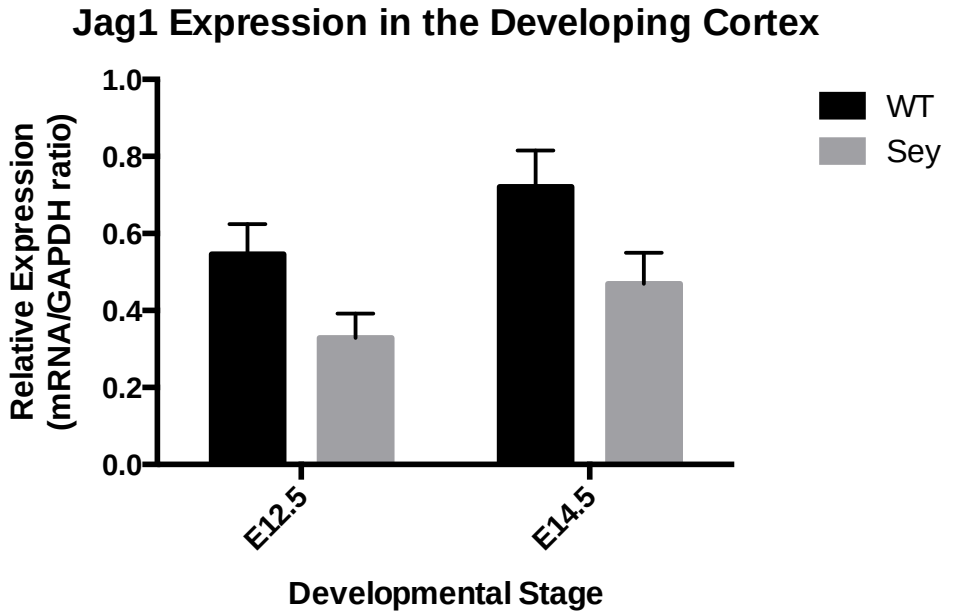

Figure 4.6 *Jag1* gene expression in the developing cortex of *Pax6*$^{-/-}$ Embryos

Detection of *Jag1* gene expression in the developing cortex by qPCR. qPCR was carried out on two developmental stages (E12.5 and E14.5) on Sey mutants and WT control littermates. Results were normalised to GAPDH. No significant decrease in Jag1 expression was detected in Sey mutants at E12.5 (p=0.136) or E14.5 (p=0.164). Wt = *Pax6*$^{+/+}$ and Sey = *Pax6*$^{-/-}$. (N = 3 embryos).

4.6 Discussion

As previously discussed, the expression pattern of the Jag1 protein has been investigated prior to this research undertaken by our group (Nelson *et al*., 2013). However, the expression pattern for the *Jag1* mRNA in the developing murine cortex has not been documented in great detail. Expression analysis by in situ hybridisation

in WT embryos at E11.5 observed light staining in the developing cortex, with stronger staining at the PSPB and strong staining in the ganglionic eminences of the ventral telencephalon. Further analysis in WT embryos at E12.5 displayed strong staining in the ganglionic eminences of the developing telencephalon and strong staining was also observed at the PSPB. Lighter staining was evident in the developing cerebral cortex, with a gradient expression pattern observed and *Jag1* expression strongest in the dorsal region of the cortex. It was observed that *Jag1* expression appeared strongest at E12.5 in WT embryos, suggesting that the gene exerts its greatest effect upon telencephalic development at this embryonic stage. In turn, *Jag1* expression in WT embryos at E14.5 appeared lighter, with no staining in the developing cortex suggesting the possibility that *Jag1* may no longer be required for cortical development by this stage of embryonic development, despite its expression still being required at the PSPB and the ganglionic eminences. However, the loss of *Jag1* at the cortex does not necessarily mean that its expression is not required for cortical development and phenotypic analysis of embryos that do not express Jag1 would be required in order to confirm that the gene is required for correct cortical development.

In contrast, investigation into *Jag1* expression in *Pax6*$^{-/-}$ embryos found a potential reduction in *Jag1* expression in the developing cortex at E12.5 and a complete loss of expression at the PSPB in all embryonic stages that were investigated. However, staining in the ganglionic eminences, where *Pax6* is not expressed in the developing telencephalon, remained intact. The fact that *Jag1* staining is originally evident at the PSPB of WT embryos and lost in embryos of *Pax6* null embryos is of particular interest due to the fact that *Pax6* is expressed in a high lateral – low medial gradient in the cortex of WT embryos. The observation that *Jag1* is expressed strongly where *Pax6* expression is at its highest and that expression is then lost in *Pax6*$^{-/-}$ mutants indicates that *Jag1* may be a direct target of *Pax6*. This assumption is based on past studies of *Pax6*, where an observed effect in the expression of genes involved in developmental processes controlled by the transcription factor has led to the eventual identification of these genes of interest as direct targets of Pax6 by bioinformatics and binding site validation by techniques such as EMSA, ChiP and luciferase assay,

rather than genes downstream of direct interactions that are subsequently indirectly regulated by the transcription factor (Scardigli *et al*., 2003; Holm *et al*., 2007; Tuoc and Stoykova, 2008; Castro and Guillemot, 2011; Castro *et al*., 2011; Mi *et al.*, 2013a).

While *Jag1* and *Pax6* are both expressed at the PSPB and *Jag1* staining is also present in the cortex where *Pax6* expression is also present, it does not display the same gradient pattern that *Pax6* does in the cortex and *Jag1* expression does not appear to be strongly affected by a loss of *Pax6* in this region. This suggests that while *Pax6* is likely to directly regulate *Jag1* at the PSPB, co-effectors could also be involved in regulating *Jag1* expression in the main body of the developing cerebral cortex. If this is the case, additional co-effectors that regulate *Jag1* in the cortex may compensate for the loss of *Pax6* expression in *Pax6*$^{-/-}$ embryos. However, evidence for transcriptional regulators for Jag1 in the cerebral cortex would be required in order to solidify this hypothesis.

The finding that *Jag1* is down-regulated in the cortex of PAX77 embryos at E12.5 was surprising as it was originally hypothesised that an increase in *Pax6* expression would be likely to result in an increase in *Jag1* expression in the cerebral cortex. However, analysis of *Jag1* expression in the cortex of E12.5 *PAX77* mutant embryos found staining to closely mirror the expression pattern for *Jag1* that was observed in *Pax6*$^{-/-}$ embryos. The strong staining present in the PSPB of WT littermates was completely absent in *PAX77* mutants, and staining in the developing cortex also appeared to be reduced. Staining in the ganglionic eminences where *Pax6* is not normally expressed remained intact and mirrored staining observed in WT littermates. Despite the fact that the opposite of what we originally hypothesised was observed in *PAX77* mutants, the result is particularly significant for furthering our understanding of how *Pax6* regulates genes involved in forebrain development. It would appear that requirement for *Pax6* during brain development and for the regulation of gene networks involved in the process, is far more sophisticated than the presence of the genes expression simply being required. The fact that an increase in *Pax6* expression can result in the same eradication of *Jag1* expression at the PSPB

suggests that a very specific level of *Pax6* is required for it to activate or repress the expression of genes that it is responsible for regulating during brain development. A similar phenomenon has been observed in eye development, where the levels of *Pax6* expressed dictates how well the eye develops (Dora *et al*., 2008; Favor *et al*., 2008).

Additional research into the effects of *Pax6* on *Jag1* expression implemented the use of our *Pax6* cKO line. Control embryos displayed the same expression for *Jag1* in the developing telencephalon at E12.5 as WT embryos from previous *Jag1* expression analysis, while cKO mutant embryos treated with Tamoxifen at E9.5 also displayed no change in *Jag1* expression in the ganglionic eminences or the PSPB at E12.5. While *Pax6* is expression is knocked out in the PSPB of $Pax6^{-/-}$ embryos, the timed deletion of *Pax6* in cKO mutant embryos is the result of a tamoxifen inducible Cre recombinase under the control of the *Emx1* locus ($Emx1CreER^{T2}$). While *Emx1* and *Pax6* are mutually expressed in the developing cerebral cortex, *Emx1* expression does not reach the PSPB, unlike *Pax6*. Consequently, *Pax6* expression at the PSPB of treated cKO embryos remains intact, resulting in no effect upon *Jag1* expression. Future analysis on the effects of timed deletions of *Pax6* on *Jag1* expression would require the use of a Cre strain whose expression encompasses both the cortex and the PSPB, or a CAG Cre which acts to universally dele *Pax6* throughout the developing embryo. Although this would resolve the issue concerning *Pax6* expression at the PSPB, the specificity of deleting *Pax6* in the cortex would be lost, opening the study to the possibility of additional compensation by co-effectors.

Quantification of *Jag1* expression in the cortices of $Pax6^{-/-}$ embryos by qPCR was undertaken at E12.5 and E14.5. No significant reduction in *Jag1* expression was observed at either developmental stage, despite the extreme loss of *Jag1* at the PSPB of mutant embryos. A likely explanation for no significant reduction despite such a visible loss of expression in a distinct region of the developing telencephalon would be the fact that there is little to no change in expression of *Jag1* in the main body of the developing cortex. As micro dissections carried out for qPCR analysis incorporated the entire developing cerebral cortex (including the PSPB), it stands to

reason that an extreme loss of *Jag1* at the PSPB would be diluted by the inclusion of the rest of the cortex where *Jag1* expression is not as radically altered. Additional qPCR analysis using dissections exclusive to the PSPB would be required in order to provide valid quantification of the reduction in *Jag1* expression observed by in situ analysis.

GENOTYPE/STAGE	***CTX JAG1 EXPRESSION***	***PSPB JAG1 EXPRESSION***	***GE JAG1 EXPRESSION***
WT E11.5	Light	Strong	Strong
SEY E11.5	Reduced	None	Strong
WT E12.5	Light	Strong	Strong
SEY E12.5	Reduced	None	Strong
WT E14.5	None	Light	Light
SEY E14.5	None	None	Light
WT (PAX77) E12.5	Light	Strong	Strong
PAX77 E12.5	Reduced	None	Strong
C (CKO) E12.5	Light	Strong	Strong
CKO E12.5	None	Strong	Strong

Table 4.1 Chapter 4 results summary

A summary of the in situ hybridisation analysis detailed in chapter 4. Light *Jag1* expression was observed in the cortex of E11.5 and E12.5 WT embryos, and strong *Jag1* expression was observed in the PSPB and GEs. In Sey mutant littermates, strong expression remained in the GEs, while reduced cortical staining and a complete loss of staining the PSPB was observed. At E14.5, No *Jag1* expression was observed in the cortex of WT embryos and only light expression was observed in the PSPB, while strong staining remained in the GEs. In Sey embryos at E14.5, *Jag1* expression was once again lost at the PSPB. In *PAX77* mutant embryos at E12.5, *Jag1* staining at the PSPB was lost and staining in the cortex was reduced when compared to WT littermates. In cKO mutant embryos at E12.5, no *Jag1* expression was detected in the cortex in comparison to the light expression observed in control littermates, while strong staining was observed at the PSPB in the GEs for both cKO mutants and their control littermates.

5.0 *Dll1* is expressed in a specific progenitor cell sub population

5.1 Introduction

Previous studies have suggested that the *Notch* pathway ligands all perform the same role during Notch signalling, in that they activate *Notch* receptors 1-4 in order to cleave the NICD that is responsible for the regulation of cellular proliferation and differentiation by activation of the proneural inhibitor *Hes* and *Hey* gene families (Iso *et al*., 2011; Kageyama *et al*., 2008a; Kopan and IIagan, 2009; Pierfelice *et al*.,2011). However, despite this, each of the four *Notch* ligands are expressed in different cortical regions and in different progenitor cell subpopulations from one another during corticogenesis (Nelson *et al*., 2013).

While Notch ligands have been identified as genes which are up-regulated in progenitor cells that are making the transition to differentiate into neural cells, each of the Notch ligands are enriched in a different progenitor cell sub population, suggesting that different Notch ligands are responsible for maintaining specific progenitor cell populations (Nelson *et al*., 2013). For example, *Jag1* has been identified as a gene that is expressed in specific telencephalic regions, specifically the PSPB and ganglionic eminences with apparent low expression in the cortex during specific regions of development, while fluorescence-activated cells sorting (FACS) analysis has identified expression as being restricted to RGCs within the VZ of the developing cortex (Nelson *et al*., 2013; Chapter 4). In contrast, the Delta family ligand *Dll3* is enriched solely within INPs residing within the SVZ during cortical neurogenesis (Campos *et al*., 2001; Nelson *et al*., 2013). However, as previously discussed, there has been some controversy as to where the Notch signalling ligand *Dll1* is expressed in terms of progenitor cell populations during mammalian embryonic neurogenesis (Chapter 3). Research into the expression of *Dll1* during forebrain development originally suggested that *Dll1* is expressed solely within the VZ from E12.5-E14.5 in murine embryos, with staining observed closer to the pial surface but still within the VZ rather than the SVZ (Campos *et al*., 2001),

while later studies suggested that *Dll1* expression is actually restricted to INPs residing within the SVZ (Mizutani *et al*., 2007; Kawaguchi *et al*., 2008; Yoon *et al*., 2008). Further confusion over the location of *Dll1* expression within the developing telencephalon was provided by a study conducted by Nelson *et al*., (2013), in which they proposed that *Dll1* is expressed in the VZ and the SVZ. This study used FACS analysis, which sorted RGC and INP cells dissociated from the forebrains of mouse embryos (Nelson *et al*., 2013).

Due to the fact that *Dll1* has been documented as being expressed within the VZ and also the SVZ, as well as within specific progenitor cell subpopulations, it would be advantageous to establish which progenitor zone and progenitor cell subpopulation *Dll1* is expressed in in WT embryos during cortical development. While it has been established that *Pax6* exerts some form of control over *Dll1* expression, it is unclear what sort of regulatory relationship exists between them or what their relationship contributes towards in terms of cortical development during embryonic neurogenesis.

As previously discussed, our working hypothesis developed from published literature suggests that *Pax6* and *Dll1* may mutually regulate one another via the cellular mechanism of Cis inhibition that occurs during the process of Notch signalling within proliferating neural progenitor cells (Chapter 1). Furthermore, not only does our working hypothesis model suggest that *Pax6* and *Dll1* co-regulate one another, we additionally suggest that *Pax6* regulates the progressive differentiation of RGCs into INPs via a regulatory influence upon *Dll1* expression (Chapter 1). Subsequently, we are suggesting that *Pax6* ultimately controls cellular proliferation and differentiation by Notch signalling via regulatory control of genes implicated in the pathway.

In order to confirm which progenitor cell subpopulation *Dll1* is expressed in, double labelling histological analysis, by fluorescent in situ hybridisation and immunohistochemistry techniques, was implemented. The aforementioned analytical approach provides insight into which progenitor cell subpopulation *Dll1* is expressed in during the process of corticogenesis by using markers for specific progenitor cell

types. Evidence of co-localisation between *Dll1* and these cell markers within cells ultimately allows the identification of which proliferative zone of the developing cortex *Dll1* is expressed in, as well as which progenitor cell population(s) it is expressed in. Further investigation using *Pax6*$^{-/-}$ embryos provided insight into how *Pax6* expression affects *Dll1* expression in progenitor cell populations, and if it causes any shift in which population *Dll1* is expressed by. Additionally, initial findings by double labelling analysis were also investigated by flow cytometry analysis.

5.2 *Dll1* expression is not co-localised with Tbr2 expression in the developing cortex.

In order to determine whether *Dll1* is expressed by INPs residing the SVZ, fluorescent double labelling analysis for *Dll1* and Tbr2 was carried out in WT and *Pax6*$^{-/-}$ mutant embryos at gestational stages E12.5 and E14.5. *Tbr2* is well documented as a marker for INPs in the SVZ of the developing cerebral cortex and its use in double labelling analysis will consequently provide insight into cortical progenitor region and progenitor cell type (Englund *et al*., 2005; Pontious *et al*., 2007; Nelson *et al*., 2013). Due to the fact that *Dll1* has previously been reported as a gene expressed by INPs, it was hypothesised that Dll1 and Tbr2 would co-express in the INP progenitor population (Mizutani *et al*., 2007; Kawaguchi *et al*., 2008; Yoon *et al*., 2008). Gestational stage E12.5, documented as the onset of peak neurogenesis (Li *et al., 2003*), was selected for analysis due to evidence from earlier work that *Dll1* is expressed at this developmental stage, with the gene having been identified as actively down-regulated in the cortex of *Pax6*$^{-/-}$ embryos (Chapter 3). Embryonic stage E14.5 was additionally selected due to the fact that previous studies selected this stage for *Dll1* expression analysis, along with the fact that E14.5 is considered an embryonic stage in which neurogenesis reaches its peak and when the SVZ has fully developed (Takashi *et al*., 1995; Li *et al*., 2003).

Dll1/Tbr2 double labelling carried out at E12.5 in the telencephalon of WT embryos showed strong Tbr2 expression spanning the length of the cortex (Figure 5.1 A-C, G-I). As expected, expression was restricted to the developing SVZ, resulting in Tbr2 expression residing in a relatively small area of the developing cortex when compared to Tbr2 expression at later developmental stages. In contrast, *Dll1* expression appeared to be restricted to the VZ of the cortex, with no co-localisation observed between *Dll1* and Tbr2. Furthermore, analysis of *Pax6*$^{-/-}$ mutant embryo littermates at E12.5 showed a notable reduction in both *Dll1* and Tbr2 expression (Figure 5.1 D-F, J-L). Additionally, no evidence of co-expression of *Dll1* and Tbr2 was observed within the cortex, implying that a loss of *Pax6* expression does not affect the specificity of *Dll1* expression by a progenitor cell type (Figure 5.1).

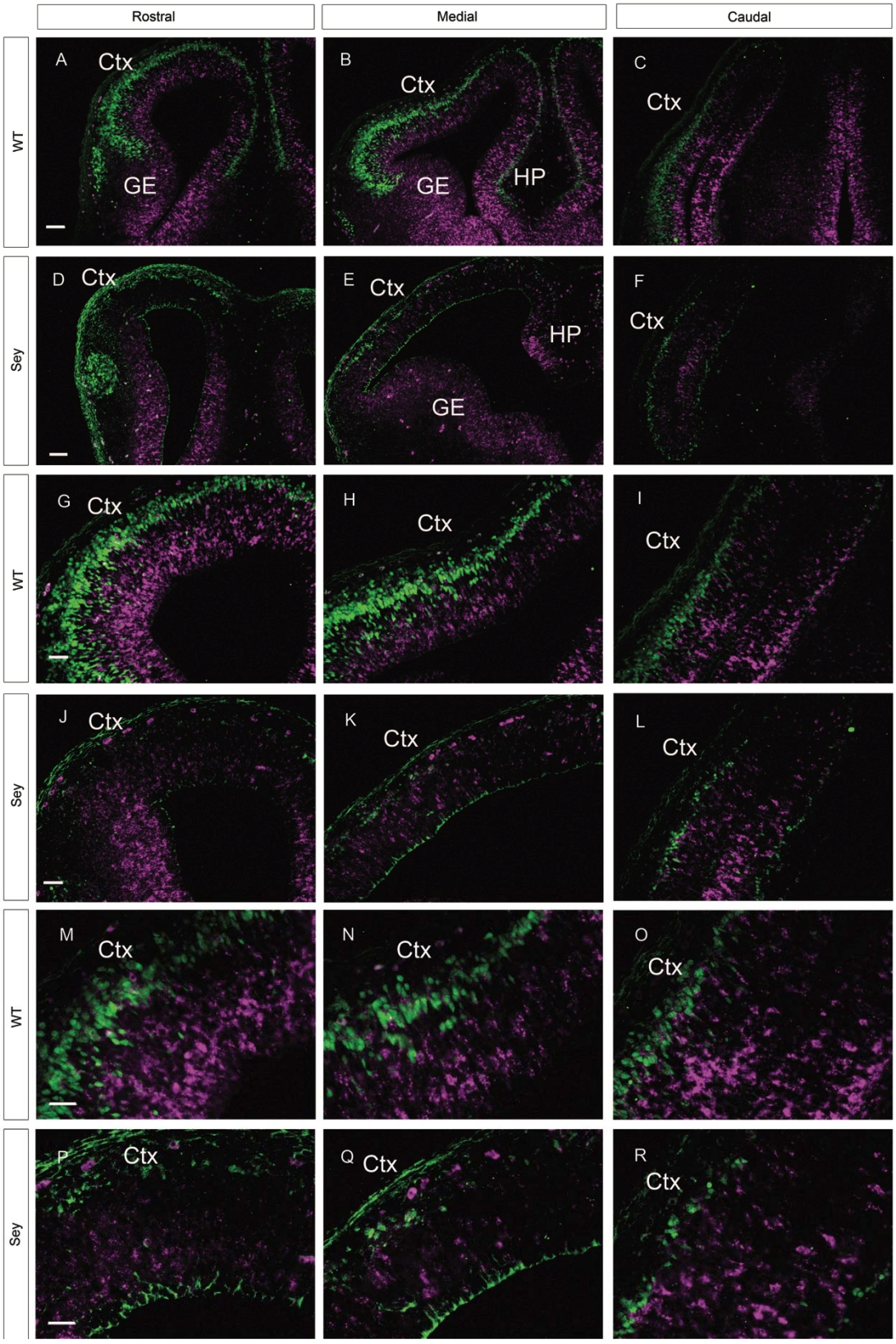

Figure 5.1 In situ hybridisation and Immunohistochemistry showing *Dll1* and Tbr2 expression in the developing cerebral cortex at E12.5

Dll1 expression (Magenta) and Tbr2 expression (green) in WT embryos (A-C and G-I) and Sey embryos (D-F and J-L). (A) Tbr2 expression in the rostral region of the telencephalon. (B) Tbr2 expression in the medial region of the telencephalon. (C) Tbr2 expression in the caudal region of the telencephalon. Tbr2 expression appears restricted to the SVZ of the developing cortex of WT embryos (A-C). (A) *Dll1* expression in the rostral region of the telencephalon. (B) *Dll1* expression in the medial region of the telencephalon. (C) *Dll1* expression in the caudal region of the telencephalon. *Dll1* expression appears restricted to the VZ of the developing cortex of WT embryos (A-C). (D) Tbr2 expression in the rostral region of the telencephalon. (E) Tbr2 expression in the medial region of the telencephalon. (F) Tbr2 expression in the caudal region of the telencephalon. Tbr2 expression appears restricted to the SVZ of the developing cortex of Sey embryos (D-F). (D) *Dll1* expression in the rostral region of the telencephalon. (E) *Dll1* expression in the medial region of the telencephalon. (F) *Dll1* expression in the caudal region of the telencephalon. *Dll1* expression appears restricted to the VZ of the developing cortex of Sey embryos (D-F). Both *Dll1* and Tbr2 expression are reduced in Sey embryos (D-F) when compared to WT embryos (A-C). (G and M) Tbr2 expression in the rostral region of the developing cortex. (H and N) Tbr2 expression in the medial region of the developing cortex. (I and O) Tbr2 expression in the caudal region of the developing cortex. (J and P) Tbr2 expression in the rostral region of the developing cortex. (K and Q) Tbr2 expression in the medial region of the developing cortex. (L and R) Tbr2 expression in the caudal region of the developing cortex. No evidence of co-expression between *Dll1* and Tbr2 is evident in the developing cortex of WT embryos (G-I) or in the cortex of Sey embryos (J-L). Sey = $Pax6^{-/-}$ and WT = $Pax6^{+/+}$. Ctx = Cortex. GE = Ganglionic Eminences. HP = Hippocampus. (A-F) Scale bars = 80µm. (G-L) = 60µm. (M-R) = 40 µm. N = 3 embryos

Double labelling analysis for *Dll1* and Tbr2 at the later embryonic stage of E14.5 in WT embryos showed a notably enlarged area of expression for Tbr2 as a result of the now fully formed SVZ accounting for the majority of the progenitor zone of the developing cortex, with the prevalence of the VZ decreasing in contrast (Figure 5.2 A-C, G-I). As was the case at E12.5, *Dll1* expression appears to be constrained to the VZ, meaning that the level of *Dll1* expression appears reduced when compared to E12.5, and no co-localisation between *Dll1* and Tbr2 was observed (Figure 5.2 G-I; Figure 5.1 G-I). Conversely, strong co-localisation was observed within the SVZ of the developing hippocampus, suggesting that INP cells in this particular region of the

developing telencephalon but not in the cerebral cortex, express *Dll1* (Figure 5.3 A and C). The fact that Dll1 expression is visible in both the VZ and SVZ of the developing hippocampus, suggests that two progenitor cell subtypes (in this case RGCs and INPs) express the ligand. This indicates that expression of Notch ligands by progenitor cell populations is structure specific rather than uniform for the telencephalons proliferative region as a whole. It also suggests that the molecular mechanisms behind neurogenesis differ slightly in different structures of the developing forebrain.

In *Pax6*$^{-/-}$ mutant littermates at E14.5 (Figure 5.2 D-F, J-I), expression for *Dll1* and Tbr2 also appeared to be markedly reduced, as was the case for *Pax6*$^{-/-}$ mutant embryos at E12.5 (Figure 5.1 D-F, J-I). Additionally, no co-localisation was observed between *Dll1* and Tbr2, as was the case in the cortex of WT embryos. Moreover, the co-localisation of *Dll1* and Tbr2 in the SVZ of the developing hippocampus appears severely disrupted in *Pax6*$^{-/-}$ mutant embryos (Figure 5.3 A and C) when compared to WT littermates, with co-expression appearing to be lost (Figure 5.3 B and D). This loss of co-localisation in the SVZ of the developing hippocampus suggests not only that *Dll1* is expressed in multiple progenitor cell populations, but also that *Pax6* may have a regulatory effect of greater significance upon *Dll1* in terms of how *Dll1* participates during Notch signalling within specific progenitor cell subtypes.

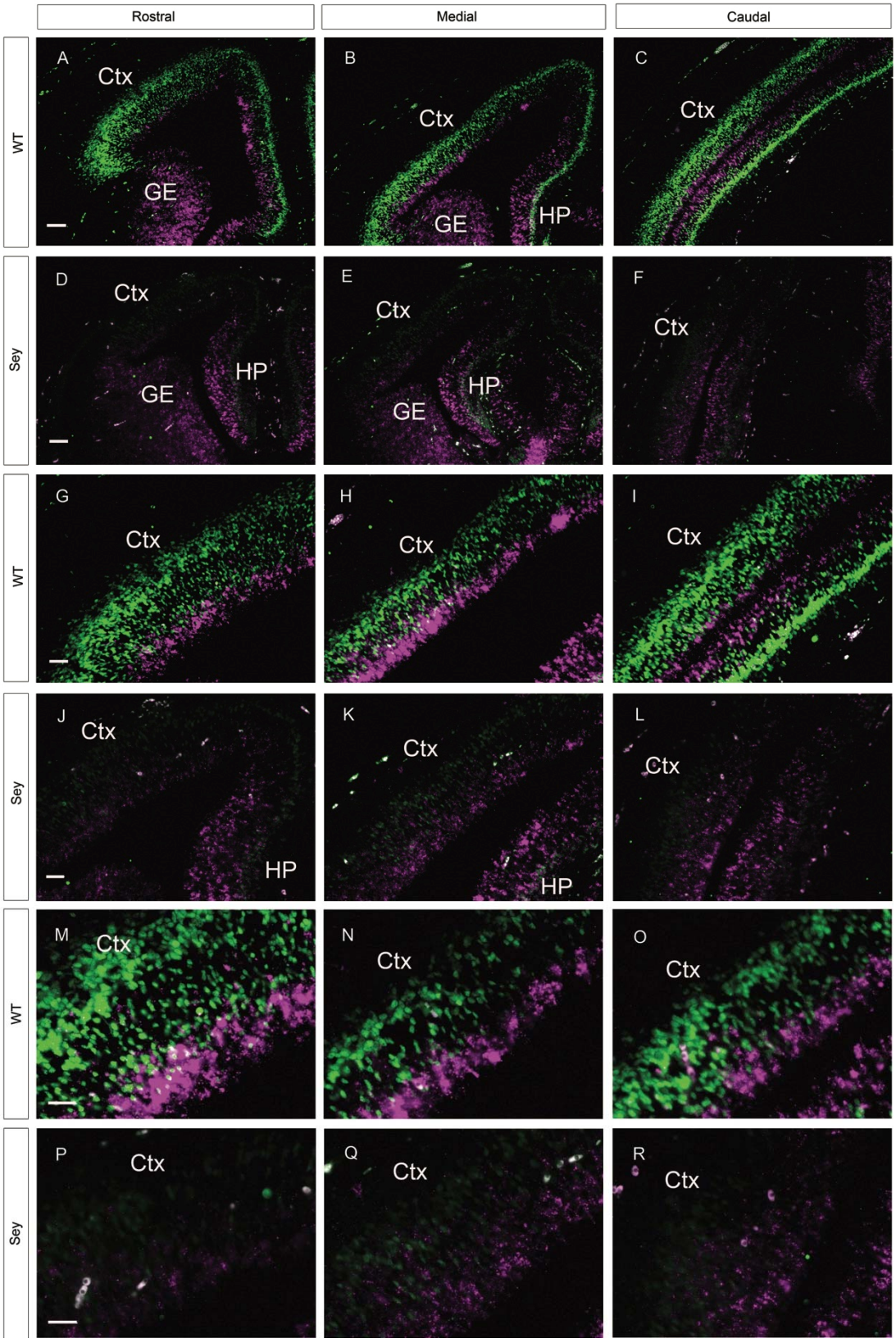

Figure 5.2 *Dll1* and Tbr2 expression in the developing cerebral cortex at E14.5

Dll1 expression (Magenta) and Tbr2 expression (green) in WT embryos (A-C and G-I) and Sey embryos (D-F and J-L). (A) Tbr2 expression in the rostral region of the telencephalon. (B) Tbr2 expression in the medial region of the telencephalon. (C) Tbr2 expression in the caudal region of the telencephalon. Tbr2 expression appears restricted to the SVZ of the developing cortex of WT embryos (A-C). (A) *Dll1* expression in the rostral region of the telencephalon. (B) *Dll1* expression in the medial region of the telencephalon. (C) *Dll1* expression in the caudal region of the telencephalon. *Dll1* expression appears restricted to the VZ of the developing cortex of WT embryos (A-C). (D) Tbr2 expression in the rostral region of the telencephalon. (E) Tbr2 expression in the medial region of the telencephalon. (F) Tbr2 expression in the caudal region of the telencephalon. Tbr2 expression appears restricted to the SVZ of the developing cortex of Sey embryos (D-F). (D) *Dll1* expression in the rostral region of the telencephalon. (E) *Dll1* expression in the medial region of the telencephalon. (F) *Dll1* expression in the caudal region of the telencephalon. *Dll1* expression appears restricted to the VZ of the developing cortex of Sey embryos (D-F). Both *Dll1* and Tbr2 expression are reduced in Sey embryos (D-F) when compared to WT embryos (A-C). (G and M) Tbr2 expression in the rostral region of the developing cortex. (H and N) Tbr2 expression in the medial region of the developing cortex. (I and O) Tbr2 expression in the caudal region of the developing cortex. (J and P) Tbr2 expression in the rostral region of the developing cortex. (K and Q) Tbr2 expression in the medial region of the developing cortex. (L and R) Tbr2 expression in the caudal region of the developing cortex. No evidence of co-expression between *Dll1* and Tbr2 is evident in the developing cortex of WT embryos (G-I) or in the cortex of Sey embryos (J-L). Sey = $Pax6^{-/-}$ and WT = $Pax6^{+/+}$. Ctx = Cortex. GE = Ganglionic Eminences. HP = Hippocampus. (A-F) Scale bars = 80µm. (G-L) = 60µm. (M-R) = 40 µm. N = 3 embryos

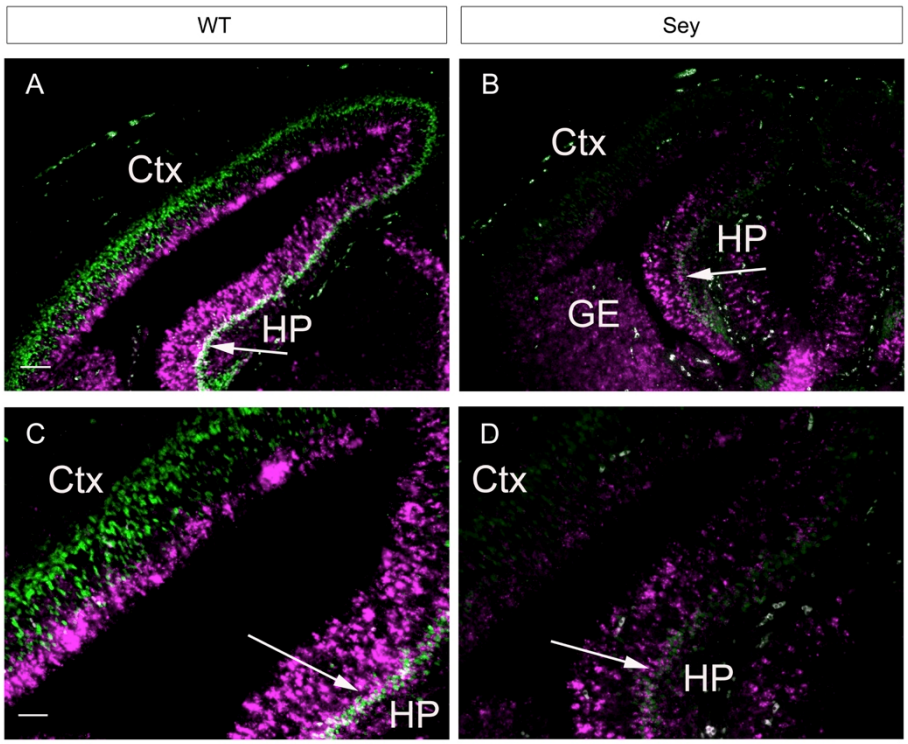

Figure 5.3 *Dll1* gene expression and Tbr2 expression in the developing hippocampus at E14.5

Dll1 expression (magenta) and Tbr2 expression (green) in WT embryos (A and C) and Sey embryos (B and D). Tbr2 expression remains restricted to the SVZ in the developing hippocampus in both WT (A) and Sey (B) embryos. *Dll1* expression is observed in both the VZ and the SVZ of the developing hippocampus of WT embryos (A and C). (A and C) white arrows show co-expression of *Dll1* and Tbr2 in WT embryos. In Sey embryos (B and D), the expression of Tbr2 and *Dll1* is reduced. Expression within regions observed WT embryos are retained in Sey embryos for both Tbr2 and *Dll1*. (B and D) white arrows depict the reduction in co-expression between *Dll1* and Tbr2 in the SVZ when compared to WT embryos (A and C). Sey = $Pax6^{-/-}$ and WT = $Pax6^{+/+}$. Ctx = Cortex. GE = Ganglionic Eminences. HP = Hippocampus. (A and B) Scale bars = 80µm. (C and D) Scale bars = 60µm. N = 3 embryos

The fact that analysis of *Dll1* and Tbr2 double in situ hybridisation/immunohistochemistry expression at E12.5 and E14.5 observed little to no co-expression between the two in the developing cortex strongly suggests that

Dll1 isn't expressed by INPs residing within the SVZ. Furthermore, *Dll1* expression was found to be restricted exclusively to the VZ in the cerebral cortex. Interestingly, co-expression was identified in the SVZ of the developing hippocampus, with *Dll1* expression apparent in the VZ and the SVZ, suggesting that the regulatory mechanisms for *Dll1* in the hippocampus differ from the cortex.

5.3 *Dll1* expression appears to co-localise with a number of *Ngn2* expressing cells in the developing cortex

While Tbr2 was used to determine which progenitor zone *Dll1* is expressed in, *Ngn2* was also used as a marker to learn more about how *Pax6* interacts with *Dll1* in progenitor cell subtypes due to previously documented regulatory relationship between *Pax6* and *Ngn2* (Scardigli *et al*., 2001; 2003), as well as the regulatory relationship between *Ngn2* and *Dll1* (Castro *et al*., 2006). Due to the results found for *Dll1*/Tbr2 expression, coupled with what we know about the regulatory relationship between *Dll1* and *Ngn2;* it was hypothesised that there would be a high level of co-expression between *Dll1* and *Ngn2* in the VZ of the developing cortex. Furthermore, it was hypothesised that *Dll1* expression would be dramatically reduced in the VZ of *Pax6*$^{-/-}$ embryonic cortices, due to the fact that Pax6 directly regulates *Ngn2* and its expression has been shown to reduce dramatically in *Pax6*$^{-/-}$ mutants (Carr, 2009; Sansom *et al*., 2009).

As was the case with fluorescent double labelling analysis carried out with *Dll1* and Tbr2, initial double analysis for *Dll1* and *Ngn2* was carried out on E12.5 WT embryos and their *Pax6*$^{-/-}$ mutant littermates (Figure 5.4). In WT embryos *Ngn2* expression was observed widely throughout the progenitor zone of the developing cerebral cortex (Figure 5.4 A-C). *Dll1* expression was also observed throughout the vast majority of the progenitor zone, suggesting that VZ accounts for the majority of the progenitor zone of the developing cortex at this stage of embryonic development. Furthermore, an abundance of double labelling between *Ngn2* and *Dll1* was evident within the cortex (Figure 5.4 G-I). In contrast, analysis using *Pax6*$^{-/-}$ mutant littermates observed a reduction in both *Dll1* and *Ngn2* staining throughout the

cortex (Figure 5.4 D-F) and as a result, an apparent reduction in the proportion of cells co-expressing the two genes (Figure 5.4 J-L).

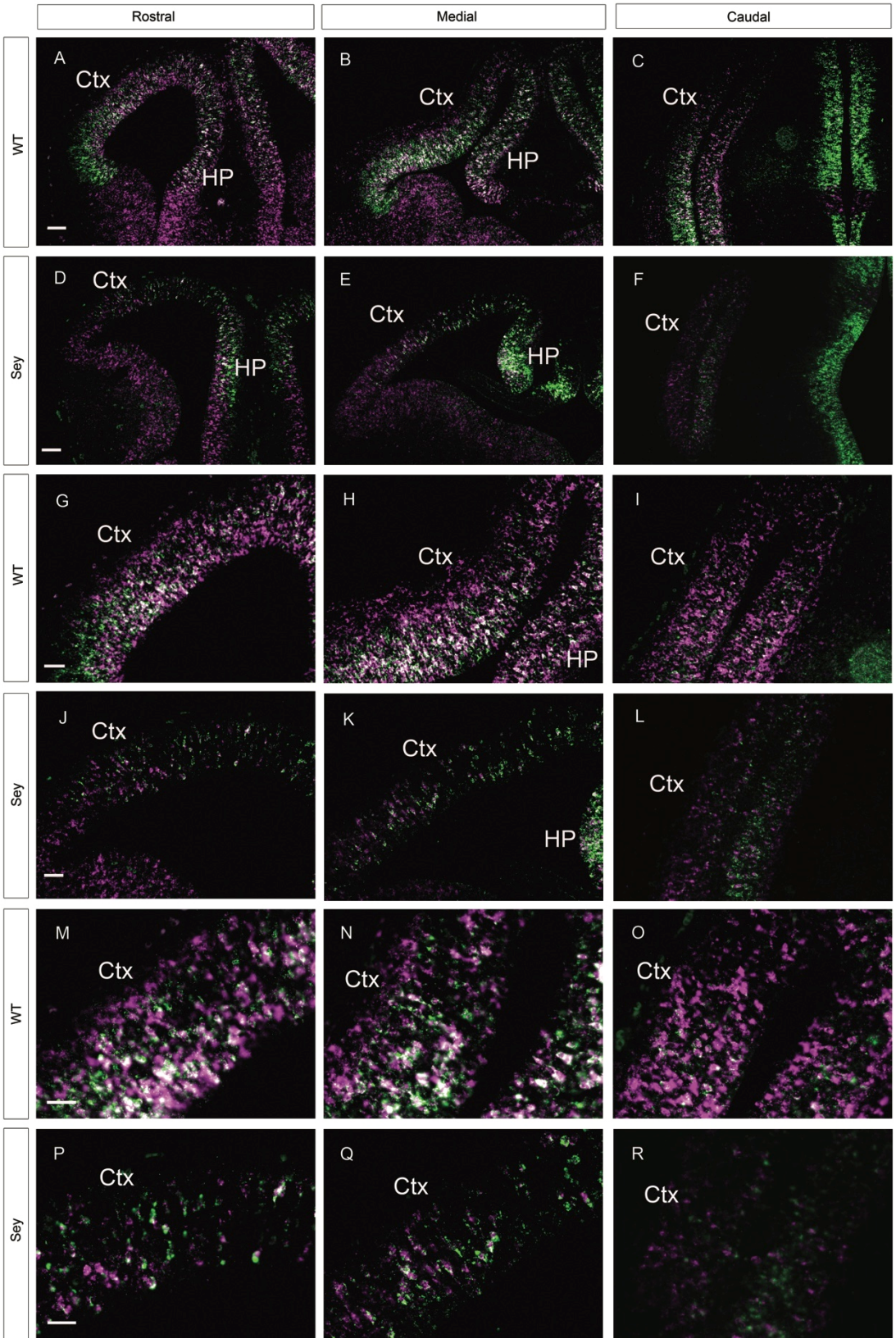

Figure 5.4 *Dll1* and *Ngn2* expression in the developing cerebral cortex at E12.5

Dll1 expression (Magenta) and *Ngn2* expression (green) in WT embryos (A-C and G-I) and Sey embryos (D-F and J-L). (A) *Dll1* and *Ngn2* expression in the rostral region of the telencephalon. (B) *Dll1* and *Ngn2* expression in the medial region of the telencephalon. (C) *Dll1* and *Ngn2* expression in the caudal region of the telencephalon. *Dll1* expression appears restricted to the VZ of the developing cortex of WT embryos (A-C). *Ngn2* expression is observed throughout the progenitor zone of the developing cortex. (D) *Dll1* and *Ngn2* expression in the rostral region of the telencephalon. (E) *Dll1* and *Ngn2* expression in the medial region of the telencephalon. (F) *Dll1* and *Ngn2* expression in the caudal region of the telencephalon. *Dll1* expression appears restricted to the VZ of the developing cortex of Sey embryos (D-F). *Ngn2* expression is observed throughout the progenitor zone of the developing cortex in Sey embryos (D-F). *Dll1* and *Ngn2* gene expression is reduced in Sey embryos (D-F) when compared to WT embryos (A-C). (G and M) *Ngn2* expression in the rostral region of the developing cortex. (H and N) *Ngn2* expression in the medial region of the developing cortex. (I and O) *Ngn2* expression in the caudal region of the developing cortex. (J and P) *Ngn2* expression in the rostral region of the developing cortex. (K and Q) *Ngn2* expression in the medial region of the developing cortex. (L and R) *Ngn2* expression in the caudal region of the developing cortex. (G-I and M-O) An abundance of co-expression between *Dll1* and *Ngn2* was observed in the VZ of the cerebral cortex of WT embryos at E12.5 (depicted in white). (J-L and P-R) Co-expression of *Dll1* and *Ngn2* (depicted in white) in the cortex of Sey embryos appears reduced when compared to WT controls (G-I). Sey = *Pax6*$^{-/-}$ and WT = *Pax6*$^{+/+}$. Ctx = Cortex. GE = Ganglionic Eminences. HP = Hippocampus. (A-F) Scale bars = 80µm. (G-L) = 60µm. (M-R) = 40 µm. N = 3 embryos.

Further *Dll1*/*Ngn2* analysis was then carried out at the later developmental stage of E14.5 (Figure 5.5). Double labelling in WT embryos identified *Ngn2* expression within the VZ of the developing cerebral cortex and within a proportion of the SVZ (Figure 5.5 A-B). *Dll1* staining remained confined to the diminishing VZ as previously observed in *Dll1*/Tbr2 double labelling experiments also performed at E14.5 (Figure 5.2). Some co-localisation between *Dll1* and *Ngn2* was observed in the VZ where *Dll1* expression was identified (Figure 5.5 G-I). Analysis of *Dll1*/*Ngn2* double labelling in *Pax6*$^{-/-}$ mutants at E14.5 showed a reduction in both *Dll1* and *Ngn2* staining in the developing cortex (Figure 5.5 D-F). Additionally, co-expression that was observed in WT littermates at E14.5 appears vastly reduced in their *Pax6*$^{-/-}$ mutant counterparts (Figure 5.5 J-L).

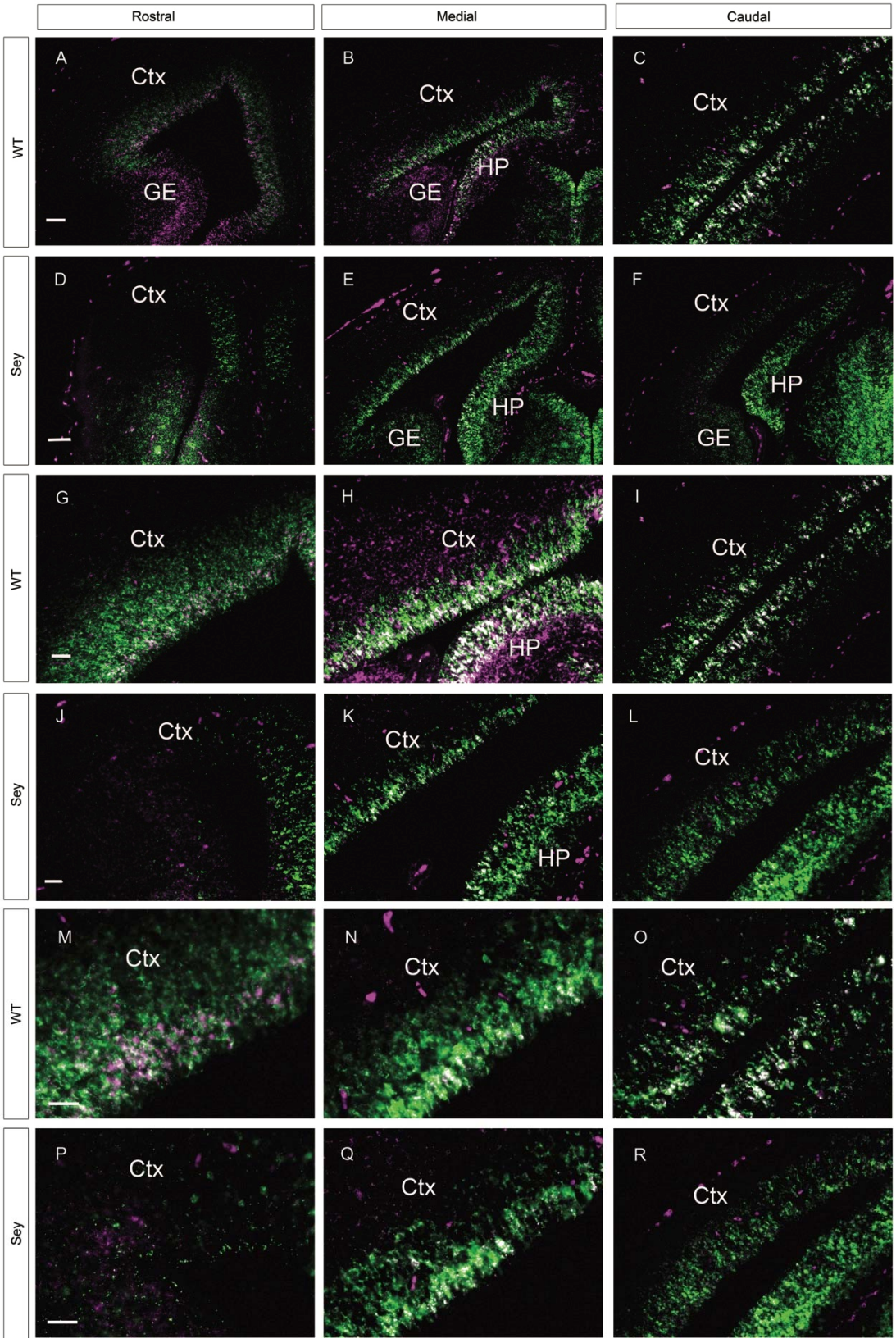

Figure 5.5 *Dll1* and *Ngn2* expression in the developing cerebral cortex at E14.5

Dll1 expression (Magenta) and *Ngn2* expression (green) in WT embryos (A-C and G-I) and Sey embryos (D-F and J-L). (A) *Dll1* and *Ngn2* expression in the rostral region of the telencephalon. (B) *Dll1* and *Ngn2* expression in the medial region of the telencephalon. (C) *Dll1* and *Ngn2* expression in the caudal region of the telencephalon. *Dll1* expression appears restricted to the VZ of the developing cortex of WT embryos (A-C). *Ngn2* expression is observed throughout the progenitor zone of the developing cortex. (D) *Dll1* and *Ngn2* expression in the rostral region of the telencephalon. (E) *Dll1* and *Ngn2* expression in the medial region of the telencephalon. (F) *Dll1* and *Ngn2* expression in the caudal region of the telencephalon. *Dll1* expression appears restricted to the VZ of the developing cortex of Sey embryos (D-F). *Ngn2* expression is observed throughout the progenitor zone of the developing cortex in Sey embryos (D-F). *Dll1* and *Ngn2* gene expression is reduced in Sey embryos (D-F) when compared to WT embryos (A-C). (G and M) *Ngn2* expression in the rostral region of the developing cortex. (H and N) *Ngn2* expression in the caudal region of the developing cortex. (I and O) *Ngn2* expression in the caudal region of the developing cortex. (J and P) *Ngn2* expression in the medial region of the developing cortex. (K and Q) *Ngn2* expression in the medial region of the developing cortex. (L and R) *Ngn2* expression in the caudal region of the developing cortex. (G-I and M-O) An abundance of co-expression between *Dll1* and *Ngn2* was observed in the VZ of the cerebral cortex of WT embryos at E14.5 (depicted in white). (J-L and P-R) Co-expression of *Dll1* and *Ngn2* (depicted in white) in the cortex of Sey embryos appears reduced when compared to WT controls (G-I). Sey = $Pax6^{-/-}$ and WT = $Pax6^{+/+}$. Ctx = Cortex. GE = Ganglionic Eminences. HP = Hippocampus. (A-F) Scale bars = 80µm. (G-L) = 60µm. (M-R) = 40 µm. N = 3 embryos.

While potential co-expression between *Dll1* and *Ngn2* was observed when analysis of double fluorescent labelling was carried by conventional fluorescence microscopy, co-localisation could not be confirmed without additional image analysis of Z stacked images produced on a confocal microscope. Z stacked images provide a comprehensive, multidimensional view of cells comprising the developing cortex, rather than the single level of depth achieved by a traditional fluorescent light microscope. Analysis of Z stacked images identified that the proposed co-localisation of *Dll1* and *Ngn2* cells was accurate, with co-localisation in whole cell bodies clearly visible (Figure 5.6).

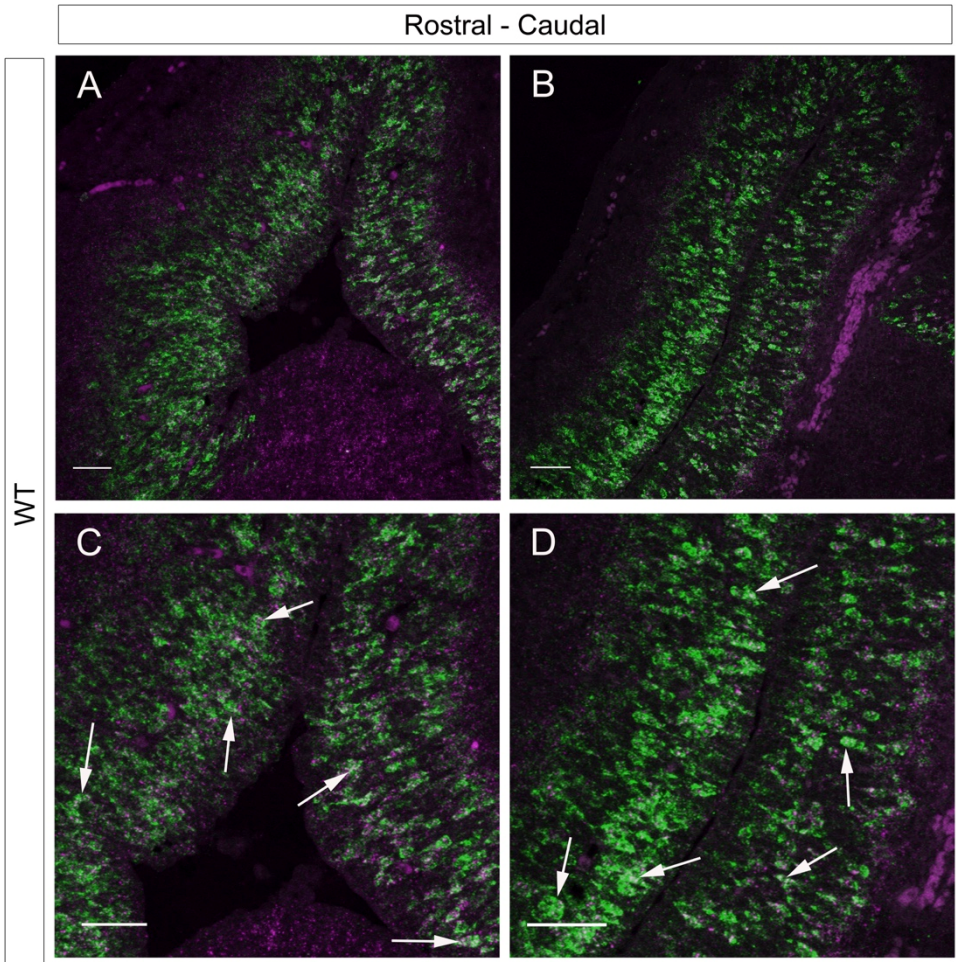

Figure 5.6 Z stack analysis of *Dll1* and *Ngn2* expression in the developing cortex at E14.5

(A) A rostral section of the developing cortex at E14.5. (B) A Caudal section of the developing cortex at E14.5. (C) Magnification of A. (D) Magnification of B. White arrows show examples of co-localisation of the two genes in individual cells within the VZ. Scale bars = 60µm. N = 3 embryos.

5.4 *Dll1* expression in the developing cortex is unaffected by a loss of *Ngn2* expression at E14.5

Further investigations into the regulatory control of *Dll1* by *Pax6* was carried out using an *Ngn2*-Cre knockin mutant mouse line previously described by Zirlinger *et*

al., (2002), which produces a homozygous Ngn2$^{-/-}$ genotype (Zirlinger *et al*., 2002). Homozygous *Ngn2*$^{-/-}$ mutant embryos were selected for the experiment and WT littermates were also selected to act as a control. Analysis of *Dll1* expression by in situ hybridisation was carried out in order to establish whether a similar or greater down regulation of *Dll1* occurs in the cortex of *Ngn2*$^{-/-}$ embryos. This approach was implemented due to our knowledge of the regulatory effects of *Pax6* on *Ngn2*, as well as previous studies which have highlighted that *Ngn2* is responsible for the activation of *Dll1* in the Notch signalling pathway during embryonic neurogenesis (Scardigli *et al*., 2001; 2003; Castro *et al*., 2006). In situ hybridisation was carried out at the developmental stage E14.5, when embryonic neurogenesis is at its peak. Quantification of in situ expression data was then carried out by cell count analysis. It was hypothesised that a significant decrease in *Dll1* expression and density would be observed and that this decrease would be greater than the decrease in *Dll1* expression observed in *Pax6*$^{-/-}$ embryonic cortices.

At E14.5, *Dll1* staining was observed as a punctate expression pattern in both *Ngn2*$^{-/-}$ mutants (Figure 5.7 D-F) and their WT control littermates (Figure 5.7 A-C). *Dll1* expression appeared to be predominantly restricted to the VZ of the developing telencephalon, with little evidence of expression outwith this proliferative region. Analysis of *Dll1* expression in the cerebral cortex observed no obvious difference in staining between *Ngn2*$^{-/-}$ mutant embryos (Figure 5.7 G-I) and their WT control littermates (Figure 5.7 J-L).

Statistical analysis of the cell density of *Dll1* expressing cells by Two-way ANOVA of both the dorsal (Figure 5.8 A) and the ventral (Figure 5.8 B) regions of the developing cortex at E14.5 reported no interaction, region or genotype effect. Further analysis by Tukey's multiple comparison testing yielded no significant differences. Analysis of total cell number in the developing cortex of *Ngn2*$^{-/-}$ and WT control embryos by two-way ANOVA also produced no interaction, region or genotype effects, and Tukey's multiple comparison tests also yielded no significant differences in both the dorsal (Figure 5.8 C) and ventral (Figure 5.8 D) regions of the developing cerebral cortex.

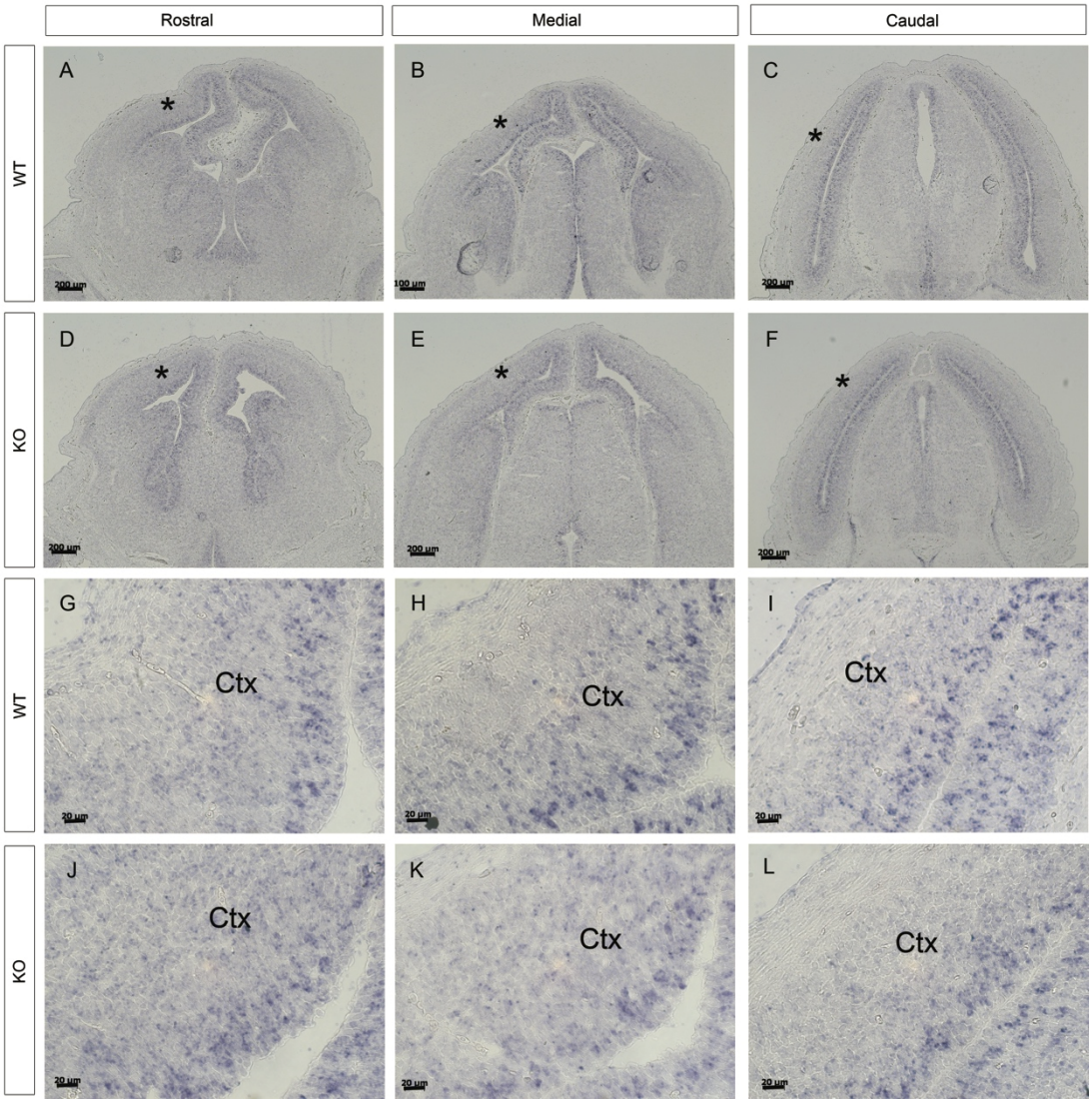

Figure 5.7 *Dll1* expression in the developing forebrain of *Ngn2*$^{-/-}$ embryos at E14.5

(A-C) *Dll1* gene expression in a WT control embryo. (A) *Dll1* expression in the rostral region of the WT forebrain. (B) *Dll1* expression in the medial region of the WT forebrain. (C) *Dll1* expression in the caudal region of the WT forebrain. (D-F) *Dll1* expression in an *Ngn2*$^{-/-}$ mutant embryo. (D) *Dll1* expression in the rostral region of the *Ngn2*$^{-/-}$ forebrain. (E) *Dll1* expression in the medial region of the *Ngn2*$^{-/-}$ forebrain. (F) *Dll1* expression in the caudal region of the *Ngn2*$^{-/-}$ forebrain. (G-I) *Dll1*s punctate expression pattern in the developing cerebral cortex of WT control embryos at E14.5. (J-L) *Dll1* expression in the developing cerebral cortex of *Ngn2*$^{-/-}$ mutant embryos. No discernable difference in *Dll1* expression is apparent between WT control (G-I) and Sey mutant (J-L) embryos. (A-F) Scale bars = 200µm. (A-F) * indicates the cortex. (G-L) Ctx = Cortex (G-L) Scale bars = 20µm. (N=3 embryos). Analysis carried out by project student Elena Purlyte.

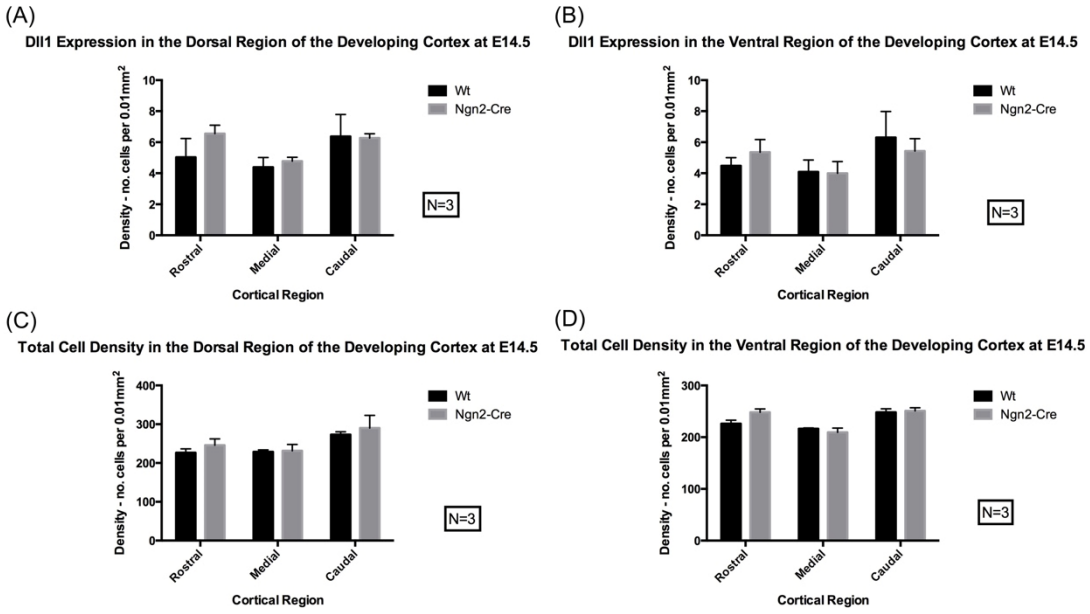

Figure 5.8 *Dll1* expression in the dorsal and ventral regions of the developing cortex of *Ngn2*$^{-/-}$ embryos at E14.5

(A) *Dll1* cell density in the dorsal region of the cortex in WT controls and *Ngn2*$^{-/-}$ mutants. (B) *Dll1* cell density in the ventral region of the cortex in WT controls and *Ngn2*$^{-/-}$ mutants. (A-B) No significant difference in *Dll1* density was detected when comparing *Ngn2*$^{-/-}$ mutants to WT controls. (C) Total cell density in the dorsal region of the cortex in WT controls and *Ngn2*$^{-/-}$ mutants. (D) Total cell density in the ventral region of the cortex in WT controls and *Ngn2*$^{-/-}$ mutants. (C-D) No significant difference in total cell density was detected when comparing *Ngn2*$^{-/-}$ mutants to WT controls. Ngn2-Cre = *Ngn2*$^{-/-}$ embryos. Analysis carried out by project student Elena Purlyte.

Analysis of *Dll1* expression and density by in situ hybridisation and cell count quantification respectively, identified no significant decrease in *Ngn2*$^{-/-}$ embryos when compared to their WT littermates. This was surprising as activation of *Dll1* is directly regulated by Ngn2. As a result, the fact that a more noteworthy decrease was observed in *Pax6*$^{-/-}$ embryos, it begs the question as to whether Pax6 plays a greater role in the regulation of *Dll1* than originally hypothesised.

5.5 *Dll1* is enriched in RGCs and INPs in the developing cortex at E14.5

In situ hybridisation analysis of *Dll1* has observed expression of the gene to be restricted to the VZ of the developing cerebral cortex (Campos *et al*., 2001; Chapter 3; Chapter 5). Furthermore, double labelling analysis of *Dll1* expression and Tbr2 expression indicated that Dll1 is not expressed by INPs (Chapter 5). It can therefore be proposed that Dll1 is likely to be expressed by RGCs residing within the VZ. However, as previously discussed, past studies have claimed that Dll1 expression is restricted to INPs predominately within the VZ. The fact that conflicting data on Dll1 analysed protein rather than mRNA expression is of particular interest and relevance in determining why there are discrepancies between studies of Dll1. One such conflicting study is the 2013 research article by Nelson *et al.,* which included FACS analysis, carried out using a Tbr2 green fluorescent protein (GFP) reporter mouse line. This study identified that Tbr2 positive GFP labelled cells also expressed Dll1. However, some anomalies exist in their data set, such as the apparent expression of Pax6 by INPs rather than RGCs. Pax6 has been well documented as a marker of RGCs during cortical development for both its mRNA and protein expression. This not only highlights the possibility that Dll1 protein may be present in INPs even though Dll1 mRNA is not, but equally brings into question the reliability of the FACS data presented by Nelson *et al*., (2013).

In order to resolve this, Dll1 protein expression was analysed by flow cytometry, a similar experiment to the FACS analysis conducted by Nelson *et al*., (2013). Double staining of Dll1 and the INP marker Tbr2 was carried out on dissociated embryonic cortical cells of WT embryos at E14.5 prior to conducting flow cytometry analysis. This gave the ability to distinguish whether Dll1 protein is expressed in INPs in the developing cerebral cortex. It was found that a proportion of Dll1 expressing cells expressed Tbr2 but not all Dll1 expressing cells were Tbr2 positive. Additionally, not all cells expressing Tbr2 also expressed Dll1 and a proportion of cells did not express either protein.

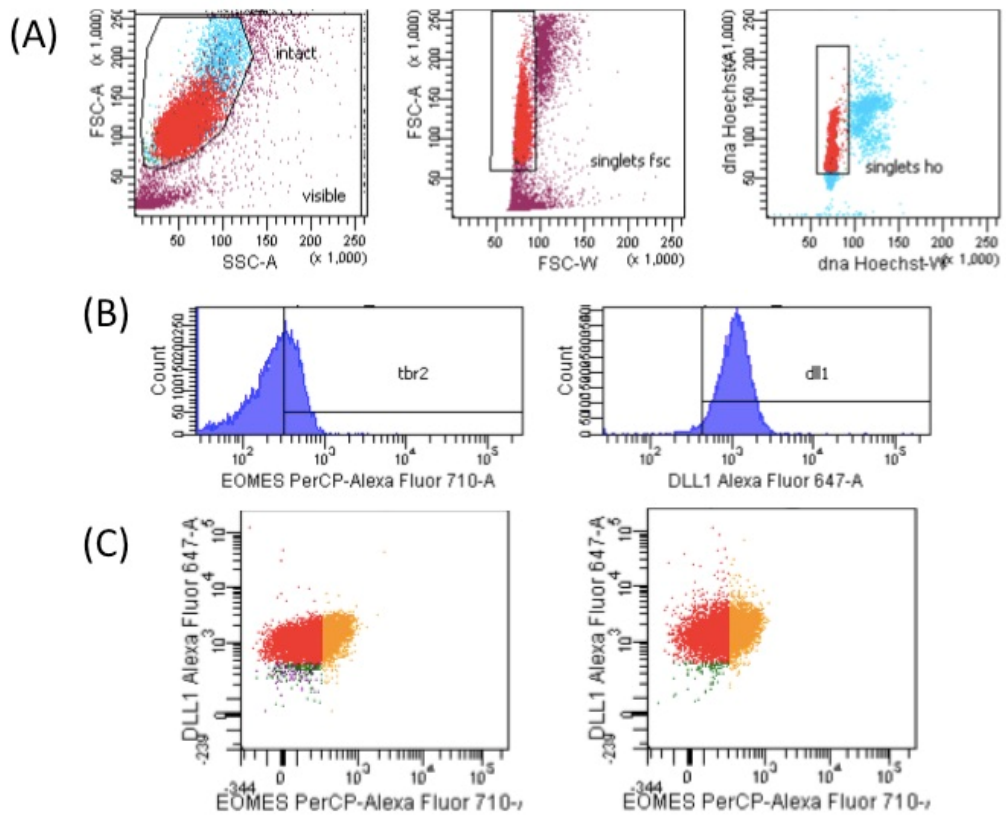

Figure 5.9 Dll1 and Tbr2 flow cytometry analysis

(A) An example of the channel gating used to select cells for analysis. (B) Gating set for Dll1 and Tbr2 expression. Expression to the left of the gate is considered as background and discounted from analysis. (C) Example scatter plots depicting Dll1 expressing cells. Histograms show that a proportion of Dll1 expressing cells also express Tbr2 (shown in orange).

5.6 Discussion

Investigations into the location of *Dll1* expression within the progenitor cell population were carried out in order to solidify which sub population the *Notch* ligand is expressed in. As previously described, past studies have produced conflicting results concerning which progenitor cell population *Dll1* is expressed in. While it could initially be concluded from the literature that *Dll1* may simply be

expressed within multiple progenitor zones, the fact that each individual study did not reflect this makes this unlikely.

In order to establish which progenitor cell population *Dll1* is expressed in, double labelling was carried out using the INP marker *Tbr2*. Co-expression of *Dll1* and *Tbr2* would signify that INP cells express *Dll1*, while any expression of *Dll1* within the progenitor zone, outwith the expression of *Tbr2*, would indicate expression of *Dll1* within RGCs residing in the VZ of the developing cortex. Analysis of WT embryos at E12.5 and E14.5 identified no co-expression of *Tbr2* and *Dll1* in the developing cerebral cortex, with *Dll1* expression residing distinctly within the VZ. This suggests that *Dll1* is expressed in RGCs rather than in INPs. However, it is possible that Dll1 could be expressed by INPs residing within the VZ. It has been suggested that INP^{VZ}s could potentially be newly generated INPs in the processes of migrating to the SVZ following the asymmetric division of a RGC within the VZ. If this is the case, Dll1 could potentially be a link between the differentiation of RGCs into INPs, with Dll1 expression signifying a RGC fated to divide to produce an INP and its expression within INP^{VZ}s acting as a remnant of the progenitor cell subtype that it was generated from (Englund *et* al., 2005; Corbin *et al*., 2009; Nelson *et al.*, 2013).

The 2013 study by Nelson *et al*., further solidified the previous claim that INPs are a major source of Dll1 expression, while also suggesting that the ligand is also expressed by INP^{VZ}s and potentially a small, subpopulation of RGCs in the VZ (Nelson *et al*., 2013). Their initial investigations implemented a FACs-based gene expression profiling approach, in order to identify genes expressed in proliferating INPs vs. proliferating RGCs. In order to achieve this, the cortices of E14.5 $Tbr2GFP^{+}$ embryos were used in order to sort replicating progenitors (>2N DNA) and then further sort INPs (GFP^{+}) from RGCs (GFP^{-}) by FACs. Sorted cells were then used as RNA sources for comparative transcriptomic profiling of the progenitor subtypes by microarray analysis. It was concluded that Dll1 is expressed exclusively by INPs, along with Notch components Dll3 and Hey1; while RGCs expressed N1-3, Hes5 and Jag1. While this aligned with previous claims that Dll1 is solely expressed by INPs (Mizutani *et al*., 2007; Kawaguchi *et al*., 2008; Yoon *et al*., 2008), this

result not only conflicts with the findings detailed in this chapter (5.2), but also with previous research (Campos *et al*., 2001) and with subsequent findings detailed in Nelson *et al*., (2013). It was noted that Pax6 expression was documented as being exclusive to INPs, a claim that can automatically be identified as incorrect due to the fact that Pax6 is well known as a marker of RGCs in the developing cortex (Manuel *et al*., 2015). As a result, this throws into question the validity of the entire FACs/microarray analysis carried out by Nelson *et al*., (2013). It is plausible that the Tbr2GFP reporter used could be leaky, labelling some RGCs as well as INPs, although this wouldn't account for Pax6 being expressed exclusively by INPs; leaving the possibility of manual/mechanical error during the experimental process or during analysis of the subsequent data. Regardless, the claim that Dll1 is expressed solely by INPs cannot be relied upon solely based upon these results. Immunohistochemical analysis of Dll1 expression by Nelson *et al*., (2013) suggested that Dll1 is expressed in the cell bodies of INPs, while expression found surrounding RGCs was located on cell process extending from INPs. However, the expression data provided was somewhat unconvincing, with few panels of low expression shown. Furthermore, investigations for this thesis using the same Dll1 antibody and immunohistochemistry methods as Nelson *et al*., (2013) were in fact abandoned due to the irreproducibility of the results and overall, faint and unconvincing expression for Dll1; even when imaged using a confocal microscope. Further evidence was provided to determine which progenitor cells express Dll1 by analysis of slice cultures and live cell imaging, which utilised embryonic cortices electroporated Dll1Lacz and Dll1YFP reporters respectively, observed Dll1 expression originating from both INPs and a subset of RGCs, suggesting that Dll1 is expressed by both progenitor cell populations (Nelson *et al*., 2013). However, how the SVZ, VZ, INPs and RGCs were distinguished is not thoroughly detailed in the paper and appears to be based on the identification of apical/apical and basal attachments in order to determine progenitor cell subtype. This method of identification relies heavily upon the quality of the images produced and leaves considerable room for human error. Additionally, the proportions of INPs and RGCs expressing Dll1 were not quantified, so the number of each cell type expressing Dll1 and whether this number is significant, is unknown. Interestingly, recent investigations by Shimojo *et al*., (2016)

into the effects of Dll1 on Notch oscillations and neurogenesis, identified an increase in expression of the INP marker Tbr2 in Dll1 mutant embryos, and a reduction in the size of the VZ and number of mitotic cells residing there. This suggests that Dll1 is likely to be expressed by RGCs in the VZ, as proliferation is disrupted within this proliferative zone of the cortex (Shimojo *et al*., 2016).

While no co-expression between *Dll1* and Tbr2 was identified in the developing cerebral cortex, apparent co-localisation between Tbr2 and *Dll1* was observed within the SVZ of the developing hippocampus at E14.5. This was of particular interest due to the fact that Notch signalling is a key player during hippocampal development, with Notch ligands and receptors being broadly expressed during all stages of the development of the hippocampus, while also orchestrating the maintenance of neural stem cells postnatally (Urban and Guillemot, 2014; Pleasure *et al*., 2000). In terms of Dll1 specifically, the ligand has previously been identified in the subgranular zone of the adult murine hippocampus, where it has been found to play a critical role in the maintenance of the quiescence of adult neural stem cells that reside there (Kawaguchi *et al*., 2013; Kirby *et al*., 2015). The fact that *Dll1* and Tbr2 were found to co-express in the SVZ of the developing hippocampus at E14.5, suggests that the molecular mechanisms that drive cell proliferation in different progenitor cells populations differ in specific telencephalic structures rather than being uniform for the proliferative region of the telencephalon as a whole. Specifically, it highlights that the mechanisms of Notch signalling vary in the progenitor cell populations in different telencephalic structures. This difference is most likely due to different co-effectors acting within the hippocampus at E14.5, resulting in the progenitor cells within its progenitor zone being maintained differently. In addition to the role of Dll1 expression in development and maintenance of both the embryonic and postnatal hippocampus, the fact that Pax6 is also required for the production and maintenance of neural progenitor cells in the hippocampus (Maekawa *et al*., 2005; Duan *et al*., 2013) is noteworthy as this evidence suggests that a regulatory relationship between Pax6 and Dll1 could exist in the hippocampus, both directly or indirectly via Pax6's control of Tbr2. Interestingly, there is no evidence of co-expression of *Dll1* and *Tbr2* in the developing hippocampus at E12.5. This suggests that genetic factors

responsible for the shift in *Dll1*s expression to multiple progenitor populations do not occur until E14.5. It would subsequently be of significance to analyse later developmental stages in order to determine if this shift continues and whether or not it applies to other telencephalic regions such as the cerebral cortex.

Analysis of *Pax6*$^{-/-}$ mutant embryos observed both *Dll1* and Tbr2 to be down regulated in the telencephalon at E12.5 and E14.5. This observation was expected due to our work highlighting *Pax6*'s regulatory effect on *Dll1*, and previous studies which have identified Tbr2 as a positive target of *Pax6* (Warren *et al., 1999;* Englund *et al.*, 2005; Carr, 2009; Sansom *et al*., 2009; Diaz-Alonso *et al*., 2014). Interestingly, the level of co-expression between *Dll1* and Tbr2 in the SVZ of the developing hippocampus is markedly reduced. This could be due to the fact that *Pax6* drives the expression of Tbr2 and *Dll1* within the same progenitor cell type, accounting for the observed reduction. However, the decrease could also purely be due to a decrease in the number of Tbr2/*Dll1* expressing cells as observed in the cortex of *Pax6*$^{-/-}$ mutant embryos, and that there is no shift in gene expression caused by a lack of *Pax6* in the hippocampus at E14.5.

In order to gain further understanding of *Pax6*'s regulatory control, *Dll1* double labelling analysis with *Dll1* and *Ngn2* was carried out at embryonic stage E12.5 and E14.5. This approach allowed us to examine the relationship between *Dll1* and a gene directly regulated by *Pax6* (Scardigli *et al*., 2003; Sansom *et al*., 2009), as well as a direct activator of *Dll1*. According to literature, if *Dll1* is an indirect target of *Pax6*, it is most likely that any regulatory control that the transcription factor exerts over *Dll1* would be via *Pax6*'s up regulation of *Ngn2*. As previously mentioned, our working hypothesis states that *Pax6* and *Dll1* may exhibit a mutual regulatory effect upon one another via the mechanism termed 'cis-inhibition' actively involved in progenitor cell maintenance by Notch signalling (Chapter 1). Consequently, it is anticipated that there should be a high level of co-localisation between *Dll1* and *Ngn2*, and that in *Pax6*$^{-/-}$ embryos, the reduction in *Dll1* and *Ngn2* expression should be relatively similar due to the fact that *Ngn2* activates *Dll1* and that Ngn2$^{-/-}$ is vastly down-regulated in Pax6$^{-/-}$ embryos (Carr, 2009; Sansom *et al*., 2009).

Double labelling analysis at E12.5 showed *Ngn2* expression throughout the VZ and the newly developing SVZ, while *Dll1* expression remained constrained to the VZ as previously shown. At E12.5 in WT embryos, an abundance of *Dll1*/*Ngn2* co-expression was apparent throughout the VZ of the developing cerebral cortex. However, not every *Dll1* expressing cell co-expresses *Ngn2*. At E14.5, *Ngn2* expression remained prevalent in the fully formed SVZ and the now diminished VZ of the cerebral cortex, with co-expression between *Dll1* and *Ngn2* remaining predominant within the boundaries of the VZ. The fact that a reduction in *Ngn2* and *Dll1* expression was identified in the cortex of *Pax6*$^{-/-}$ mutant embryos at E12.5 and E14.5 was unsurprising due to the conclusions drawn from previous investigations from our lab and the published research of other groups (Chapter 3; Chapter 5; Carr 2009; Scardigli *et al*., 2001; 2003). However, the fact that *Dll1* expression does not appear to be as reduced as *Ngn2* expression at both stages of embryonic development is of particular interest as it signifies that *Ngn2* is not solely responsible for the activation of *Dll1*.

Further research into the literature surrounding *Dll1* uncovered that the proneural gene *Mash1* is also responsible for the activation of *Dll1* (Casarosa *et al*., 1999; Castro *et al*., 2006). This link is of key significance to our observation that *Dll1* does not appear to be as reduced as *Ngn2* in the developing cortex of *Pax6*$^{-/-}$ mutant embryos, due to the fact that Mash1 and Ngn2 have opposing levels of expression in the developing cortex (Carr *et al*., 2009; Sansom *et al*., 2009). *Mash1* has been identified as a target of *Pax6* and is up-regulated in Pax6$^{-/-}$ mutant embryos (Kroll *et al*., 2005; Carr, 2009; Sansom *et al*., 2009), meaning that *Pax6* acts to repress *Mash1* expression in the developing cortex of WT embryos. It stands to reason that an up-regulation of *Mash1* would account for the fact that *Dll1* does not display as striking a reduction in expression as *Ngn2*, due to the up-regulation in *Mash1* accounting for any decrease in *Dll1* as a result of a decrease in *Ngn2* expression. However, the up-regulation of *Mash1* does not completely restore *Dll1* expression in WT embryos (Chapter 3) suggesting that the activation of *Dll1* by *Mash1* does not fully compensate for the loss of *Dll1* activation by *Ngn2*. This implies that *Ngn2* is

responsible for a higher proportion of *Dll1* expression than *Mash1*, most likely resulting in the reduction in *Dll1* expression observed in the cortex of *Pax6*$^{-/-}$ mutant embryos due to the up-regulation of *Mash1* expression being unable to fully compensate for the down-regulation in *Ngn2* in relation to activating *Dll1*.

In order to further investigate the hypothesis that *Pax6* is likely to be regulating *Dll1* via *Ngn2*, further analysis using an *Ngn2* mutant mouse line was implemented. It was observed that *Ngn2* mutant embryos did not appear to display any difference in *Dll1* gene expression at E14.5 when compared to WT control littermates. Furthermore, cell count analysis yielded no significant difference in *Dll1* expression between WT control and *Ngn2* mutant embryos. This result was of key interest to our study of *Pax6*'s regulatory effects upon *Dll1*, as it did not match our hypothesis based upon previous studies of the regulatory relationship between *Ngn2* and *Dll1*. Our initial expectation was that we would observe a dramatic reduction in *Dll1* expression due to the fact that *Ngn2* has been documented as one of the proneural genes responsible for the activation of *Dll1*. However, no significant difference was observed, suggesting that the loss of *Dll1* activation by *Ngn2* is compensated for in the cortex of *Ngn2* mutant embryos. This observation could be the result of an increase in *Mash1* expression, as previous studies of *Ngn2* mutant embryos have identified that *Mash1* is up regulated in the developing cerebral cortex and that *Mash1* is habitually repressed by *Ngn2* in the cortex of WT embryos (Fode *et al*., 2000). Conversely, while a similar phenomenon occurs in *Pax6*$^{-/-}$ mutant embryos, a significant decrease in *Dll1* expression is observed. This indicates that *Mash1* could potentially be up regulated to a higher degree in *Ngn2* mutants when compared to *Pax6* mutants, or that another co-effector is responsible for the regulation of *Dll1* and is compensating for the loss of *Dll1* activation by *Ngn2*. The fact that *Dll1* expression is reduced in *Pax6* mutants suggests that any compensation observed in *Ngn2* mutants could be due to *Pax6* expression directly regulating the gene, or indirectly via another gene other than *Ngn2* and *Mash1*. In order to identify whether the steady expression of *Dll1* in *Ngn2*$^{-/-}$ mutants and their WT counterparts is due to a higher level of *Mash1* expression in *Ngn2*$^{-/-}$ mutants than the up regulation of *Mash1* observed in *Pax6*$^{-/-}$ mutants, qPCR could be utilised. This would allow *Mash1* expression levels to be

efficiently compared in the developing cortex of *Ngn2*$^{-/-}$, *Pax6*$^{-/-}$ and WT control embryos at a variety of different embryonic stages. If no discernable difference in *Mash1* expression levels were detected by qPCR, the hypothesis that *Pax6* could be regulating *Dll1* levels via a different proneural gene such as *Math1* (Gazit *et* al., 2004; Duprac *et al*., 2006), or directly, could be investigated further. It is also worth acknowledging that previous research has identified that most neural progenitor cells express only Pax6 or only Tbr2, suggesting that Pax6 is expressed by the vast majority of RGCs in the cerebral cortex, while Tbr2 is expressed by the INPs; as when 1989 cells that were immunoreactive for Pax6 and Tbr2 were analysed at E14.5, 55.7 ± 9.9% were Pax6 positive, 32.8 ± 10.2% were Tbr2 positive, and 11.5 ± 1.0% were Pax6 and Tbr2 positive (Englund *et al.,* 2005). This suggests that it would be highly likely that the majority (if not all) *Dll1* positive cells in the VZ would also co-express *Pax6*, although future cell counts for *Dll1*/*Pax6* in situ hybridisation would have to be carried out in order to ascertain this.

Flow cytometry analysis confirmed that Dll1 protein is expressed in INPs, with a proportion of Dll1 expressing cells found to be positive for the INP marker Tbr2. However, the fact that some Dll1 stained cells did not co-express Tbr2 suggests that Dll1 is also expressed by RGCs. The fact that Dll1 mRNA expression is restricted to the VZ while Dll1 protein expression is not is initially puzzling. However, it is possible that Dll1 protein expression remains 'switched on' in a cell longer than its mRNA counterpart does due to the fact that the expression of a protein is not instantaneous but rather a gradual increase and decrease as its expression is instigated and then stopped (Englund *et al*., 2005). Therefore, Dll1 protein expression could originate in RGCs residing in the VZ, where Dll1 mRNA is expressed, and could remain present while RGCs go on to produce INPs and migrate to the SVZ where Dll1 protein expression slowly diminishes. This would explain why we see Dll1 mRNA expression in the VZ and no expression in INPs residing within the SVZ, as well as detecting Dll1 protein expression within a proportion of INPs. However, further investigations would need to be undertaken to confirm whether this hypothesis is correct, such as lineage tracing of progenitor cells and looking at protein levels of Dll1 in RGCs and INPs during corticogenesis.

STAGE/GENOTYPE	*DLL1*/TBR2	*DLL1*/*NGN2*
E12.5 WT	***Dll1*:** Restricted to VZ **Tbr2:** Restricted to SVZ **Co-expression:** None	***Dll1*:** Restricted to the VZ ***Ngn2*:** Expressed throughout progenitor zone of cortex **Co-expression:** *Dll1*/*Ngn2* co-expression in the VZ of the cortex
E12.5 SEY	***Dll1*:** Reduced staining compared to WT Restricted to VZ **Tbr2:** Reduced staining compared to WT Restricted to SVZ **Co-expression:** None	***Dll1*:** Reduced staining compared to WT Restricted to the VZ ***Ngn2*:** Reduced staining compared to WT Expressed throughout progenitor zone of cortex **Co-expression:** Reduced *Dll1*/*Ngn2* co-expression in the VZ of the cortex compared to WT
E14.5 WT	***Dll1*:** Restricted to VZ in the cortex Expression in the VZ and SVZ of the hippocampus **Tbr2:** Restricted to SVZ **Co-expression:** None in the cortex *Dll1*/*Ngn2* co-expression in the SVZ of the hippocampus	***Dll1*:** Restricted to the VZ ***Ngn2*:** Expressed throughout progenitor zone of cortex **Co-expression:** *Dll1*/*Ngn2* co-expression in the VZ of the cortex
E14.5 SEY	***Dll1*:** Reduced staining compared to WT Restricted to VZ in cortex Expression in the VZ and SVZ of the hippocampus **Tbr2:** Reduced staining compared to WT Restricted to SVZ **Co-expression:** None in the cortex Reduced *Dll1*/*Ngn2* co-	***Dll1*:** Reduced staining compared to WT Restricted to the VZ ***Ngn2*:** Reduced staining compared to WT Expressed throughout progenitor zone of cortex **Co-expression:** Reduced *Dll1*/*Ngn2* co-expression in the VZ of the cortex compared to WT

	expression in the SVZ of the hippocampus compared to WT			

STAGE/COMPARISON	*DLL1* DORSAL	*DLL1* VENTRAL	CELL DENSITY DORSAL	CELL DENSITY VENTRAL
E14.5 WT/*NGN2-CRE*	No difference	No difference	No difference	No difference

Table 5.1 Chapter 5 results summary (1/2)

A summary of the double in situ hybridisation/immunohistochemistry (*Dll1*/Tbr2) results, and the double in situ hybridisation (*Dll1/Ngn2)* results detailed in chapter 5. At E12.5 and E14.5, *Dll1* was found to be restricted to the VZ of the cortex and Tbr2 to the SVZ. The expression of both *Dll1* and Tbr2 were reduced in Sey embryos compared to WT littermates and both developmental stages. At E14.5, *Dll1* expression was observed in the VZ and the SVZ of the developing hippocampus, and co-expression of *Dll1* and Tbr2 was observed in the SVZ. At E12.5 and E14.5, *Ngn2* expression was observed in the VZ and the SVZ of the developing cortex, and co-expression of *Dll1* and *Ngn2* was evident in the VZ. *Dll1* and *Ngn2* expression was reduced in Sey embryos compared to WT control littermates at E12.5 and E14.5.

STAGE/GENOTYPE	CORTICAL CELLS EXPRESSING DLL1 ONLY	CORTICAL CELLS EXPRESSING TBR2 ONLY	CORTICAL CELLS CO-EXPRESSING DLL1 AND TBR2
E14.5 WT	Yes	Yes	Yes

Table 5.2 Chapter 5 results summary (2/2)

Summaries of the cell count analysis and flow cytometry results detailed in chapter 5. Analysis of the density of *Dll1* expressing cells and total cell density in WT/*Ngn2-Cre* embryos at E14.5 observed no significant differences in the dorsal and ventral regions of the cerebral cortex. Flow cytometry analysis of WT E14.5 dissociated cortical cells observed cell populations that expressed Dll1 only, Tbr2 only, and a population that co-expressed Dll1 and Tbr2.

6.0 *Jag1* as a direct target of *Pax6* expression during corticogenesis

6.1 Introduction

As previously discussed in chapter 4, in situ hybridisation analysis of Jag1 expression in Pax6$^{-/-}$ mutant embryos and their WT littermates provides convincing evidence to support Jag1 as a prime candidate of direct regulation by Pax6 in the developing cerebral cortex (Chapter 4). The complete loss of Jag1 expression at the PSPB of Pax6$^{-/-}$ and Pax77 mutants suggests that not only is Jag1 likely to be directly activated by Pax6, but that Jag1 is also highly sensitive to levels of Pax6 expression. Furthermore, the observation that *Jag1* is a target of Pax6 at the PSPB by microarray analysis, also provides support to the hypothesis that Jag1 could potentially be a direct target of Pax6 as there is evidence that Pax6 does regulate the gene, although it is unknown whether it is direct or indirect target (Carr, 2009).

Previous studies that have identified direct targets often began with the assumption that a substantial increase or decrease in gene expression when Pax6 expression is lost would lead to the discovery that the gene in question is a direct target of Pax6 (Holm *et* al., 2007; Wen *et* al., 2008; Sansom *et* al., 2009; Mi *et al*., 2013a). The 2003 study by Scardigli *et al*., is one such example, where the vast effect upon Ngn2 gene expression in Pax6$^{-/-}$ mice was noted and subsequent research identified putative binding sites for Pax6 (Scardigli *et al*., 2001; 2003). Furthermore, work in our own lab identified the cell cycle gene Cdk6 as a direct target of Pax6, with the discovery that Pax6 represses Cdk6 expression in the developing cerebral cortex during embryogenesis (Mi *et al*., 2013b). Due to the fact that such a dramatic decrease in Jag1 expression is shown at the PSPB of Pax6$^{-/-}$ mutant embryos, it is plausible that Pax6 could be directly regulating Jag1 gene expression in this region of the developing telencephalon.

In order to ascertain whether Pax6 directly regulates potential gene targets, past studies have implemented bioinformatics to reveal potential binding sites (Coutinho

et al., 2011; Bhatia *et al*., 2013; Mi *et al*., 2013a; Ravi *et al*., 2013). Work by Coutinho *et al*., (2011) implemented a bioinformatics approach and identified over 600 putative Pax6 binding sites and over 200 predicted direct target genes by utilising hidden Markov models (HMMs) generated from experimentally validated Pax6 binding sites (Countinho *et al*., 2011). This led to the identification of several novel target genes, such as Foxp2, implicated in development and disease (Countinho *et al*., 2011). Further studies implementing a bioinformatics approach identified numerous targets of *eyeless (*the *Drosophila Melanogaster* Pax6 gene) including the early retinal development genes *eya*, *so*, *Optix* and *ato* (Ostrin *et al*., 2006), while studies in Medaka fish identified and validated Atoh7, Pax2, Pax5 and Pax8 as direct targets of Pax6 (Del Bene *et al*., 2007; Ramialison *et al*., 2008). As previously discussed, work by Scardigli *et al*., (2001; 2003) and Mi *et al*., (2013) identified and validated Ngn2 and Cdk6 respectively as direct targets of Pax6, and implemented bioinformatics in order to identify putative binding sites. Bioinformatics screening provides a useful complementary resource alongside conventional "wet lab" approaches such as ChIP screening and expression analysis experiments (Countinho *et al*., 2011). Ultimately, bioinformatics allows a relatively quick and cost effective resource to screen candidate genes and identify potential putative binding sites for transcriptional regulators such as Pax6, which can be analysed and explored further in order to validate them (Stormo, 2000; Countinho *et al*., 2011).

It can therefore be assumed that screening by bioinformatics is an ideal strategy to further explore the possibility that Pax6 may directly regulate Jag1. Consequently, it was determined that a bioinformatics approach would be implemented in order to determine if there were any likely binding sites for Pax6. Past studies have determined that many enhancer and binding sites for the activation or repression of a gene tend to be relatively close to the promoter region of the gene in question, usually within a few Kb upstream of the 5'UTR (Bulger and Groudine, 2010). With this in mind, it was decided that Jag1 gene would be screened and 10Kb upstream and downstream of the gene would also be included.

If screening of Jag1 by bioinformatics is found to be successful, binding sites will be analysed by their position and conservation score to determine which are the most likely candidates to be true binding sites of Pax6. Selected binding sites will be tested further to establish whether they are genuine putative Pax6 binding sites and to conclude whether Pax6 directly regulates Jag1. Our bioinformatics approach will utilise previously designed position weight matrixes (PWMs) for a validated consensus Pax6 binding site and the use of the UCSC genome browser to identify areas of high sequence alignment across 30 vertebrate species. This will allow us to identify potential conserved regulatory elements for Jag1. We will then be able to screen for and identify sequences of high conservation between regulatory elements for Jag1 and the consensus Pax6 binding site, providing us with a comprehensive list of potential putative binding sites for Pax6.

In order to assess whether Pax6 directly binds to our selected candidate binding sites, a cloning approach will be implemented to clone our site of interest into a luciferase construct. This approach will involve designing primers to clone our region of interest from genomic DNA and then using an in-fusion PCR approach to clone our region of interest into a luciferase construct. Following production of our construct, the candidate sites will be tested by luciferase assay in order to ascertain whether Pax6 directly activates them.

Luciferase assay analysis will be implemented using HEK cells transfected with luciferase constructs containing our candidate sites of interest cloned upstream of the firefly reporter and a renilla construct to act as an internal control. HEK cells will also be transfected with increasing amounts of a Pax6 expressing construct. If Pax6 binds to Jag1UE and activates firefly expression as a result, we should observe an increase in firefly expression for each expression as Pax6 dosage increased, as well as an increase in comparison to any of our control experiments (Chapter 2.14). This would not only validate our candidate sites, but also provide evidence to support our hypothesis that Jag1 is a direct regulatory target of Pax6.

6.2 Bioinformatic screening of *Jag1*

Bioinformatics was implemented using a custom made PaxPWM-CEs track built by Dr Ian Simpson. The track utilised four different Pax6 consensus site PWMs: M00808 (Hufnagel *et al*., 2007); M00097 (Epstein *et al*., 1994); M00979 (Roth *et al*., 1991; Duncan *et al*., 1996; Sander *et al*., 1997; Duncan *et al*., 1998; Zhou *et al*., 2000) and C0000010 (Countinho *et al*., 2011) (Figure 6.1). The designed track screened the aforementioned PWMs for Pax6 against highly conserved regions on or flanking Jag1 across 30 vertebrate species. This allowed for screening for high conservation between regulatory elements and the consensus Pax6 binding site. Position specific estimates of evolutionary constraint (GERP scores) were then used to discover multiple positions that combine to give a signal that is indicative of a putative functional element (constrained elements). Constrained elements were determined and scored using a sum of log-likelihoods to provide a 'score' for the likelihood of a particular base pair residing in a specific position within the sequence. An algorithm was then implemented to compare highly conserved areas surrounding the Jag1 gene to the Pax6 motifs. This produced a set of probable Pax6 targets which could be visualised on the custom made track on the UCSC genome browser (Figure 6.2). Dr Ian Simpson (Informatics Forum) carried out all bioinformatics screening and the resulting scores were then analysed by our own lab.

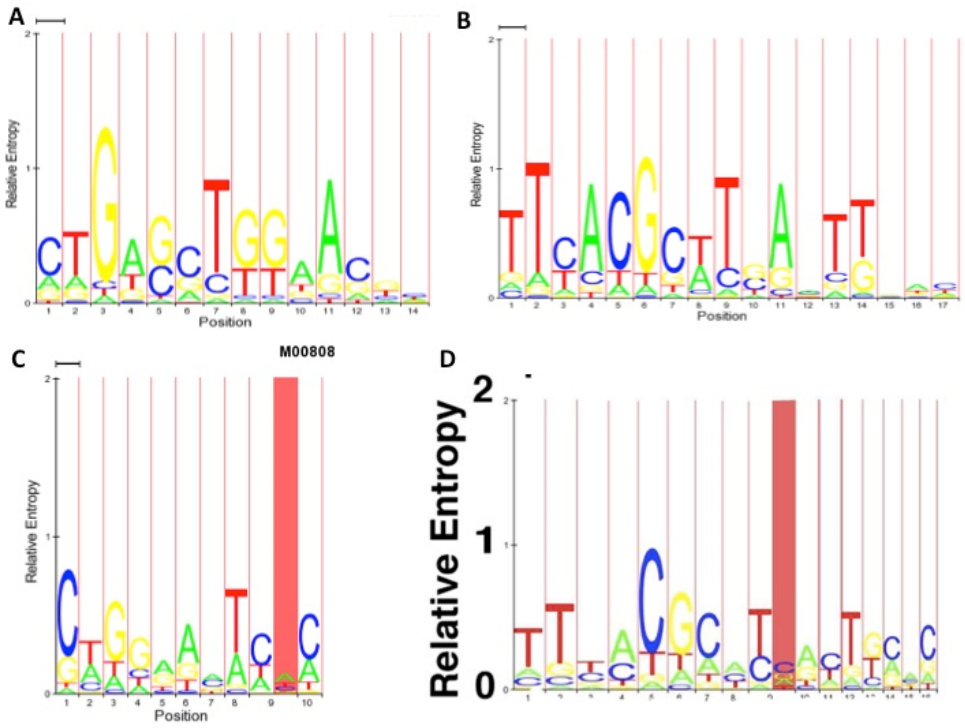

Figure 6.1 Pax6 consensus binding site motifs

Images taken from Countinho *et al*., 2011 and www.snnper.chip.org. The four validated Pax6 consensus binding site motifs utilised in our bioinformatic screening for Jag1 putative Pax6 bindings sites. (A) M00097 (Epstein *et al*., 1994) (B) M00979 (Roth *et al*., 1991; Duncan *et al*., 1996; Sander *et al*., 1997; Duncan *et al*., 1998; Zhou *et al*., 2000) (C) M00808 (Hufnagel *et al*., 2007) (D) C0000010 (Countinho *et al*., 2011). Position = bp position in sequence. Relative Entropy = probability of bp distributions occurring at a particular position within the sequence.

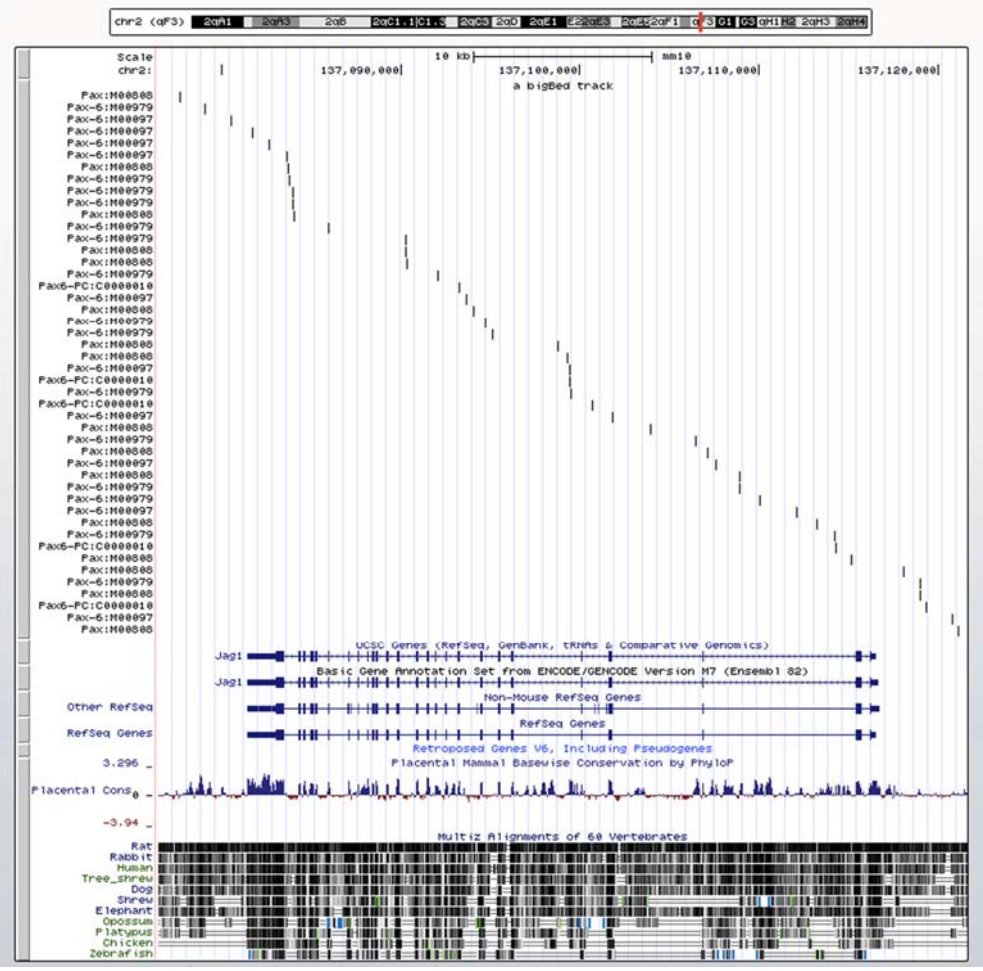

Figure 6.2 Customised *Jag1* Pax6PWM_CEs track

Developed by Dr Ian Simpson. Pax6PWM_CEs track applied to the UCSC genome browser to screen for and visualise sequences of high conservation between Jag1 regulatory elements and the consensus Pax6 binding site. Using the UCSC genome browser to find areas of high sequence alignment across 60 vertebrate species including rat, rabbit, human, dog and elephant screened for potential regulatory elements for Jag1. Potential binding sites are marked by black lines and labelled with the Pax6 consensus motif they align with.

Analysis of the scores for each conserved site found that six of the constrained elements with the highest scores were all located within a 3Kb radius of one another (Figure 6.3A). Further analysis of the custom track also determined that the constrained elements were located around 1.5Kb upstream of the 5'UTR of Jag1. The number and positioning of the constrained elements made them a particularly

attractive candidate as an enhancer element for Jag1, as enhancers are typically located upstream or downstream of the target gene (Pennacchio *et al*., 2013).

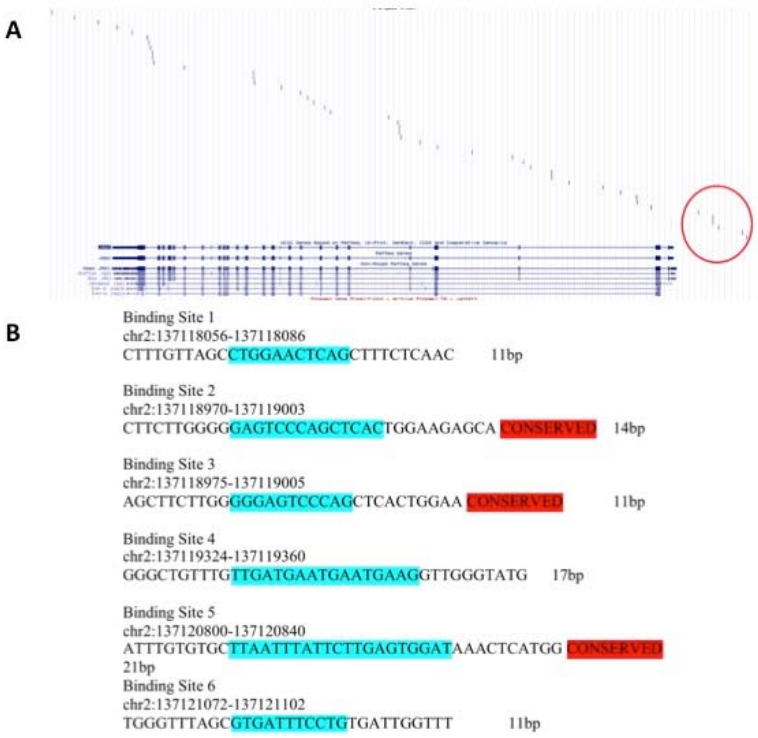

Figure 6.3 Visualisation of candidate binding sites on the Pax6PWM_CEs track and binding site chromosome positions and sequences

(A) The six constrained elements selected as a potential enhancer element (Jag1UE) visualised on the Jag1/Pax6PWM_CEs track. Jag1UE is located 1.5Kb upstream of the 5'UTR for Jag1. All of the six constrained elements are within 3.5Kb of one another. (B) The chromosome positions and sequences for each of the six constrained elements that constitute Jag1UE. The sequences for the constrained elements are highlighted in blue. Three of the constrained elements are highly conserved amongst the screened vertebrate species and are highlighted in red.

As a result, it was determined that the six constrained elements should be treated as a potential enhancer element and dubbed 'Jagged1 upstream enhancer' (Jag1UE). Jag1UE was selected as the most likely predicted putative Pax6 binding site with the

hypothesis that Pax6 was likely to directly bind to one, several or all of the constrained elements that make up Jag1UE.

6.3 Cloning Jag1UE

Once Jag1UE was identified, the region was cloned into a luciferase vector in order to carry out analysis of the enhancer by luciferase assay. Due to the fact that Jag1UE is situated 1.5Kb upstream of the 5'UTR, within the 'gene desert' of the genome (large tracts of the genome devoid of protein coding genes), BLAT was used to obtain the entire sequence encompassing Jag1UE. This was achieved by using the 5'UTR sequence of Jag1 and the sequences of the six individual constrained elements obtained from the Jag1 specific PaxPWM-CEs track (Figure 6.3B). Once the sequence was obtained, primers were designed that encompassed the six constrained elements (Figure 6.4A) and In-fusion PCR software was used to convert them to in-fusion PCR primers which were specific to our region of interest and our selected luciferase vector (Figure 6.4B). Jag1UE was cloned from genomic DNA and sequenced. In-fusion PCR was then carried out to clone Jag1UE into our selected luciferase vector, pGL4.23, in order to produce pGL4.23+Jag1UE: a luciferase vector with Jag1UE inserted upstream of a minimal promoter which will drive expression of the firefly reporter when activated (Figure 6.5).

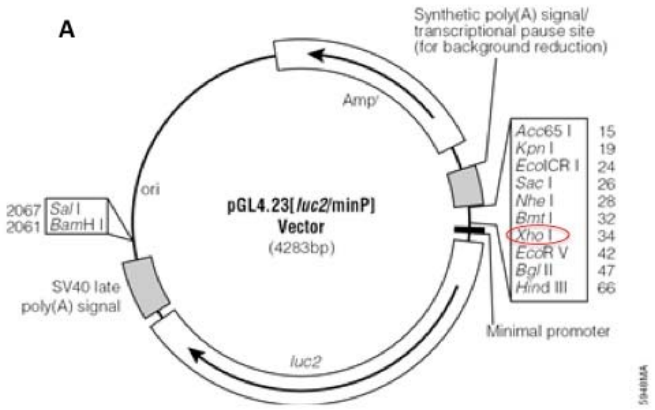

B

Jag1UE F Primer (Jag1UE F)
5'GCTCGCTAGCCTCGAGCGCATCTTCTGAGCAGG

Jag1UE Primer R Primer (Jag1UE R)
5'TCTTGATATCCTCGATTGCGTTGAGCCTGTCCT

Figure 6.4 A map of the pGL4.23 luciferase vector with a minimal promoter and the developed In-Fusion PCR primer sequences for cloning Jag1UE.

(A) pGL4.23 was selected as the luciferase vector to clone Jag1UE into due to the fact that it contains a minimal promoter and we were unable to identify the exact location of the promoter for Jag1UE. Due to the fact that our region of interest is located 1.5Kb upstream of the 5'UTR for Jag1, we presumed that the region does not contain the promoter region for Jag1 and chose to treat our region of interest as a potential enhancer for Jag1. (B) The primer sequences designed for cloning Jag1UE. Standard 16bp primers (highlighted in blue) were initially designed and then run through Clontech In-Fusion PCR software to produce primers specific to Jag1UE and pGL4.23. The developed primers will only produce and insert Jag1UE in a specific orientation into pGL4.23 linearized with XhoI.

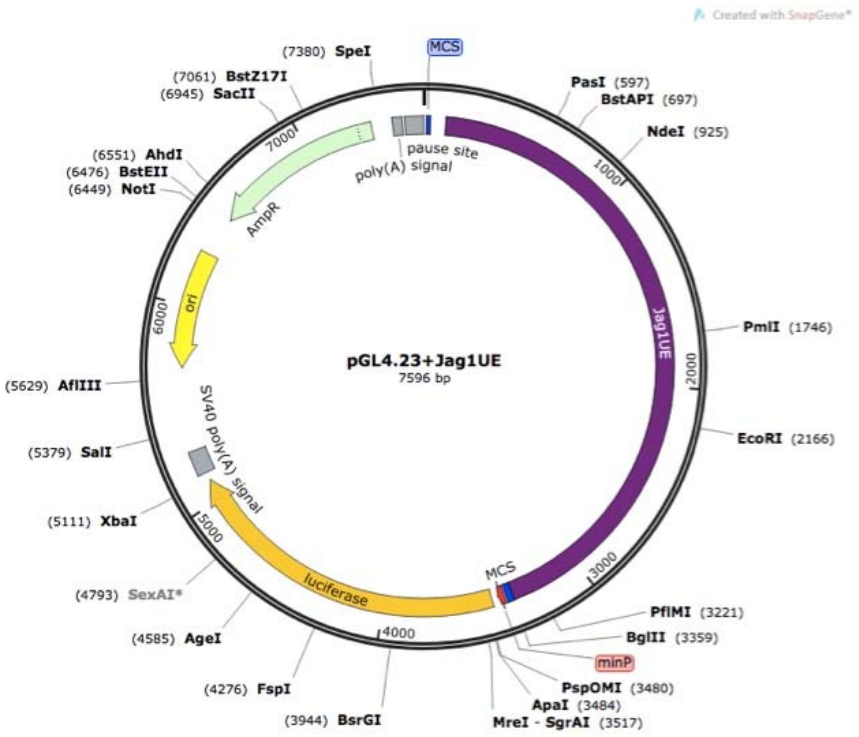

Figure 6.5 pGL4.23+Jag1UE construct map

A map of Jag1UE (purple) inserted into the Xho1 site within the multiple cloning site (blue) of pGL4.23. Jag1UE will work to activate the minimal promoter (red) of pGL4.23 when regulated by the presence of Pax6 expression. pGL4.23+Jag1UE = 7596bp.

6.4 The effect of Pax6 on Jag1UE Expression

Analysis of Jag1UE as a putative Pax6 binding site was carried out by luciferase assay, utilising the pGL4.23+Jag1UE construct described in 6.5. Pax6 non-expressing HEK293 cells were transfected with pGL4.23+Jag1UE and increasing amounts of Pax6 in order to demonstrate that Pax6 binds and activates Jag1UE (Figure 6.6). This allowed us to fully investigate the effects of Pax6 upon Jag1UE without having to compensate for background Pax6 expression. HEK293 cells were also transfected with a Renilla luciferase control and with different levels of Pax6 (0ng, 50ng, 100ng, 200ng, 400ng, 500ng) per transfection. Three additional controls were used as standard for each luciferase assay experiment: an empty pGL4.23 vector control to demonstrate that firefly is being activated by Pax6's effect on

Jag1UE, an empty pCMV vector in order to demonstrate that Pax6 is responsible for the increase in firefly activity, and a no transfection control to account for background levels of Firefly and Renilla. Analysis by linear regression yielded no significant difference in Jag1UE expression (P=0.1494) as Pax6 levels increased (0ng-500ng) and an R^2 value = 0.1254 (Figure 6.6A). Additionally, no significant difference was found for the expression of the pGL4.23 control (P=0.3048) as pax6 levels increased (0ng-500ng) and an R^2 value = 0.06564 (Figure 6.6B). In order to demonstrate that Pax6 levels increased as Pax6 transfection dosage increased, western blot analysis of the transfected HEK 293 cells was carried out. Western blot analysis showed that Pax6 levels increased as the dose of Pax6 plasmid that the cells were transfected with increased (Figure 6.7). The increase in Pax6 expression as dose of Pax6 increases (Figure 6.7C) correlates with the slight increase in Jag1UE expression (Figure 6.6A). However, the slight increase in Jag1UE expression was not found to be significant by linear regression analysis.

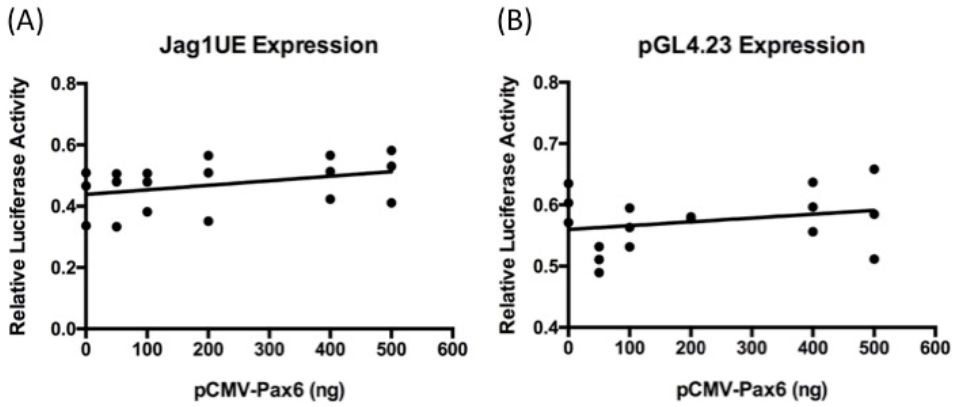

Figure 6.6 Luciferase assay analysis of Jag1UE expression

(A) Measure of firefly luciferase activity (relative to Renilla control) in HEK293 cells transfected with a range of Pax6 levels (0-500ng). Statistical analysis by linear regression detected no significant difference in Jag1UE expression (P=0.1494). R^2=0.1254. (B) Measure of firefly luciferase activity (relative to Renilla control) in HEK293 cells transfected with a range of Pax6 levels (0-500ng). Statistical analysis by linear regression detected no significant difference in pGL4.23 expression (P=0.3048). R^2=0.06564.

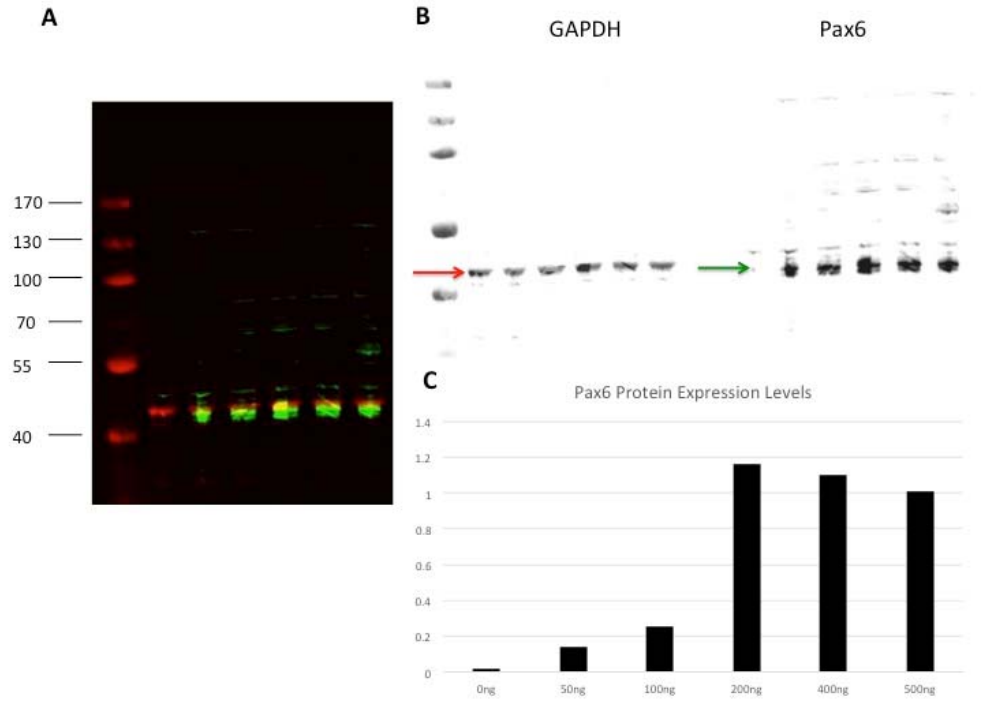

Figure 6.7 Western blot carried out on transfected HEK293 cells

(A) Western blot for GAPDH and Pax6. Lane 1 = ladder shown in red. Lanes 2-7 = 0ng-500ng Pax6 transfected HEK293 cells, red = GAPDH and green = Pax6. GAPDH used as a positive control to normalise to. (B) GAPDH and Pax6 western blot results separated for analysis. GAPDH expression indicated by red arrow and Pax6 expression indicated by green arrow. Little to no Pax6 expression is apparent in HEK293 cells that were transfected with 0ng of Pax6. (C) Quantitative analysis of western blot for Pax6 expression. Pax6 pixel intensity for 0ng-500ng HEK293 cells was calculated and results were normalised to the GAPDH pixel intensity for each sample.

6.5 Discussion

Bioinformatic screening for putative Pax6 binding sites yielded a potential enhancer element for Jag1 (6.2). The potential enhancer site, dubbed Jag1UE, was successfully cloned into the pGL4.23 construct with a minimal promoter and analysis by luciferase assay was carried out in order to validate Jag1UE as an enhancer element activated by direct Pax6 binding. However, while a small increase in firefly

expression was observed as Pax6 expression increased, it was not deemed statistically significant when tested by linear regression analysis. While it could automatically be assumed that this result suggests that Jag1UE is not an enhancer element activated by Pax6, this conclusion is likely to be too hasty and a non-significant result could be due to multiple reasons that will be outlined below.

While the use of HEK293 cells for transfection gave us a distinct advantage due to the fact that they do not express Pax6, they are vastly removed from mouse embryonic cortical cells. It is impossible to confirm whether the same relationship between Jag1 and Pax6 applies in kidney cells or in human embryos without further investigation. As a result, future attempts to analyse the effects of Pax6 on Jag1UE by luciferase assay would be best to utilise dissociated cortical cells from $Pax6^{-/-}$ mutant embryos. Not only would this provide experimental conditions as close as possible to the conditions implemented for our expression data analysis for Jag1, but it would also provide cells that do not normally express Pax6 but with all of the components required for Pax6 regulation. Additionally, a further analysis could be carried out using WT cortical cells and *PAX77* cortical cells in order to further examine the effects of Pax6 levels upon Jag1UE.

In order to further validate the luciferase assay experiment in the future, additional positive controls could be included. This would most effectively be achieved by including a previously tested construct that has been validated as a direct target of Pax6. Furthermore, while the Pax6 construct used for this experiment has successfully identified a Pax6 target previously (Mi *et al*., 2013b), re-confirming that the Pax6 protein used is functional would be advantageous in order to validate the luciferase assay experiment carried out for this thesis. The best way to achieve the aforementioned points would be to carry out an additional control run using the validated Cdk6 constructs detailed in Mi *et al*., (2013b). As this study used the same experimental design for their luciferase assay, the Cdk6 construct would provide the best positive control in order to validate this experimental set-up, and would also provide evidence that the Pax6 protein used is functional (Mi *et al*., 2013b).

Another explanation for our luciferase assay results could be that Pax6 may only bind to one or a few of the binding sites that make up Jag1UE. Similar instances have been documented previously, where a region that included multiple binding sites was initially tested as a whole before each individual site was re-tested and it was discovered that only one or two of the binding sites were actually directly activated by Pax6 (Scardigli *et al*., 2003; Mi *et al*., 2013a). If this is the case it could be that inclusion of the additional binding sites having a repressive effect upon the activity of Jag1UE as a whole (Whitfield *et al*., 2012). In order to determine whether this is in fact the case with Jag1UE, testing each individual binding site by designing constructs for each individual binding site and different combinations of the binding sites would confirm whether this was the case, or mutating combinations of the binding sites within Jag1UE to render them non-functional would help to prove or disprove this hypothesis.

It is also plausible that Pax6 may only be partially responsible for the activation of Jag1UE and that another transcription factor is also responsible for its activation (Brindle *et al*., 1990). This would account for such a small increase in firefly expression as Pax6 expression increases. However, taking our Jag1 expression data into consideration (Chapter 4) would suggest that Pax6 expression should evoke a much larger effect upon an enhancer element for Jag1. This would suggest that if there is an additional transcription factor responsible for binding and activating Jag1UE, HEK293 cells might not express it. Furthermore, it could also be possible that Pax6 exerts its direct regulatory effects on Jag1 by binding to additional putative Pax6 binding sites located at a different region of the genome. This is highly likely as our bioinformatic screening of Jag1 against Pax6 yielded over 60 potential binding sites. In order to test this, further analysis of these additional binding sites would need to be undertaken and selected candidates would have to be tested by luciferase assay.

While analysis by luciferase assay is a suitable approach to identify whether Pax6 directly binds Jag1UE, it is also far removed from what occurs in the developing cerebral cortex during murine embryogenesis. As a result, an in vitro approach may

be too removed from the biological process occurring between Pax6 and Jag1 in an embryo and as a result, it may cease to function correctly. As a result, an in vivo approach would be more suitable to test Pax6's effects upon Jag1UE. A microinjection approach as described in Scardigli *et al*., (2003) would be ideal as a Jag1UE construct with a LacZ reporter could be integrated into the DNA of developing WT embryos and then they could be analysed at specific developmental stages. If Pax6 activates Jag1UE, the reporter would visualise Jag1's expression pattern at the PSPB (Scardigli *et al*., 2013). Mutation of the binding sites that comprise Jag1UE would further validate Jag1UE as expression should be lost if some/all of the binding sites are disrupted.

Although the luciferase assay results were not significant, a small increase in firefly expression was evident as Pax6 levels increased. Due to the fact that WB validated increasing Pax6 levels, technical issues may have resulted in no statistically significant increase in firefly expression as Pax6 levels increase. While carrying out luciferase assay experiments, extreme difficulties with transfection rates were initially experienced. While transfection efficiency was optimised as much as possible within the time constraints of the project, it is possible that transfection efficiency was still was still relatively poor for one if not all of the experimental constructs used. If this were the case, poor transfection efficiency would account for no significant increase in firefly expression as Pax6 levels increase. In order to combat this, future luciferase experiments would need to optimise transfection efficiency further and confirm that each repeat had similar transfection efficiencies for all constructs.

While the results from our analysis of Jag1UE by luciferase assay remain inconclusive, it is still likely that Jag1UE could be an enhancer element or contains at least one putative Pax6 binding site. Further research into Jag1UE in order to validate it as an enhancer element would be required, and analysis of the other potential putative Pax6 binding sites may also be required in order to ascertain whether Jag1 is a direct target of Pax6.

RELATIVE LUCIFERASE ACTIVITY OF CELLS TRANSFECTED WITH A RANGE OF PAX6 LEVELS (0-500NG)	LINEAR REGRESSION ANALYSIS
JAG1UE	No significant difference
PGL4.23	No significant difference

AMOUNT PAX6 TRANSFECTED (NG)	INCREASE IN PAX6 EXPRESSION LEVELS COMPARED TO PREVIOUS TRANSFECTION
0	No
50	Yes
100	Yes
200	Yes
400	No
500	No

Table 6.1 Chapter 6 results summary

A summary of the luciferase assay results and western blot results detailed in chapter 6. Linear regression analysis of luciferase expression for Jag1UE and the control pGL4.23 construct observed no significant difference. Western blot analysis of Pax6 expression levels by cells transfected with increasing amounts of Pax6 (0ng-500ng) observed an increase in Pax6 levels up to 200ng and then a decrease for 400ng and 500ng.

7.0 General discussion

7.1 Pax6 regulates Dll1 and Jag1 during cortical development

The initial aim of this project was to discover new target genes of Pax6 implicated in the development of the embryonic cerebral cortex (Chapter 1). Notch pathway genes were highlighted from past microarray (Carr *et al*., 2009) and ChIP (Sansom *et al*., 2009) studies and some were confirmed as Pax6 targets including *N1* and *Hes5* (Dorà, 2011). Both Dll1 and Jag1 were identified as potential targets of Pax6 (Carr *et al*., 2009; Sansom *et al*., 2009).

Expression analysis of *Dll1* by in situ hybridisation and subsequent quantification by cell count analysis found that *Dll1* expression is significantly reduced in areas of the cerebral cortex from E11.5-E12.5 in *Pax6*$^{-/-}$ and from E12.5-E13.5 in cKO embryos (Chapter 3). This allowed us to conclude that *Dll1* is a Pax6 target. However, it is unclear whether *Dll1* is directly or indirectly regulated by the transcription factor. Analysis carried out in chapter 3 suggests that *Dll1* is more likely to be an indirect target due to the fact that it is not as severely affected as some validated Pax6 targets such as Ngn2 where expression is severely reduced in the cortex of *Pax6*$^{-/-}$ mutant embryos (Stoykova et al., 2000; Toresson et al., 2000; Yun et al., 2001; Scardigli et al., 2003; Holm et al., 2007; Quinn et al., 2007; Sansom and Livesey, 2009 and Cdk6 (Mi *et al*., 2013a; 2013b). Although *Dll1* appears to be most likely only indirectly regulated by Pax6, their relationship could potentially be particularly interesting to study further due to the role of both Pax6 and *Dll1* in cell proliferation (Pierfelice *et al*., 2007; Manuel *et al*., 2013). As a result, their relationship could be integral to the process of cortical neurogenesis during embryonic development.

While the relationship between *Dll1* and *Pax6* appears to be quite complex, the relationship between *Pax6* and *Jag1* is likely to be much more straightforward. Expression analysis of *Jag1* in *Pax6*$^{-/-}$ embryos from E11.5-E14.5 saw a complete loss of *Jag1* expression at the PSPB and diminished expression in the main body of

the developing cortex (Chapter 4). Taking the dramatic change in expression levels of validated Pax6 targets like *Ngn2* into consideration, Jag1 is a likely direct target of Pax6 due to the complete loss of *Jag1* expression at the PSPB of *Pax6*$^{-/-}$ mutant embryos. Interestingly, Jag1 expression was also lost at the PSPB of *PAX77* mutant embryos (Chapter 4), suggesting that specific levels of Pax6 are required to activate Jag1 expression in this telencephalic region. Dll1, on the other hand, saw no significant increase or decrease in expression when analysed in *PAX77* embryos (Chapter 3). This suggests that Pax6 interacts with the two Notch ligands in very different ways, despite Dll1 and Jag1 fundamentally carrying out the same role during embryonic neurogenesis.

7.2 *Dll1* mRNA is expressed in the VZ and Dll1 protein is co-expressed with Tbr2 in a subset of progenitor cells

Following the identification of two notch ligands as Pax6 targets, we endeavoured to learn as much as possible about the relationships between them. While we concluded that the regulatory relationship between Pax6 and Jag1 was likely to be relatively straightforward, it was determined that the relationship between Pax6 and Dll1 was likely to be far more complex. In order to form a hypothesis centred on how Pax6 and Jag1 may interact with one another during cortical development, an extensive research of the literature on Dll1 during forebrain development was carried out. As previously discussed, many discrepancies in the literature were discovered for the location of Dll1 expression in the developing cerebral cortex during embryogenesis (Chapter 5).

To briefly summarise what has already been covered in chapter 5, some studies determined that Dll1 is expressed in the VZ of the developing cortex (Campos *et al*., 2001), while others reported that Dll1 is expressed within the SVZ (Mizutani *et al*., 2007; Kawaguchi *et al*., 2008; Yoon *et al*., 2008). A further study conducted by Nelson *et al*., (2013) suggested that Dll1 is predominately expressed in INPs residing within the SVZ, but also expressed in the VZ in a subpopulation of INPs that reside

there (INP^{VZ}) (Nelson *et al*., 2013). These inconsistencies in the published literature proved detrimental to our analysis of the relationship between Pax6 and Dll1, as it was unclear whether the fundamental basics the model developed from our hypothesis were correct (Chapter 1). As a result, we carried out analysis of Dll1 expression in order to determine where the ligand is expressed in the embryonic cerebral cortex (Chapter 3, Chapter 5).

Single and double labelling expression data concluded that Dll1 is expressed within the VZ of the developing cerebral cortex (Chapter 3 and Chapter 5) and that INP cells do not express Dll1 (Chapter 5). However, studies describing Dll1 expression in the SVZ and in INPs analysed Dll1 protein expression rather than Dll1 mRNA expression (Nelson *et al*., 2013). In order to disprove or validate these findings; we carried out flow cytometry analysis of Dll1 and Tbr2 expression in dissociated E14.5 WT cortical cells (Chapter 5). A proportion of cells were found to co-express Tbr2 and Dll1 (Chapter 5), but not all cells expressing Dll1 also expressed Tbr2 and vice versa. In chapter 5, the notion that Dll1 mRNA expression diminishes before Dll1 protein expression was considered (Chapter 5). This would account for Dll1 protein expression in INP cells and possibly RGCs, as well as Dll1 mRNA expression in RGCs only. However, it is also plausible that the co-expression of Dll1 and Tbr2 observed in our flow cytometry analysis could be in INP^{VZ} s that are still expressing Dll1 and are beginning to express Tbr2 as they migrate to the SVZ where they settle as fully matured INPs that no longer express Dll1.

7.3 Dll1 and Jag1 as direct targets of Pax6

As previously discussed, Jag1 was identified as a candidate gene for direct regulation by Pax6 (Chapter 4; Chapter 7.1). Subsequent screening by bioinformatics yielded a comprehensive list of around 30 constrained elements on or around Jag1 that were likely putative Pax6 binding sites (Chapter 6.2). We determined that a cluster of 6 constrained elements around 1.5Kb upstream of the 5”UTR of Jag1 was likely to be an enhancer element for the gene (Chapter 6.2). However, analysis of the proposed

enhancer element (Jag1UE) by luciferase analysis did not yield a significant result to validate Jag1UE as an enhancer. Despite this, as discussed in detail in chapter 6, it is still possible that Jag1UE may be an enhancer element that binds Pax6 (Chapter 6.5). Additionally, there is the distinct possibility that some of the untested binding sites from our bioinformatics screen could be putative Pax6 sites (Chapter 6.5). Consequently, although Jag1 was not confirmed as a direct target of Pax6 by our investigations, it remains a prime candidate and further research is required to confirm or disprove it.

While we approached Dll1 as a likely indirect target of Pax6 regulation due to our initial investigations in chapter 3, it cannot be disproved as a potential direct target without further research. Our investigations into Dll1 expression in the developing cortex of *Ngn2*$^{-/-}$ mutant embryos showed that expression levels are not significantly reduced like they are in *Pax6*$^{-/-}$ embryos (Chapter 5). As discussed in chapter 5, Dll1 is a direct target of Ngn2 (Castro *et al*., 2006) so it was initially surprising that Dll1 expression was not reduced. While compensation by Mash1 is the likely resolution, it does not explain the significant reduction in Dll1 expression in Pax6 mutant embryos (Chapter 3), as Mash1 is up-regulated in the cortex of *Pax6*$^{-/-}$ embryos (Kroll *et* al., 2005; Carr, 2009). This ultimately begs the question of whether Mash1 is simply up-regulated to a greater degree in the cortex of *Ngn2*$^{-/-}$ embryos when compared to *Pax6*$^{-/-}$ embryos or whether Pax6 may have a different regulatory relationship with Dll1 than originally presumed. However, if this were found not to be the case, it would provide circumstantial evidence that Pax6 could potentially directly regulate Dll1 rather than indirectly regulate it. Subsequently, it would be advantageous to investigate Dll1 as potential direct target of Pax6 in the future.

7.4 The Pax6/Notch ligand model revisited

In light of the findings of this project highlighted in sections 7.1-7.3, the experimental model (Figure 1.8) produced from our initial hypothesis (Chapter 1.11)

may require revising. Three potential revisions of the model are described in the following paragraphs.

In light of our findings, a new model depicting that Dll1 mRNA and protein are first expressed in RGCs residing within the VZ could be applied. In this revision of our model, both Dll1 mRNA and protein would continue to be expressed by newly generated INP^{VZ}s, with Dll1 mRNA levels starting to slowly diminish as INP^{VZ}s (Figure 7.1a) migrate towards the SVZ. In order to account for the fact that Dll1 mRNA is not expressed in the SVZ but that Dll1 protein has been visualised in the SVZ (Nelson *et al*., 2013), the model would depict that mature INPs residing in the SVZ do not express Dll1 mRNA (Figure 7.1a) but do continue to express Dll1 protein (Figure 7.1b). This phenomenon would be explained by the notion that once Dll1 mRNA is no longer expressed, the protein levels persist for some time. This would suggest that Dll1 expression in the SVZ is the result of Dll1 protein produced by RGCs and that its protein expression lingers long after Dll1 mRNA is no longer expressed. As a result, it is likely that Dll1 protein levels in INPs slowly diminish until Dll1 is no longer expressed.

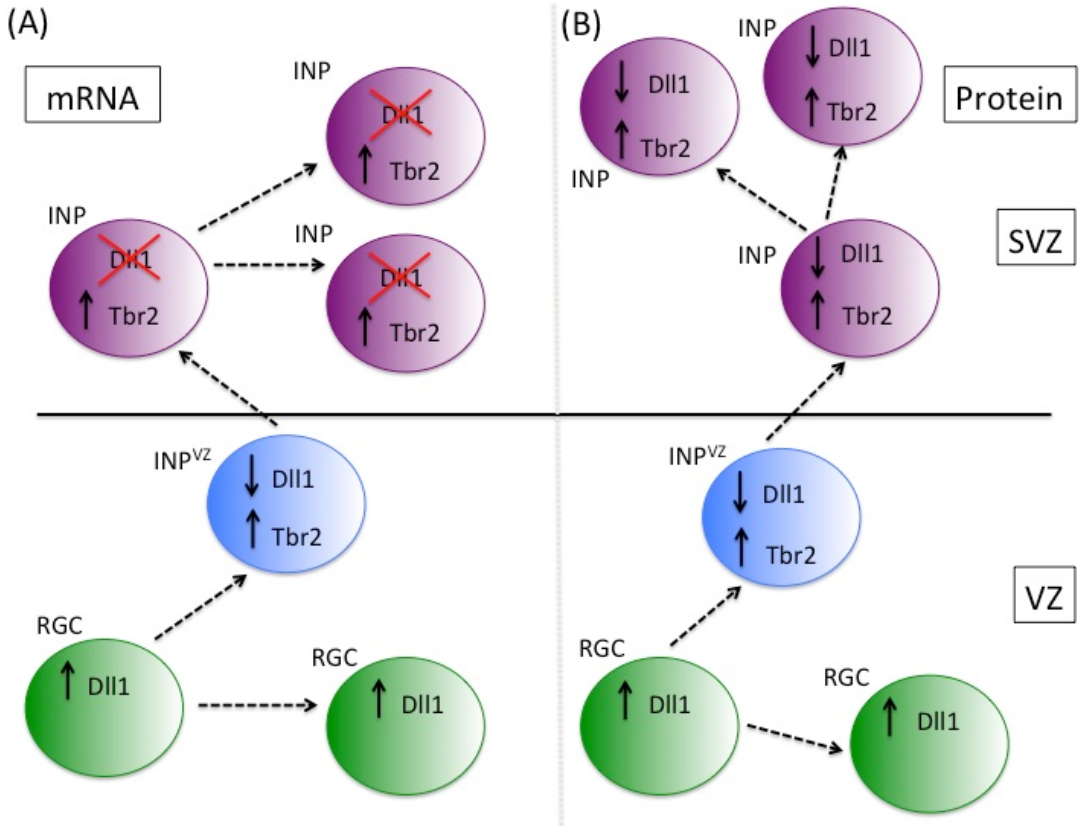

Figure 7.1 Adapted hypothesis model

(A) *Dll1* mRNA expression in progenitor cell subpopulations during corticogenesis. *Dll1* is expressed in RGCs. Newly generated INPs (INP^{VZ}s) still express *Dll1* but mRNA levels decrease as INP^{VZ}s migrate to the SVZ where they settle as mature INPs. INPs do not express *Dll1.* (B) Dll1 protein is expressed by RGCs and expression of Dll1 is retained in INP^{VZ}s and INPs. It is likely that Dll1 expression slowly diminishes in INPs until the protein is no longer expressed. Green cell = RGC. Blue cell = INP^{VZ}. Purple cell = INP. ↑ = sustained expression. ↓ = diminishing expression. □ = No longer expressed.

An additional possible revision of the existing model would depict that Dll1 is only expressed by RGCs and INP^{VZ}s in the VZ, and not in INP cells in the SVZ. This would account for our Dll1 mRNA expression data (Chapter 3, Chapter 5) and the results of our flow cytometry analysis (Chapter 5), as well as some of the data from previous Dll1 forebrain studies (Campos *et* al., 2001; Nelson *et al*., 2013). However, the fact that data from Nelson *et al*., 2013 suggested that cells expressing Dll1 also

co-express Tbr2 and that Dll1 was also visualised in cells within the SVZ using a GFP reporter makes this scenario far less likely (Nelson *et al*., 2013).

The final potential revision of our existing model explores the idea that Dll1 could be expressed in INP^{VZ}s only. This would account for cells that co-express Dll1 and Tbr2, as well as Dll1 expression in the VZ. However, in situ hybridisation analysis suggested that Dll1 is expressed in the majority of cells residing in the VZ and INP^{VZ} cells comprise a relatively small percentage of the VZ in comparison to RGCs (Englund *et* al., 2005; Götz and Huttner, 2005; Corbin *et al*., 2009; Nelson *et al*., 2013), making this revision of the model redundant.

Taking all of the experimental evidence from this project as well as previous studies into account, the first revision of our original model seems to be the most likely scenario. Furthermore, this model would still incorporate the proposed co-regulatory relationship between Dll1 and Pax6 from the original (Chapter 1.11), although the possibility that Dll1 and Pax6 may both be co-expressed in RGCs provides the possibility for an alternative regulatory relationship between the two genes, whether this is a revision of the original version (Chapter 1.1) that compensates for the molecular signalling mechanism of RGCs, or an additional regulatory model unique to RGCs.

7.5 Pax6 controls cortical cell proliferation/differentiation via is regulation of *Dll1* and *Jag1*

As previously stated, it is largely accepted that Pax6 is critical during cortical development and is a key regulator of cell proliferation and differentiation during corticogenesis (Stoykova *et al*., 2000; England *et al*., 2005; Georgala *et al*., 2011a; 2011b). Although the molecular mechanisms that Pax6 controls to exert its effects upon cell proliferation are still poorly understood (Carr, 2009; Sansom *et al*., 2009). Interestingly, the discovery that components of the Notch signalling pathway (namely *Dll1* and *Jag1*) appeared to be targets of Pax6, provided potential

explanation as to how Pax6 could be exerting its effects upon cell proliferation during corticogenesis (Carr, 2009; Sansom *et al*., 2009; Dorà 2011; Chapter 1.11). The Notch signalling pathway is known to play a critical role in orchestrating the balance between cell proliferation and differentiation – maintaining the progenitor cell pool and dictating when cells differentiate into neurons that form the multiple layers of the murine cerebral cortex (Pierfelice *et al*., 2011). When Notch signalling is disrupted, there is a depletion of the neural progenitor cell pool and as a result, a decrease in the production of neurons, resulting in the layers of the cortex failing to form correctly and as a result an overall decrease in cortical size and optimal function (Kageyama *et al*., 2008; Pierfelice *et al*., 2011; Shimojo *et al*., 2016).

Our discovery that a loss of Pax6 reduces the expression of Notch ligands *Dll1* and *Jag1* (Chapter 3; Chapter 4) has given rise to the hypothesis that Pax6 controls corticogenesis via is regulation of key components of the Notch signalling pathway. Furthermore, our conclusions that support previous findings that *Jag1* and *Dll1* are expressed in the VZ and most likely by RGCs/predominately by RGCs, gives our hypothesis traction; as Pax6 could be directly regulating *Dll1* and *Jag1* within the RGC population, subsequently instructing RGCs to remain in a proliferative state within the neural progenitor pool (Chapter 5).

The original model of the hypothesis presented in this thesis depicts the direct regulation of *Jag1* by Pax6 in RGCs, consequently instructing a proliferative cell fate in neighbouring RGCs (Figure 1.8) (Chapter 1.11). Previous research presented Jag1 as a gene expressed by RGCs within the VZ (Nelson *et al*., 2013). This part of the model was predominately supported by our findings as Jag1 expression decreased in the cortex of *Pax6*$^{-/-}$ embryos and was completely lost at the PSPB, where Pax6 expression is highest (Chapter 3). Furthermore, while our findings from Chapter 6 were inconclusive, it is still feasible that *Jag1* could be a direct target of Pax6.

While the original hypothesis model (Figure 1.8) described in Chapter 1.11 relied heavily upon evidence described by Nelson *et al*., (2013), our findings largely contradicted the data presented in the aforementioned article and as a result, our own

original hypothesis. While the hypothesis model (Figure 1.1) suggested that Pax6 and Dll1 indirectly regulate one another in INPs residing within the VZ (Chapter 1.11), the findings detailed in this thesis do not support this and instead suggest that *Dll1* is in fact expressed solely within the VZ and by RGCs, as there is no co-expression between *Dll1* and Tbr2; a known marker of the INP cell population, that is also expressed by INP^{VZs} (Pontious *et al*., 2007; Nelson *et al*., 2013). While our findings detailed in Chapter 5.2 contradict Nelson *et al*., (2013), they compliment the findings of Shimojo *et al*., (2016), where a disruption in correct *Dll1* expression resulted in the quenching of Notch pathway oscillations and a decrease in the proliferation of RGCs within the VZ.

The observations by Shimojo *et al*., 2016 surrounding *Dll1* are of particular interest in regards to the work undertaken in this thesis. The fact that a disruption in *Dll1* expression resulted in the quenching of Notch oscillations and consequently, a disturbance in normal levels of cell proliferation vs differentiation in the VZ, demonstrated that Dll1 is a key player in maintaining Notch signalling and subsequently, correct cortical development. This was demonstrated by the observation that not only was there a reduction in the size of the VZ in Dll1 mutant mice as a result of a reduction in Notch signalling, but also by the fact that there was an overall reduction in the size of the cerebral cortex; suggesting that as proliferative cell pool within the VZ reduced, it resulted in an insufficient neuron yield to allow for correct structural development (Shimojo *et al*., 2016). The fact that Dll1 has been highlighted as playing a critical role in Notch signalling, with no apparent compensation provided by other Notch pathway components; aids our hypothesis that Pax6 controls cell proliferation by regulating genes involved in Notch signalling. As it is generally accepted that Notch signalling is a critical for the mediation between cell proliferation and differentiation during neurogenesis, the fact that a loss of normal Dll1 expression disrupts this so severely gives traction to our hypothesis that Pax6 controls cell proliferation during corticogenesis due to the fact that Pax6 has been proven to regulate the expression of a gene that is vital to the process (Shimojo *et* al., 2016; Chapter 3; Chapter 5).

7.6 Future work

In order to ascertain which version of our model is correct, further experiments need to be conducted outwith the time constraints of this project. This would allow us to answer the remaining questions from this project and would allow us to prove or disprove further aspects of the model for Pax6s regulation of Dll1 and Jag1 during cortical neurogenesis.

In order to validate Jag1 as a direct target of Pax6, follow up experiments for Jag1UE would need to be conducted, as well as further testing of other putative bindings sites that were highlighted in our bioinformatics screen (Chapter 6.2). As previously discussed in depth in chapter 6, further optimisation of our original luciferase assay experiment, coupled with an in *in vivo* approach would be ideal (Chapter 6.5). While additional testing of other candidate binding sites by our luciferase method would be beneficial if the sites that comprise Jag1UE are disproved entirely.

Results from this project raised the question of whether Dll1 is truly an indirect target of Pax6 or if it may actually be a direct target. In order to examine the developing hypothesis that it could be a direct target, a bioinformatics approach like the one carried out for Jag1 (Chapter 6.2) could be implemented. This would provide a comprehensive list of any potential putative Pax6 binding sites for Dll1 that could be analysed further and then tested by the same luciferase assay approach implemented for Jag1 (Chapter 6.6).

In light of our original model, which suggests that Pax6 and Dll1 may be capable of indirectly co-regulating one another within INP^{vz}s, it would be beneficial to examine whether Dll1 and Pax6 are capable of mutually co-regulating one another. This would further solidify our model and provide insight into the relationship between Pax6 and Dll1 during cell proliferation. Examining the effects of a loss of Dll1 on Pax6 expression in the embryonic cerebral cortex would be a straightforward approach to beginning to answer this complex question. This could be conducted

using Dll1 mutant line like the one described by Hrabe de Angelis *et* al., (1997) and Machka *et al*., (2005) and would allow examination of Pax6 expression at different stages of development (Hrabe de Angelis *et al*., 1997; Machka *et al*., 2005). Complimentary gain-of-function studies for both Pax6 and Dll1 by electroporation in order to assess the affect on the other would also be a favourable approach (Marin *et al*., 2013).

Due to time constraints, whether Dll1 is expressed in RGCs was never tested. The fact that a great deal of our model hinges on the precise location of Dll1 expression in progenitor cells subpopulations makes this an increasingly crucial question that requires a definitive answer. Double in situ hybridisation and flow cytometry for Dll1 and a RGC marker would provide the evidence required to prove or disprove whether RGCs express Dll1. Use of Pax6 to undertake these experiments would not only provide evidence that Dll1 is expressed in RGCs, but would also confirm whether Pax6 and Dll1 are co-expressed by progenitor cells. This would not only, prove areas of our existing model, but also provide evidence to prove and disprove some of the revised versions of the model outlined in section 7.4.

To further solidify our model and allow us to revise aspects of it, providing evidence that INP^{VZ}s simultaneously express Dll1, Tbr2 and Pax6 would be of the utmost importance. A triple label flow cytometry approach would confirm whether there are cortical cells that express all three simultaneously but would not confirm that these cells are INP^{VZ} cells. INP^{VZ}s are typically characterised by their position within the cortex and their expression of Tbr2. A an adaptation of the live-cell imaging approach of slice cultures transfected with a Dll1 reporter construct as described by Nelson *et al*., (2013) and subsequent immunohistochemical labelling would allow the identification of INP^{VZ}s and confirm whether they simultaneously express Dll1,Tbr2 and Pax6.

7.7 Conclusion

This study has identified that the Notch ligands Dll1 and Jag1 are Pax6 targets. Steps have also been taken in identifying the specifics surrounding regulatory relationships that Pax6 has with Dll1 and Jag1. Potential putative Pax6 binding sites for Jag1 have been identified but further testing is required to validate them. The precise location of Dll1 in the proliferative zone of the cortex was previously inconclusive, with multiple studies stating that it was expressed by different progenitor cells. This study has identified that Dll1 mRNA expression is restricted to the VZ, while Dll1 protein expression is co-expressed by a proportion of Tbr2 positive cells. However, it cannot be concluded if these are INP cells or INP^{VZ} cells. A model for how Pax6 may control cell proliferation during neurogenesis has been designed but revisions of the original and further testing is required in order to validate it. As a result, this study has identified a potential mechanism by which Pax6 exerts control over cell proliferation during cortical neurogenesis by controlling the Notch signalling pathway via regulation of two of its ligands.

Abdipranoto, A., Wu, S., Stayte, S., Vissel, B. (2008). The Role of Neurogenesis in Neurodegenerative Diseases and its Implications for Therapeutic Development. *CNS Neurol Discord Drug Targets.* **7.** 187-210.

Akhtar, A.A., Breunig, J.J. (2015). Lost Highway(s): Barriers to Postnatal Cortical Neurogenesis and Implications for Brain Repair. *Front Cell Neurosci.*

Anderson, S., Vanderhaeghen, P. (2014). Cortical Neurogenesis from Pluripotent Stem Cells: Complexity Emerging from Simplicity. *Curr Opin Neurobiol.* **27.** 151-157.

Appolloni, I., Calzolari, F., Barilari, M., Terrile, M., Daga, A., Malatesta, P. (2012). Antagonistic Modulation of Gliomagenesis by Pax6 and Olig2 in PDGF-Induced Oligodendroglioma. *Int J Cancer.* **131.** E1078-87.

Artavanis-Tsakonas, S., Rand, M.D., Lake, R.J. (1999). Notch Signaling: Cell Fate Control and Signal Integration in Development. *Science.* **284.** 770-776.

Assimacopoulos, S., Grove, E.A., Ragsdale, C.W. (2003). Identification of a Pax6-Dependent Epidermal Growth Factor Family Signaling Source at the Lateral Edge of the Embryonic Cerebral Cortex. *J Neurosci.* **23.** 6399–6403.

Azevedo, F. A. C., Carvalho, L. R. B., Grinberg, L. T., Farfel, J. M., Ferretti, R. E. L., Leite, R. E. P., Filho, J.W., Lent, R.,Herculano-Houzel, S. (2009). Equal numbers of neuronal and non neuronal cells make the human brain an isometrically scaled-up primate brain. *J. Comp. Neurol.* **513.** 532-541.

Basak, O., and Taylor, V. (2007) Identification of self-replicating multipotent progenitors in the embryonic nervous system by high Notch activity and Hes5 expression. **25.** 1006-1022.

Bettenhausen, B., Hrabě de Angelis, M., Simon, D., Guénet, J.L., Gossler, A. (1995). Transient and Restricted Expression during Mouse Embryogenesis of Dll1, a Murine Gene Closely Related to Drosophila Delta. *Development.* **121.** 2407-2418.

Bertuccioli, C., Fasano, L., Jun, S.,Wang, S., Sheng, G., Desplan, C. (1996). In vivo requirement for the paired domain and homeodomain of the paired segmentation gene product. *Development*. **122.** 2673–2685.

Bhatia, S., Monahan, J., Ravi, V., Gautier, P., Murdoch, E., Brenner, S., van Heyningen, V., Venkatesh, B., Kleinjan, D.A. (2014). A Survey of Ancient Conserved Non-coding Elements in the PAX6 Locus Reveals a Landscape of Interdigitated Cis-regulatory Archipelagos. *Dev Biol.* **387.** 214-228.

Bishop, K. M., Goudreau, G., O'leary, D. D. (2000). Regulation of area identity in the mammalian neocortex by Emx2 and Pax6. *Science.* **288.** 344–349.

Bishop, K. M., Rubenstein, J. L., O'leary, D. D.(2002). Distinct actions of Emx1, Emx2, and Pax6 in regulating the specification of areas in the developing neocortex. *J. Neurosci.* **22.** 7627–7638.

Borello, U., Cobos, I., Long, J.E., Murre ,C., Rubenstein, J.L. (2008). FGF15 Promotes Neurogenesis and Opposes FGF8 Function During Neocortical Development. *Neural Dev.* **3.** 17.

Borrell, V., Cárdenas, A., Ciceri, G., Galcerán, J., Flames, N., Pla, R., Nóbrega-Pereira, S., García-Frigola, C., Peregrín, S., Zhao, Z., Ma, L., Tessier-Lavigne, M., Marín, O. (2012). Slit/Robo Signaling Modulates the Proliferation of Central Nervous System Progenitors. *Neuron.* **76.** 338-352.

Breunig, J.J., Silbereis, J., Vaccarino, F.M., Sestan, N., Rakic, P. (2007). Notch Regulates Cell Fate and Dendrite Morphology of Newborn Neurons in the Postnatal Dentate Gyrus. *Proc Natl Acad Sci U S A.* **104.** 20558-20563.

Brindle, P.K., Holland, J.P., Willett, C.E., Innis, M.A., Holland, M.J. (1990). Multiple Factors Bind the Upstream Activation Sites of the Yeast Enolase Genes ENO1 and ENO2: ABFI Protein, Like Repressor Activator Protein RAP1, Binds Cis-acting Sequences Which Modulate Repression or Activation of Transcription. *Mol Cell Biol.* **10.** 4872-4885.

Bulger, M., Groudine, M. (2010). Enhancers: The Abundance and Function of Regulatory Sequences beyond promoters. *Dev Biol.* **339.** 250-257.

Campos-Ortega, J.A. (1993). Mechanisms of Early Neurogenesis in Drosophila Melanogaster. *J Neurobiol.* **24.** 1305-1327.

Campos, L.S., Duarte, A.J., Branco, T., Henrique, D. (2001). mDll1 and mDll3 Expression in the Developing Mouse Brain: Role in the Establishment of the Early Cortex. *Journal of neuroscience research.* **64.** 590–598.

Cappello, S., Attardo, A., Wu, X., Iwasato, T., Itohara, S., Wilsch-Bräuninger, M., Eilken, H. M., Rieger, M. A., Schroeder, T. T., Huttner, W. B., Brakebusch, B., Götz, M. (2006). The Rho-GTPase cdc42 regulates neural progenitor fate at the apical surface. *Nat. Neurosci.* **9.** 1099 – 1107.

Caric, D., Gooday, D., Hill, R.E., McConnell, S.K., Price, D.J. (1997). Determination of the Migratory Capacity of Embryonic Cortical Cells Lacking the Transcription Factor Pax-6. *Development*. **124.** 5087-5096.

Carr, C. (2009) Microarray Investigation of the Role of Pax6 at the PSPB using a novel TauGFP-Pax6 Reporter Mouse. PhD Thesis. University of Edinburgh.

Cartier, L., Laforge, T., Feki, A., Arnaudeau, S., Dubois-Dauphin, M., Krause, K. H. (2006). Pax6-induced alteration of cell fate: shape changes, expression of neuronal alphatubulin, postmitotic phenotype, and cell migration. *J. Neurobiol.* **66.** 421–436.

Casarosa, S., Fode, C., Guillemot, F. (1999). Mash1 Regulates Neurogenesis in the Ventral Telencephalon. *Development.* **126.** 525-534.

Castro, D.S., Skowronska-Krawczyk, D., Armant, O., Donaldson, I.J., Parras, C., Hunt, C., Critchley, J.A., Nguyen, L., Gossler, A., Göttgens, B., Matter, J.M., Guillemot, F.

(2006). Proneural bHLH and Brn Proteins Coregulate a Neurogenic Program through Cooperative Binding to a Conserved DNA Motif. *Dev Cell.* **11.** 831-844.

Castro, D.S., Guillemot, F. (2011). Old and New Functions of Proneural Factors Revealed by the Genome-wide Characterization of their Transcriptional Targets. *Cell Cycle.* **10.** 4026-4031.

Castro, D.S., Martynoga, B., Parras, C., Ramesh, V., Pacary, E., Johnston, C., Drechsel, D., Lebel-Potter, M., Garcia, L.G., Hunt, C., Dolle, D., Bithell, A., Ettwiller, L., Buckley, N., Guillemot, F. (2011). A Novel Function of the Proneural Factor Ascl1 in Progenitor Proliferation Identified by Genome-wide Characterization of its Targets. *Genes Dev.* **25.** 930-945.

Chapouton, P., Gärtner, A., Götz, M. (1999). The Role of Pax6 in Restricting Cell Migration between Developing Cortex and Basal Ganglia**.** *Development*. **126.** 5569-5579.

Chenn, A., and McConnell, S.K. (1995). Cleavage Orientation and the Asymmetric Inheritance of Notch1 Immunoreactivity in Mammalian Neurogenesis. *Cell*. **82.** 631-641.

Chi, N., Epstein, J.A. (2002). Getting your Pax Straight: Pax Proteins in Development and Disease. *Trends Genet.* **18.** 41-47.

Chitnis, A., Henrique, D., Lewis, J., Ish-Horowicz, D., and Kintner, C. (1995). Primary Neurogenesis in Xenopus Embryos Regulated by a Homologue of the Drosophila Neurogenic Gene Delta. *Nature*. **375.** 761–766.

Cocas, L.A., Georgala, P.A., Mangin, J.M., Clegg, J.M., Kessaris, N., Haydar, T.F., Gallo, V., Price, D.J., Corbin, J.G. (2011). Pax6 is Required at the Telencephalic Pallial-subpallial Boundary for the Generation of Neuronal Diversity in the Postnatal Limbic System. *J. Neurosci*. **31.** 5313-5324.

Coffman, C.R., Skoglund, P., Harris, W. A., and Kintner, C.R. (1993). Expression of an Extracellular Deletion of Xotch Diverts Cell Fate in Xenopus Embryos. *Cell*. **73.** 659–671.

Corbin, J.G., Gaiano, N., Juliano, S.L., Poluch, S., Stancik, E., and Haydar, T.F. (2009) *J. Neurochem.* **106.** 2272-2287.

Couso, J.P., Knust, E., Martinez Arias, A. (1995). Serrate and Wingless Cooperate to Induce Vestigial Gene Expression and Wing Formation in Drosophila. *Curr Biol.* **5.** 1437-1448.

Coutinho, P., Pavlou, S., Bhatia, S., Chalmers, K.J., Kleinjan, D.A., van Heyningen, V. (2011). Discovery and Assessment of Conserved Pax6 Target Genes and Enhancers. *Genome Res.* **21.** 1349-1359.

Davidson, E.H. (2010). Emerging Properties of Animal Gene Regulatory Networks. *Nature.* **468.** 911-920.

del Álamo, D., Rouault, H., Schweisguth, F. (2011). Mechanism and Significance of Cis-inhibition in Notch Signalling. *Curr Biol.* **21.** R40-47.

de Antonellis, P., Medaglia, C., Cusanelli, E., Andolfo, I., Liguori, L., De Vita, G., Carotenuto, M., Bello, A., Formiggini, F., Galeone, A., De Rosa, G., Virgilio, A.,

Scognamiglio, I., Sciro, M., Basso, G., Schulte, J.H., Cinalli, G., Iolascon, A., Zollo, M. (2011). MiR-34a Targeting of Notch Ligand Delta-like 1 Impairs CD15+/CD133+ Tumor-propagating Cells and Supports Neural Differentiation in Medulloblastoma. *PLoS One.* **6.** e24584.

de Celis, J.F., and Bray, S. (1997). Feed-back Mechanisms Affecting Notch Activation at the Dorsoventral Boundary in the Drosophila Wing. *Development.* **124.** 3241–3251.

Del Bene, F., Ettwiller, L., Skowronska-Krawczyk, D., Baier, H., Matter, J.M., Birney, E., Wittbrodt, J. (2007). In Vivo Validation of a Computationally Predicted Conserved Ath5 Target Gene Set. *PLoS Genet.* **3.** 1661–1671.

Díaz-Alonso, J., Aguado, T., de Salas-Quiroga, A., Ortega, Z., Guzmán, M., Galve-Roperh, I. (2014). CB1 Cannabinoid Receptor-Dependent Activation of mTORC1/Pax6 Signaling Drives Tbr2 Expression and Basal Progenitor Expansion in the Developing Mouse Cortex. *Cerebral Cortex.* **25.** 2395-2408.

Doherty, D., Feger, G., Younger-Shepherd, S., Jan, L.Y., Jan, Y.N. (1996). Delta is a Ventral to Dorsal Signal Complementary to Serrate, another Notch Ligand, in Drosophila Wing Formation. *Genes Dev.* **10.** 421-434.

Dohrmann, C., Gruss, P., Lemaire, L. (2000). Pax Genes and the Differentiation of Hormone-producing Endocrine Cells in the Pancreas. *Mech Dev.* **92.** 47-54.

Dorà, E. (2011). The Role of the Notch Signalling Pathway by Pax6. Msc Dissertation. University of Edinburgh.

Dorà, N., Ou, J., Kucerova, R., Parisi, I., West, J.D., Collinson, J.M. (2008). PAX6 Dosage Effects on Corneal Development, Growth, and Wound Healing. *Dev Dyn.* **237.** 1295-1306.

Duan, D., Fu, Y., Paxinos, G., Watson, C. (2013). Spatiotemporal expression patterns of Pax6 in the brain of embryonic, newborn, and adult mice. *Brain Struct. Funct.* **218(2).** 353-72.

Duparc, R.H., Abdouh, M., David, J., Lépine, M., Tétreault, N., Bernier, G. (2006). Pax6 Controls the Proliferation Rate of Neuroepithelial Progenitors from the Mouse Optic Vesicle. *Dev Biol.* **301.** 374-387.

Duncan, M.K., Li, X., Ogino, H., Yasuda, K., Piatigorsky, J. (1996). Developmental regulation of the chicken beta B1-crystallin promoter in transgenic mice. *Mech. Dev.* **57.** 79–89.

Duncan, M.K., Haynes, J.I., Cvekl, A., Piatigorsky, J. (1998). Dual roles for Pax-6: a transcriptional repressor of lens fiber cell-specific beta-crystallin genes. *Mol. Cell. Biol.* **1998.** 18:5579–5586.

Egger, B., Gold, K.S., Brand, A.H. (2011). Regulating the Balance Between Symmetric and Asymmetric Stem Cell Division in the Developing Brain. *Fly (Austin).* **5.** 237-241.

Englund, C., Fink, A., Lau, C., Pham, D., Daza, R.A.M., Bulfone, A., Kowalczyk, T., and Hevner, R.F. (2005). Pax6, Tbr2, and Tbr1 Are Expressed Sequentially by Radial Glia,

Intermediate Progenitor Cells, and Postmitotic Neurons in Developing Neocortex. *J. Neurosci.* **25(1).** 247-251.

Epstein, J., Cai, J., Glaser, T., Jepeal, L., Maas, R. (1994). Identification of a Pax Paired Domain Recognition Sequence and Evidence for DNA-dependent Conformational Changes. *J. Biol. Chem.* **269.** 8355–8361.

Eriksson, P.S., Perfilieva, E., Björk-Eriksson, T., Alborn, A.M., Nordborg, C., Peterson, D.A., Gage, F.H. (1998). Neurogenesis in the Adult Human Hippocampus. *Nat Med.* **4.** 1313-1317.

Estivill-Torrus, G., Pearson, H., van Heyningen, V., Price, D.J., Rashbass, P. (2002). Pax6 is Required to Regulate the Cell Cycle and the Rate of Progression from Symmetrical to Asymmetrical Division in Mammalian Cortical Progenitors. *Development.* **129.** 455-466.

Estrach, S., Cordes, R., Hozumi, K., Gossler, A., and Watt, F.M. (2008). Role of the Notch Ligand Delta1 in Embryonic and Adult Mouse Epidermis. *J. Invest. Dermatol.* **128.** 825–832.

Farkas, L.M., and Huttner, W.B. (2008). The Cell Biology of Neural Stem and Progenitor Cells and its Significance for their Proliferation Versus Differentiation During Mammalian Brain Development. *Current Opinion in Cell Biology*. **20.** 707-715.

Favor, J., Gloeckner, C.J., Neuhäuser-Klaus, A., Pretsch, W., Sandulache, R., Saule, S., Zaus, I. (2008). Relationship of Pax6 Activity Levels to the Extent of Eye Development in the Mouse, Mus Musculus. **179.** 1345-1355.

Fiaschetti, G., Schroeder, C., Castelletti, D., Arcaro, A., Westermann, F., Baumgartner, M., Shalaby, T., Grotzer, M.A. (2014). NOTCH Ligands JAG1 and JAG2 as Critical Pro-survival Factors in Childhood Medulloblastoma. *Acta Neuropathol Commun.* **7.** 39.

Fietz, S. A., Kelava, I., Vogt, J., Wilsch-Bräuninger, M., Stenzel, D., Fish, J. L., Corbeil, D., Riehn, A., Distler,W., Nitsch, R. (2010). OSVZ progenitors of human and ferret neocortex are epithelial-like and expand by integrin signaling. *Nat. Neurosci.* **13.** 690-699.

Florio, M., Huttner, W. B. (2014) Neural progenitors, neurogenesis and the evolution of the neocortex. *Development*. **141.** 2182-2194.

Fode, C., Ma, Q., Casarosa, S., Ang, S. L., Anderson, D. J., and Guillemot, F. (2000). A Role for Neural Determination Genes in Specifying the Dorsoventral Identity of Telencephalic Neurons. *Genes Dev.* **14.** 67-80.

Fortini, M.E. (2012). Introduction – Notch in Development and Disease. *Semin Cell Dev Biol.* **23.** 419-420.

Franklin, J.L., Berechid, B.E., Cutting, F.B., Presente, A., Chambers, C.B., Foltz, D.R., Ferreira, A., and Nye, J.S. (1999). Autonomous and Non-autonomous Regulation of Mammalian Neurite Development by Notch1 and Delta1. *Curr. Biol.* **9.** 1448–1457.

Fung, L.K., Quintin, E.M., Haas, B.W., Reiss, A.L. (2012). Conceptualizing Neurodevelopmental Disorders through a Mechanistic Understanding of Fragile X Syndrome and Williams Syndrome.

Gaiano, N., Nye, J. S. and Fishell, G. (2000). Radial Glial Identity Is Promoted by Notch1 Signaling in the Murine Forebrain. *Neuron*. **26.** 395-404.

Gal, J.S., Morozov, Y.M., Ayoub, A.E., Chatterjee, M., Rakic, P., Haydar, T.F. (2006). Molecular and Morphological Heterogeneity of Neural Precursors in the Mouse Neocortical Proliferative Zones. *J. Neurosci.* **26.** 1045–1056.

Gammil, L.S., Bronner-Fraser, M. (2003). Neural Crest Specification: Migrating into Genomics. *Nat Rev Neurosci.* **4**. 795-805.

Gazit, R., Krizhanovsky, V., Ben-Arie, N. (2004). Math1 Controls Cerebellar Granule Cell Differentiation by Regulating Multiple Components of the Notch Signaling Pathway. *Development.* **131.** 903-913.

Georgala PA, Manuel M, Price DJ. (2011a). The Generation of Superficial Cortical Layers is Regulated by Levels of the Transcription Factor Pax6. *Cereb Cortex.* **21.** 81-94.

Georgala, P.A., Carr, C.B., Price, D.J. (2011b). The Role of Pax6 in Forebrain Development. *Dev Neurobiol.* **71.** 690-709.

Glittenberg, M., Pitsouli, C., Garvey, C., Delidakis, C., and Bray, S. (2006). Role of Conserved Intracellular Motifs in Serrate Signalling, Cis-inhibition and Endocytosis. *EMBO J.* **25.** 4697–4706.

Götz, M., Stoykova, A., Gruss, P. (1998). Pax6 Controls Radial Glia Differentiation in the Cerebral Cortex. *Neuron.* **21.** 1031-1044.

Götz M. (2001) Cerebral Cortex Development. *Encyclopaedia of Life Sciences*

Götz, M., Hartfuss, E. and Malatesta, P. (2002). Radial Glial Cells as Neuronal Precursors: A New Perspective on the Correlation of Morphology and Lineage Restriction in the Developing Cerebral Cortex of Mice. *Brain Research Bulletin*. **57(6).** 777–788.

Götz, M. and Barde, A. (2005). Radial Glial Cells: Defined and Major Minireview Intermediates between Embryonic Stem Cells and CNS Neurons. *Neuron*. **46.** 369-372.

Götz, M. and Huttner, W. B. (2005). The Cell Biology of Neurogenesis. *Molecular Cell Biology*. **6.** 777-788

Götz, M., and Sommer, L. (2005). Cortical Development: the Art of Generating Cell Diversity. *Development*. **132.** 3327-3332.

Guillemot, F., Joyner, A.L. (1993). Dynamic Expression of the Murine Achaete-Scute Homologue Mash-1 in the Developing Nervous System. *Mech Dev.* **42.** 171-185.

Guruharsha, K.G., Kankel, M.W., Artavanis-Tsakonas, S. (2012). The Notch Signalling System: Recent Insights into the Complexity of a Conserved Pathway.

Hack, M.A., Sugimori, M., Lundberg, C., Nakafuku, M., Gotz, M. (2004). Regionalization and fate specification in neurospheres: the role of Olig2 and Pax6. *Mol. Cell. Neurosci.* **25.** 664–678.

Halilagic A, Zile MH, Studer M. (2003). A Novel Role for Retinoids in Patterning the Avian Forebrain During Presomite Stages. *Development.* 2003. **130.** 2039–2050.

Halilagic A, Ribes V, Ghyselinck NB, Zile MH, Dolle P, Studer M. (2007). Retinoids Control Anterior and Dorsal Properties in the Developing Forebrain. *Dev Biol*. **303.** 362–375.

Hämmerle, B., Tejedor, F.J. (2007). A Novel Function of DELTA-NOTCH Signalling Mediates the Transition from Proliferation to Neurogenesis in Neural Progenitor Cells. *PLoS One.* **2.** e1169.

Hansen, D.V., Lui, J.H., Parker, P.R.L.,Kriegstein, A.R. (2010). Neurogenic radial glia in the outer subventricular zone of human neocortex. *Nature.* **464.** 554-561.

Hanson, I.M., Seawright, A., Hardman, K., Hodgson, S., Zaletayev, D., Fekete, G., van Heyningan, V. (1993) Pax6 mutations in aniridia. *Human Molecular Genetics.* **2(7):** 915-920.

Hanson, I., Van Heyingen, V. (1995). Pax6: More than Meets the Eye. *Trends Genet.* **11.** 268-272.

Hatakeyama, J., Bessho, Y., Katoh, K., Ookawara, S., Fujioka, M., Guillemot, F., and Kageyama, R. (2004). Hes Genes Regulate Size, Shape and Histogenesis of the Nervous System by Control of the Timing of Neural Stem Cell Differentiation. *Development*. **131(2).** 5539-5550.

Hatakeyama, J., and Kageyama, R. (2006). Notch1 Expression Is Spatiotemporally Correlated with Neurogenesis and Negatively Regulated by Notch1-Independent Hes Genes in the Developing Nervous System. *Cerebral Cortex*. **16.** 132-137.

Haubensak, W., Attardo, A., Denk, W., Huttner, W.B. (2004). Neurons Arise in the Basal Neuroepithelium of the Early Mammalian Telencephalon: a Major Site of Neurogenesis. *Proc. Natl. Acad. Sci. U.S.A.* **101.** 3196–3201.

Haubst, N., Berger, J., Radjendirane, V., Graw, .J, Favor, J., Saunders, G.F., Stoykova, A., Gotz, M. (2004). Molecular Dissection of Pax6 Function: the Specific Roles of the Paired Domain and Homeodomain in Brain Development. *Development*. **131.** 6131-6140.

Heins, N., Malatesta, P., Cecconi, F., Nakafuku, M., Tucker, K. L., Hack, M. A., Chapouton, P., Barde, Y. and Götz, M. (2008) Glial Cells Generate Neurons: the Role of the Transcription Factor Pax6. *Nature Neuroscience*. **5(4).** 308-315.

Heins, N., Malatesta, P., Cecconi, F., Nakafuku, M., Tucker, K.L., Hack, M.A., Chapouton, P., Barde, Y.A., Götz, M. (2002). Glial Cells Generate Neurons: the Role of the Transcription Factor Pax6. *Nat Neurosci.* **5.** 308-315.

Henrique, D., Adam, J., Myat, A., Chitnis, A., Lewis, J., and Ish-Horowicz, D. (1995). Expression of a Delta Homologue in Prospective Neurons in the Chick. *Nature*. **375.** 787–790.

Henrique, D., Hirsinger, E., Adam, J., Le Roux, I., Pourquie, O., Ish-Horowicz, D., and Lewis, J. (1997). Maintenance of Neuroepithelial Progenitor Cells by Delta-Notch Signalling in the Embryonic Chick Retina. *Curr. Biol*. **7.** 661–670.

Hevner, R. F. (2006). From Radial Glia to Pyramidal-Projection Neuron**.** Transcription Factor Cascades in Cerebral Cortex Development. *Molecular Neurobiology*. **33(1).** 33-50.

Hill, R.E., Favor, J., Hogan, B.L., Ton, C.C., Saunders, G.F., Hanson, I.M., Prosser, J., Jordan, T., Hastie, N.D., van Heyningen, V. (1991). Mouse Small Eye Results from Mutations in a Paired-like Homeobox-containing Gene. *Nature*. **354.** 522-525.

Hitoshi, S., Tropepe, V., Ekker, M., van der Kooy, D. (2002). Neural Stem Cell Lineages are Regionally Specified, but not Committed, Within Distinct Compartments of the Developing Brain. *Development*. **129.** 233–244.

Hoch, R.V., Rubenstein, J.L., Pleasure, S. (2009). Genes and signaling events that establish regional patterning of the mammalian forebrain. *Semin Cell Dev Biol.* **20.** 378-386.

Holm, P.C., Mader, M.T., Haubst, N., Wizenmann, A., Sigvardsson, M., Götz, M. (2007). Loss- and Gain-of-function Analyses Reveal Targets of Pax6 in the Developing Mouse Telencephalon. *Mol Cell Neurosci.* **34.** 99-119.

Hrabe de Angelis, M., McIntyre, J., Gossier, A. (1997). Maintenance of Somite Borders in Mice Requires the Delta Homologue DII1. **386.** 717-721.

Hufnagel, R. B., Riesenberg, A. N., Saul, S. M., Brown, N. L. (2007). Conserved regulation of Math5 and Math1 revealed by Math5-GFP transgenes. *Mol. Cell. Neurosci.* **36(4).** 435–448.

Hui, Z., Yongchao, Z., Yongqing, Z. (2015). Recent Progresses in Molecular Genetics of Autism Spectrum Disorders. *Yi Chuan.* **37.** 845-854.

Huttner, W.B., Kosodo, Y. (2005). Symmetric Versus Asymmetric Cell Division during Neurogenesis in the Developing Vertebrate Central Nervous System. *Curr Opin Cell Biol.* **17.** 648-657.

Ignatova, T.N., Kukekov, V.G., Laywell, E.D., Suslov, O.N., Vrionis, F.D., Steindler, D.A. (2002). Human cortical glial tumors contain neural stem-like cells expressing astroglial and neuronal markers in vitro. *Glia.* **39.** 193-206.

Imayoshi, I., Kageyama, R. (2011). The Role of Notch Signaling in Adult Neurogenesis. *Mol Neurobiol.* **44.** 7-12.

Imayoshi, I., Shimojo, H., Sakamoto, M., Ohtsuka, T., Kageyama, R. (2013). Genetic Visualization of Notch Signaling in Mammalian Neurogenesis. *Cell Mol Life Sci.* **70.** 2045-2057.

Imayoshi, I., Isomura, A., Harima, Y., Kawaguchi, K., Kori, H., Miyachi, H., Fujiwara, T.K., Ishidate, F., Kageyama, R. (2013). Oscillatory control of factors determining multipotency and fate in mouse neural progenitors. *Science*. **342.** 1203–1208.

Imayoshi, I., Kageyama, R. (2014). bHLH factors in self-renewal, multipotency, and fate choice of neural progenitor cells. *Neuron.* **82.** 9–23.

Ishibashi M, McMahon AP. (2002). A Sonic Hedgehog-dependent Signaling Relay Regulates Growth of Diencephalic and Mesencephalic Primordia in the Early Mouse Embryo**.** *Development.* **129.** 4807-4819.

Iso, T., Kedes, L., Hamamori, Y. (2003). HES and HERP Families: Multiple Effectors of the Notch Signaling Pathway. *J Cell Physiol.* **194.** 237-255.

Itoh, M., Kim, C.H., Palardy, G., Oda, T., Jiang, Y.J., Maust, D., Yeo, S.Y., Lor- ick, K., Wright, G.J., Ariza-McNaughton, L., et al. (2003). Mind Bomb is a Ubiq- uitin Ligase that is Essential for Efficient Activation of Notch Signaling by Delta. *Dev. Cell.* **4.** 67–82.

Jin, L., Lloyd, R.V. (1997). In situ hybridization: Methods and applications. *Journal of Clinical Laboratory Analysis.* **11(1).** 1098-2825.

Jubb, A.M., Browning, L., Campo, L., Turley, H., Steers, G., Thurston, G., Harris, A.L., Ansorge, O. (2012). **Expression of Vascular Notch Ligands Delta-like 4 and Jagged-1 in Glioblastoma.** *Histopathology.* **60.** 740-747.

Jun, S., Desplan, C. (1996). Cooperative Interactions between Paired Domain and Homeodomain. *Development.* **122.** 2639-2650.

Kageyama, R., Ohtsuka, T., Kobayashi, T. (2008a). Roles of Hes Genes in Neural Development. *Dev. Growth. Differ.* **50.** S97-S103.

Kageyama, R., Ohtsuka, T., Shimojo, H., Imayoshi, I. (2008b). Dynamic Notch Signaling in Neural Progenitor Cells and a Revised View of Lateral Inhibition. *Nat Neurosci.* **11.** 1247–1251.

Kageyama, R., Ohtsuka, T., Shimojo, H., Imayoshi, I. (2009). Dynamic Regulation of Notch Signaling in Neural Progenitor Cells. *Curr Opin Cell Biol.* **21.** 733-740.

Kawaguchi, D., Furutachi, S., Kawai, H., Hozumi, K., Gotoh, Y. (2013) Dll1 maintains quiescence of adult neural stem cells and segregates asymmetrically during mitosis. *Nat. Commun.* **4.** 1880.

Kessaris, N., Fogarty, M., Iannarelli, P., Grist, M., Wegner, M., Richardson, W.D. (2006) Competing Waves of Oligodendrocytes in the Forebrain and Postnatal Elimination of an Embryonic Lineage. *Nat Neurosci.* **9.** 173-179.

Kirby, E. D., Kuwahara, A. A., Messer, R. L., Wyss-Coray, T. (2015). Adult hippocampal neural stem and progenitor cells regulate the neurogenic niche by secreting VEGF. *Proc. Natl. Acad. Sci. U S A.* **112(13).** 4128-33.

Klein, T., Brennan, K., Arias, A.M. (1997). An Intrinsic Dominant Negative Activity of Serrate that is Modulated during Wing Development in Drosophila. *Dev. Biol.* **189.** 123–134.

Kopan, R., Nye, J.S., and Weintraub, H. (1994). The Intracellular Domain of Mouse Notch: A Constitutively Activated Repressor of Myogenesis Directed at the Basic Helix-loop-helix Region of MyoD. *Development*. **120.** 2385–2396.

Kopan, R., Ilagan, M.X. (2009). The Canonical Notch Signaling Pathway: Unfolding the Activation Mechanism. *Cell.* **137.** 216-233.

Kovach, C., Dixit, R., Li, S., Mattar, P., Wilkinson, G., Elsen, G.E., Kurrasch, D.M., Hevner, R.F., Schuurmans, C. (2013). Neurog2 Simultaneously Activates and Represses Alternative Gene Expression Programs in the Developing Neocortex. *Cereb Cortex.* **23.** 1884-1900.

Kozmik, Z. (2008). The Role of Pax Genes in Eye Evolution. *Brain Res Bull.* **75.** 335-339.

Kroll, T.T., O'Leary, D.D. (2005) Ventralized Dorsal Telencephalic Progenitors in Pax6 Mutant Mice Generate GABA Interneurons of a Lateral Ganglionic Eminence Fate. *Proc. Natl. Acad. Sci. U S A.* **102.** 7374-7379.

Laguesse, S., Peyre, E., Nguyen, L. (2015). Progenitor Genealogy in the Developing Cerebral Cortex. *Cell Tissue Res.* **359.** 17-32.

Lavado, A., Lagutin, O.V., Chow, L.M., Baker, S.J., Oliver, G. (2010). Prox1 is Required for Granule Cell Maturation and Intermediate Progenitor Maintenance During Brain Neurogenesis. *PLoS Biol.* **8.** e1000460.

Lavado, A., Oliver, G. (2014). Jagged1 is Necessary for Postnatal and Adult Neurogenesis in the Dentate Gyrus. *Dev Biol.* **388.** 11-21.

Levitt, P., Barbe, M. F. and Eagleson, K. L. (1997). Patterning and specification of the cerebral cortex. *Annu. Rev. Neurosci.* **20.** 1-24.

Lewandoski, M. (2001). Conditional Control of Gene Expression in the Mouse. *Nat Rev Genet.* **2.** 743-755.

Li, H.S., Wang, D., Shen, Q., Schonemann, M.D., Gorski, J.A., Jones, K.R., Temple, S., Jan, L.Y., and Jan, Y.N. (2003). Inactivation of Numb and Numblike in Embryonic Dorsal Forebrain Impairs Neurogenesis and Disrupts Cortical Morphogenesis. *Neuron*. **40.** 1105–1118.

Li, X.J., Liu, X.J., Yang, B., Fu, Y.R., Zhao, F., Shen, Z.Z., Miao, L.F., Rayner, S., Chavanas, S., Zhu, H., Britt, W.J., Tang, Q., McVoy, M.A., Luo, M.H. (2015). Human Cytomegalovirus Infection Dysregulates the Localization and Stability of NICD1 and Jag1 in Neural Progenitor Cells. **89.** 6792-6804.

Limbourg, A., Ploom, M., Elligsen, D., Sörensen, I., Ziegelhoeffer, T., Gossler, A., Drexler, H., Limbourg, F.P. (2007). Notch Ligand Delta-like 1 is Essential for Postnatal Arteriogenesis. *Circ Res.* **100.** 363-371.

Lindsell, C.E., Shawber, C.J., Boulter, J., Weinmaster, G. (1995). Jagged: a Mammalian Ligand that Activates Notch1. *Cell.* **80.** 909-917.

Lindsell, C.E., Boulter, J., diSibio, G., Gossler, A., Weinmaster, G. (1996). Expression Patterns of Jagged, Delta1, Notch1, Notch2, and Notch3 Genes Identify Ligand-receptor Pairs that May Function in Neural Development. *Mol Cell Neurosci.* **8.** 14-27.

Liu, M., Inoue, K., Leng, T., Guo, S., Xiong, Z.G. (2014). TRPM7 Channels Regulate Glioma Stem Cell through STAT3 and Notch Signaling Pathways. *Cell Signal.* **26.** 2773-2781.

Liu, Y., Deng, W. (2015). Reverse Engineering Human Neurodegenerative Disease Using Pluripotent Stem Cell Technology. *Brain Res.* **15.** S0006-8993.

Louvi, A., and Artavanis-Tsakonas, S. (2006). Notch Signalling in Vertebrate Neural Development. *Nat. Rev. Neurosci.* **7.** 93–102.

Lowell, S., Jones, P., Le Roux, I., Dunne, J., and Watt, F.M. (2000). Stimulation of Human Epidermal Differentiation by Delta-notch Signalling at the Boundaries of Stem-cell Clusters. *Curr. Biol.* **10.** 491–500.

Ma, D.K., Kim, W.R., Ming, G., Song, H. (2009). Activity-dependent Extrinsic Regulation of Adult Olfactory Bulb and Hippocampal Neurogenesis. *Ann N Y Acad Sci.* **1170.** 664-673.

Machka, C., Kersten, M., Zobawa, M., Harder, A., Horsch, M., Halder, T., Lottspeich, F., Hrabé de Angelis, M., Berckers, J. (2005) Identification of Dll1 (Delta1) Target Genes during Mouse Embryogenesis using Differential Expression Profiling. **6.** 94-101.

MacLennan, A.H., Thompson, S.C., Gecz, J. (2015). Cerebral Palsy: Causes, Pathways, and the Role of Genetic Variants. *Am J Obstet Gynecol.* **213.** 779-788.

Maekawa, M., Takashima, N., Arai, Y., Nomura, T., Inokuchi, K., Yuasa, S., Osumi, N. (2005). Pax6 is required for production and maintenance of progenitor cells in postnatal hippocampal neurogenesis. *Genes Cells.* **10(10).** 1001-14.

Mansouri, A., Hallonet, M., Gruss, P. (1996). Pax Genes and their Roles in Cell Differentiation and Development. *Curr Opin Cell Biol.* **8.** 851-857.

Manuel, M., Georgala, P.A., Carr, C.B., Chanas, S., Kleinjan, D.A., Martynoga, B., Mason, J.O., Molinek, M., Pinson, J., Pratt, T., Quinn, J.C., Simpson, T.I., Tyas, D.A., van Heyningen, V., West, J.D., Price, D.J. (2007). Controlled overexpression of Pax6 in vivo negatively autoregulates the Pax6 locus, causing cell-autonomous defects of late cortical progenitor proliferation with little effect on cortical arealization. *Development*. **134**:545--555.

Manuel, M.N., Mi, D., Mason, J.O., Price, D.J. (2015). Regulation of Cerebral Cortical Neurogenesis by the Pax6 Transcription Factor. *Front Cell Neurosci.* **9.** 70.

Manzini, M.C., Walsh, C.A. (2011). What Disorders of Cortical Development Tell Us About the Cortex: One Plus One Does Not Always Make Two. *Curr Opin Genet Dev.* **21.** 333-339.

Martínez-Cerdeño, V., Noctor, S.C., Kriegstein, A.R. (2006). The role of intermediate progenitor cells in the evolutionary expansion of the cerebral cortex. *Cerebral Cortex*. **16**:i152-i161.

Mathieu, P., Adami, P.V., Morelli, L. (2013). Notch Signaling in the Pathologic Adult Brain. *Biomol Concepts.* **4.** 465-476.

Mi, D., Carr, C.B., Georgala, P.A., Huang, Y.T., Manuel, M.N., Jeanes, E., Niisato, E., Sansom, S.N., Livesey, F.J., Theil, T., Hasenpusch-Theil, K., Simpson, T.I., Mason, J.O., Price, D.J. (2013a). Pax6 Exerts Regional Control of Cortical Progenitor Proliferation Via Direct Repression of Cdk6 and Hypophosphorylation of pRb. *Neuron.* **78.** 269-284.

Mi, D., Huang, Y.T., Kleinjan, D.A., Mason, J.O., Price, D.J. (2013b). Identification of Genomic Regions Regulating Pax6 Expression in Embryonic Forebrain using YAC Reporter Transgenic Mouse Lines. *PLoS One.* **8.** e80208.

Mikkola, I., Bruun, J.A., Holm, T., Johansen, T. (2001). Superactivation of Pax6-Mediated Transactivation from Paired Domain-binding Sites by Dna-independent Recruitment of Different Homeodomain Proteins. *J Biol Chem.* **276.** 4109-4118.

Mishra, R., Gorlov, I.P., Chao, L.Y., Singh, S., Saunders, G.F. (2002). PAX6, Paired Domain Influences Sequence Recognition by the Homeodomain. *J Biol Chem.* **277.** 49488-49494.

Miyata, T., Kawaguchi, A., Saito, K., Kawano, M., Muto, T., Ogawa, M. (2004). Asymmetric Production of Surface-dividing and Non-surface-dividing Cortical Progenitor Cells. *Development.* **131.** 3133–3145.

Mizutani, K., Yoon, K., Dang, L., Tokunaga, A., Gaiano, N. (2007). Differential Notch Signalling Distinguishes Neural Stem Cells from Intermediate Progenitors. *Nature.* **449.** 351–355.

Molotkova N, Molotkov A, Duester G. (2007). Role of Retinoic Acid During Forebrain Development Begins Late when Raldh3 Generates Retinoic Acid in the Ventral Subventricular Zone. *Dev Biol.* **303.** 601–610. □

Morriss-Kay, G., Ruberte, E., Fukiishi, Y. (1993). Mammalian Neural Crest and Neural Crest Derivatives. *Ann Anat.* **175.** 501-507.

Morriss-Kay, G., Wood, H., Chen, W.H. (1994). Normal Neurulation in Mammals. *Ciba Found Symp.* **181.** 51-63.

Muzio, L., Mallamaci, A. (2003). Emx1, emx2 and pax6 in specification, region-alization and arealization of the cerebral cortex. *Cereb. Cortex.* **13.** 641–647.

Muzio, L., Dibenedetto, B., Stoykova, A., Boncinelli, E., Gruss, P., Mallamaci, A. (2002). Emx2 and Pax6 control regionalization of the pre-neuronogenic cortical primordium. *Cereb.Cortex*. **12.** 129–139.

Nelson, B.R., Reh, T.A. (2008). Relationship Between Delta-like and Proneural bHLH Genes during Chick Retinal Development. *Dev Dyn.* **237.** 1565-1580.

Nelson, B.R., Hodge, R.D., Bedogni, F., Hevner, R.F. (2013). Dynamic Interactions Between Intermediate Neurogenic Progenitors and Radial Glia in Embryonic Mouse Neocortex: Potential Role in Dll1-Notch Signaling. **33(21).** 9122-9139.

Nieto, M., Schuurmans, C., Britz, O., Guillemot, F. (2001). Neural bHLH Genes Control the Neuronal Versus Glial Fate Decision in Cortical Progenitors. *Neuron.* **29.** 401-413.

Ninkovic, J., Pinto, L., Petricca, S., Lepier, A., Sun, J., Rieger, M.A., Schroeder, T., Cvekl, A., Favor, J., Götz, M. (2010). The Transcription Factor Pax6 Regulates Survival of Dopaminergic Olfactory Bulb Neurons Via Crystallin αA. *Neuron.* **68.** 682-694.

Noctor, S.C., Flint, A.C., Weissman, T.A., Dammerman, R.S., Kriegstein, A.R. (2001). Neurons Derived from Radial Glial Cells Establish Radial Units in Neocortex. *Nature*. **409.** 714-720.

Noctor, S. C., Martínez-Cerdeño1, V., Ivic1, L. and Kriegstein, A. R. (2004). Cortical Neurons Arise in Symmetric and Asymmetric Division Zones and Migrate Through Specific Phases. *Nature Neuroscience*. **7(2).** 136-144.

Nye, J.S., Kopan, R., and Axel, R. (1994). An Activated Notch Suppresses Neurogenesis and Myogenesis but not Gliogenesis in Mammalian Cells. *Development*. **120.** 2421–2430.

Ochiai, W., Nakatani, S., Takahara, T., Kainuma, M., Masaoka, M., Minobe, S., Namihira, M., Nakashima, K., Sakakibara, A., Ogawa, M., and Miyata, T. (2009). Periventricular Notch Activation and Asymmetric Ngn2 and Tbr2 Expression in Pair-generated Neocortical Daughter Cells. *Mol. Cell. Neurosci*. **40.** 225–233.

Ohtsuka, T., Ishibashi, M., Gradwohl, G., Nakanishi, S., Guillemot, F., Kageyama, R. (1999). Hes1 and Hes5 as Notch Effectors in Mammalian Neuronal Differentiation. *Embo J.* **18.** 2196-2207.

Osumi, N., Shinohara, H., Numayama-Tsuruta, K., Maekawa, M. (2008). Concise Review: Pax6 Transcription Factor Contributes to both Embryonic and Adult Neurogenesis as a Multifunctional Regulator. *Stem Cells.* **26.** 1663-1672.

Ostrin, E., Li, Y., Hoffman, K., Liu, J., Wang, K.Q., Zhang, L., Mardon, G., Chen, R. (2006) Genome-wide identification of direct targets of the Drosophila retinal determination protein Eyeless. *Genome Res.* **16.** 466–476.

Pennacchio, L.A., Bickmore, W., Dean, A., Nobrega, M.A., Bejerano, G. (2013). Enhancers: five essential questions. *Nat Rev Genet.* **14.** 288-295.

Peter, I.S., Davidson, E.H. (2011). **Evolution of Gene Regulatory Networks Controlling Body Plan Development.** *Cell.* **144.** 970-985.
Pierfelice T, Lavinia A, Gaiano N. (2011) Notch in the vertebrate nervous system: an old dog with new tricks. *Neuron*. **69**: 840-855.

Pleasure, S.J., Collins, A.E., Lowenstein, D.H. (2000). Unique expression patterns of cell fate molecules delineate sequential stages of dentate gyrus development. *J. Neurosci.* **20.** 6095–6105.

Piñon, M.C., Tuoc, T.C., Ashery-Padan, R., Molnár, Z., Stoykova, A. (2008). Altered Molecular Regionalization and Normal Thalamocortical Connections in Cortex-specific Pax6 Knock-out Mice. *J Neurosci.* **28.** 8724-8734.

Politis, P.K., Rohrer, H., Matsas, R. (2007). Expression Pattern of BM88 in the Developing Nervous System of the Chick and Mouse Embryo. *Gene Expr Patterns.* **7.** 165-177.

Pontious, A., Kowalczyk, T., Englund, C. and Hevner R. F. (2007). Role of Intermediate Progenitor Cells in Cerebral Cortex Development. *Developmental Neuroscience*. **30.** 24-32.

Pratt, T., Vitalis, T., Warren, N., Edgar, J.M., Mason, J.O., Price, D.J. (2000). A Role for Pax6 in the Normal Development of Dorsal Thalamus and its Cortical Connections. *Development.* **127.** 5167-5178.

Pratt, T., Quinn, J.C., Simpson, T.I., West, J.D., Mason, J.O., Price, D.J. (2002). Disruption of Early Events in Thalamocortical Tract Formation in Mice Lacking the Transcription Factors Pax6 or Foxg1. *J Neurosci.* **22.** 8523-8531.

Purow, B.W., Haque, R.M., Noel, M.W., Su, Q., Burdick, M.J., Lee, J., Sundaresan, T., Pastorino, S., Park, J.K., Mikolaenko, I., Maric, D., Eberhart, C.G., Fine, H.A. (2005). Expression of Notch-1 and its Ligands, Delta-like-1 and Jagged-1, is Critical for Glioma Cell Survival and Proliferation. *Cancer Res.* **65.** 2353-2363.

Quinn, J.C., Molinek, M., Martynoga, B.S., Zaki, P.A., Faedo, A., Bulfone, A., Henver, R.F., West, J.D., Price, D.J., (2007). Pax6 Controls Cerebral Cortical Cell Number by Regulating Exit from the Cell Cycle and Specifies Cortical Cell Identity by a Cell Autonomous Mechanism. *Dev Biol*. **302.** 50-65.

Rakic, P. (1972). Mode of Cell Migration to the Superficial Layers of Fetal Monkey Neocortex. *J Comp Neurol*. **145.** 61-84.

Rakic, P. (1988). Specification of Cerebral Cortical Areas. *Science*. **8.** 170–176.

Rallu, M., Machold, R., Gaiano, N., Corbin, J.G., McMahon, A.P., Fishell, G. (2002). Dorsoventral Patterning is Established in the Telencephalon of Mutants Lacking Both Gli3 and Hedgehog Signaling. *Development.* **129.** 4963–4974.

Ramialison, M., Bajoghli, B., Aghaallaei, N., Ettwiller, L., Gaudan, S., Wittbrodt, B., Czerny, T., Wittbrodt, J. (2008). Rapid Identification of PAX2/5/8 Direct Downstream Targets in the Otic Vesicle by Combinatorial Use of Bioinformatics Tools. *Genome Biol.* **9.** R145.

Rash, B.G., Grove, E.A. Patterning the Dorsal Telencephalon: a Role for Sonic Hedgehog? *J Neurosci.* **27.** 11595–11603.□

Ravi, V., Bhatia, S., Gautier, P., Loosli, F., Tay, B.H., Tay, A., Murdoch, E., Coutinho, P., van Heyningen, V., Brenner, S., Venkatesh, B., Kleinjan, D.A. (2013). Sequencing of Pax6 Loci from the Elephant Shark Reveals a Family of Pax6 Genes in Vertebrate Genomes, Forged by Ancient Duplications and Divergences. *PLoS Genet.* **9.** e1003177.

Reillo, I., de Juan Romero, C., Garcia-Cabezas, M. A. and Borrell, V. (2011). A role for intermediate radial glia in the tangential expansion of the mammalian cerebral cortex. *Cereb. Cortex.* **21.** 1674-1694.

Ribes, V., Wang, Z., Dolle, P., Niederreither, K. (2006). Retinaldehyde Dehydrogenase 2 (RALDH2)-mediated Retinoic Acid Synthesis Regulates Early Mouse Embryonic Forebrain Development by Controlling FGF and Sonic Hedgehog Signaling. *Development.* **133.** 351–361.

Roth, H.J., Das, G.C., Piatigorsky, J. (1991). Chicken beta B1-crystallin gene expression: presence of conserved functional polyomavirus enhancer-like and octamer binding-like promoter elements found in non-lens genes. *Mol. Cell Biol.* **11.** 1488–1499.

Rubenstein, J.L., Beachy, P.A. (1998). Patterning of the Embryonic Forebrain. **8.** 18-26.

Sakamoto, K., Ohara, O., Takagi, M., Takeda, S., and Katsube, K. (2002). Intracellular Cell-autonomous Association of Notch and its Ligands: a Novel Mechanism of Notch Signal Modification. *Dev. Biol.* **241.** 313–326.

Sander, M., Neubuser, A., Kalamaras, J., Ee, H.C., Martin, G.R., German, M.S. (1997). Genetic analysis reveals that PAX6 is required for normal transcription of pancreatic hormone genes and islet development. *Genes Dev.* **11.** 1662–1673.

Sansom, S.N., Griffiths, D.S., Faedo, A., Kleinjan, D.J., Ruan, Y., Smith, J., van Heyningen, V., Rubenstein, J.L., Livesey, F.J. (2009a) The level of the transcription factor Pax6 is essential for controlling the balance between neural stem cell self-renewal and neurogenesis. *PLoS Genetics.* **5.** 1-16.

Sansom, S.N., Livesey, F.J. (2009b). Gradients in the Brain: the Control of the Development of Form and Function in the Cerebral Cortex. *Cold Spring Harb Prospect Biol.* **1.** a002519.

Scardigli, R., Schuurmans, C., Gradwohl, G., Guillemot, F. (2001). Crossregulation between Neurogenin2 and Pathways Specifying Neuronal Identity in the Spinal Cord. *Neuron.* **31.** 203-217.

Scardigli, R., Bäumer, N., Gruss, P., Guillemot, F., and Le Roux, I. (2003). Direct and Concentration-dependent Regulation of the Proneural Gene Neurogenin2 by Pax6. *Development*. **130.** 3269-3281.

Schmahl, W., Knoedlseder, M., Favor, J., Davidson, D. (1993). Defects of Neuronal Migration and the Pathogenesis of Cortical Malformations are Associated with Small Eye (Sey) in the Mouse, a Point Mutation at the Pax-6-locus. *Acta Neuropathol*. **86.** 126-135.

Schneider, R.A., Hu, D., Rubenstein, J.L., Maden, M., Helms, J.A. (2001). Local Retinoid Signal- ing Coordinates Forebrain and Facial Morphogenesis by Maintaining FGF8 and SHH. *Development.* **128.** 2755–2767. □

Sessa, A., Mao, C., Hadjantonakis, A., Klein, W., Broccoli, V. (2008). Tbr2 Directs Conversion of Radial Glia into Basal Precursors and Guides Neuronal Amplification by Indirect Neurogenesis in the Developing Neocortex. *Neuron.* **60.** 56–69.

Sheng, G., Thouvenot, E., Schmucker, D.,Wilson, D.S., Desplan, C. (1997). Direct regulation of rhodopsin1 byPax-6/eyeless in Drosophila: evidence for a conserved function in photoreceptors. *Genes Dev.* **11.** 1122–1131.

Shimojo, H., Ohtsuka, T., and Kageyama, R. (2008). Oscillations in Notch Signaling Regulate Maintenance of Neural Progenitors. *Neuron*. **58.** 52-64.

Shimojo, H., Isomura, A., Ohtsuka, T., Kori, H., Miyachi, H., Kageyama. R. (2016). Oscillatory control of Delta-like1 in cell interactions regulate dynamic gene expression and tissue morphogenesis. *Genes Dev.* **30.** 102–116.

Shimojo, S., Kageyema, R. (2016). Oscillatory control of Deltalike1 in somitogenesis and neurogenesis: A unified model for different oscillatory dynamics. *Seminars in Cell & Dev. Biol.* **49.** 76–82.

Simpson, T.I., Pratt, T., Mason, J.O., Price, D.J. 2009. Normal ventral telencephalic expression of Pax6 is required for normal development of thalamocortical axons in embryonic mice. *Neural Dev*. **4.** 19.

Singh, S., Tang, H.K., Lee, J. Y., Saunders, G.F. (1998). Truncation mutations in the transactivation region of PAX6 result in dominant-negative mutants. *J. Biol.Chem.* **273.** 21531–21541.

Singh, S., Stellrecht, C.M., Tang, H.K., Saunders, G. F. (2000). Modulation of PAX6 homeodomain function by the paired domain. *J. Biol.Chem.* **275.** 17306–17313.

Singh, S., Chao, L. Y., Mishra, R., Davies, J., Saunders, G. F. (2001).Missense mutation at the C-terminus of PAX6 negatively modulates homeodomain function. *Hum.Mol.Genet.* **10.** 911–918.

Smith, J.L., Schoenwolf, G.C. (1997). Neurulation: Coming to Closure. *Trends Neurosci.* **20.** 510-5.

Sommer, L., Ma, Q., Anderson, DJ. (1996). Neurogenins, a Novel Family of Atonal-related bHLH Transcription Factors, are Putative Mammalian Neuronal Determination Genes that Reveal Progenitor Cell Heterogeneity in the Developing CNS and PNS. *Mol Cell Neurosci.* **8.** 221-241.

Stormo, G.D. (2000). DNA binding sites: Representation and discovery. *Bioinformatics.* **16.** 16–23.

Stoykova A, Gruss P. (1994). Roles of Pax-genes in developing and adult brain as suggested by expression patterns. *J. Neurosci*. **14.** 1395-1412.

Stoykova, A., Fritsch, R., Walther, C., Gruss, P. (1996). Forebrain Patterning Defects in Small Eye Mutant Mice. *Development.* **122.** 3453-3465.

Stoykova, A., Götz, M., Gruss, P., Price, J. (1997). Pax6-dependent Regulation of Adhesive Patterning, R-cadherin Expression and Boundary Formation in Developing Forebrain. *Development.* **124.** 3765-3777.

Stoykova, A., Treichel, D., Hallonet, M., Gruss, P. (2000). Pax6 Modulates the Dorsoventral Patterning of the Mammalian Telencephalon. *J Neurosci*. **20(21).** 8042-8050.

Sun, J., Rockowitz, S., Xie, Q., Ashery-Padan, R., Zheng, D., Cvekl, A. (2015). Identification of in Vivo DNA-binding Mechanisms of Pax6 and Reconstruction of Pax6-dependent Gene Regulatory Networks during Forebrain and Lens Development. *Nucleic Acids Res.* **43.** 6827-6846.

Tabata, H. (2015). Diverse Subtypes of Astrocytes and their Development During Corticogenesis. *Front Neurosci.* **7.** 114.

Takahashi, T., Nowakowski, R.S., Caviness, V.S. (1995). Early Ontogeny of the Secondary Proliferative Population of the Embryonic Murine Cerebral Wall. *J Neurosci.* **15.** 6058-6068.

Tan, X., Shi, S.H. (2013). Neocortical Neurogenesis and Neuronal Migration. *Wiley Interdiscip. Rev. Dev. Biol.* **2.** 443–459.

Tang, H.K., Singh, S., Saunders, G.F. (1998).Dissection of the transactivation function of the transcription factor encoded by the eye developmental gene PAX6. *J. Biol.Chem.* **273.** 7210–7221.

Temple, S., Alvarez-Buylla, A. (1999). Stem Cells in the Adult Mammalian Central Nervous System. *Curr Opin Neurobiol.* **9.** 135-141.

Toresson, H., Potter, S.S., Campbell, K. (2000). Genetic Control of Dorsal-ventral Identity in the Telencephalon: Opposing Roles for Pax6 and Gsh2. *Development.* **127.** 4361-4371.

Tuoc, T.C., Stoykova, A. (2008). Er81 is a Downstream Target of Pax6 in Cortical Progenitors. *BMC Dev Biol.* **8.** 23.

Tuoc, **T.C., Radyushkin, K., Tonchev, A.B., Piñon, M.C., Ashery-Padan, R., Molnár, Z., Davidoff, M.S., Stoykova, A.** (2009). Selective Cortical Layering Abnormalities and Behavioral Deficits in Cortex-specific Pax6 Knock-out Mice. *J Neurosci.* **29.** 8335-8349.

Ulloa, F., Briscoe, J. (2007). Morphogens and the Control of Cell Proliferation and Patterning in the Spinal Cord. *Cell Cycle.* **6.** 2640-2649.

Urban, N., Guillemot, F. (2014). Neurogenesis in the embryonic and adult brain: same regulators, different roles. *Front. Cell. Neurosci.* **8.** 396.

Van den Akker, N.M., Winkel, L.C., Nisancioglu, M.H., Maas, S., Wisse, L.J., Armulik, A., Poelmann, R.E., Lie-Venema, H., Betsholtz, C., Gittenberger-de Groot, A.C. (2007). PDGF-B Signaling is Important for Murine Cardiac Development: its Role in Developing Atrioventricular Valves, Coronaries, and Cardiac Innervation. *Dev Dyn.* **237.** 494-503.

Wahi, K., Bochter, M.S., Cole, S.E. (2014). The Many Roles of Notch Signaling during Vertebrate Somitogenesis. *Semin Cell Dev Biol.* **S1084-9521.** 00320-00326.

Walcher, T., Xie, Q., Sun, J., Irmler, M., Beckers, J., Öztürk, T., Niessing, D., Stoykova, A., Cvekl, A., Ninkovic, J., Götz, M. (2013). Functional Dissection of the Paired Domain of Pax6 Reveals Molecular Mechanisms of Coordinating Neurogenesis and Proliferation. *Development.* **140.** 1123-1136.

Walther, C., Gruss, P. (1991). Pax-6, a Murine Paired Box Gene, is Expressed in the Developing CNS. *Development.* **113.** 1435-1449.

Warren, N., Caric, D., Pratt, T., Clausen, J.A., Asavaritkrai, P., Mason, J.O., Hill, R.E, Price, D.J. (1999). The Transcription Factor, Pax6, is Required for Cell Proliferation and Differentiation in the Developing Cerebral Cortex. *Cereb Cortex.* **9.** 627-635.

Wen, J., Hu, Q., Li, M., Wang, S., Zhang, L., Chen, Y., Li, L. (2008). Pax6 Directly Modulate Sox2 Expression in the Neural Progenitor Cells. *Neuroreport*. **19**. 413-417.

Wettstein, D.A., Turner, D.L., and Kintner, C. (1997). The Xenopus Homolog of Drosophila Suppressor of Hairless Mediates Notch Signaling During Primary Neurogenesis. *Development*. **124.** 693–702.

Whitfield, T.W., Wang, J., Collins, P.J., Partridge, E.C., Aldred, S.F., Trinklein, N.D., Myers, R.M., Weng, Z. (2012). Functional Analysis of Transcription Factor Binding Sites in Human Promoters. *Genome Biol.* **13.** R50.

Wilson, S.W., Rubenstein, J.L. (2000). Induction and Dorsoventral Patterning of the Telencephalon. *Neuron.* **28.** 641-651.

Wilson, S.W., Houart, C. (2004). Early Steps in the Development of the Forebrain. *Dev Cell.* **6.** 167-181.

Wolf, L.V., Yang, Y., Wang, J., Xie, Q., Braunger, B., Tamm, E.R., Zavadil, J., Cvekl, A. (2009). Identification of Pax6-dependent Gene Regulatory Networks in the Mouse Lens. *PLoS One.* **4.** e4159.

Woo, S.M., Kim, J., Han, H.W., Chae, J.I., Son, M.Y., Cho, S., Chung, H.M., Han, Y.M., Kang, Y.K. (2009). Notch Signaling is Required for Maintaining Stem-cell Features of Neuroprogenitor Cells Derived from Human Embryonic Stem Cells. *BMC Neurosci.* **10.** 97.

Xie, Q., Cvekl, A. (2011). The Orchestration of Mammalian Tissue Morphogenesis through a Series of Coherent Feed-forward Loops. *J Biol Chem.* **286.** 43259–43271

Xie, Q., Yang, Y., Huang, J., Ninkovic, J., Walcher, T., Wolf, L., Vitenzon, A., Zheng, D., Götz, M., Beebe, D.C., Zavadil, J., Cvekl, A. (2013). Pax6 interactions with chromatin and identification of its novel direct target genes in lens and forebrain. *PLoS One*. **8.** e54507.

Yamaguchi, Y., Sawada, J., Yamada, M., Handa, H., Azuma, N. (1997). Autoregulation of Pax6 Transcriptional Activation by Two Distinct DNA-binding Subdomains of the Paired Domain. *Genes Cells.* **2.** 255–261.

Yoon, K., and Gaiano, N. (2005). Notch Signalling in the Mammalian Central Nervous System: Insights from Mouse Mutants. *Nature Neuroscience*. **8(6).** 709-1411.

Yoon, K.J., Koo, B.K., Im, S.K., Jeong, H.W., Ghim, J., Kwon, M.C., Moon, J.S., Miyata, T., Kong, Y.Y. (2008). Mind Bomb 1-expressing Intermediate Progenitors Generate Notch Signaling to Maintain Radial Glial Cells. *Neuron.* **58.** 519–531.

Yun, K., Potter, S., Rubenstein, J.L. (2001). Gsh2 and Pax6 Play Complementary Roles in Dorsoventral Patterning of the Mammalian Telencephalon. *Development.* **128.** 193–205.

Zaret, K.S., Carrol, J.S. (2011). Pioneer Transcription Factors: Establishing Competence for Gene Expression. *Genes Dev.* **25.** 2227-2241.

Zhang, X.P., Zheng, G., Zou, L., Liu, H.L., Hou, L.H., Zhou, P., Yin, D.D., Zheng, Q.J., Liang, L., Zhang, S.Z., Feng, L., Yao, L.B., Yang, A.G., Han, H., Chen, J.Y. (2008). Notch activation promotes cell proliferation and the formation of neural stem cell-like colonies in human glioma cells. *Mol Cell Biochem.* **307.** 101–108.

Zhou, Y., Zheng, J.B., Gu, X., Li, W., Saunders, G.F. (200). A novel Pax-6 binding site in rodent B1 repetitive elements: coevolution between developmental regulation and repeated elements? *Gene.* **245.** 319–328.

Zirlinger, M., Lo, L., McMahon, J., McMahon, A.P., Anderson, D.J. (2002). Transient Expression of the bHLH Factor Neurogenin-2 Marks a Subpopulation of Neural Crest Cells Biased for a Sensory but not a Neuronal Fate. *Proc Natl Acad Sci U S A.* **99.** 8084-8089.

Appendix 1

1.1 Adaption of Promega dual-luciferase assay system protocol

Kit preparation

Passive lysis buffer preparation:

Prepare 1X passive lysis buffer solution (1ml 5X passive lysis buffer solution (supplied with kit) + 4ml ddH_2O).

LAR II:

Resuspend the lyophilized Luciferase Assay Substrate in Luciferase Assay Buffer II. Store at -20°C for 1 month or at -70°C for 1 year.

Stop and Glo Reagent:

Add 2.1ml of 50X Stop and Glo Substrate to 105ml of Stop and Glo Buffer in the stop and Glo bottle provided. Vortex for 10 seconds. Store at -20°C for up to 15 days.

Cell Preparation

Wash cells in 500µl of 1X PBS.
Remove 1X PBS and add 100µl of 1X passive lysis buffer (PLB) to each well of transfected cells.
Place on a rocking platform for 15 minutes at RT.
Use a plastic cell scraper (Fisher Scientific) to collect all cell lysate into a 2ml eppendorf tube.
Centrifuge at 13000rpm for 5 minutes at 4°C.

Collect supernatant. Aliquot 25µl into 0.25ml PCR tubes and retain for luciferase assay analysis. Aliquot the remaining supernatant into an additional 0.25ml PCR tube and retain for western blot analysis. Freeze at -20°C (or -70°C if being stored for longer than 1 month).

Luciferase Assay

Aliquot 20ul of cell lysis into each well of the 96 well plate.

Transfer LAR II and Stop and Glo Reagent into 30ml universal tubes for use with the GloMax luminometer .

Appendix 2

2.1 Operation of Promega Glomax Luminometer

Follow the Dual Luciferase Reporter Assay System Technical Manual for the Preparation of samples and reagents.

1. Turn on computer and then turn on luminometer.
2. Computer User name is Glomax and Password is blank.
3. Double-click on the Glomax X icon.
4. Select 'Run Promega Protocol'
5. Double-click on DLR folder
6. Select 'DLR with 2 injections column format' option
7. Prepare the injectors for use as follows:

Flush both injectors:

i) Remove the injector tips from the injector tip holders and place them into Waste beaker.

ii) Flush the injectors 3 times each in the following sequence:

ddH_2O
70% EtOH
ddH_2O
Air

Prime both injectors:

i) Insert inlet tubing into reagent bottles as follows:

Line 1 into LAR II and Line 2 into STOP and Glo reagent bottles.

ii) Remove the injection tips from the injection tips holder and place them in waste container

iii) Prime (into waste container).

iv) Return injection tips to the injection tip holder.

8. Place Multiwell plate containing lysates (20ul each) in luminometer and select wells for measurement via ‘Options’

A whole row can be selected by clicking on letter to left of row

9. Press START to start the assays

10. At the end of the run save a copy of the excel file containing the renilla and firefly measurements.

11. Calculate the averages for each set of triplicate measurements and then calculate the fold change in luciferase activity relative to the control.

Appendix 3

3.1 Protein transfer

1L 1X transfer buffer recipe:

NuPAGE Transfer Buffer (20X) – 50ml
Methanol – 100ml
ddH_2O – 850ml

Cut nitrocellulose to the correct size and soak in 1x transfer buffer for 10 minutes. Additionally, soak scotch-brite pads and filter papers in transfer buffer for 10 minutes.

Remove the gel from the western blot tank and soak in transfer buffer for 10 minutes so that any gel shrinkage occurs prior to transfer. Assemble transfer as below:

Insert into transfer module:

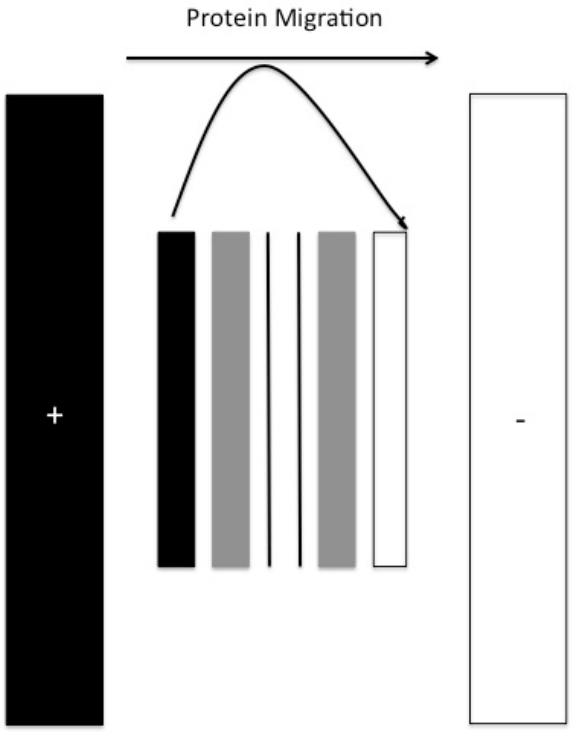

Cover the whole module with transfer buffer. After transfer take apart and treat nitrocellulose with care.